SEISMIC STRENGTHENING OF REINFORCED CONCRETE FRAMES

USING POST-TENSIONED BRACING SYSTEMS

by

JOSE ANTONIO PINCHEIRA, Ingeniero Civil, M.Sc.

DISSERTATION

Presented to the Faculty of the Graduate School of

The University of Texas at Austin

in Partial Fulfillment

of the Requirements

for the Degree of

DOCTOR OF PHILOSOPHY

THE UNIVERSITY OF TEXAS AT AUSTIN

August 1992

SEISMIC STRENGTHENING OF REINFORCED CONCRETE FRAMES
USING POST-TENSIONED BRACING SYSTEMS

APPROVED BY
DISSERTATION COMMITTEE:

To Paulette and José Pablo

To my parents

ACKNOWLEDGMENTS

The author would like to express his sincere and deepest gratitude to Dr. James O. Jirsa for his guidance, encouragement, continuous support and friendship during the development of this research. His leadership, professional ethics and human excellence are virtues that I can only aspire to follow in my life. It has been a privilege and a pleasure to work with such a remarkable man.

Sincere thanks are extended to Dr. Michael E. Kreger for his advice, friendship and support during my studies. The valuable suggestions of Dr. José M. Roesset and Dr. Michael D. Engelhardt to the present study are greatly appreciated. Thanks are extended to Dr. Stelios Kyriakides for serving on the supervising committee.

The author would also like to express his sincere appreciation to Dr. John E. Breen for his encouragement, friendship and support throughout his studies. The advice and support of Dr. Joseph A. Yura and Dr. Richard E. Klingner are also gratefully acknowledged.

The support provided by the staff of the Ferguson Structural Engineering Laboratory is greatly appreciated. Special thanks are expressed to April Jenkins whose assistance was extremely helpful from the moment of my arrival at Austin. Sincere thanks are extended to Jean Gerhke, Sharon Cunningham and Laurie Golding. Thanks are also extended to Alec Tahmassebi and Ryan Green for their assistance in solving many of the hardware/software glitches during the development of this project. The technical support provided by Lawrence (Nubz) Newberg with the VAX systems is appreciated.

The friendship and support of fellow graduate students (too many to name them all) at Ferguson Laboratory are sincerely appreciated and will always be remembered. The friendly environment created by the faculty, staff and students make Ferguson Laboratory a place that anyone would look forward to going to work every day. Thanks to y'all once again.

The author is indebted to his wife Paulette whose patience, understanding and encouragement made the tough times much easier. Thank you for your love and for giving me that little "earthquake" named José Pablo.

The author would also like to express his heartfelt gratitude to his parents whose continuous support and encouragement were vital to the completion of his goals. Thank you for everything.

José A. Pincheira

Austin, Texas

March, 1992

vi

SEISMIC STRENGTHENING OF REINFORCED CONCRETE FRAMES

USING POST-TENSIONED BRACING SYSTEMS

Publication No. _____

José Antonio Pincheira, Ph.D.

The University of Texas at Austin, 1992

Supervisor: James O. Jirsa

Many existing buildings in the United States designed and constructed according to past standards are often found inadequate to withstand major earthquakes. Non-ductile reinforced concrete frames have been identified among the types of structures that pose the greatest hazard to society. Accordingly, significant research effort has been devoted to developing and evaluating different techniques for the seismic retrofit of such buildings.

The present study focusses on the use of a technique that involves the addition of high strength, post-tensioned braces (steel strands or rods) as an alternate retrofit scheme for non-ductile reinforced concrete frames. The main objectives of the study are to evaluate analytically the performance of the post-tensioned bracing system as a retrofit technique and to identify the benefits and inadequacies of the system.

To study the behavior of the post-tensioned bracing system, inelastic dynamic and

static analyses are conducted on three non-ductile reinforced concrete structures. The buildings represent typical low and medium rise construction of the 1950's and 1960's in the United States. Dynamic analyses are conducted using five ground motions representative of major earthquakes on firm and soft soil conditions. For buildings located on soft soils, the effects of soil-structure interaction are included in the analyses using a simplified procedure.

Overall, the results indicate that the post-tensioned bracing system can control lateral drifts and prevent collapse of low and medium rise structures on firm and soft soil sites. The technique is most suitable for low-rise buildings on soft soils, but can be used for low and medium rise buildings on firm soils. For medium rise buildings on soft soils, the performance of the system depends on the characteristics of the earthquake record. A high level of initial brace prestressing maximizes energy dissipation of the system and reduces overall response of the building. For low and medium rise buildings, the technique provides a performance level comparable to that of X-bracing and to the addition of a structural wall.

TABLE OF CONTENTS

CHAPTER V   ON THE BEHAVIOR OF POST-TENSIONED BRACING SYSTEMS

CHAPTER I

INTRODUCTION

1.1 GENERAL

Many existing buildings in the United States designed and constructed according to past standards and practices are often found to be inadequate to withstand major earthquakes. Although many of these buildings may perform satisfactorily in future earthquakes, a large number of structures or building components are likely to fail catastrophically posing a serious hazard to the occupants. The tragic collapse of the Cypress Viaduct and the billions in damage caused by the Loma Prieta earthquake of October 17, 1989, are the most recent testimonies of the vulnerability of older construction to seismic events.

In recent years, a significant research effort has been undertaken to identify potentially hazardous structures and to develop techniques to improve their seismic resistance. Non-ductile reinforced concrete frame buildings have been identified as one of the types of structures which appear to represent the greatest hazard to the society [1]. As a consequence, an important amount of research has been devoted to evaluating the performance of retrofit techniques to enhance the seismic behavior of reinforced concrete frame structures and frame members. The techniques for the seismic retrofit, or seismic rehabilitation, of structures can be varied depending on the structural properties of the existing structure and the performance level desired. The most common retrofit schemes are steel or reinforced concrete jacketing, the addition of infill walls and the addition of steel bracing systems.

To date, a major part of the research work has focussed on experimental verification of different retrofit techniques which examine the behavior of subassemblages under static cyclic load reversals. While these studies provide valuable information on stiffness and strength of the retrofitted structure, they do not provide information on the ability of the system to satisfy the strength, displacement and ductility demands during an earthquake. The actual forces and deformations developed during ground motion can only be

1

determined by dynamic shaking table tests, pseudo-dynamic tests or by dynamic analyses. Most retrofit techniques will result in an increase in stiffness with minor increases in mass and thus shortening of the period of vibration of the structure. A shortening in the period of vibration often results in an increase in the strength and ductility demands of the retrofitted structure. Thus, the retrofit scheme will be successful only if increases in strength and ductility capacity of the structure are greater than or equal to increases in demands imposed by the earthquake.

In a previous analytical study, Jordan [49] evaluated the inelastic dynamic response of prototype non-ductile reinforced concrete frames rehabilitated with reinforced concrete jacketing or infill walls. The study showed that while all retrofit schemes increased the stiffness and strength of the existing structure, not every scheme performed adequately under any seismic event selected. Jordan attributed the inadequate performance of the retrofit schemes to the inability of the systems to control lateral drifts and prevent severe damage to "non-strengthened" elements in the structure. From his study, it can be concluded that the effectiveness of the retrofit scheme was dependent not only on the structural properties of the existing structure, but also on the characteristics of the ground motion.

Steel bracing systems have been found, in general, well-suited for the retrofit of reinforced concrete frames. If correctly designed, they provide the structure with increased stiffness and strength and can be detailed to exhibit good hysteretic behavior. However, previous studies on bracing systems with low slenderness ratio braces have shown that alternate inelastic buckling and yielding of braces is linked with large local deformations at the brace connection. Such behavior can lead to a premature failure of the connections and ultimately to the sudden loss of one or more braces. A previous study [51] showed that due to the relatively low ductility and redundancy of existing frame structures, the redistribution of forces following the sudden loss of a brace results in almost immediate failure of the existing non-ductile reinforced concrete members. Such behavior limits the strength and energy dissipation capacity of the structure and can lead to collapse of the building during a major earthquake.

To prevent braces from buckling inelastically, it has been suggested [25] to design the brace with a very low or a very high slenderness ratio. For braces with very low slenderness

' ratios, yielding takes place instead of buckling. With high slenderness ratios (such as steel rods or strands), braces buckle elastically and the negative effects of inelastic buckling are thus avoided.

The present study centers on the use of a retrofit technique that involves addition of post-tensioned braces (steel rods or strands) to improve the seismic response of reinforced concrete frames. With the use of high strength steel rods or strands the lateral strength of the structure can be increased very efficiently with relatively small amounts of material. Also, steel strands or rod braces can be initially prestressed to increase the lateral stiffness of the building and to reduce the likelihood of shortening the braces to a point where they become slack. If braces remain in tension, the reductions in lateral stiffness are minimized. Though the technique has received limited attention in the U.S, it has been used to retrofit low-rise buildings in Mexico City after the 1985 Mexico earthquake.

1.2 OBJECTIVES

The purpose of this study is to evaluate analytically the seismic performance of post-tensioned bracing systems (cables or rods) as a retrofit scheme for low and medium rise frames of reinforced concrete. In addition, the study will identify benefits and inadequacies of the system and will identify cases for which the post-tensioned bracing technique is most suitable.

To compare the behavior of the post-tensioned bracing system, the performance of two common retrofit schemes is also evaluated, namely the addition of an X-bracing system and the addition of structural walls.

The behavior of the different retrofit schemes is examined in light of available code provisions for new and existing construction. Based on this evaluation and the results obtained from analyses, a procedure for determining the minimum requirements of stiffness and strength for adequate performance of the retrofit scheme is developed. Design recommendations for the use of post-tensioned bracing, X-bracing and the addition of structural walls are proposed.

1.3 SCOPE

Evaluation and retrofit of the buildings considered for study are restricted to moment resisting frames of reinforced concrete. The buildings are prototype designs and were designed to represent typical low and medium rise construction of the 1950's and 1960's in the United States. The evaluation of the retrofit schemes is performed by examining in-plane, inelastic dynamic response of buildings. The buildings selected for study possess a regular distribution of stiffness and strength in plan so that dynamic effects of higher torsional modes of vibration are minimal and two-dimensional analyses are appropriate.

Five earthquake records representative of major earthquakes in the U.S. and elsewhere are used in the present study. Three of these records are used to study the response of buildings on firm soil conditions, while the other two are used to evaluate the response of buildings on soft soil sites. A simplified procedure is used to model soil-structure interaction effects on buildings located on soft soil sites.

Retrofit schemes are limited to post-tensioned bracing, X-bracing and addition of structural walls. In this study, all three schemes confine retrofit operations to the exterior of the building, by providing braces or wall(s) only to the perimeter frames.

CHAPTER II

LITERATURE REVIEW AND BACKGROUND INFORMATION

2.1 GENERAL

The seismic retrofit of existing structures has been defined as the judicious modification of the structural properties to improve the performance in future earthquakes[7]. Seismic retrofit of an existing building may be called upon to repair and strengthen damaged members after a major earthquake, or simply to improve the seismic characteristics of the structure anticipating inadequate performance in future seismic events. The criteria for seismic retrofit projects often require unique design considerations because the structural properties of the existing building and the goals of the retrofit vary considerably for different structures. The strength, stiffness and ductility characteristics of existing buildings depend on the structural system provided (moment frames, bearing walls, braced frames, etc), the type and existing condition of the construction materials and, the design provisions in effect at the time of erection of the structure. Although several strengthening techniques have been proposed, there are no specific regulations for the seismic retrofit of existing buildings. Currently, the decision to retrofit a structure is, for the most part, made on a voluntary basis, and therefore the goals of the seismic retrofit are determined by common agreement between the engineer and the owner. With the lack of precise regulations, the selection of the appropriate retrofit scheme is left solely to the judgement of the design engineer. The techniques and schemes for the retrofit of buildings are diverse, and depend on the available strength and ductility of the existing structure and on the goals of the retrofit as discussed above.

In this chapter, current techniques oriented specifically towards the improvement of the seismic performance of non-ductile moment resisting frames of reinforced concrete are reviewed. Common structural problems associated with reinforced concrete frames constructed 20 years ago or more are identified and are examined in light of current design provisions for seismic zones. The design strategies for the selection of appropriate retrofit schemes for moment frames are discussed and design criteria for the retrofit schemes selected for study are presented.

5

2.2 EARTHQUAKE DESIGN PHILOSOPHY FOR FRAME STRUCTURES

A brief review of basic criteria of earthquake resistant design of building frame structures will serve to facilitate an understanding of the problems associated with the evaluation and subsequent retrofit strategies for existing buildings presented below.

Figure 2.1 shows the lateral force and lateral displacement relationships for two hypothetical structures with identical initial stiffness but different lateral strengths, both responding to the same earthquake. Structure A is able to respond the given earthquake completely in the elastic range, while structure B reaches its elastic limit and deforms beyond its elastic range. Because structure B responds inelastically to the earthquake, the maximum displacement could be, in

Figure 2.1 Load and displacement relationships.

general, equal to, smaller than or larger than the maximum displacement developed by structure A. It can be seen from Fig. 2.1 that structure B can be designed for a lower lateral strength S_B than the elastic force S_A, provided that inelastic deformations and resulting damage are controlled. The level of the design force S_B is a function of the structure's ability to dissipate energy during inelastic response. The larger the energy dissipation capacity of the system, the lower the required strength. Although it is possible to design a structure to respond elastically during a major event, current social and economic priorities dictate that such design is both uneconomical and impractical.

The design principles presented above form the basis of current design philosophy for earthquake resistant structures. Due to the uncertainties involved in estimating the magnitude and return period of earthquake ground shaking during the service life of a structure, the performance level specified by code provisions has associated with it an implied risk. A building structure design according to current code provisions is expected to:

    a) resist minor earthquakes without damage (essentially in the elastic range)

b) resist moderate earthquakes without structural damage, but with some non-structural damage

c) resist major earthquakes with non-structural as well as *structural damage*, but *without collapse*.

The last statement is most significant because it deviates from standard design procedures for static loadings. It establishes that, under a major earthquake, the structure is expected to yield and deform well beyond the elastic limit of the structure. Furthermore, frame members are expected to withstand several cycles of reversed inelastic deformation without significant degradation of stiffness or strength. In other words, frame members are expected to have good energy absorption capacity, sometimes expressed in terms of *ductility*, the ratio between the ultimate deformation of the member and the deformation at yield.

Current design codes rely on *member ductility*, or in general, the *system ductility* to specify the design lateral loads. The design lateral forces prescribed by current codes are **reduced** from elastic forces by *response modification factors* that primarily account for the ductility of the structural system. Other aspects included in response modification factors are damping, the degree of redundancy in the structure and overstrength capacity above that where design loads cause "significant yield"[15]. Different structural systems have different energy absorption capacity or levels of ductility for which codes specify different values for the response modification factors. Note that if the structure were to respond elastically during a major event, no reduction would be allowed in the level of lateral forces.

To ensure ductile behavior during a major earthquake, current design provisions require special detailing of frame members and connections. In addition, code provisions are oriented towards the design of structural systems capable of resisting large inelastic deformations without collapse. Figure 2.2 shows two possible failure mechanisms for frame buildings, often referred to as the *strong-beam weak-column* mechanism and the *weak-beam strong-column* mechanism. The former mechanism (*strong-beam weak-column*) is an undesirable collapse mechanism for several reasons, but mainly because yielding of columns in a given story means increased likelihood of collapse of the entire building. In contrast, the *weak-beam strong-column* mechanism enforces yielding of beams in flexure prior to hinging of columns which allows energy dissipation with less likelihood of collapse
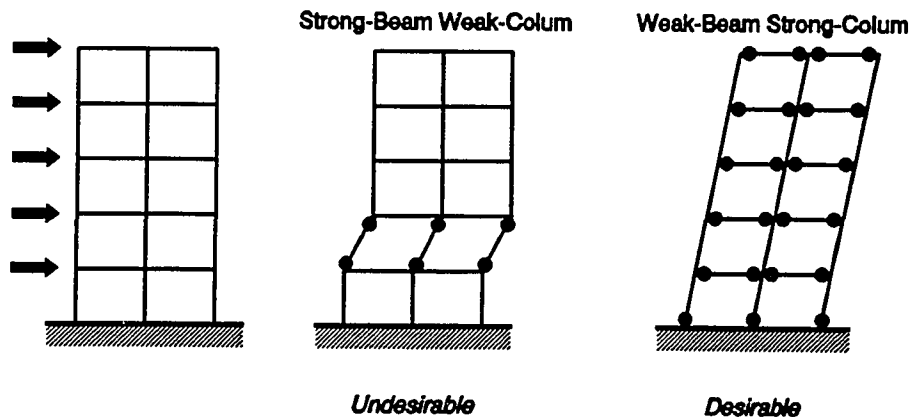
Figure 2.2   Possible failure mechanisms for frame structures under lateral loads.

of the building. In a static failure mode, as shown in Fig. 2.2, plastic hinges in a *weak-beam strong-column* mechanism form at the base of columns only in first story columns. Under dynamic loading, plastic hinges may also form in many column ends throughout the structure and therefore columns should always be provided with adequate ductility.

Under current code provisions, the *weak-beam strong-column* mechanism is implemented by requiring that the summation of the flexural strengths of columns at a joint be larger than that of the beams. Such a provision does not necessarily prevent the columns from yielding under earthquake loading, but it reduces the likelihood of yielding in columns prior to yielding of beams.

2.3 NEED FOR SEISMIC RETROFIT

The need for seismic retrofit of existing buildings in the U.S. has been recognized over the last two decades, and is perhaps, one of the most urgent problems at the present time. Because of advances in the understanding and knowledge of earthquake resistant design of structures, it is now well recognized that most buildings constructed two decades ago or more have inadequate earthquake resistance and may pose a serious hazard to society.   In California, the collapse of the Cypress viaduct during the Loma Prieta Earthquake is perhaps the most tragic testimony of the need for seismic retrofit of existing structures. In the eastern U.S., studies have shown that earthquakes are less frequent than

in California, but they may pose just as large a threat to society[62]. The threat is of special concern because most structures in the east have not been designed for earthquake loading.

The reasons for the seismic retrofit of an existing building may be diverse, namely, repair/strengthening of damage due to previous earthquakes, deteriorated condition of structural materials, changes in the building occupancy, etc. Nonetheless, the most common reason is probably the upgrading of seismic provisions of local codes. Upgrading of seismic code provisions includes two main revisions which are: a significant increase in the level of the design lateral forces and a significant improvement in detailing of members for ductile behavior. Both aspects are interrelated and have a significant impact in the evaluation and later selection of the appropriate retrofit strategy. These two aspects are discussed in detail in the following sections.

2.3.1 Comparison of Lateral Force Code Provisions - 1955 to 1991

The design lateral force levels required in the provisions of the Uniform Building Code (UBC) are compared for the years 1955[8], 1964[6] and 1991[3]. In addition, the recommendations of the National Earthquake Hazards Reduction Program (NEHRP) of 1988 [15] are also compared.

Because the design procedures for lateral forces have changed significantly throughout the years within the specifications of the UBC, a direct comparison of older code provisions with current ones cannot be made without including certain design assumptions. Unlike most recent versions of the UBC, the 1955 UBC does not provide a direct expression to compute the base shear coefficient from the building period. Instead, it specifies lateral forces directly which are based on the number of stories of the building. For the purpose of the comparison, the empirical equation: T (secs) $= 0.1 N$ (N being the number of stories), was used to compute an equivalent period of vibration of a reinforced concrete frame structure.

Probably the most significant difference in the design procedures for reinforced concrete building structures was the change from the working stress design (WSD) method to the Ultimate Strength Design (USD) method that took place during the 1960's and the early part of the 1970's. Because of the difference in load factors, strength reduction factors

and load combinations (among others), the design lateral forces as obtained from these two different design procedures cannot be compared directly. To account for this difference, the lateral forces obtained using the WSD method must be factored upward for comparison with those obtained using the USD method. There is no single factor to use, but a factor of 1.4 seems reasonable.

Based on the assumptions presented above, the base shear coefficient and the building period relationship was calculated using the old and current provisions of the UBC and NEHRP recommendations, as shown in Fig. 2.3. In this figure, the base shear coefficient and building period relationship has been plotted for Ordinary Moment Resisting Space Frames (OMRSF) of reinforced concrete, in zones of highest seismicity (Zone 4 according to the current UBC classification), and on firm soil (soil type 2 of the 1991 UBC).

As can be seen in Fig. 2.3, there has been a significant increase in the design lateral forces for reinforced concrete frame structures, particularly since the publication of the 1964
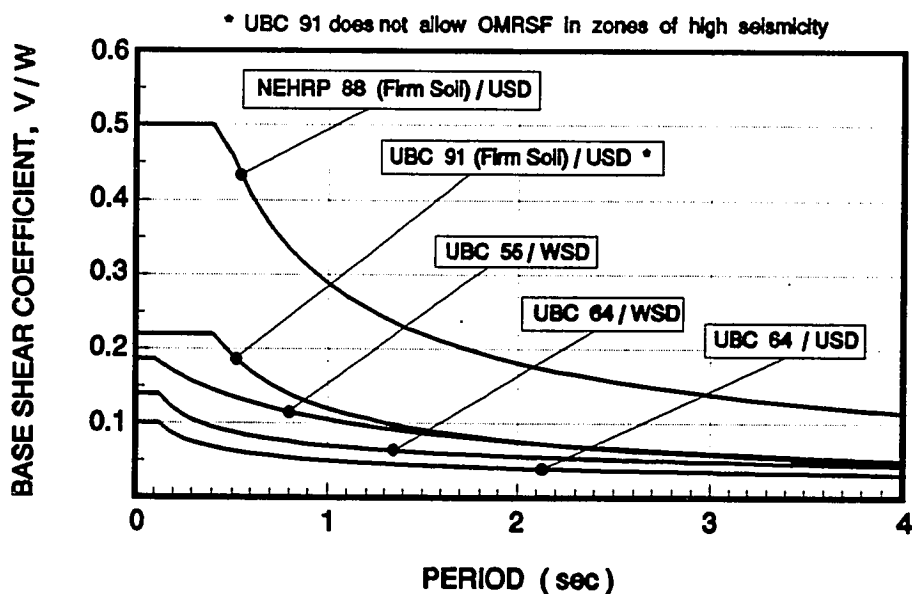
Figure 2.3 Comparison of base shear coefficient versus building period for ordinary moment-resisting frames (OMRSF) of reinforced concrete in zones of high seismic risk.

edition of the UBC. The main source of the increment in the design lateral force level in current codes (1991 UBC and 1988 NEHRP) comes from the recognition that older codes did not have adequate provisions for detailing of reinforcement that would ensure ductile behavior of the reinforced concrete members. Thus, a larger lateral force level is required to supplement the lack of ductility in the structure.

Note that the WSD provisions of the 1955 UBC would result in higher lateral design forces than those obtained from a more recent code such as the WSD approach of the 1964 UBC. It also appears that the use of the USD procedure of the 1964 UBC results in a lower lateral strength of the building than the corresponding WSD approach.

While the current 1991 UBC does not require the same level of lateral forces as the 1988 NEHRP code, it must be recognized that ordinary moment resisting space frames are prohibited in zones of high seismicity by the current UBC. Furthermore, OMRSF are only permitted in zones of low seismicity (zone 1 of the 1991 UBC). On the other hand, the recommendations of the 1988 NEHRP do permit the erection of OMRSF in zones of high seismic risk, provided that a high penalty is imposed on the design lateral force level. This can be clearly seen in Fig 2.3, where the base shear coefficient required for a short period structure by the 1988 NEHRP is almost 2.3 times larger than that required by the 1991 UBC.

2.3.2 Typical Detailing of Reinforced Concrete Frames in Older Construction

Since the level of lateral forces prescribed in older codes was much lower than those required by present code provisions, the design of reinforced concrete frame structures was often governed by gravity loads and not by earthquake loading. As a result, most frame structures built in the late 1950's or 1960's have been detailed primarily for gravity loads and consequently lack adequate ductility. In addition, the knowledge and understanding of the behavior of reinforced concrete members subjected to cyclic load reversals have improved significantly in the last two decades. Therefore, buildings constructed in the 1950's or 1960's lack proper detailing of members for seismic loads simply because of the absence of specific requirements for earthquake loading, even if design lateral forces had been higher.

Following is a description of critical details that are typical of past design practice. Critical details are based partly on a review of design codes and detailing manual used since

1950, and partly on previous studies on seismic retrofit of building structures [11, 25, 28, 49, 55]. The implications of inadequate detailing of frame members on the expected behavior of the structure are also discussed.

a) *Shear Reinforcement of Frame Members:*

Typically, transverse reinforcement in column and beam members was designed for shear forces obtained directly from analyses of the building using *design* lateral forces. While this procedure followed standard practice in effect at the time, it does not prevent the premature brittle shear failure of members. As discussed earlier, the *design* lateral forces used to design the shear reinforcement were much smaller than those required by current code provisions. Even under current code procedures, the actual forces that the structure will experience during severe ground motion are much smaller than those implied by the codes because it is assumed that frame members will dissipate energy through inelastic response. Thus, unless frame members possess strengths comparable to the elastic forces developed during an earthquake, the members will fail in shear in the event of a major earthquake. Maximum shear forces of a frame member are related to the flexural capacity at its ends rather than to factored shear forces indicated by lateral load analyses. For these reasons, current design provisions [4] require frame members to be designed for the forces associated with the maximum moment strengths at the member ends to ensure a flexural mode of failure of the members (*capacity design philosophy*), as illustrated in Fig. 2.4.

The latter provisions were first introduced in the ACI code in 1971 and included only column members. As a result, column and beam members designed according to earlier editions of the ACI code are likely to experience premature shear failure prior to developing their full flexural capacity under earthquake loadings. In addition, because the forces used in design were significantly lower than those required by current codes, shear failure of these members would probably occur in the early stages of a major event and at small lateral drifts.
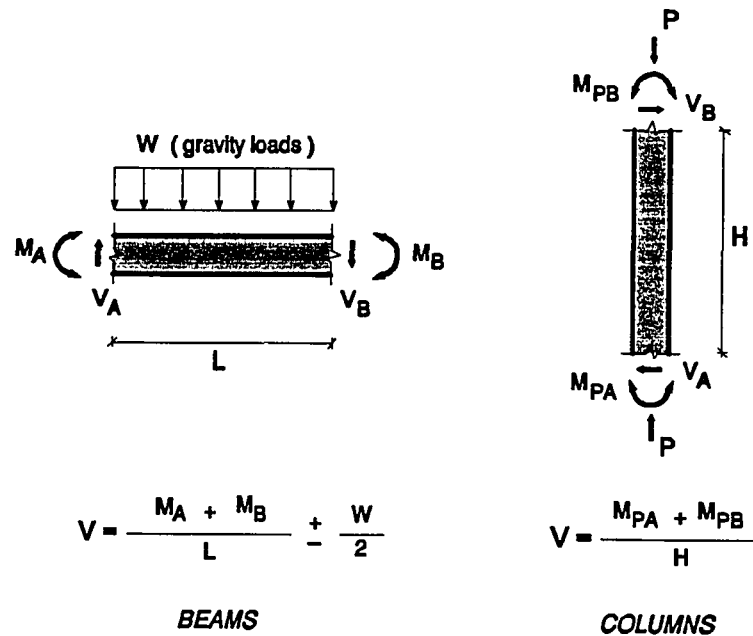
Figure 2.4 Design shear forces for beam and column members under current provisions (*capacity design philosophy*).

b) <u>*Lap Compression Splices in Columns:*</u>

Since design lateral loads in older codes were relatively low, the design of building frames was primarily governed by gravity loading. As a result, columns were often considered as "compression members" and lap splices were designed accordingly. To simplify construction, splices in columns were typically located just above the slab at each floor level where a construction joint was specified, as shown in Fig. 2.5. The length of lap splices specified in older codes was typically 20 bar diameters (ACI-1956[9]) or 24 bar diameters (ACI-1963[2]). For the concrete strengths used at the time (typically 3000 psi), such a splice length is insufficient to develop yielding in tension of most sizes of a Grade 60 bar. The amount of transverse reinforcement present in the splice region in most buildings
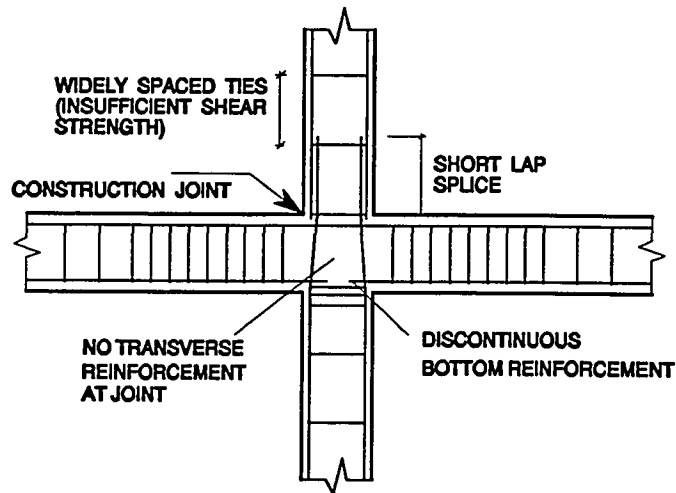
Figure 2.5   Typical reinforcing details of moment frames designed in the late 1950's and 1960's.

is minimal and provides little improvement in the splice capacity. The section at the base of columns with lap splices may not be able to develop flexural yielding and therefore the capacity of these sections will be limited to that of the splice in tension. Note that under earthquake loading the end sections of a column are regions of maximum bending in the structure and therefore critical for the safety of the building. Furthermore, the base sections of columns are potential hinging regions where energy dissipation is expected to take place under a major earthquake. A premature splice failure will not only reduce the lateral resistance of the building but it will also limit the energy absorption capacity of the frame.

c) *Discontinuous Bottom Reinforcement in Beams:*

Since gravity loads often governed the design of older frame buildings, "positive" bending moments at the beam ends were not anticipated. As a result, bottom ("positive") reinforcement in beams was typically embedded into the beam column-joint, as shown in Fig. 2.5. At least one-fourth of the area of the "positive" reinforcement in continuous spans was required to be embedded 6 in. into the support. Such a detail corresponds to past and present practices of members that are not part of a primary lateral load resisting system [2, 4, 9].

During a major earthquake the beam ends will be subjected to large moment reversals which will counteract the "negative" moment induced by gravity loads and cause the bottom reinforcement to act in tension. An embedment length of 6 in. is insufficient to develop yielding of any commercially available reinforcing bar (Grades 40 and 60). Thus, pull-out of the bars from the joint is likely to occur under a major event which will limit the "positive" moment capacity of the beam and the lateral resistance of the building. The brittle nature of a pull-out failure will also limit the energy absorption capacity of the frame building.

d) *Beam-Column Joints:*

In building frame structures, the role of the beam-column joint is to transfer the forces developed in the columns and beams. Therefore, adequate strength of the joint is essential for the development of the full capacity of the framing members. However, the design and detailing of beam-column joints received little, if any, attention in the past and it has not been until the last fifteen years that detailing of joints has been studied more comprehensively. Joint provisions for structures subjected to seismic loading were not introduced until the 1971 edition of the ACI code [57] in which transverse reinforcement was first required throughout the connection. As a result, most building structures built prior to this date are likely to have beam-column joints that have not been designed for seismic forces and that contain no transverse reinforcement through the joint (see Fig. 2.5). Under severe ground motion, the joint may be subjected to high shear forces which eventually can cause failure of the joint and limit the lateral resistance and ductility of the frame structure. The absence of transverse reinforcement in the joint aggravates the problem since the confinement necessary for transfer of the forces through the joint region is not available and a more brittle mode of failure is likely.

There is, however, one aspect that could benefit the behavior of the joint and prevent its failure during a severe earthquake. Because the members framing into the joint are likely to have limited strength (failure of column splices, pull-out of bottom reinforcement in beams) the maximum forces to be transferred at the joint are also limited. For these reasons, joint shear failure is unlikely to occur unless framing members are strengthened to develop their full capacity. In the

latter case, the beam-column joint will most likely have to be strengthened as well.

Other deficiencies such as inadequate spacing of shear reinforcement, insufficient development of reinforcing bars, etc., are also likely to be present in old construction and will have an effect on the performance of the building under lateral loads. However, the critical details indicated above represent the deficiencies that are most likely to govern the lateral strength and ductility of the building.

In addition to deficient detailing of members, building frames constructed in the past may also present an inadequate structural system for resisting lateral loads. Many building frames will display a *strong-beam weak-column* mechanism mode of failure, which is an undesirable mechanism for a lateral load resisting system, as discussed earlier in this chapter. Another deficiency of structural systems designed in the past is the so called "soft story". Typically, the first story of a building frame was designed to be taller than the upper stories in the building, which in many cases led to a more flexible (soft) first story. In addition, the lateral strength of the first story was designed to be lower than that of the upper stories (*weak first story*), so that all deformations and inelastic behavior was concentrated in the fist floor. Such a design concept became popular in the late 1960's [58], but it was later recognized that the first story concept would seriously jeopardize the stability of the super-structure because of large concentrated drifts in the first story.

2.4 SEISMIC REHABILITATION OF REINFORCED CONCRETE FRAMES

2.4.1 General

The rehabilitation of building structures may involve many different aspects that are intrinsic to each individual project and often make the selection of the proper retrofit scheme a unique problem. There are, however, certain considerations that are common to most retrofit operations and can be regarded as general for the retrofit of building structures. It is often found uneconomical and impractical to strengthen the entire structural system to achieve the required level of upgrading and, therefore, the retrofit is usually restricted to the strengthening of only certain portions of the structure. In general, solutions that confine retrofit operations to the perimeter of the structure are often preferred, mainly because they expedite the rehabilitation process and minimize disturbance to the occupants in the interior

of the building. In some instances the building may even remain occupied while the retrofit is underway. The latter aspect can be a very important economic and social factor strongly influencing the selection of the retrofit scheme.

Concentrating rehabilitation to the exterior portions of the structure may leave some "non-strengthened" elements in the interior of the structure. These elements may lack adequate strength, but more likely, will lack the ductility required to withstand the large deformations imposed on the structure under a severe ground motion. While understrength of "non-strengthened" elements can be accounted for in design, the lack of ductility cannot. Current seismic design procedures for new construction assigns "overall" system ductilities (response modification factors) to reduce elastic forces provided that all members that are properly detailed for ductility. As discussed above, an existing or retrofitted building may contain both ductile and brittle elements. The latter elements will limit the ductility of the system and therefore the provisions for new construction (design forces) are not directly applicable for the retrofit of buildings. In addition, the presence of non-strengthened elements may require limiting lateral drifts to much lower values than those permitted for new "ductile" buildings.

Currently in the U.S., there are no specific provisions for the retrofit of existing buildings and therefore the engineer has to find a retrofit solution and the appropriate level of lateral forces and drift limits with little or no guidance. The solutions for compensating for inadequate strength and ductility can vary considerably, and in current practice depend primarily on the engineer's judgement and on the owner's requirements. It is clear, however, that in the design of the retrofit scheme the designer must carefully contemplate the presence of these "non-ductile" elements and either modify the structure to avoid local failure of elements and/or limit the level of damage in these members. The definition of acceptable level of damage is not universal and, although it can be described qualitatively, it is quite difficult to express it in quantitative terms.

2.4.2 Evaluation of Existing Structures

The first step in the rehabilitation process of an existing structure is to establish the adequacy of the building to withstand the maximum probable earthquake expected for the site. Then, if the building is found inadequate a decision must be made to either retrofit the

building or demolish it and replace it by a new structure. To establish the adequacy of an existing structure, information on strength of materials, detailing of reinforcement, specifications and calculations is of primary importance. Original design and "as-built" plans of the building are indispensable for the evaluation; however, original drawings are often unavailable. A field inspection may be required to asses field conditions, modifications to original plans and the current state of deterioration of materials.

Once the basic information is gathered, an evaluation of the strength, stiffness and ductility characteristics can be performed. To determine the lateral capacity of an existing building there exists several documents to assist the engineer in the evaluation process. In Japan, the Japan Disaster Prevention Association has published two standards aimed at the evaluation, repair and strengthening of building structures [59, 60]. In the U.S., the Applied Technology Council has published two relatively new documents oriented to the evaluation of existing buildings, namely ATC-14 [61] published in 1987 and more recently ATC-22 [12] published in 1989. The ATC-22 recommendations are based partly on the methodology used in the ATC-14, but also follow criteria specified in the NEHRP Recommended Provisions for the Development of Seismic Regulations for New Buildings [15]. In this study the ATC-22 document is used as a reference for the evaluation of the buildings and is briefly discussed in the following.

2.4.2.1 ATC-22 Recommendations - A Brief Review

The methodology presented in ATC-22 (and in ATC-14) was aimed at developing comprehensive, but at the same time practical guidelines to assist engineers in the U.S. in evaluating existing buildings. Primarily, the provisions are intended to identify the different structural systems or building components that could endanger human lives during a severe ground motion. Hence, a major portion of the methodology is devoted to directing the engineer in determining the weak links in the structure that could precipitate structural or component failures. A summary of the ATC-22 provisions relevant to the structural systems investigated in this study are presented in Appendix A.

During the development of the ATC-14 provisions, later adopted by ATC-22, it was considered that less conservatism could be tolerated in an existing building because "for the review of existing buildings, the primary aim is to evaluate the true strength of the structure

when subjected to an earthquake"[61]. Thus, the input ground motion considered in ATC-22 is reduced with respect to that used for new construction. The lateral force level, base shear, specified in ATC-22 is based on a mean response spectra rather than the mean plus one standard deviation spectra usually specified for new construction. Response modification factors used in ATC-22 are the same as those specified in the NEHRP provisions for new construction [15].

In contrast to the reduction in the level of lateral forces, ATC-22 specifies **increased** load factors associated with seismic forces for *brittle* and *semi-ductile* elements in order to account for the lack of ductility of these elements. The higher load factors specified for buildings with *brittle* and/or *semi-ductile* elements partly compensate for the reduction in lateral forces. Thus, the lateral strength required by ATC-22 for buildings with *brittle* and/or *semi-ductile* elements may be as high as that of similar structural systems designed under current provisions, even though the level of lateral forces has been reduced as indicated earlier. However, for buildings provided with ductile elements, response modification factors and load factors are the same as those specified for new construction. Therefore, the lateral strength of ductile systems required by ATC-22 will be lower than that required for new buildings. The latter provisions are consistent with the intent of the document in that less conservatism is tolerated for an existing *ductile* system, but for *brittle* structures the strength and conservatism are similar to those required for new construction.

While ATC-22 provides minimum requirements for the evaluation of existing building, the document provides no recommendations for the "design" or evaluation of retrofit systems. Thus, as indicated earlier, the designer must determine an appropriate level of forces and drift limits for the existing building with no guidance.

2.4.2.2 Experimental Studies of Structural Systems with Inadequate Detailing for Seismic Zones.

Experimental work on the behavior of building structures/components with inadequate reinforcing details for seismic zones is scarce. Such information can provide valuable insight for a more accurate evaluation of the structural properties and behavior of existing buildings.

In 1990, Pessiki et al. [11] conducted a series of tests on full-scale cruciform-shaped specimens that represented the interior connection of a moment resisting frame. The specimens were tested under reversed cyclic loading and included column axial forces to represent gravity loads present during earthquake loading, as shown in Fig. 2.6. The main variables studied included the effects of short lap splices at the base of columns, embedded bottom reinforcement in beams and transverse reinforcement in the joint. The level of axial force and the presence of transverse beams (perpendicular to the plane of the specimen) to study the influence of transverse confinement were also among the variables studied.
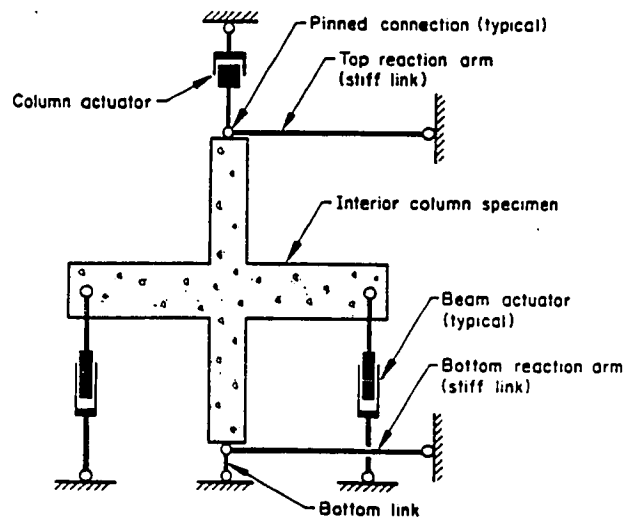
Figure 2.6 Test specimen and test set-up in Pessiki's tests (Ref. 11)

The test specimens included lightly-confined column lap splices located in the maximum moment region just above the floor level and discontinuous bottom beam reinforcement (some specimens included continuous bottom beam reinforcement as well). All top beam reinforcement was continuous through the beam-column joint. Bottom reinforcement in beams consisted of either 2#6 or 2#8 reinforcing bars of grade 60 ksi steel embedded 6 in. into the beam-column joint in accordance with past design practice (see section 2.3.2.c). Longitudinal reinforcement in columns consisted of either 8#7, 6#8 or 4#10 reinforcing bars. The splice length was 30 bar diameters in all cases, which exceeds the 20 or 24 bar diameter requirement of ACI 1956 and ACI 1963 (see section 2.3.2.b). The

28-day compressive concrete strength varied for beams and columns, and ranged from 2800 psi to 5500 psi. The conclusions relevant to the present study are summarized below:

a) Failure of specimens with discontinuous bottom reinforcement always initiated by pull-out of the bottom reinforcement from the beam-column joint. The peak pull-out resistance was independent of the bar sizes (#6 or #8) and also independent of the two axial force levels examined. However, larger beam rotations occurred in the presence of the smaller axial force. Fig. 2.7 shows typical moment and rotation relationship for the specimens with embedded reinforcement. It can be seen that the anchorage failure of bottom beam bars caused significant degradation of stiffness and strength of the member. Note that even though the top reinforcement in beams was continuous through the joint, there is also a reduction in the bending capacity for "negative" moment after the failure of the bottom reinforcement. This result is not addressed by the authors, but it is believed that such behavior may have been the result of significant deterioration of the concrete in the bottom region of the beam caused by the pull-out failure of bottom bars. Concrete may have spalled off as bars were pull-out form the joint which would cause a reduction in the size of the compression block and lever arm of the section in "negative" moment leading to a reduced "negative" moment capacity. However, a closer examination of test results may be required to support this conclusion.
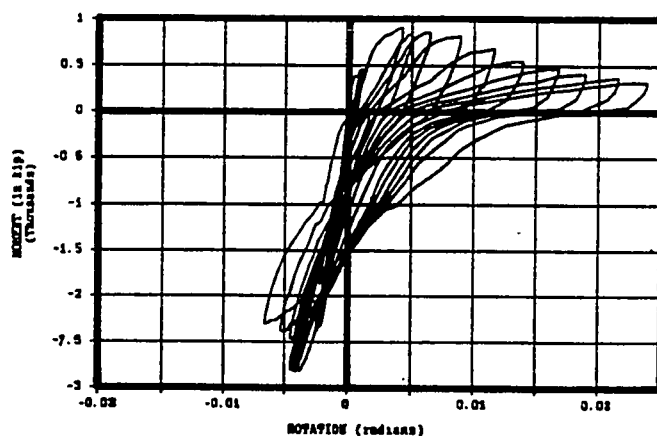
Figure 2.7   Moment and rotation relationship for specimens with embedded bottom beam reinforcement (Ref. 11).

b) Column splice failure was not observed in any of the test specimens considered in the study, even though splitting of the concrete cover was detected in the splice region. As noted above, the splice length provided in the specimens exceeded the lap prescribed in older code provisions and therefore the results regarding the performance of column splices are inconclusive. The presence of axial load in the columns may have significantly improved the capacity of the splice, a condition that does not represent the most unfavorable situation for evaluating the capacity of the splice. Compressive axial forces in columns may be reduced significantly during an earthquake; the presence of tensile forces due to overturning moments are not uncommon in exterior columns of moment frames.

Chai et. al [69] have recently conducted reversed cyclic loading tests on circular bridge columns with lapped starter bars. The longitudinal reinforcement of prototype columns consisted of #6 reinforcing bars of Grade 40 steel, with a 20 bar diameter lap splice at the base of the column. The 28-day compressive strength of the concrete in the column specimens varied from 4725 psi to 5600 psi. While the detailing of the bridge column specimens is somewhat different than that encountered in columns of frame structures, test results indicated that bond distress occurred at the base of the columns. Note that the yield strength of the rebars used in those tests was only 40 ksi and therefore it is highly likely that rebars of Grade 60 steel, commonly used in building construction, will develop bond distress for similar lap lengths.

Recent studies by Valluvan et. al [28] on prototype column specimens with lap splices subjected to cyclic axial loading have shown that a 24 bar diameter lap is insufficient to develop yielding in tension of #6 rebars of Grade 60 steel. The compressive strength of the concrete used in these tests averaged 4000 psi at 28 days. While the hysteretic response of splices in direct tension may be different from that of splices in flexure, it is believed that the peak capacity of the splice is adequately represented by the pure tension tests. Column tests with short lap splices subjected to lateral load reversals are currently underway [50], which will help verify this conclusion.

2.4.3 Retrofit Schemes and Related Research

Several techniques have been developed for the strengthening and repair of building components. Most of the techniques are oriented to the improvement of strength and

' ductility of the elements in existing buildings. In 1989, the Federal Emergency Management Agency (FEMA) published a comprehensive document on the different techniques recommended for the seismic strengthening of existing buildings [62]. The FEMA document includes techniques for the retrofit of different structural systems of steel, reinforced concrete, masonry and wood, etc. In addition, there has been substantial research work in this area [28, 46, 50, 51, 56, 63, 64, 67, 70] in which the behavior of different strengthening techniques are evaluated. The following describes the techniques developed specifically for moment frames of reinforced concrete. The advantages and disadvantages of each of the techniques presented are briefly discussed.

2.4.3.1 Reinforced Concrete or Steel Jacketing

The "jacketing" technique consists of encasing existing columns and/or beams with a new shell of reinforced concrete or steel. A typical jacketing scheme is illustrated in Fig. 2.8. The jacketing technique is intended to improve the axial, flexural and shear strength
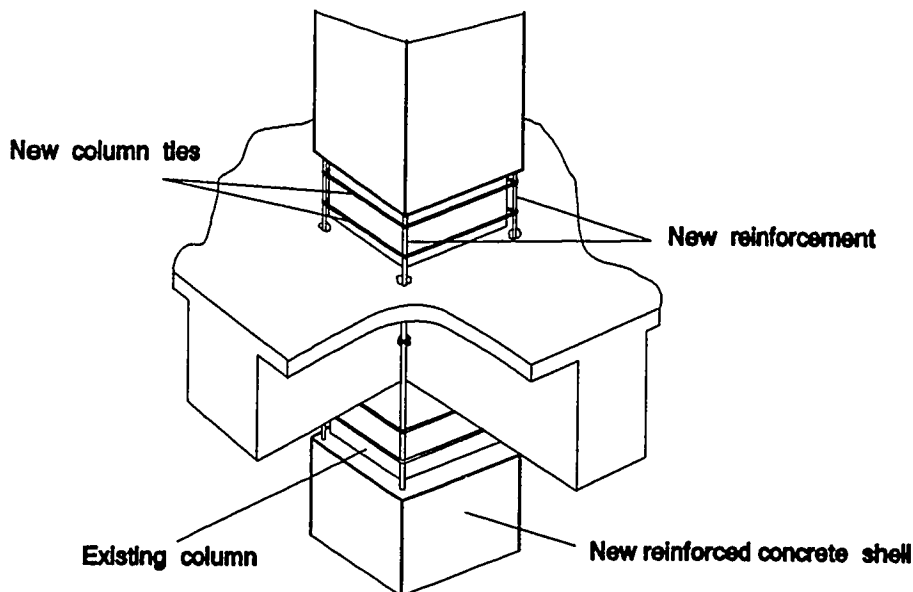
Figure 2.8 Strengthening of a an existing column using reinforced concrete jacketing. (Adopted form Ref. 62)

of existing members. Strengthened elements will possess higher and better energy absorption characteristics which will help enhance the ductility of the overall structural system. If the goal is to increase only the shear capacity of the member, the jacketing can be terminated with a small gap at the ends of the member, as shown in Fig. 2.9. In this manner, the flexural capacity at the member ends remains unchanged, while the shear capacity is increased. Notice that while improving the strength and ductility of existing members, the jacketing technique maintains the original characteristics of the structural system, i.e. the building remains as a moment resisting frame after retrofit.
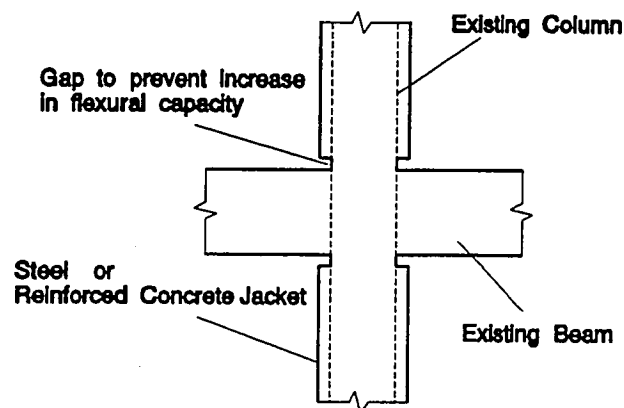
Figure 2.9 Strengthening of an existing column to increase shear strength only.

In general, the technique requires few or minor modifications to existing foundations. Also, only minor changes in the original layout of the building makes the jacketing technique attractive from an architectural standpoint.

The performance of reinforced concrete jacketing has received significant attention in recent years. Alcocer et. al [63] conducted an experimental program using large-scale beam-column subassemblages, to evaluate the performance of reinforced concrete jackets and to investigate the suitability of the technique as a retrofit scheme. Fig. 2.10 shows the test specimen and test set-up used in the program. The beam-column subassemblages represented an existing structure designed according to Mexican and American practices of the 1950's. All specimens were tested under bi-directional reversed cyclic loading. The
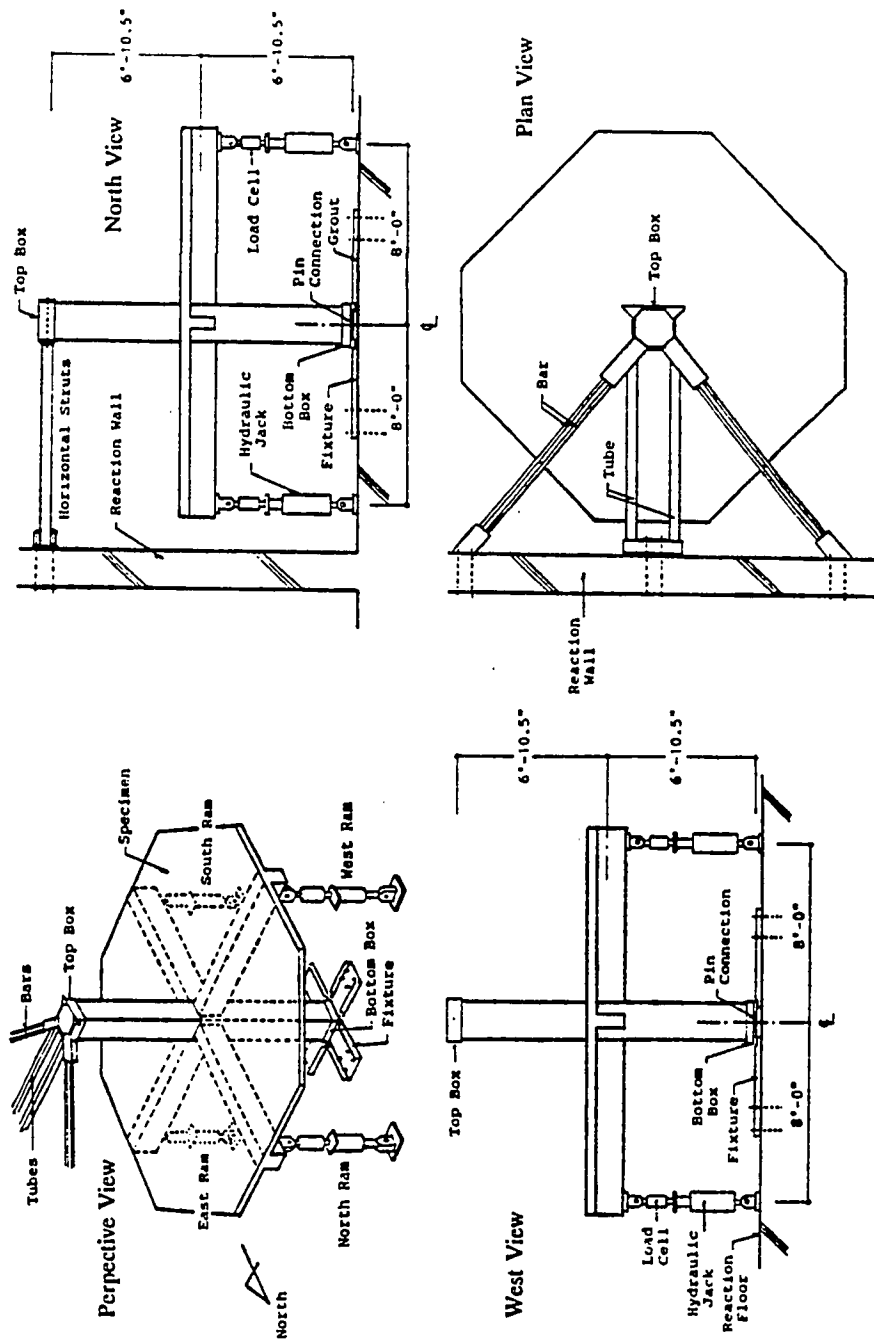
Figure 2.10 Test specimen and test set-up of Alcocer et. al tests (Ref. 63).
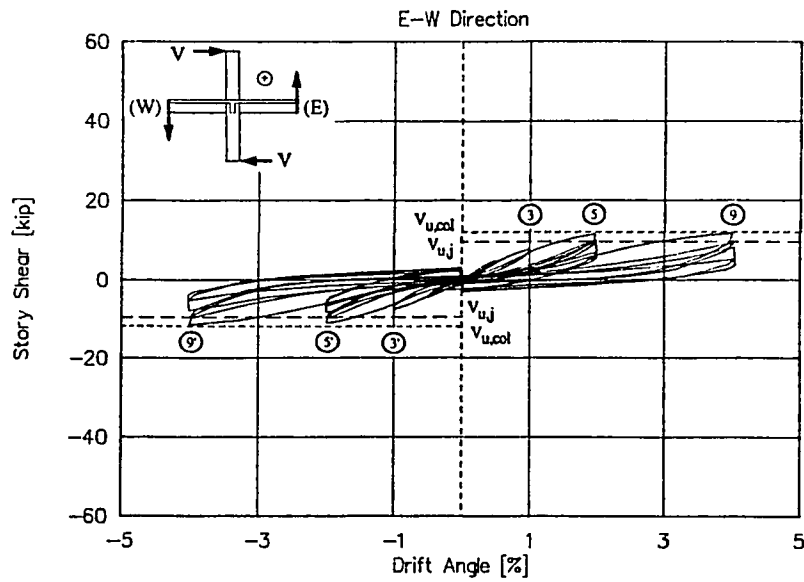
Specimen O - Story Shear vs. Drift Angle (E-W Direction)
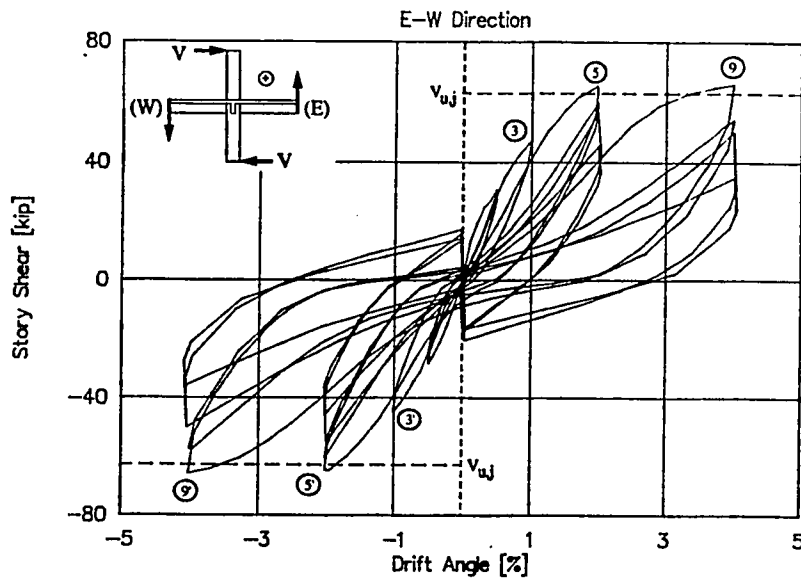
Specimen SD-B - Story Shear vs. Drift Angle (E-W Direction)

Figure 2.11 Comparison of hysteretic behavior of original and retrofit specimens using reinforced concrete jacketing (Ref. 63).

jacketing consisted of encasing columns, beams and the joint region with new reinforcement and a new concrete shell. Fig. 2.11 compares the hysteretic response for the original "non-jacketed" specimen and the response of the same original specimen encased with one of the jacketing schemes used in the program. It can be seen that the increases in strength and stiffness with the jacketing scheme are substantial. Even though the hysteresis loops of the retrofitted specimen show some pinching, the cycles were stable and showed moderate strength degradation.

In a previous study, Bett [70] studied the performance of reinforced concrete jackets to repair and strengthen short columns lacking shear strength. In all cases, the repaired and strengthened specimens showed greater strength and ductility than the original "non-strengthened" column. In addition, the mode of failure of strengthened specimens was changed to a more ductile flexural-shear failure mode and the observed hysteretic behavior became stable at larger lateral drifts.

Overall, test results show that the reinforced concrete jacketing technique always improved the strength, stiffness and energy dissipation characteristics of existing frame members. However, it has been noted that due to the intensive labor required to place the new materials around the existing members and the high costs of formwork, the technique may be uneconomical for the American practice [63].

Steel jacketing has been used extensively to rehabilitate structures in the past, although there is only limited experimental evidence on the behavior the technique [71]. Similar to the results obtained for reinforced concrete jacketing, steel jackets help enhance the strength and energy dissipation capabilities of the existing structure.

2.4.3.2 Addition of Infill Panels or Structural Walls

The addition of infill panels of reinforced concrete in one or more bays of an existing moment frame is a common technique for improving lateral strength. Fig. 2.12 illustrates a typical design of an infill panel scheme. Of primary concern is the shear transfer capacity between the infill wall and the existing frame members. As shown in Fig. 2.12, infill walls are usually connected to the boundary frame elements by mechanical connectors or by epoxy grouted bars. The reinforced concrete infill is usually made of cast in place concrete or shotcrete. In both procedures a serious quality control problem may arise—a gap between
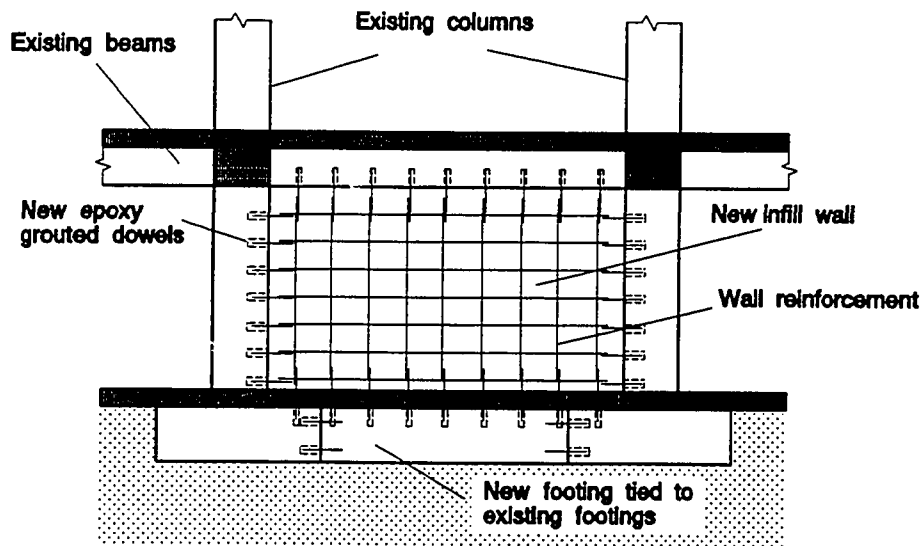
Figure 2.12 Strengthening of an existing concrete frame building with a reinforced concrete infill panel. (Adopted from Ref. 62)

the infill and the top floor beam [46, 64].

As discussed earlier, columns of existing frames typically have short lap splices which are likely to be inadequate to develop yielding in tension. In an infill wall scheme, existing columns act as boundary elements of the infill and therefore columns are subjected to large compressive and axial forces. Consequently, and as shown by previous studies [64], the benefits of adding an infill wall will be limited by the premature failure of column splices in tension, unless existing columns are strengthened as well.

In addition to providing infill panels, existing columns can be provided with a reinforced concrete jacket to prevent column splice failure and to allow columns to effectively act as boundary elements for the new wall (see Fig. 2.13). The advantage of the latter technique is that the infill panel and the reinforced concrete jacket are cast as one unit, thus minimizing the shear transfer problems between the panel and the frame members.

The behavior of infill panels and structural walls in an existing frame have been studied experimentally [46, 64]. In these studies a large-scale, single-story, one-bay reinforced concrete frame was strengthened using first an infill panel, similar to the scheme shown in
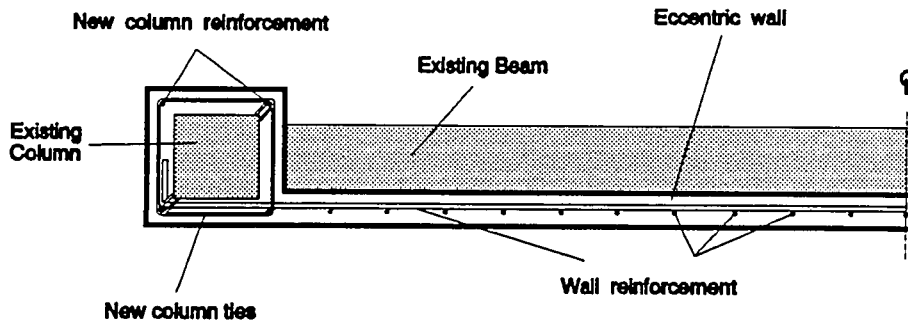
Figure 2.13 Strengthening of an existing building frame with an eccentric wall and reinforced concrete jacket of columns.

Fig. 2.12. The second scheme consisted of an eccentric wall connected to the existing frame by a concrete jacket around the existing columns similar to the scheme shown in Fig. 2.13. Both specimens were tested under reversed cyclic loading to failure. In Fig. 2.14, the lateral load and drift envelopes for the two specimens are compared. It can be seen that the eccentric wall showed higher initial stiffness and ultimate strength than the infill wall. Furthermore, column splice failure was prevented by the reinforced concrete jacket in the eccentric wall scheme. Flexural reinforcement in existing frame columns developed strains well beyond yielding with no signs of splice failure. In contrast, the capacity of the infill wall specimen was limited by failure of column splices in boundary elements. A comparison of the hysteretic behavior of the specimens revealed that the energy absorption capacity of the eccentric wall was significantly higher than that of the infill panel. Also, the transfer of shear from the existing frame to the eccentric wall was achieved with virtually no slip between surfaces[46].

Overall, the structural wall technique has proved to be more efficient and more effective than the addition of infill panels only, although the technique is clearly more expensive. If properly detailed, the addition of infill panels or new structural walls can substantially increase the lateral stiffness, strength and ductility of an existing building. Depending on the size and number of walls provided in the building, the behavior of the original moment frame structure can be changed to wall-frame system. Since the added wall(s) are much stiffer and stronger than the existing frame, the behavior of the retrofitted will generally be controlled by the structural wall(s).
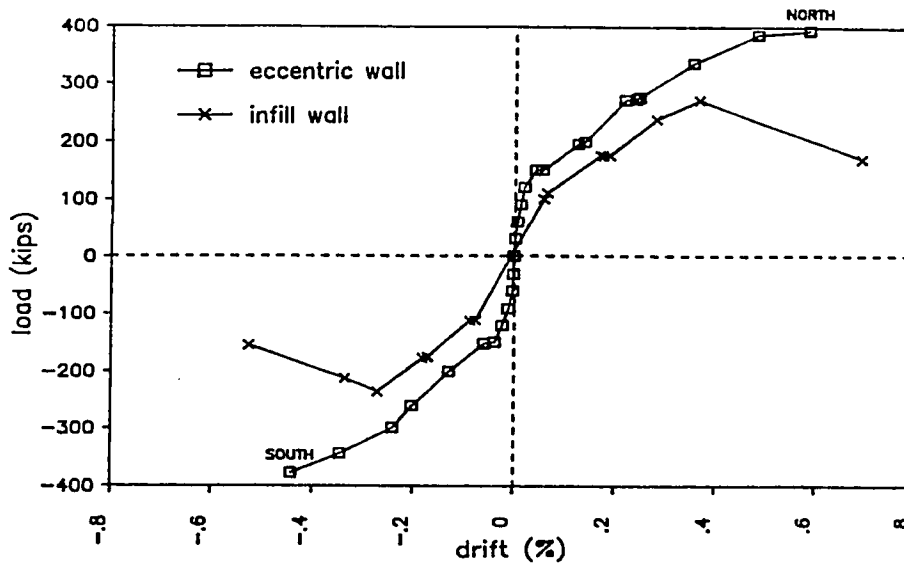
Figure 2.14 Comparison of lateral load and drift envelopes for a concrete frame strengthened with an infill panel and with an eccentric wall (Ref. 46).

Because walls are much stiffer than the frame elements they attract most of the lateral loads imposed on the building, and therefore the addition of walls to a frame structure will normally require extensive modifications to existing foundations. Modifications to foundations may require intensive labor, particularly if the quality of the foundation soil is poor. For these reasons, even though structural walls could be designed to provide a suitable retrofit scheme, they often result in an expensive solution.

2.4.3.3 Addition of Wing Walls

This technique combines the concepts of reinforced concrete jacketing and infill wall schemes. It consists of increasing the lateral strength of the structure by adding *wing walls* of reinforced concrete to the sides of existing columns, as shown in Fig. 2.15. The technique is most suitable for structures in which a strong-beam weak-column failure mechanism is anticipated. By increasing the size of existing columns, the column flexural and shear strengths are increased. Thus, failure is shifted to the beams, which results in a weak-beam strong-column mechanism of failure. The wing walls may be either precast or

Existing frame　　　　　New Wing Walls

New Wing Walls of Reinforced Concrete

Existing columns　　　　Existing beams
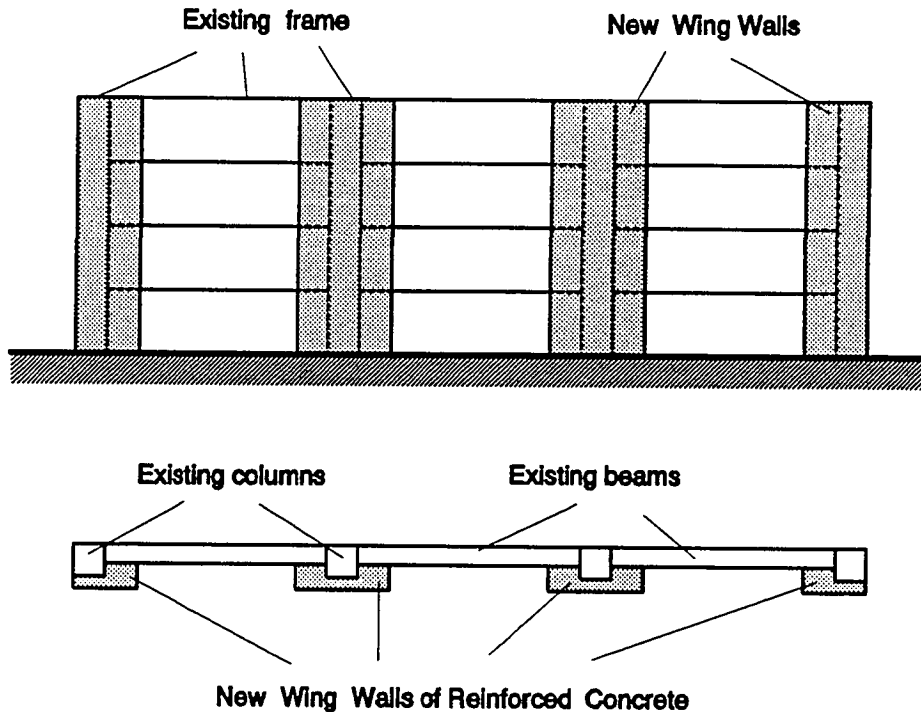
Figure 2.15　Strengthening of a concrete frame using wing walls.

cast in place panels. The connections between the panel and the existing frame members can be accomplished using wedge or adhesive anchors. Such connections pose problems similar to those encountered for the shear transfer in infill walls.

The behavior of the wing wall technique has been studied experimentally to strengthen a prototype moment frame with deep spandrel beams and short columns, similar to the one shown in Fig. 2.15. Details of the experimental program can be found in Ref. 51. The test specimen was subjected to several cycles of lateral load to different drift levels. Test results indicated that the addition of wing walls significantly increased the lateral stiffness and resistance of the existing structure, but most importantly, it changed the mode of failure of the structure from a "weak-column shear failure mechanism" to a weak-beam strong-column flexural mode of failure. Hysteresis loops of the strengthened structure were stable up to drifts of 1% with relatively minor degradation of strength.

The wing wall technique offers an alternative retrofit scheme for those cases in which a reinforced concrete jacketing scheme is insufficient to satisfy the demands of the retrofit, but at the same time the addition of infill walls or structural walls is either not possible or uneconomical. Similar to reinforced concrete jacketing, the wing wall scheme requires intensive labor during construction. In addition, because the size of columns is significantly increased to the size of a concrete pier, the scheme will likely require modifications to existing foundations.

2.4.3.4 Steel Bracing Systems

Steel braces have been extensively used in the design of steel frames to help carry lateral forces and to limit lateral drifts of buildings. The fact that bracing systems can be designed to improve the lateral resistance of building frames led to the concept of using steel bracing systems as possible retrofit schemes for existing reinforced concrete frames. One of the main advantages of the bracing system is the wide range of possible bracing configurations that can be selected to meet different levels of performance. Depending of the original layout of the building, the number of braced bays, configuration and/or brace size can be designed to satisfy different levels of lateral strength and/or stiffness. A disadvantage of the bracing system is that braces will introduce axial forces in existing column and beam members. Compressive forces are, in general, welcome in beams, and depending on the level of axial forces from gravity loads they can also benefit the behavior of columns. However, axial tensile forces are undesirable in both beams and columns. Should tension forces develop as a consequence of the bracing scheme, existing members will most likely have to be strengthened to carry these forces.

The behavior of steel braces under cyclic loading have been studied extensively in the past. In Fig. 2.16, the hysteretic behavior of steel braces is compared qualitatively in terms of the energy dissipation capabilities as a function of the effective slenderness ratio, KL/r. If the slenderness ratio of the brace is very low ($KL/r < 40$), the brace yields in tension and compression, and the energy dissipation capability reaches a maximum. As the slenderness ratio increases ($120 < KL/r < 40$), the brace buckles in compression and the energy dissipation capabilities are reduced. Braces with very high slenderness ratios ($KL/r > 120$) have almost negligible buckling strength, which reduces the energy dissipation capacity of the brace even further, as shown in Fig. 2.16. Ideally, braces should be
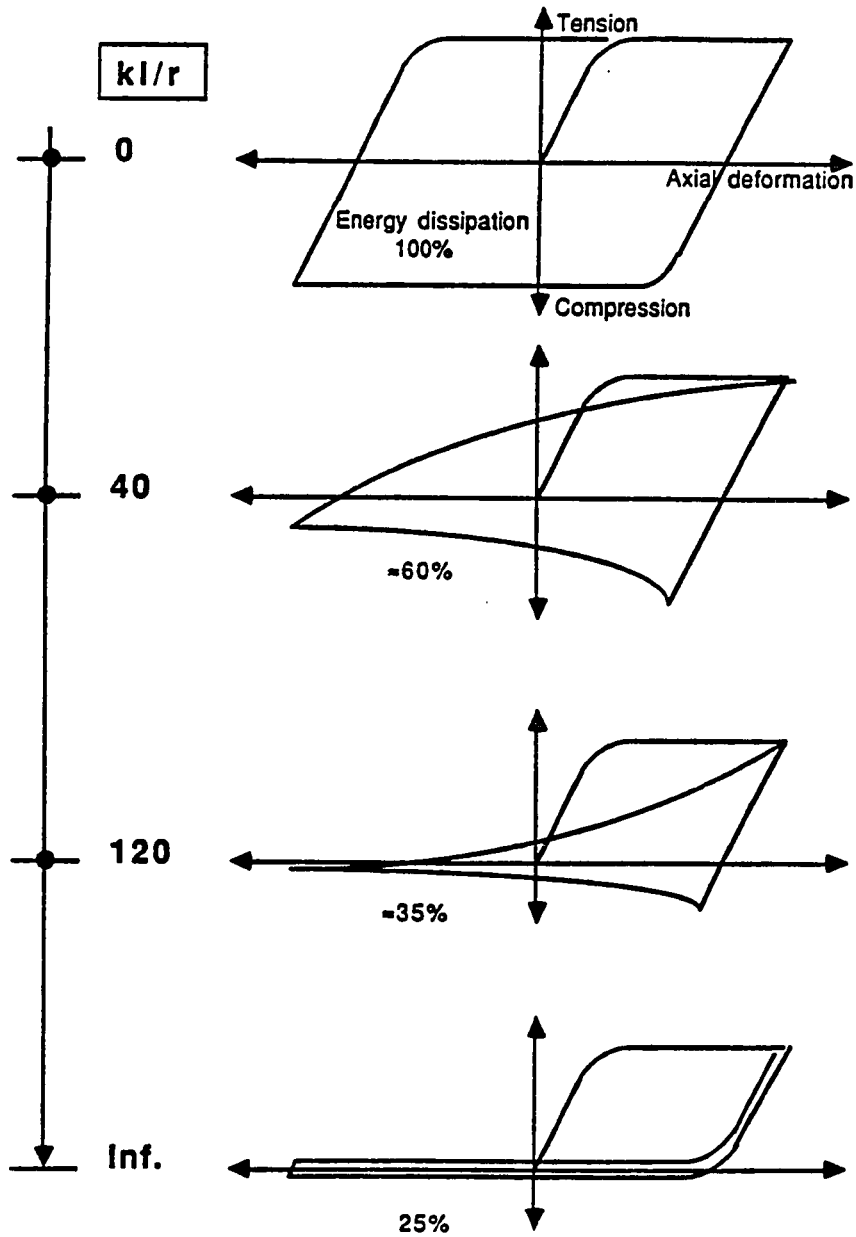
Figure 2.16 Comparison of hysteretic behavior for steel braces with different slenderness ratios (Ref. 25)

designed to have the smallest possible unbraced length (slenderness ratio) for maximum energy dissipation. In practice, however, it is seldom possible to design braces short enough to prevent buckling completely. In addition, the design of braces to yield in compression would, in general, call for heavy sections which would make bracing an expensive solution. In this study, two different types of braces are considered as possible retrofit schemes, and are classified according to their behavior under reversed cycling loadings. Braces with medium slenderness ratios (50 < KL/r < 120) and braces with very high slenderness ratios (KL/r > 120) will be studied.

a) *Medium Slenderness Ratio Bracing Systems (50 < KL/r < 120)*

The performance of frames with medium slenderness ratio braces can be defined by two systems: concentrically braced frames (CBF) and eccentrically braced frames (EBF). The latter bracing system has shown very favorable seismic behavior in new construction and may represent an attractive alternative for the retrofit of existing concrete frames. The behavior of eccentric bracing in existing reinforced concrete frames is not included in this study, but it is currently under investigation in a parallel study. Depending on the

Diagonal Bracing   X - Bracing

K - Bracing   V - Bracing   Chevron
or Inverted V - Bracing
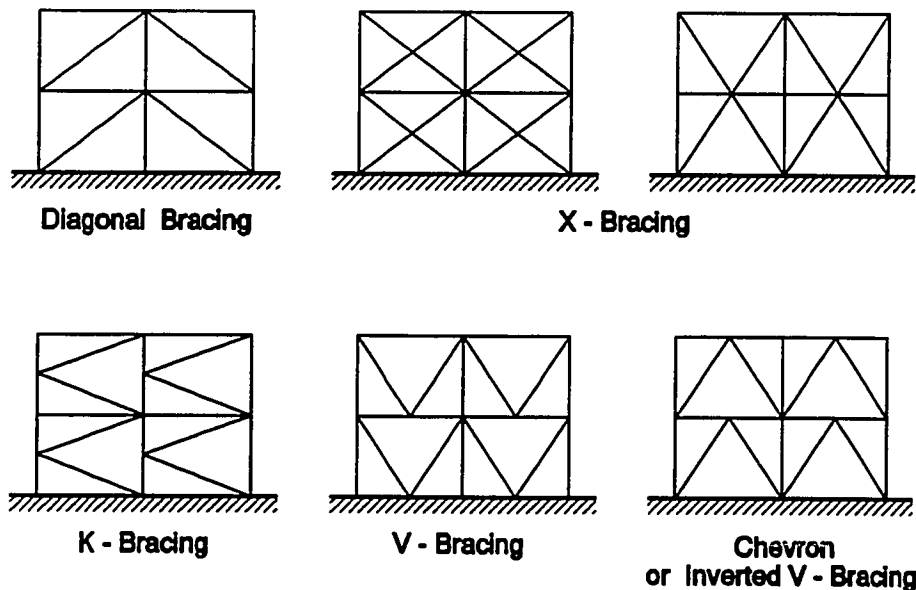
Figure 2.17 Typical configurations for concentric bracing systems.

configuration pattern, concentric bracing systems may consist of Diagonal bracing, X-bracing, K-bracing, V-bracing, Chevron or inverted V-bracing, as shown in Fig. 2.17. Due to special problems when one of the braces buckles, K-bracing and V-bracing, are not recommended for improving the seismic resistance of building frames [45]. In fact, K- bracing is prohibited in zones of high seismic risk in the Seismic Provisions for Structural Steel Buildings - Load and Resistance Factor Design [45]. V-bracing is not prohibited, but the required design strength of V-brace members should be at least 20% larger than would be required for other concentric bracing systems, thus discouraging the use of such configurations in seismic zones. Consequently, diagonal bracing or X-bracing are the only concentric bracing systems that appear to be viable solutions for the retrofit of reinforced concrete frames.

X-bracing can significantly increase the lateral stiffness and strength of existing frames. However, the addition of the bracing system can induce high axial forces in beams and columns which may cause a premature failure in tension or compression of these members. To prevent such failure, steel jacketing could be provided to augment the axial load carrying capacity of columns and beams. The use of X-bracing has become popular for the retrofit of reinforced concrete frames and has been used in Japan, Mexico [25] and lately in the U.S [52].

In 1987, Bush [51] conducted an experimental study on the behavior of X-bracing as a retrofit scheme for a reinforced concrete frame. The test specimen consisted of a prototype reinforced concrete frame with deep spandrels and short columns, as shown in Fig. 2.18. Braces consisted of modified wide-flange sections of 36 ksi yield strength. In addition to the brace members, steel collectors (structural tees and steel channels) were provided around beams and columns to help transfer the brace forces to the existing reinforced concrete frame (see Fig. 2.18). The collector members were attached to beams and columns with anchor bolts embedded in the frame members. All connections between steel braces and collector elements were welded to produce a fixed-fixed end restraint condition for the braces. The effective slenderness ratio of braces was estimated to be 70, and therefore inelastic buckling of braces was anticipated. The braced frame was tested under reversed cyclic lateral loading to failure.
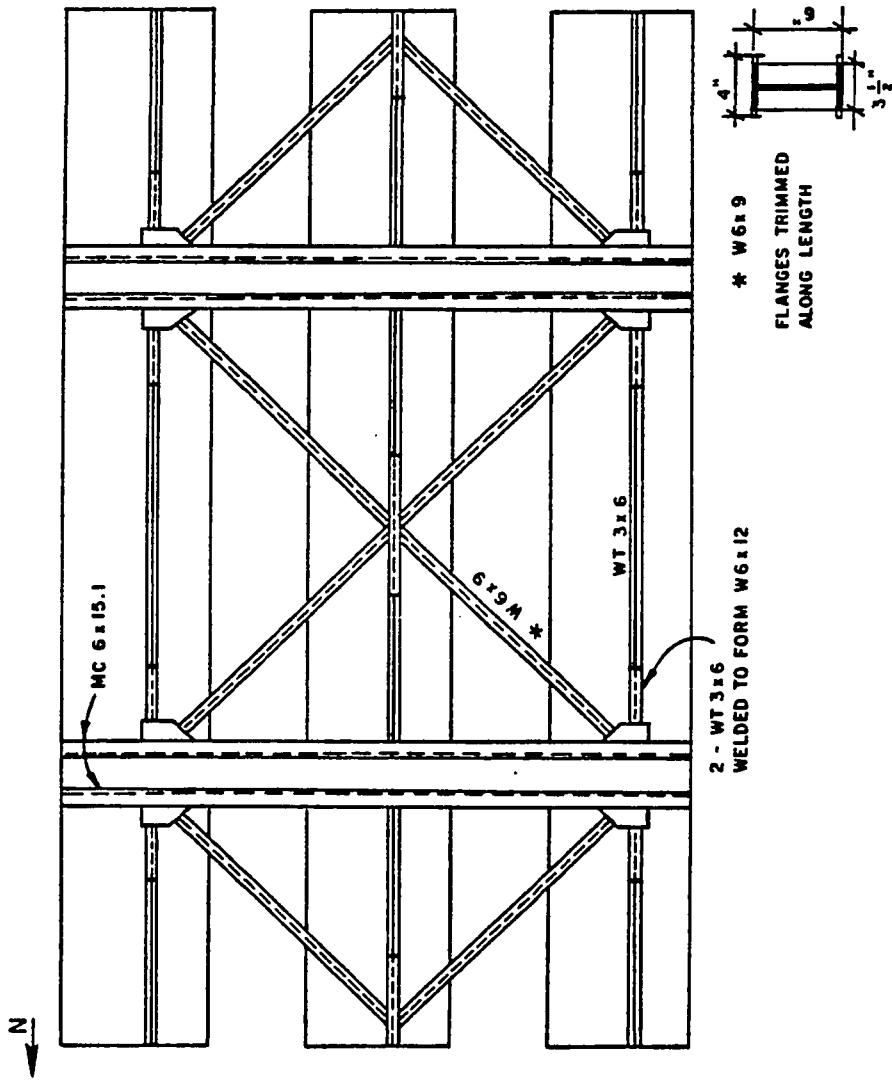
Figure 2.18   Prototype reinforced concrete frame specimen strengthened with X-bracing steel sections (Ref. 51).

Test results indicated that the bracing system significantly increased the lateral stiffness and strength (about six times stronger) of the existing frame. During the test, second story braces reached yielding and buckled after several load reversals. However, the ultimate load of the braced frame was reached when one of the welded connections suddenly failed. The sudden loss of the brace resulted in a load redistribution in which second story columns were overloaded and failed in shear. The high local deformations generated by alternate yielding and buckling of braces led to the premature failure of the welded connection. Thus, while the bracing scheme significantly increased the lateral load capacity of the frame, the strength and, more importantly, the ductility of the braced frame was limited by the quality of the welded connections.

In a companion study, Badoux [25] conducted a parametric study on a *subassemblage* structure (single-degree-of-freedom-system) representative of a reinforced concrete frame strengthened with steel braces. The main objective of the study was to investigate analytically the behavior of the steel-braced reinforced concrete frame under static cyclic lateral loading. The results of the study indicated that the major advantage of the bracing retrofit scheme was its ability to increase the strength and stiffness of the braced structure. However, unless inelastic buckling was prevented, the ductility of the braced frame was considered unreliable and such systems should be used with caution. The latter conclusion added to the substandard performance of the welded connections found in Bush's tests led, in part, to the idea that inelastic buckling of braces should be avoided in order for the steel bracing system to be suitable as a retrofit technique. Badoux suggested that steel braces should be designed with either very low or very high slenderness ratios. If the slenderness ratio is very low ($KL/r << 50$), braces would yield instead of buckling in compression, and inelastic buckling would be prevented. The hysteretic behavior of low slenderness ratio braces is optimum, and would, at least in theory, provide the structure with good energy absorption capacity. On the other hand, if the slenderness ratio is very high ($KL/r > 120$), such as in cables, braces would buckle elastically and inelastic buckling would be prevented.

b) *High Slenderness Ratio Bracing Systems (KL/r < 120)*

The use of bracing systems with high slenderness ratio braces have been discouraged in zones of high seismic risk because of their low energy dissipation

capabilities. As illustrated in Fig. 2.16, the compression strength of a brace with high slenderness ratio is negligible in comparison to the yielding capacity in tension. Consequently, a bracing system consisting of only high slenderness ratio braces resist lateral forces almost exclusively through the braces in tension and thus, it is normally referred to as *tension-only* bracing system. Under reversed cyclic loading, the concern of *tension-only* bracing systems is that during the first yield cycle, braces in tension stretch and become slack when the loading is removed. When tension is applied in following cycles the loading may be applied abruptly and may cause premature fracture of the brace. A further concern is that, if there are only a few braced bays, the building lacks redundancy.

The drawbacks of *tension-only* bracing systems can be overcome if braces are designed to behave elastically. An elastic design approach would probably require the braces to resist large axial forces and would call for large brace sizes, if regular steel were used. However, with the current availability of high strength materials such as steel strands or alloy steel rods, braces can be designed for high forces with relatively small amounts of material. In addition braces could be initially prestressed to increase the initial lateral stiffness of the frame. The bracing system consisting of initially prestressed high slenderness ratio braces will be referred to hereafter as a *Post-Tensioned Bracing System*. Depending of the level of initial prestress, initial brace prestressing will allow braces to yield in tension without becoming slack upon removal of the load. In addition, the initial brace prestress could help delay, if not prevent, the braces which shorten to become slack under lateral loads. Thus, initial brace prestressing would eliminate, or at least significantly reduce the problems associated with the sudden loading on the braces as described above. If braces are designed to yield under a major event, the bracing system will provide the building with energy absorbing capacity and the overall response will be reduced. Also, the high strength of the steel strands and steel rods can provide the building with lateral strength very efficiently, making the post-tensioned bracing technique an attractive alternative when lack of strength and stiffness are the main deficiencies of an existing building.

In addition to improving the behavior of the bracing system, initial brace prestressing will induce, in general, axial compressive forces in existing columns and beams which can be beneficial for the flexural and shear behavior of these elements. Whether the forces induced by initial prestressing of braces are beneficial or harmful to the existing members

will depend on many factors, such as bracing configuration, brace size, level of prestress, initial level under gravity loads, etc. These and other aspects of the post-tensioned bracing system will be discussed in detail in Chapter V.

The post-tensioned bracing system has received little attention among the engineering community in the U.S. However, the system has already been used in Mexico City, Mexico, to strengthen low-rise buildings. Fig. 2.19 shows the tendons provided on the exterior of a two-story school building prior to initial prestressing of braces. A typical anchorage for the tendons at the foundation level is presented in Fig. 2.20. As can be seen, the anchorage of the tendons may require modifications to the existing foundations and possibly the design of special connection devices at the points of anchorage to transfer the brace forces to the existing structure.

While the post-tensioned bracing system can be a promising technique to increase the stiffness and strength of existing buildings, there have been only a few studies on the behavior of the system as a retrofit scheme. Miranda et. al [65, 66] conducted an analytical study on the use of post-tensioned steel rods as retrofit of reinforced concrete frames. The study considered typical low-rise school buildings located on the Pacific coast of Mexico and included earthquake records on firm and soft soil sites representative of major events of the Pacific Coast of Mexico. The results showed that the post-tensioned bracing system produced significant increases in the stiffness and strength of the low-rise buildings investigated. The technique was found to be particularly beneficial for soft soil sites where the increase in stiffness and strength usually results in a reduction of the demands imposed by the earthquake on short-period (low-rise) buildings. The results also indicated that the system could also be used for buildings located on medium to hard soils, provided that adequate strength and stiffness was added to the existing building.

Experimental studies on post-tensioned bracing systems have not been reported to date. In 1980, Sugano et. al reported test results on the strengthening of reinforced concrete frames using a tension-only bracing system as one of the retrofit schemes studied. However, the braces used in the study were non-prestressed. The investigation was conducted on a one-third scale, single story reinforced concrete frame which was strengthened with two 28 mm. ($\approx$ 1.1 in.) diameter steel bars for each brace. The yield

Figure 2.19 Post-tensioned bracing of a low-rise building in Mexico City (tendons prior to initial prestressing).
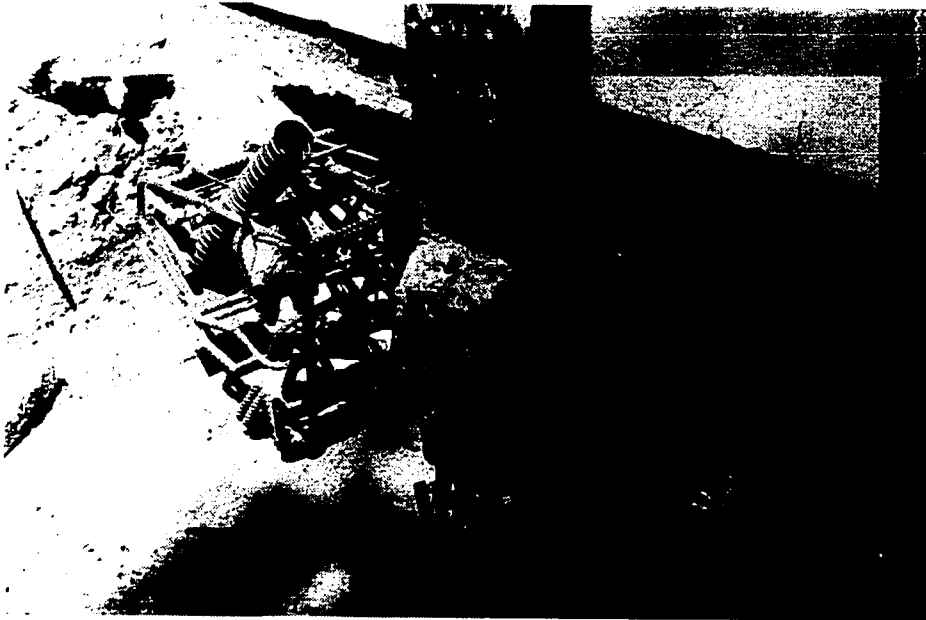
Figure 2.20 Anchorage of tendons at the foundation level.
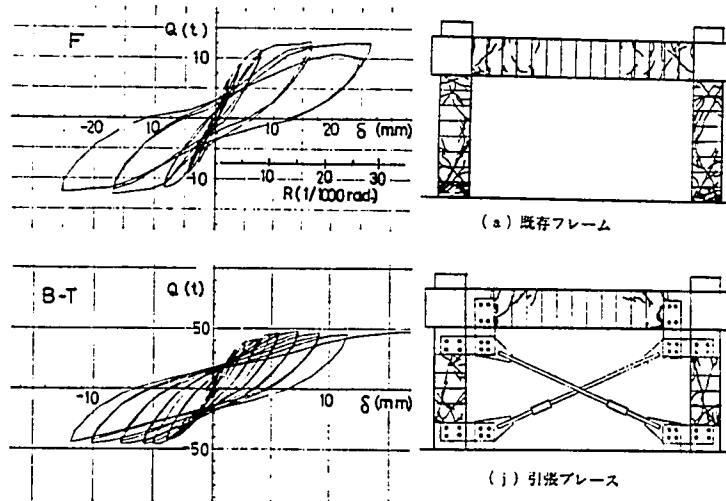
Figure 2.21 Comparison of original bare frame and braced frame with steel rods in Sugano's tests (Ref. 67).

strength of the bars was 3080 kg/cm^2 ($\approx$ 44 ksi). The frame was subjected to several cycles of reversed static loading until failure.

In Fig. 2.21, the behavior of the original bare frame and the braced frame tested by Sugano are compared. The increase in the lateral stiffness and strength of the braced frame is apparent. Unexpectedly, the hysteresis loops of the braced frame were remarkably stable with minor pinching after several load reversals, and even after significant yielding of the braces in tension. As described earlier, in tension-only bracing systems braces are expected stretch and become slack once they yield in tension. The elongated brace then becomes ineffective in tension upon reloading of the structure until the brace is deformed to its new length. Such behavior is expected to produce significant pinching of the hysteresis loops under load reversals. The fact that the original structure exhibited only moderate pinching of the hysteresis loops does not explain the hysteretic behavior of the braced frame. Close examination of the connection details of the braces suggested that braces may have had some resistance in compression and dissipated energy either through inelastic buckling or yielding of the connection in compression, or a combination thereof. The latter behavior would explain in part the hysteretic behavior observed for the braced frame. However, further experimental studies would be required to support or refute the findings of Sugano's

study. In addition, dynamic loading tests would be required to evaluate the effects on the braces and the connection produced by the sudden loading that is likely to occur when braces become slack and are suddenly stressed in tension as described earlier.

2.4.4 Design Strategy for Seismic Retrofit

The selection of the appropriate retrofit scheme for an existing building requires consideration of economical, architectural and structural aspects. Nonetheless, the criterion for determining the adequacy of retrofit schemes has been primarily based on *life-safety*, although the issue of *continuity of operation* has been raised as an equally important criterion for the seismic retrofit of structures [68]. The design strategies for the selection of the adequate retrofit scheme for structures with different combinations of initial strength and ductility have been discussed in detail by Jirsa et al. in previous studies [25, 68]. The present section discusses specific criteria that apply to the building frames considered for study. In the present study, adequacy of the selected retrofit scheme is based exclusively on providing *life-safety* to the occupants. Other criteria to select the appropriate retrofit scheme is ignored. Under the *life-safety* criterion, the retrofit of the building centers primarily on the improvement of the strength and ductility of the existing building.

2.4.4.1 Buildings on Firm Soil Sites

Consider in Fig. 2.22 a typical smoothed response spectra for a single-degree-of-freedom-system (SDOF) on firm soil conditions for different levels of ductility. The response spectra represent the design earthquake for which an existing structure needs to be evaluated. The lateral load and drift relationship for the same structure is presented in Fig. 2.23. The building is assumed to have lateral strength S_o, a ductility capacity μ_o and a fundamental period T_o. For simplicity, the ductility capacity of the building will be defined as the ratio between the maximum allowable deformation and the deformation at yield. The maximum allowable deformation is defined as the maximum drift that the building can tolerate without collapse. Using the response spectra shown in Fig. 2.22, the required strength for the original building with fundamental period T_o and ductility μ_o is C_o. Therefore, the original structure would be considered adequate only if the lateral strength S_o is greater or equal to the required strength, C_o. For the purpose of discussion, it will be

SEISMIC COEFFICIENT

Period Range

short   medium   long

Elastic

μ_0

μ_1

$\mu_0 < \mu_1$

C_0'

C_1

C_0

0   T_{R2} T_{R1} T_0 2   4

FUNDAMENTAL PERIOD (secs)
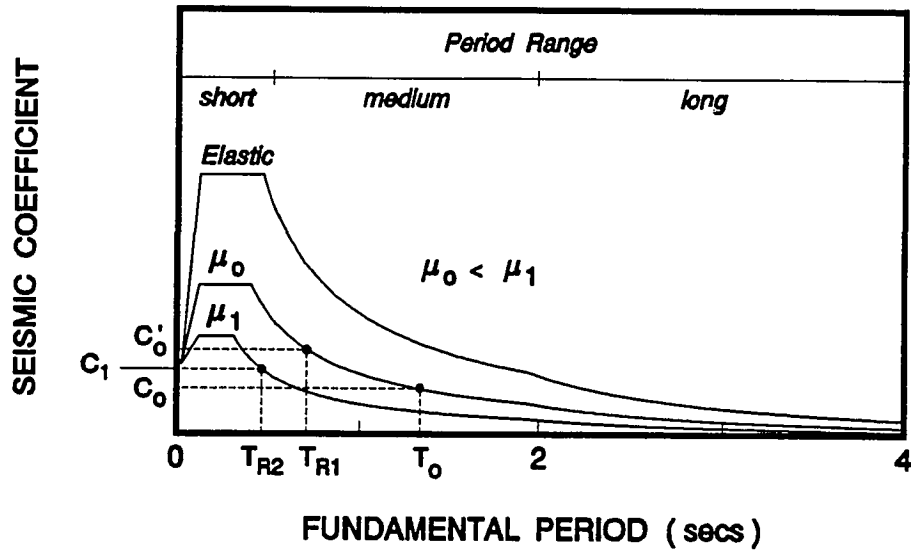
Figure 2.22   Smoothed pseudo-acceleration response spectra for firm soil conditions.

LATERAL STRENGTH

S_{R2} Scheme R_2 $\mu_{R2} = \dfrac{\Delta_u}{\Delta_y^{R2}}$

S_{R1} Scheme R_1 $\mu_{R1} = \mu_0$

S_0 Original $\mu_0 = \dfrac{\Delta_u}{\Delta_y^0}$

Δ_y^{R2} Δ_y^0 Δ_u
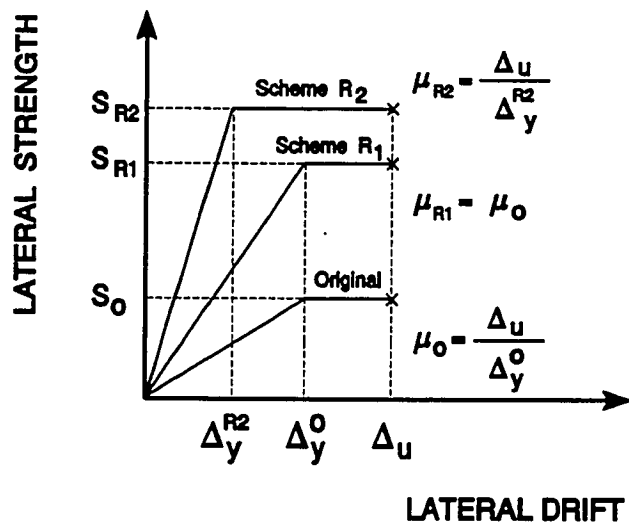
LATERAL DRIFT

Figure 2.23   Lateral strength and drift relationships for original and retrofitted structures.

assumed that the lateral strength of the original structure, S_o, is less than the demands of strength, C_o, and therefore the original building is rendered inadequate.

To improve the behavior of the original building, the structure is strengthened with retrofit scheme, R_1, which provides the existing building with an increased lateral strength. The load and drift relationship for scheme R_1 is indicated in Fig. 2.23. In the following, it is assumed that scheme R_1 has lateral strength S_{R1} equal to the demand C_o required for the original building above. The ductility capacity of scheme R1, μ_{R1}, is assumed to remain the same as that of the original building, i.e. $\mu_{R1} = \mu_o$. As a consequence of the retrofit, the initial stiffness of the building is increased and the fundamental period of the retrofitted building is shortened to T_{R1} (it is assumed that the retrofit does not involve significant modifications to the mass of the building). According to the response spectra of Fig. 2.22, the required strength for the building with retrofit R_1 with period T_{R1} and ductility $\mu_{R1} = \mu_o$ is now C_o', which is greater than the strength of the retrofit building $S_{R1} = C_o$. Thus, even though the retrofit scheme augmented the lateral strength of the existing building, the increases in lateral strength are offset by the increases in the demands of strength due to the shortening in the fundamental period of vibration of the structure.

The behavior described above will be typical of many of the retrofit situations for buildings with a medium to short fundamental periods of vibration located on firm soils. In such cases, the retrofit scheme would be adequate only if the increases in lateral strength provided by the retrofit scheme are larger than the increases in the demands of strength as indicated above. Clearly, a retrofit scheme which provides an increase in both lateral strength and the ductility capacity of the building will have a better chance of being a successful scheme. Such is the case of retrofit scheme R_2, which has lateral strength S_{R2} and a ductility capacity μ_{R2}, as shown in Fig. 2.23. For the purpose of discussion, the ductility capacity μ_{R2} will be assumed to be equal to μ_1. The fundamental period of scheme R_2 is T_{R2}, and is shorter than that of retrofit scheme R_1. As shown in Fig. 2.22, because of the larger ductility of scheme R_2, the required strength for scheme R_2 with fundamental period T_{R2} is C_1, which is smaller than the strength C_o' required for scheme R_1 above. Retrofit scheme R_2 need only satisfy strength demands C_1, and will be adequate as long as the lateral strength S_{R2} is greater or equal to C_1.

For building with longer periods of vibration (tall frame buildings) the design strategies may be somewhat different than those described above. Consider in Fig. 2.24, the displacement response spectra derived from the smoothed pseudo-acceleration response spectra for the SDOF system shown in Fig. 2.24. Previous studies [55] have shown that there exists a period range in which the maximum inelastic displacement is approximately the same as the elastic displacement, regardless of the lateral strength of the system. However, the system must have enough ductility to achieve the maximum inelastic displacement. Such a period range corresponds in practice to buildings with relative long periods of vibration and it is represented by the horizontal line of the displacement response spectrum shown in Fig. 2.24. Notice in Fig. 2.22 that in the long period range the demands of strength show little variation for different ductilities. In the medium to short period range, displacements are reduced with a shortening in the period of vibration of the building. Also, for buildings with short periods of vibration, maximum inelastic displacements increase with increasing ductility of the system.
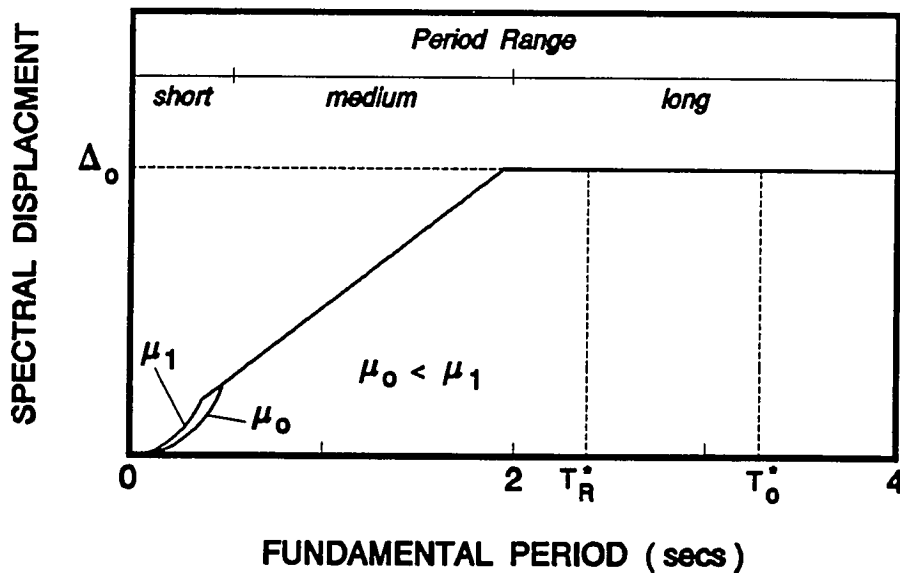
Figure 2.24 Smoothed displacement response spectra for firm soil conditions.

Consider in Fig. 2.24, an existing building of fundamental period T_0^* and a possible retrofit scheme with fundamental period T_R^*. As shown in Fig. 2.24, the maximum displacements for the original and retrofitted structures would be the same, even though the retrofit scheme may significantly increase the strength and ductility of the system. Assuming that damage and displacements (drift) are interrelated, the fact that inelastic and elastic displacements are the same for the long period range indicates that stiffness (fundamental period) of the retrofit scheme would control damage to the structure, while increases in strength could be relatively unimportant. The observations presented above suggest that for long period structures the retrofit strategy should be oriented towards increasing stiffness of the existing building rather than increasing its strength, which in some cases may require significant changes in the structural system of the building.

2.4.4.2 Buildings on Soft Soil Sites

Consider in Fig. 2.25 a smoothed design spectra for SDOF system on soft soil conditions similar to those found in the clay deposits of Mexico City [44]. Under these conditions, maximum demands of strength occur for structures in the medium to long period range. Consider the same original and retrofit schemes described in Fig. 2.23. Unlike the observations made for the buildings on firm soils, an increase in lateral stiffness of the existing structure (period shortening), results in a decrease on the demands of strength. Thus, both retrofit schemes, R_1 and R_2, are likely to perform adequately under the design earthquake. However, it must be remembered that inelastic behavior causes the period of vibration of the building to elongate during the response. Thus, for buildings with schemes R_1 and R_2 the elongation in the period of vibration will result in an increase in strength and displacement demands. If lateral deformations are not limited during inelastic response, the building may go into resonance and perform inadequately despite the retrofit.

For buildings in the long period range, the design strategies are expected to be similar to those anticipated for buildings with medium periods of vibration on firm soil conditions discussed above. Because long period structures (T_0^* and T_R^*) are located to the right of the maximum response of the system, an increase in lateral stiffness will result in an increase in strength demands, as shown in Fig. 2.25.
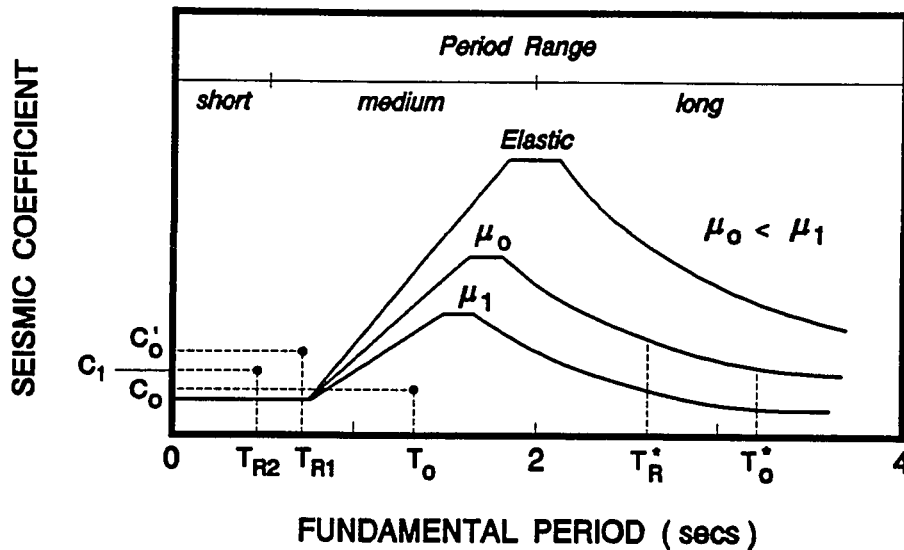
Figure 2.25 Smoothed pseudo-acceleration response spectra for soft soil conditions.

scheme that Is adequate for firm soil conditions may be Inadequate under soft soils and vice-versa.

The design principles presented above are based on the behavior of SDOF systems and should be Interpreted as a tool to estimate the overall behavior that can be expected for buildings. The dynamic response of multi-story buildings Includes many different aspects such as higher modes of vibration, variations of stiffness and strength with height, etc, that are difficult to represent with SDOF systems alone, particularly if inelastic response occurs. The present study Is aimed at providing new Information on the seismic retrofit by examining analytically the inelastic dynamic response of several possible retrofit techniques for frames of reinforced concrete. As discussed earlier In Chapter I, the study focusses on the behavior of post-tensioned bracing systems, but also Includes the performance of X-bracing systems and the addition of structural walls.

CHAPTER III

BUILDING MODELING TECHNIQUES

3.1 GENERAL

In this chapter, the analytical models used to idealize the inelastic behavior of the reinforced concrete members and steel braces of the buildings selected for study are presented. The hysteretic behavior of such members is examined, and, main properties and parameters used in the inelastic models are presented. Also, basic assumptions involved in the modeling of the building structures are discussed. The effects of foundation materials on building response are briefly introduced and the procedure adopted to include soil-structure interaction effects is described.

Current modeling techniques of the inelastic behavior of members may vary from refined non-linear finite element analyses to more discrete models that involve the use of the so called *non-linear beam* elements in which inelastic behavior is assumed to be concentrated at specific locations in the member. Ideally, inelastic models should be developed using basic material behavior (stress-strain relationships) combined with mechanics principles to predict the behavior of any structural member subjected to any loading condition. One such ideal model is the fiber or layer-by-layer technique, which can be used to predict with accuracy the inelastic behavior of members, particularly under static loading conditions. However, the application of this technique (or finite elements) for the dynamic analysis of structures demands significant computational effort and becomes particularly inefficient for the analysis of multi-story structures under earthquake loading. In addition, for moment resisting frame structures, inelastic behavior is, in general, concentrated at the column (beam) ends, which makes the use of *non-linear beam* elements an attractive modeling technique. Consequently, significant research effort has been devoted to the development of these simplified models which are based primarily on numerous experimental observations[48]. Because of the ease of use, the simplified modeling technique was selected for the analyses conducted in the present study.

48

3.2 COMPUTER PROGRAM

Analysis of the structures considered in this study was carried out using a modified version of the **DRAIN - 2D** computer program [18], originally developed at the University of California, Berkeley. The program consists of a *'base'* subroutine (which essentially determines the displacement response of the structure) and a series of *element subroutines* that are intended to idealize the behavior of different types of structural members (reinforced concrete, steel beam-columns, braces, etc). Three element subroutines were used to model the behavior of the structural members required by the present study, namely: reinforced concrete beams, columns, and structural walls, and steel braces. The main features, background information and the modifications that were introduced to these subroutines to idealize the behavior of these members are presented in detail in the following sections.

The main assumptions considered in the analytical models include the following:

a) The buildings are idealized as a series of planar frames connected at each floor level with a rigid diaphragm.

b) Masses are assumed to be lumped at the nodes of the elements at each floor level.

c) Elastic axial deformations of column and wall members are included in the analyses.

d) Elastic shear deformations of beams, columns and walls are included.

e) The joint region of beams is assumed infinitely rigid.

f) The effects of gravity loads and initial prestressing on the elements are considered as initial member end actions. Any end forces due to dynamic loading are simply added to these initial forces.

g) Torsional response of the building is neglected.

h) Earthquake excitation is defined only in the horizontal direction and all support points are assumed to move in phase.

i) Secondary moments due to P - Δ effects are neglected in the analyses.

3.2.1 Algorithm of Solution and Integration Interval

The dynamic equilibrium equations of a multi-degree-of-freedom, MDOF, system subjected to a ground acceleration can be written in its incremental form as:

$$[M] \{\Delta \ddot{u}_r\} + [C_T] \{\Delta \dot{u}_r\} + [K_T] \{\Delta u_r\} = -[M] \{ \Delta \ddot{u}_g \} \tag{3.1}$$

in which $[M]$ is the mass matrix and $[C_T]$, $[K_T]$ are the *tangent* values of the damping and stiffness matrices of the structure in its current state. The vectors $\{ \Delta \ddot{u}_r \}$, $\{ \Delta \dot{u}_r \}$, $\{ \Delta u_r \}$ are finite increments of the acceleration, velocity and displacement, respectively, relative to the ground. The vector $\{ \Delta \ddot{u}_g \}$ represents finite increments of ground acceleration, in which terms appear only for the horizontal translation components of the acceleration.

To solve Eq. 3.1, the constant acceleration method [18,19] was adopted in the program. The accuracy of the constant acceleration method, as in any step-by-step integration procedure, depends largely upon the time integration interval. Although the DRAIN -2D program includes some provisions to avoid the systematic accumulation of errors within each time step (equilibrium unbalance due to changes in the yield status of the structural elements), an adequate time step is essential for the accuracy of the calculated response of the structure. Clearly, greater accuracy can be expected as the integration time step is reduced. On the other hand, it is important to select as long a time step as possible in order to minimize the computational effort. To determine an appropriate time step, several trial analyses were conducted on the building structures with different time integration steps: 0.02, 0.01, 0.005 and 0.001 seconds. A comparison of the response of the building using these time steps revealed that time steps of 0.02 and 0.01 seconds resulted in a significant accumulation of errors. However, the response of the structure showed no appreciable difference when integration time steps of 0.005 and 0.001 seconds were used. Based on these results, it was concluded that an integration interval of 0.005 seconds yielded sufficiently accurate results and it was therefore used for all subsequent dynamic analyses of the buildings.

3.2.2 Viscous Damping

Damping Coefficients

Damping of the structure is considered in the analyses through the damping matrix $[C_T]$, (See Eq. 3.1), that represents the amount of viscous damping present in the structure. In this study, it is assumed that the viscous damping matrix $[C_T]$ is a linear combination of the mass and stiffness matrices (Rayleigh damping), as follows:

$$[C_T] = \alpha [M] + \beta [K_T] \tag{3.2}$$

in which α and β are coefficients to be specified for the desired amount of critical damping. Note in Eq. 3.2 that the stiffness matrix will change every time the stiffness of a structural element varies, and the damping matrix will be updated accordingly. If the system is assumed to be uncoupled into normal modes, the amount of critical damping can be specified at two different periods of vibration through the following relationships:

$$\alpha = \frac{4\pi \ (T_j \xi_j - T_i \xi_i)}{T_j^2 - T_i^2} \tag{3.3a}$$

$$\beta = \frac{T_i T_j \ (T_j \xi_i - T_i \xi_j)}{\pi (T_j^2 - T_i^2)} \tag{3.3b}$$

in which T_i and T_j are the periods for two selected modes of vibration of the structure, and ξ_i and ξ_j are the damping ratios to be specified for the selected two modes. Typically, T_i and T_j are selected as the first two modes of vibration of the structure, which largely dominate the dynamic response of building structures.

Figure 3.1 shows the relationship between the damping ratio and period of vibration that is obtained using Eqs. 3.3a and 3.3b. Note that ξ_1 and ξ_2 can be specified to have the same value, in which case the first two modes of vibration will have the same amount of damping. The procedure described above will in general yield sufficiently accurate results for the *elastic* analysis of building structures. In such analysis, the stiffness matrix remains

unchanged and the specified amount of damping remains the same during the entire response of the structure. In an inelastic analysis, however, the yielding and stiffness degradation of structural elements will increase the flexibility of the structure. Consequently, the fundamental period of the structure will increase with increasing inelastic behavior, and so will the damping ratio associated with the fundamental mode of vibration (See Fig. 3.1). The increase in damping will depend on the amount of inelastic behavior undergone by the structure and on the particular relationship between the damping coefficients α, β and the periods of vibration of the structure.
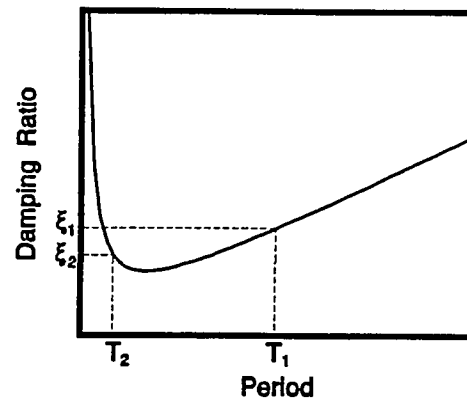
Figure 3.1 Relationship between damping ratio and period of vibration for Rayleigh damping.

To minimize the influence of inelastic behavior on the amount of damping, and ultimately on the overall response of the building, the damping coefficients α, β were determined so that minimum damping was obtained for the fundamental period of vibration of the structure, as shown by the solid line in Fig. 3.2. Clearly, higher modes of vibration of the structure are heavily damped in this case. An additional improvement can be acquired by modifying the damping coefficients so that the resulting curve has a more gradual increase in damping with increasing fundamental period of the structure, as shown by the dotted line in Fig. 3.2. The latter procedure is tedious, time consuming and it does not always yield a better
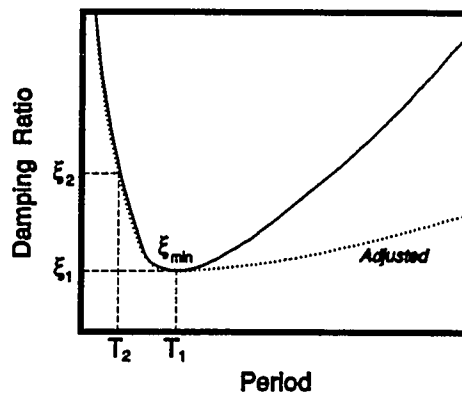
Figure 3.2 Criterion for selecting minimum damping for the fundamental mode of vibration.

relationship without introducing excessively large damping ratios for higher modes of vibration.

Several analyses were conducted on the buildings using the two criteria presented above for determining the damping coefficients; i.e.: First, by directly applying Eqs. 3.3a and 3.3b with $\xi_1 = \xi_2$. Second, by specifying minimum damping ratio for the fundamental period of vibration of the structure, $\xi_1 = \xi_{min}$ (solid line in Fig. 3.2). The target value for the damping ratio was in both cases 2%.

The analyses using the damping coefficients defined above indicated in all cases an increased response when the second criterion was used (i.e. when minimum amount of damping is specified for the fundamental period, $\xi_1 = \xi_{min}$). The adjustment introduced to the relationship (dotted line in Fig. 3.2) showed, in general, little effect on the response of the structures. On the basis of these results and on the simplicity of the method, damping coefficients were specified using the second criterion described above; ξ_{min} for the fundamental period of the structure. In addition, the latter procedure yields results that are conservative.

Damping Values for Building Structures

Viscous-damping is probably one of the most important parameters in the dynamic response of structural systems. While the many sources of damping have been identified qualitatively, recommended values for viscous damping to be used in dynamic analyses to mimic observed response abound. It is important to realize that many of the suggested values are intended for the *elastic* analyses of structures. In such cases, sources other than pure viscous-damping, such as hysteretic damping, are introduced as an "equivalent" viscous-damping, which result in larger amounts of viscous-damping than those really associated with material viscosity[20]. While the validity of this simplification is debatable, hysteretic damping is already accounted for in the present study through the inelastic response of structural members.

Recommended values of viscous-damping for reinforced concrete structures vary from 2 to 10 % depending on the level of deformation and strain induced in the structure. Previous studies[21,22] have measured damping values as low as 2% in low amplitude tests and as high as 11% in structures subjected to extensive inelastic behavior. Based on these

results and assuming that viscous-damping is the main source of damping in low amplitude tests, a value of 2% of viscous-damping was adopted for the analyses of the present study. This value will in general yield conservative results. Note that the 2% value of viscous-damping corresponds to the structure in its fixed-base condition, and it will be subsequently modified to include the effects of soil-structure interaction as discussed in the following sections.

3.2.3 Reinforced Concrete Members - Beams and Columns

Inelastic behavior of beam and column elements was idealized using the *one-component model*, originally presented by Giberson[23]. The element model possess flexural and axial stiffness; however, all inelastic deformations are assumed to be concentrated in plastic hinges at the element ends. Structural members are idealized by a linear elastic sub-element connected to nodes by non-linear rotational springs, as shown in Fig. 3.3. All inelastic deformations are introduced by means of moment - rotation relationships for the non-linear springs, while elastic deformations are considered by the central element.

To model the inelastic behavior of reinforced concrete members under reversed cyclic loading, a modified version of Takeda's model[24] was adopted. The model assumes a bi-linear relationship in which the initial stiffness and strain hardening ratio are determined from monotonic loading conditions for flexural deformations only. Figure 3.4 illustrates some of the main features of the hysteretic laws for the moment- rotation relationship at the element ends obtained with Takeda's model. This model can include stiffness degradation upon load reversals, but it
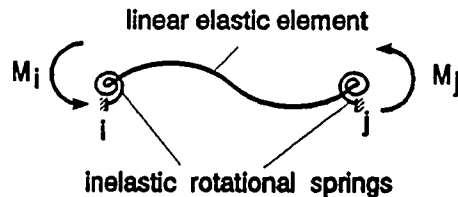
Figure 3.3 One-component model of non-linear element.
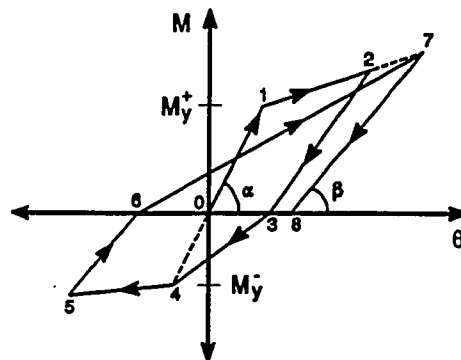
Figure 3.4 Moment - rotation relationship for Takeda's model.

does not include strength degradation of the member. In order to model the failure of members which lack adequate strength and ductility (such as those encountered in older construction), the existing version of Takeda's model was modified to include two specific modes of failure: anchorage failure of flexural reinforcement and shear failure of members.

3.2.3.1 Modeling of Members with Anchorage Failure of Flexural Reinforcement

The modifications introduced to the Takeda's model were intended to represent the failure of the short embedment lengths that are encountered for the bottom flexural reinforcement of beams. At the same time, it was important to be able to use the same model to represent the failure of short lap splices in column members. Typically, these modes of failure are characterized by a sudden loss of the flexural strength of the section after reaching peak moment capacity. To idealize such behavior, an additional segment with a negative slope following peak moment capacity of the member was introduced as part of the moment-rotation envelope. The main features of the moment - rotation envelope and the hysteric laws for the modified model are illustrated in Fig. 3.5. In this figure, M_p represents the maximum (peak) moment capacity of the member and it can be specified to be greater than or smaller than the yielding moment capacity. In the latter case, initiation of inelastic behavior can be specified for the cracking moment, as indicated in Fig. 3.5. Note that a residual moment M_r and rotation θ_r variables have been specified at the end of the descending branch that are used to specify the slope of the segment. Once the residual moment is reached an additional segment with a very small negative slope is defined, mainly to prevent moment reversal with increasing rotation.

Basic hysteresis behavior of the modified model is similar to that of the original Takeda model. However, notice that once the member has reached the peak moment capacity, it never recovers its original strength (segments 1 - 2 and 2 - 3 in Fig. 3.5). Upon unloading and loading in "negative" bending the member follows segments 3 - 4 and 4 - 5. The slope of segment 3 - 4 may be different from that of 0 - 1 to account for stiffness degradation of the member. At point 5, the member reaches its peak moment capacity in "negative" bending and follows segment 5 - 6, whose slope may be different from that of segment 2-3. At point 6, the member reaches its residual moment capacity, and further loading of the member in negative bending results in segment 6 - 7. If the moment is reversed at point 7,
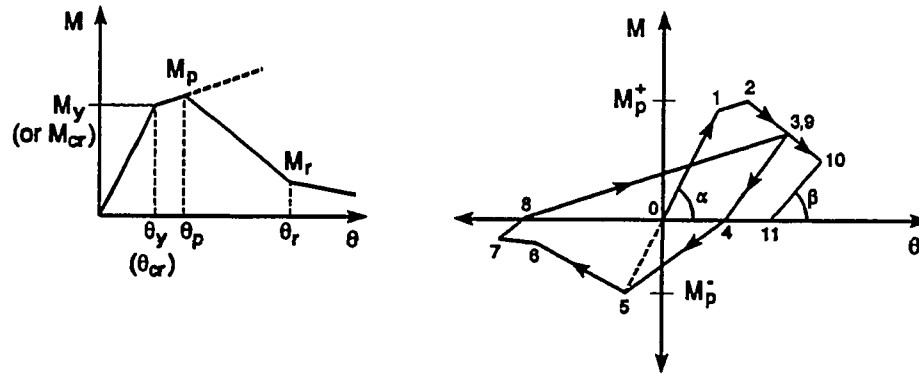
Figure 3.5 Modified moment - rotation envelope and hysteretic laws for reinforced concrete elements.

the member follows segments 7 - 8 and 8 - 9. The bending moment level at point 9 corresponds to that prevailing when the member was unloaded during the previous cycle (point 3). Further loading in "positive" moment and then unloading results in segments 9 - 10 and 10 - 11, respectively.

The model does not include "pinching" of the hysteresis loops which many reinforced concrete members exhibit during large cyclic deformation reversals. However, for members which exhibit limited ductility (such as those found in older construction), "pinching" of the hysteresis loops have been shown to have only minor influence on the response of the building [49]. The effects introduced by the strength degradation of the member are believed to be much more important in the response of the building than those introduced by "pinching" of the loops. Thus, the latter effects were not considered in the present study.

3.2.3.2 Modeling of Members with Failure in Shear

A variety of models have been proposed to emulate the shear failure of reinforced concrete members. One such model considered the shear failure of reinforced concrete members by using an element similar to the one described in the previous section [24]. In this model, shear failure of the member is fictitiously introduced by activating the descending branch of the moment - rotation relationship at both ends of the member when the specified shear capacity is reached. The disadvantages of this technique are that it assumes that the

member is subjected to equal and opposite end moments at all times, but most importantly, it introduces negative stiffness coefficients at both ends of the member. Since shear failure of columns and anchorage failure of reinforcement in beams is anticipated for the buildings under study, the use of such a model will likely result in a negative stiffness coefficient in the diagonal of the stiffness matrix (rotational or translational). This numerical condition cannot be solved with the current solution algorithm of the **DRAIN - 2D** program.

An alternative model that eliminates the problem of introducing negative stiffness coefficients upon shear failure of the member consists in the use of a secant shear modulus, G, which is modified according to previously established hysteretic laws [26]. Nonetheless, to introduce such a model to the program it was essentially required to write an entire new subroutine. While such a model could reasonable represent the strength degradation that follows the shear failure of reinforced concrete members, the derivation and subsequent calibration of such model are beyond the scope of the present study.

Because of the brittle and sudden nature of the shear failure, such failure cannot be allowed in the design of earthquake resistant structures. The purpose of including a shear model for the evaluation of existing structures was aimed at determining the strength of the building and the consequences of the failure of some members in the response of the structure, rather than predicting the behavior of members failing in shear. Therefore, a simpler, more direct approach was adopted.

In deriving a model for shear failure of reinforced concrete members, it was assumed that the member loses its lateral strength completely after reaching peak shear capacity. Such assumption is based on numerous tests of reinforced concrete columns such as the one shown in Fig. 3.6. In this figure, it can be seen that the loss of strength of the member within one load cycle after reaching peak shear strength is about 50%. Strength and stiffness degradation in following cycles is apparent. The shear failure of the members was introduced in the program by removing from the stiffness matrix all stiffness coefficients associated with the lateral strength of the member, leaving only its axial stiffness. The remaining axial capacity of reinforced concrete members after a shear failure has not been fully investigated and needs further experimental evidence. Previous tests on short columns have shown that the axial compression load increases the rate of strength degradation after peak shear capacity [73]. The tests also showed that columns with axial loads of 20% of the
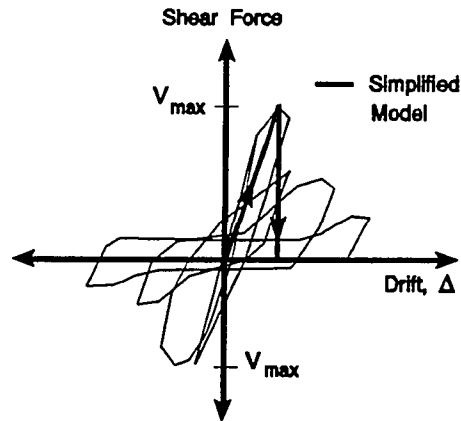
Figure 3.6 Typical hysteretic behavior of shear dominated behavior in short columns (Ref. 73), and simplified model.

ultimate compression capacity were able to sustain lateral drifts of at least twice that at peak shear capacity with no sign of axial failure [25,73]. On the basis of the available data it seemed reasonable to assume that the member would be able to maintain part of its axial stiffness and strength (at least in compression) after reaching peak shear capacity. With this model, the behavior of the element after shear failure is essentially that of a truss element. Figure 3.7 illustrates schematically the modeling of such a failure with the model.

Members failing in shear
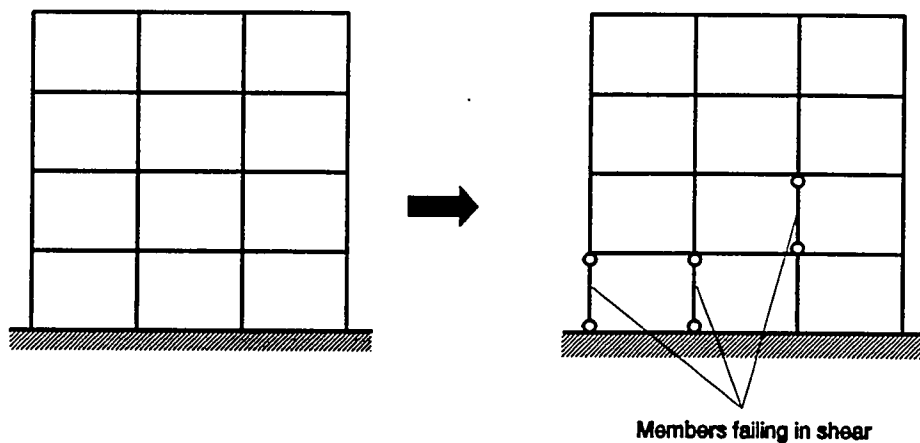
Figure 3.7 Simplified model of reinforced concrete members failing in shear.

To satisfy equilibrium, the forces being resisted by the element prior to failure are transferred to the remaining structure as member end forces in the following time step. Although the model described above does not accurately represent the behavior that follows the shear failure of the member, it is believed that it adequately represents the effects of member shear failure in the response of the structure and the sudden transfer of forces to the rest of the members in the structure.

3.2.3.3 Modeling Parameters and Procedure

Moment - rotation relations are obtained by direct integration of the moment - curvature relationships. In determining these properties, it is assumed that the bending distribution of the member is such that the point of inflection remains fixed at mid-span during the entire loading history. Such distribution approximately corresponds to the elastic moment distribution in frame members under lateral loads. The simplification is introduced in the model to avoid load path dependency of the stiffness coefficients of the rotational springs.

Moment - curvature relationships are computed for critical sections of the members using the program RCCOLA [13]. In this program, the stress - strain relationship proposed by Park and Kent [14] was used to idealize the behavior of concrete. Steel - strain relationship of the reinforcing bars was idealized as shown in Fig. 3.8. In beams, a portion of the slab was assumed as a compression flange to compute the flexural behavior of the member. The effective flange width followed current ACI-318 committee recommendations [4]. The contribution of slab reinforcement was not included in the calculations for the beam capacity in "negative" moment.

To account for the effects of gravity loads on the flexural behavior of columns, moment - curvature relationships were calculated for the axial force level carried by each column as obtained from a gravity load analysis of the building. Axial load in beams was neglected in the calculation of
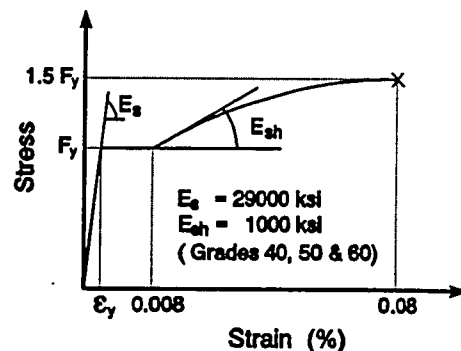
Figure 3.8 Stress - strain relationship for reinforcing bars. Grades 40, 50 and 60.

the moment - curvature relationships in all instances, including the case of braced frames. As indicated earlier, the effects of gravity loads were incorporated in both static and dynamic analyses of the buildings by initializing the member end forces (bending moments and shear forces). The influence of these initial member actions on the response of the members will depend upon the ratio between the gravity induced forces and the "yielding" strength of the member, and it is, in general, more relevant in beams than in columns. The presence of an initial "negative" bending moment in beams will delay moment reversals at the beam ends, but it will cause early yielding of the sections where "negative" moments from gravity loads and earthquake forces add together.

For sections in which yielding is anticipated, the **DRAIN - 2D** program [18] requires that the properties of the non-linear springs at the member ends be based on bi-linear moment - rotation envelope. In the present study, the continuous moment - curvature relationships obtained from the program **RCCOLA** [13] were fit to a bi-linear relation, by defining the yield moment as that causing first yielding of the tension reinforcement. Initial effective flexural stiffness of the member (EI) was obtained directly from the fit bi-linear moment - curvature relationship. However, when the member exhibited different yield moment capacities for "positive" and "negative" bending, the initial stiffness was determined by averaging the initial stiffness of opposite ends (this procedure was based on the assumption that the member is expected to be bent in double curvature). Notice that on the basis of this procedure, reinforced concrete members are assumed to be initially cracked.

To determine the anchorage capacity of reinforcing bars with short embedment lengths or short lap splices, the relationship proposed by Orangun et al. [10] was adopted:

$$f_s = \frac{4 l_{db}}{d_b} \sqrt{f'_c} \left(1.2 + \frac{3 c}{d_b} + \frac{50 d_b}{l_{db}} + \frac{A_{tr} f_{yt}}{500 s d_b} \right) \tag{3.4}$$

in which:

d_b = bar diameter (in)

l_{db} = splice or development length (in)

c = cover parameter (in)

A_{tr} = area of transverse reinforcement resisting splitting (in^2)

s = spacing of transverse reinforcement

f'_c = concrete cylinder strength (psi)

f_{yt} = yield strength of transverse reinforcement (psi)

The above relationship provides an accurate estimate of the maximum stress that can be developed by a reinforcing bar prior to an anchorage failure under monotonic load conditions. However, recent tests have indicated that this relationship still provides accurate estimates under reversed cyclic loading [28]. Using this relationship the maximum moment capacity of sections having an anchorage failure can be estimated. Such moment capacity was assigned as the peak moment capacity of the member to be used in the model described in section 3.2.3.1.

For sections in which pull-out of reinforcement or a splice failure was anticipated, the moment - rotation relationships were based on bi-linear or tri-linear relationships, depending upon whether such failure occurred prior to or after flexural yielding of the sections. Because the failure modes of the members in the buildings considered for study vary considerably, the parameters and procedure adopted to represent member behavior are presented in detail for each of the buildings analyzed in Chapter IV.

Shear capacity of the members was estimated using the provisions of the ACI code[4]. Joint shear capacity was estimated using the recommendations of the ACI-ASCE committee 352 [27].

3.2.4 Reinforced Concrete Members - Structural Walls

As discussed in Chapter II, infill panels can substantially increase the lateral stiffness and strength of existing frame buildings. These infill walls can be effectively anchored to the existing frame structure by using dowels along the wall-frame interface and by providing a reinforced concrete jacket around existing columns. Such construction procedure allows for the composite action between the new infill wall and the existing frame. In this study, full composite behavior is assumed and the addition of infill panels is considered to produce a structural wall (or *shear wall*) in which the boundary elements are the columns of the existing frame. To model the structural wall a wide - column analogy (column with inertia of the wall and rigid beams at each floor level- see Fig. 3.9) is used. Inelastic behavior of wall elements was modelled with the same element used for the beams and columns

described above. However, unlike beam and column elements, walls are expected to deformed in single curvature rather than in double curvature, unless the walls are connected with very rigid and strong beams (coupled walls). To idealize the single curvature behavior of the wall, each wall element is subdivided in short sub-elements within each story level as shown in Fig. 3.9. By using this procedure, the variation of bending moment over the length of any yielding element is small and each sub-element is subjected to nearly a constant moment. Under these assumptions, it is reasonable to assume that the moment - curvature and the moment - rotation relationships are directly proportional. In this study, the number of sub-elements was determined so that the difference in moment between the sub-element ends varied within 10%. Because of the larger gradient of moment at the base of the wall, a larger number of sub-elements was required for the lower stories of the building.

WIDE - COLUMN ANALOGY

Figure 3.9 Wide - Column analogy used to model structural walls.

Wall stiffness and strength typically were varied over the height of the buildings. The addition of structural walls to the frame structures considered in this study almost always resulted in a significant increase in stiffness and strength of the existing frame. Thus, walls added a significant contribution to the overall lateral stiffness of the building and an accurate estimation of the wall stiffness was critical in the evaluation of the response of the structure. Since a bi-linear relationship was used to idealize the behavior of the wall, the uncracked, cracked, and yielding stages of the wall could not be considered simultaneously with such a model. The wall sub-elements were therefore considered either in the uncracked/cracked or cracked/yielding stages. The actual bending stiffness of each wall sub-element was then determined on the basis of the maximum level of moment attained during a given seismic event. This procedure required several analyses to obtain convergence between the assumed properties and those experience by the elements during the seismic event.

3.2.5 Steel Brace Elements

3.2.5.1 High Slenderness Ratio Braces (KL/r > 120)

Inelastic behavior of high slenderness ratio braces (steel strands or steel rods) was idealized using the *truss element model* of the DRAIN - 2D program. The truss element model is a *two-component model*, in which the only element deformation considered is its axial deformation. Inelastic behavior of the element adopted for this study considered yielding in tension and *elastic* buckling in compression, as shown in Fig. 3.10. The behavior of the element in compression is thus *non-linear elastic*; i.e. the loading and unloading paths are always the same, even after the element has reached its assumed buckling capacity (segments A-B and C-D in Fig. 3.10).

Because of the high slenderness ratio of steel rod or strand braces, their buckling capacity is negligible. While a bundle of
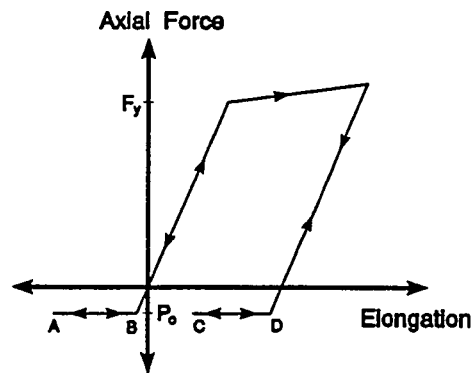
Figure 3.10 Element behavior for high slenderness ratio braces (KL/r > 120).

steel strands or steel rods may possess some strength in compression, the magnitude of the capacity in compression is insignificant compared to their yielding strength in tension. Therefore, the compression capacity of these type of braces was assumed to be zero in the analyses. Strain hardening effects after yielding in tension can be included, and were considered in the analyses as described in the following section.

Initial prestressing of the truss elements was considered by specifying initial fixed end forces. These forces are algebraically added to those obtained from gravity loads in order to include the combined action of these two main sources of initial forces in the structure.

Modeling Parameters and Procedure

Two different types of prestressing steel, commonly used in the prestressing industry, were considered for the braces. These are: high strength steel rods with a nominal ultimate

strength of 178 ksi and steel strands of nominal ultimate strength of 250 ksi. Typical stress- strain relationships for these two materials are presented in Fig. 3.11. Also shown in this figure is the stress-strain relationship for conventional Grade 60 ksi reinforcing steel for comparison. The main characteristic of prestressing rods and strands is their high yield point and ultimate strength. Steel rods considered in this study possess a yield point of about 156 ksi and a steel plateau that is well defined as shown in Fig. 3.11. Steel strands,

Figure 3.11 Stress - strain relationships for high strength and conventional rebar steels.

however, do not exhibit a yield plateau and possess an equivalent yield stress level of about 235 ksi (as defined by the strain at a stress of 1%).

While yielding and ultimate strength of prestressing steel (rods and strands) is much higher than that of conventional steel, its elongation at ultimate is lower, particularly for strands. Steel rods can develop up to 6 % elongation at ultimate compared to only 4% for strands (ultimate elongation values are based on a gage length of 10 times the bar diameter). Because steel rods present a well defined yield point followed by a flat plateau,

an elasto-plastic model was appropriate to represent the behavior of rod braces for elongations up to about 1.1%. For steel strands, however, such a simple model may not be representative of the stresses and deformations in the braces. To emulate the gradual change of stiffness of strands beyond the elastic range with a bi-linear model, a slope equal to 3% of the initial modulus of elasticity was adopted as strain hardening, as shown in Fig. 3.12. This slope reasonably predicts the stresses in the
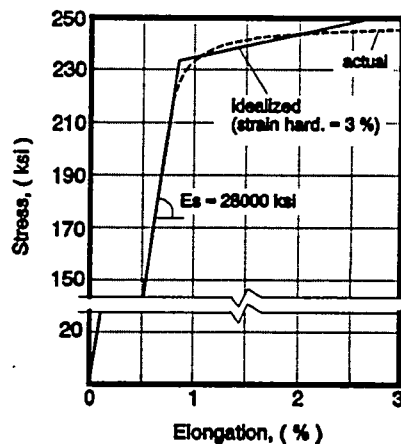
Figure 3.12 Idealized stress - strain relationships adopted for strands.

strand for elongations up to 2.5 %, but will probably overestimate stresses for elongations beyond 3%.

As will be discussed in Chapter V, maximum total elongation for these types of braces is not expected to exceed twice the deformation at yielding, and the selected model will be appropriate as long as the aforementioned deformations are not exceeded.

3.2.5.2 Medium Slenderness Ratio Braces (50 < KL/r < 120)

Behavior of steel braces with medium slenderness ratios was idealized with the *buckling element* of the computer program. The model, originally developed at the University of Michigan, Ann Arbor, presents a multi-linear hysteresis model for axially loaded, pin - ended bracing members[29]. The model is based on extensive experimental evidence on different types of concentric braces, primarily hollow square tube sections and, single and double angle sections. Hysteretic laws of the model include an elasto-plastic behavior of the element in tension and the post-buckling behavior observed for these types of braces, as discussed in Chapter II. Such post-buckling behavior consists of a continuous reduction of the initial buckling load capacity with repeated cycles. However, it has been observed that after a few cycles the buckling capacity appears to become stable at a small fraction of the initial buckling load, referred to as residual buckling load in the present study.

Figure 3.13 shows the basic hysteretic behavior of the buckling element. In this figure, the load level P_c, corresponds to the buckling load capacity under monotonic loading and it can be reached only once during the entire loading history. After the member buckles at the load level P_c, the member follows segment 3 - 4 of negative slope, which represents the strength degradation that follows initial buckling of the member. The slope of segment 3 - 4 is defined by the residual buckling capacity of the member, P_r, and a compression displacement equal to five times the tension yield displacement, Δ_y. These parameters are both based on experimental results[29]. Upon reversal of the load at point 4 and reloading in tension, the member follows segments 4 - 5, 5 - 6 and 6 - 7. Point 6 is introduced in the model to represent "pinching" effects that follow post-buckling behavior of the member. Note that point 7 differs from point 2 to include the effects of strength reduction due to repeated cycles.
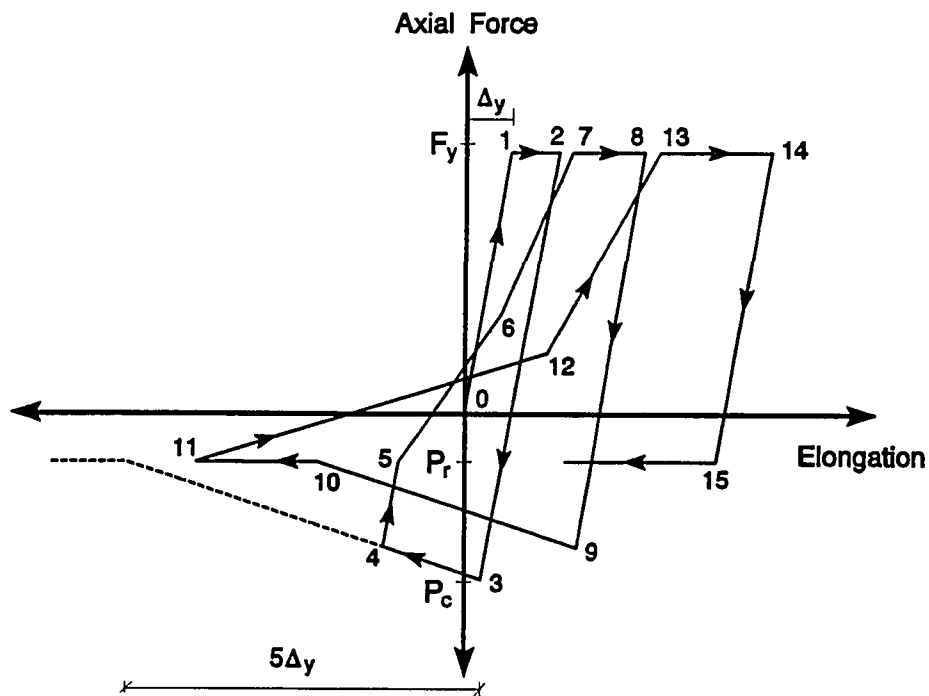
Figure 3.13 Element behavior for medium slenderness ratio braces. (50 < KL/r < 120)

Unloading in tension and reloading in compression results in segment 8 - 9. The load at point 9 corresponds to that prevailing when the member was unloaded in the previous compression cycle (point 4). The member follows then segment 9 - 10, which has the same slope as that of segment 3 - 4. At point 10, the member reaches its residual buckling load, P_r, and continues in compression following segment 10 - 11. If the axial load is reversed at point 11, the member follows segments 11 - 12 and 12 - 13. As above, point 12 reflects "pinching" of the hysteresis loop. Further loading in tension and then unloading in compression results in segments 13 - 14 and 14 - 15. The load at point 15 corresponds in this case to the residual buckling load of the member, P_r.

The parameters that govern the hysteretic laws of the model presented above are largely based on empirical relationships, some of which have been directly incorporated into the element subroutines. The description of all the variables involved in the development of the model can be found in detail in Reference 29. However, main parameters that control

most of these laws are the yield load, F_y, the buckling load, P_c, the residual buckling load capacity, P_r, and the effective length of the member, KL. As indicated above, the initial buckling load, P_c, corresponds to the compression capacity under monotonic loading and can be calculated by using the provisions of the Load and Resistance Factor Design (LRFD) for steel construction [30]. The residual buckling load, P_r, is in general specified as a fraction of the buckling load for the first cycle, P_c, and varies from 20% to 60% of the initial buckling capacity depending upon the effective slenderness ratio of the member [29]. For tubular sections, the residual buckling load can be taken as [31]:

$$P_r = (0.4 - 0.0025 \frac{KL}{r}) P_c \qquad for \ \frac{KL}{r} < 120 \qquad (3.5)$$

in which:

P_r = residual buckling load

P_c = buckling load for the first cycle

K = effective length factor

L = unbraced length of member

r = radius of gyration

and due to the absence of more specific data, the same expression was adopted to compute the residual buckling load for double-angle sections.

Effective length factors for concentric bracing are influenced primarily by the rigidity of the end connections and the connection at the intersection of the two braces. These factors vary depending upon the cross section of the brace member and also vary for in-plane or out-of-plane buckling. For X-bracing, several values have been proposed [32,33] for single and double angles, and for tubular sections, with effective length factors ranging from 0.425 to 0.5 for in-plane buckling and from 0.5 to 0.85 for out-of-plane buckling (effective length factors apply to the full brace length). In the present study, effective length factors were considered as 0.5 for in-plane buckling and 0.67 for out-of-plane buckling of the members, values that are commonly used in standard design practice.

Yielding strength of brace members was taken as 46 ksi for tubular sections and 50 ksi for double-angle sections. Elastic modulus was taken as 29000 ksi.

3.3 SOIL-STRUCTURE INTERACTION EFFECTS

For structures supported on rock or hard soil, it is common to assume that the motion at the base of the structure is the same as that of the free-field ground motion. This assumption is normally justified because the deformations in the foundation material due to the motion of the structure are negligible under the earthquake induced stresses. For structures founded on soft soils, however, the motion at the foundation level is generally different from the free-field motion due to the dynamic interaction between the soil and the super-structure. The foundation motion may include in this latter case an important rotational or rocking component, θ_f, in addition to a translational or lateral component, δ_f, as shown in Fig. 3.14. This rocking component can be particularly important for tall structures[34]. Depending on the dynamic properties of the structure, those of the soil, and the characteristics of the ground motion, soil-structure interaction effects may increase, decrease or have no effect on the magnitude of the forces induced in the structure.
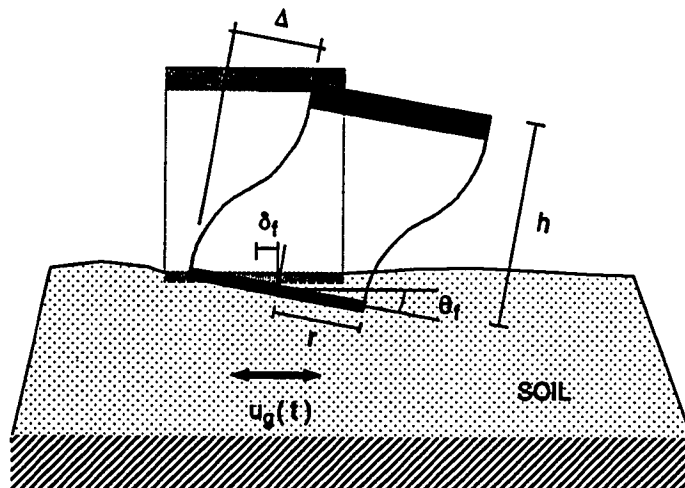
Figure 3.14 Schematic representation of soil-structure interaction effects.

3.3.1 Soil-Structure Interaction Analysis

The models of analysis of the soil-structure system may vary from refined finite element methods that account for the effects of foundation embedment, variations of soil properties in depth, etc, to simplified procedures that utilize axial and rotational springs and corresponding dashpots to simulate the stiffness and damping of the foundation soil.

3.3.1.1 Simplified Procedures

Two simplified procedures can be used to account for the effects of the soil-structure interaction [34]. The first approach involves modifying the free-field ground motion and analyzing the response of the fixed-base structure using the modified ground motion. The second procedure involves modifying the dynamic properties of the structure and the evaluation of the response of a modified structure to the free-field motion. The latter approach is used in the present study.

In the second approach, interaction effects are introduced by an increase in the fundamental period of the structure, and by a change (usually an increase) in the *effective damping* of the interacting soil-structure system. The increase in the fundamental period of the structure is a result of the flexibility of the foundation soil, whereas the change in damping results mainly from the effects of energy dissipation in the soil due to structural, radiation damping and, hysteretic or inelastic action in the soil usually referred to as *soil material damping*. This procedure yields results that are in close agreement to those of a more "exact" procedure, despite the simplifications introduced in the model [34].

Stiffness (Flexibility) of the Foundation Material

To obtain the stiffness of the foundation material, the structure is assumed to be supported on a rigid mat foundation of negligible thickness at the surface of a homogeneous elastic half-space. For a rigid circular mat, the *static* translational and rotational stiffnesses of the foundation material are defined respectively by Veletsos [34] as:

$$K_x = \frac{8}{2-\mu} Gr \qquad (3.6)$$

$$K_\theta = \frac{8}{3(1-\mu)} Gr^3 \tag{3.7}$$

In which r is the radius of the foundation, G is the shear modulus, and μ is the Poisson's ratio of the soil. The shear modulus, G, varies for different soil types and depends, in general, on the level of strain induced in the soil.

In order to account for embedment and layer depth, the static stiffness expressions can be corrected for small embedments as follows [35, 36, 37]:

$$\bar{K}_x = K_x [1 + \frac{2}{3}\frac{E}{r}][1 + \frac{5}{4}\frac{E}{H}][1 + \frac{1}{2}\frac{r}{H}] \tag{3.8}$$

$$\bar{K}_\theta = K_\theta [1 + 2\frac{E}{r}][1 + 0.7\frac{E}{H}][1 + \frac{1}{6}\frac{r}{H}] \tag{3.9}$$

where E denotes the embedment of the foundation, r the radius (or equivalent radius) of the foundation, H the depth of the layer of soil and, K_x and K_θ the static stiffness of the foundation material defined above. These expressions can be used for mat foundations of arbitrary shape, provided that an equivalent radius is used for the foundation. For the translational stiffness the equivalent radius is calculated as:

$$r_x = \sqrt{\frac{A_0}{\pi}} \tag{3.10}$$

where A_0 is the effective area of contact between the foundation and the soil. Similarly, the equivalent radius for the rotational stiffness is specified as:

$$r_\theta = \sqrt[4]{\frac{4 I_0}{\pi}} \tag{3.11}$$

where I_0 is the moment of inertia of the foundation about a horizontal centroidal axis normal to the direction in which the analysis is being considered.

Note that the use of the static stiffness in the solution of the soil-structure interaction problem is not strictly correct because, in general, the stiffness, mass and damping associated with the soil are frequency dependent. However, the static stiffness values have been found to be more than adequate for most practical applications [15].

Effective Damping of the Soil-Structure System

The effective damping factor of the interacting system, $\bar{\xi}$, is given approximately [40] by:

$$\bar{\xi} = \bar{\xi}_0 + \frac{\xi}{(\bar{T}/T)^3} \tag{3.12}$$

where $\bar{\xi}_0$ represents the effects of energy dissipation in the soil due to radiation and material damping, and ξ corresponds to the percentage of critical damping for the structure in its fixed-base condition. T corresponds to the fundamental period of the fixed-base system and, $\bar{T}$, is the fundamental period supported on soft soil, commonly referred to as the *effective natural period* of the interacting system. $\bar{T}$ is determined by applying dynamic principles to the soil-structure model, using the stiffness properties for the foundation material presented above. Alternatively, the effective period of the system can be approximately estimated from the following relationship:

$$\bar{T} = T \sqrt{1 + \frac{k}{K_x}[1 + \frac{K_x h^2}{K_\theta}]} \tag{3.13}$$

where k is the lateral stiffness of the structure in its fixed-base condition for the mode of interest, and h is the height measured from the base of the structure to the centroid of the inertia forces (effective height of the building for motion in its fundamental natural mode).

The foundation damping factor, $\bar{\xi}_0$ (See Eq. 3.12), depends on the geometry of the contact area of the foundation and on the properties of the structure and those of the underlying soil deposits. Nonetheless, the three most important parameters which affect the value of $\bar{\xi}_0$ are: the period lengthening ratio $\bar{T}/T$, the ratio of the effective height of the structure to radius of the foundation h/r, and the damping capacity of the soil. The damping capacity can be related to the hysteretic damping ratio, λ, and is usually measured

from the amount of energy absorbed in one complete load cycle and the peak strain energy for a soil specimen undergoing harmonic shear deformation [15,38]. The hysteretic damping ratio, λ, is a function of the imposed peak strain, increasing with increasing level of strain induced on the soil (or increasing intensity of the excitation).

The variation of the foundation damping $\tilde{\xi}_0$ with these three main parameters has been the subject of extensive parametric studies [34, 39, 40] which have resulted in the charts reproduced in Fig. 3.15. In this figure, the foundation damping factor, $\tilde{\xi}_0$, is plotted versus the period lengthening ratio, $\tilde{T}/T$, for different values of the ratio h/r and for two values of
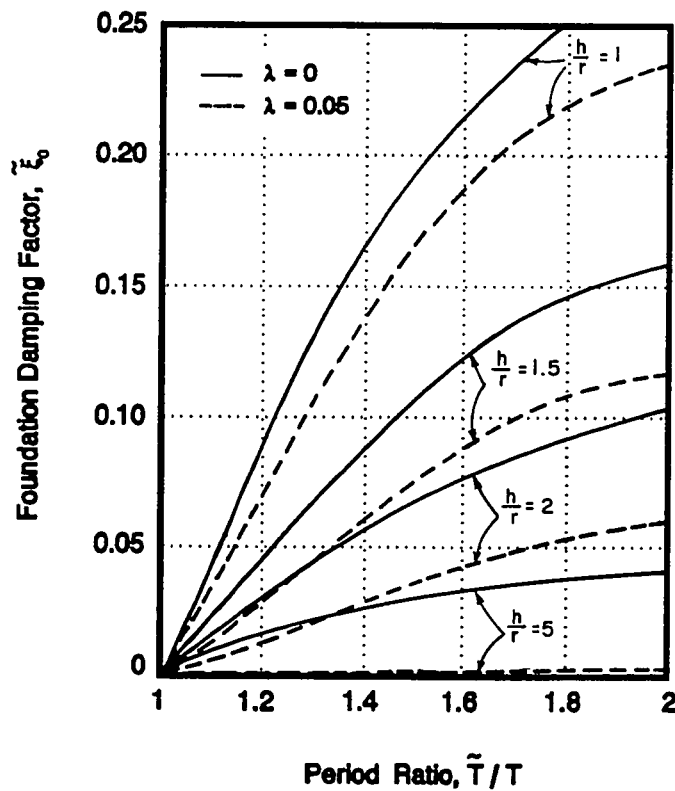
Figure 3.15 Foundation damping factor, $\tilde{\xi}_0$, for structures supported on elastic and visco-elastic half-space (After Veletsos [34]).

the hysteretic damping ratio (or two levels of excitation). Note that foundation damping can have a significant contribution to the overall damping of the system, and that the contribution of hysteretic action (λ = 0.05) may be particularly significant for tall structures (h/r = 5), for which the contribution of radiation damping is generally small (λ = 0) [34].

The magnitude of the effective natural period, $\bar{T}$, is always greater than the fixed-base fundamental period T. It follows then, from Eq. 3.12, that the effective damping of the system, $\bar{\xi}$, may be greater, equal to or smaller than ξ. However, since the damping factor ξ is normally based on the results of full-scale structures which reflect the overall damping of the foundation-structure system, it is recommended that $\bar{\xi}$ be taken no less than the value of ξ [34].

Limitations of Procedure

a) The approach presented above has been based upon the analysis of single-degree-of-freedom systems; however, it can be applied to multi-story structures which respond essentially as a SDOF system in a fixed-base condition [34]. For structures with lumped masses, it is only necessary to compute h as:

$$h^{\bullet} = \frac{\sum m_i \, x_i \, h_i}{\sum m_i \, x_i}$$

(3.14)

where x_i is the modal displacement of the ith floor (fixed-base) located at a distance h_i from the base and m_i is the total lumped mass at the ith floor.

b) A second limitation of the procedure is the assumption of linear response of the super-structure. In general, the super-structure is expected to deform beyond the elastic range during strong earthquakes, and therefore a significant amount of inelastic action may develop in the structure. The main effect of such inelastic behavior is to increase the relative flexibility of the super-structure with respect to that of the supporting medium, which tends to reduce the interaction effects [17, 41]. Thus, the use of the procedure described above in the analysis of inelastic systems will lead to results that may be somewhat conservative.

3.3.2 Modeling Parameters and Procedure

To model the soil-structure interaction system, the structure was assumed to be supported on an infinitely rigid mat foundation, which in turn is supported on axial springs representative of the flexibility of the soil material. Due to the unavailability of appropriate rotational springs in the DRAIN-2D program, rotational stiffness of the foundation material was idealized by a set of vertical springs, as shown in Fig. 3.16. Translational stiffness of the soil was idealized by a horizontal spring.

Evaluation of the soil-structure interaction effects relies primarily on two
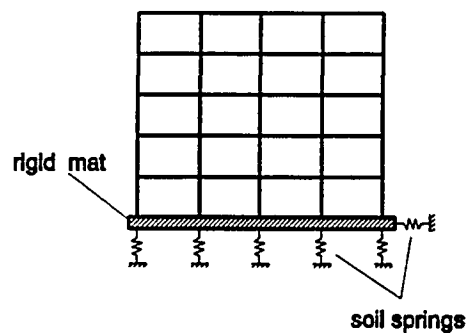
Figure 3.16 Modeling of the soil flexibility.

main factors: the shear modulus, G, and the amount of hysteretic damping, λ, of the foundation soil. Both parameters vary for different soil types and depend, in general, on the strain level induced in the soil during the earthquake motion. The present study considers structures located in two types of soft soil conditions. One such soil type corresponds to the silty clay deposits found on the lake bed area in Mexico City, Mexico. The second type of soil corresponds to the bay mud found in the San Francisco Bay area in California, U.S.A. Previous studies [42] have shown that for the silty clay deposits of Mexico City, both the shear modulus and the hysteretic damping ratio remain almost constant for shear strains up to 0.1%. Thus, it seemed reasonable to use a single value for the shear modulus and the hysteretic damping ratio of the soil in the evaluation of soil-structure effects. For the San Francisco Bay Mud, however, the shear modulus and the hysteretic damping ratio have been found to vary appreciably for strains larger than 0.01% [38,43]. Based on these studies, two levels of shear strain, namely: 0.01% and 0.1%, were used to evaluate soil-structure interaction effects for the buildings located on the San Francisco Bay Mud. Table 3.1 shows the shear modulus and hysteretic damping coefficients adopted for study.

Table 3.1 Soil parameters for soil-structure interaction effects.

Type of Soil		Shear Modulus (ksi)	Hysteretic Damping Ratio (%)	Peak Shear Strain (%)
Silty Clay Deposits (Mexico City)		1.09 [†]	2 [††]	0.1
Bay Mud (San Francisco, Ca.)	Case I	2.00 [†††]	3 [†††]	0.01
	Case II	1.50 [†††]	7 [†††]	0.1

[†] After reference 44.

[††] After reference 42.

[†††] After references 38,43.

CHAPTER IV

BUILDING STRUCTURES AND GROUND MOTIONS
SELECTED FOR STUDY

4.1 GENERAL

Three buildings were selected for study. The buildings are prototype designs and represent typical low and medium rise construction of the 1950's and 1960's in the United States. Low-rise construction is represented by a three story reinforced concrete frame, while medium-rise construction is represented by seven and twelve story high frame buildings of reinforced concrete.

A description of the buildings selected for study is presented. Each building is evaluated and studied separately by examining the structural properties and the possible modes of failure of their members. Based on estimated member capacities, the lateral strength of the buildings is estimated through an incremental, inelastic static analysis procedure. The predicted lateral strength is then compared to current applicable standards and to the codes in effect at the time of erection of the buildings.

4.2 PROTOTYPE STRUCTURE I - THREE-STORY BUILDING

4.2.1 General Description

A plan view and typical elevation in the longitudinal direction of the building are presented in Figs. 4.1 and 4.2 respectively. The lateral load resisting system of this structure consists of an ordinary moment-resisting space frame (OMRSF). Perimeter and interior frames have 18 in. by 18 in. columns with 14 in. by 20 in. beams over the entire height of the building. Spandrel beams are eccentric with respect to the column axis, flush with the interior face of the columns. Beams of interior frames are aligned with respect to the column axis. Slab thickness is 7 in. in all floor levels. Normal weight concrete with a compressive strength of 3000 psi was used in all members. Longitudinal and transverse steel reinforcement was assumed to be Grade 60.

76
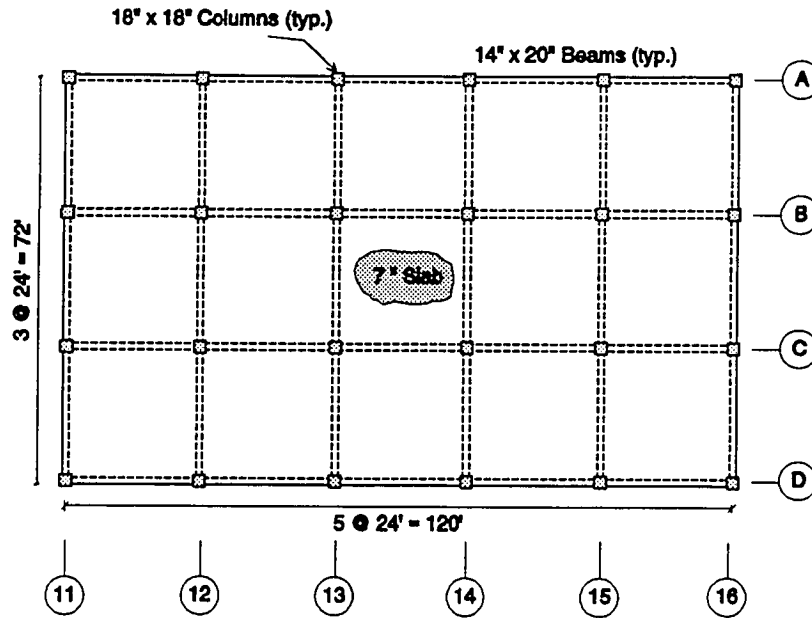
Figure 4.1 Plan view of the three-story building.
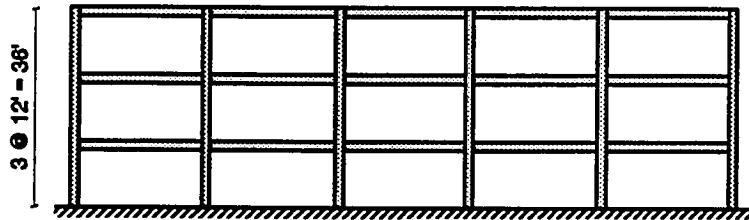
Figure 4.2 Elevation in the longitudinal direction of the three-story building.

4.2.2 Seismic Evaluation

The design lateral forces for the building were obtained from the specifications of the 1964 UBC[6], while proportioning and detailing of the reinforced concrete members were based on the provisions for ultimate strength design of the 1963 ACI code[2]. Under current equivalent design provisions, 1991 UBC[3] and 1989 ACI[4], erection of this structure would

not be permitted in zones of moderate to high seismic risk because it would not meet the minimum ductility requirements for the design of its members. As stated in chapter II, the specified lateral forces in the 1964 UBC were much lower than those required by current provisions. Consequently, the design of members of the building was governed primarily by gravity loads which resulted in relatively low member strengths and poor detailing of reinforcement. The structure is unlikely to withstand major earthquakes satisfactorily.

4.2.2.1 Reinforcing Details and Member Strength

Typical cross section details and reinforcement schedule for beams and columns are presented in Figs. 4.3 and 4.4 respectively. Details of the reinforcement in the beam-column joint area are illustrated in Fig. 4.5. Evaluation of the reinforcement layout revealed several deficiencies which were considered critical to the safety of the structure under a strong ground motion, as follows:

a) *Lap Splices of Column Reinforcement:*

Since the design of the building was governed by gravity loads, column members were considered as compression elements. Lap splices for the longitudinal reinforcement were therefore designed as "compression splices", resulting in a splice length of only 24 bar diameters, as required by the provisions of the 1963 ACI code [2]. In addition, to simplify construction column splices were located just above the slab at each floor level, as shown in Fig. 4.5. The lap length provided for the splice is inadequate in tension (splice failure will occur prior to yielding of the bars) and therefore the flexural capacity of the sections at the base of the columns will be limited to the capacity of the splice. Furthermore, transverse reinforcement in the splice region is widely spaced as show in Figs. 4.4 and 4.5. Such detail provides little confinement to maintain the integrity of the concrete around spliced bars, and will significantly limit the ductility of the member.

b) *Discontinuous Bottom Reinforcement in Beams:*

Because the lateral forces used to design the structure were much smaller than those from gravity loads, moment reversals at the beam ends due to seismic loads were not anticipated. Accordingly, anchorage of bottom reinforcement

79

BEAM REINFORCING SCHEDULE

FLOOR #	COLUMN LINE	A	B	C	D	E
1st to 2nd	A & D	2#8	1#6	1#7	2#6	-
1st to 2nd	B & C	2#9	2#8	2#9	2#8	1#6
3rd	A & D	2#7	-	-	2#6	-
3rd	B & C	2#8	-	1#9	2#8	-

1.5" (clear)

14"

7" 13"

Typical beam cross section

STIRRUP SCHEDULE

1st & 2nd Floor

A & D	9 #3@5	#3@9	#3@9	9 #3@5
B & C	9 #3@5	#3@9	#3@9	9 #3@5

| | 9 #3@5 | #3@9 | #3@9 | 9 #3@5 |
| | | #3@9 | #3@9 | |

3rd Floor

| A & D | #3@9 | #3@9 | #3@9 | #3@9 |
| B & C | #3@9 | #3@9 | #3@9 | #3@9 |

Figure 4.3 Beam cross section details and reinforcing schedule for the three-story building.

MAIN REINFORCEMENT		
Story Level	All cols. on lines A, D	All cols. on lines B, C
All Stories	8 # 6	8 # 7
	TIES	
All Stories	# 3 @ 12"	# 3 @ 14"
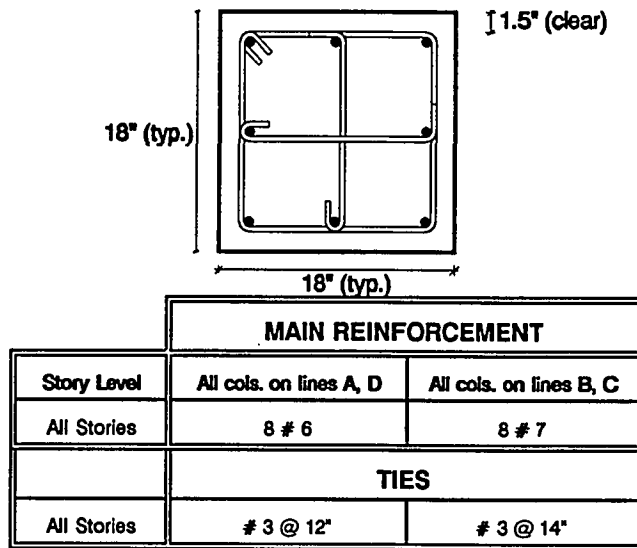
Figure 4.4 Column reinforcement details and schedule for the three-story building.
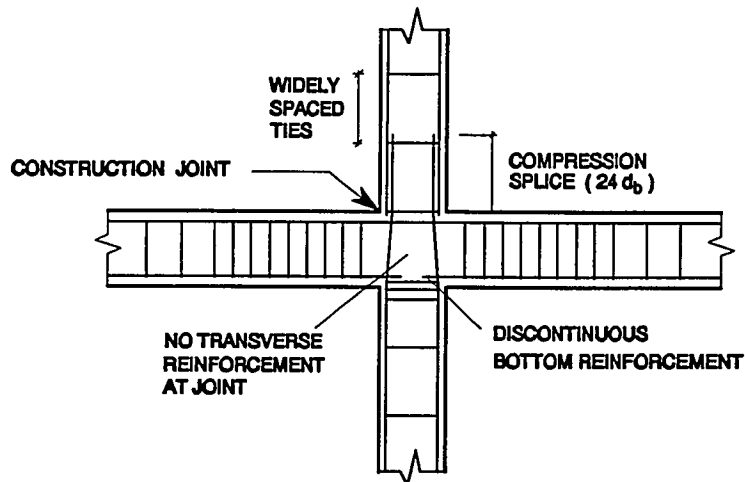
Figure 4.5 Beam-column joint details for the three-story structure.

was designed to meet the requirements of a member that was not part of a lateral load resisting system. The bars were embedded only 6 inches into the joint which is insufficient to develop the yield strength of the bars in tension. Under a strong earthquake, moment reversals at the beam ends will occur and will most likely cause the pull-out of the bottom bars from the joint. Anchorage failure of these bars at low tensile stresses will essentially create a hinge for "positive" bending moment in the early stages of a severe event, which may cause a reduction in the stiffness, strength and ductility of the structure.

c) *Shear Strength of Beams and Columns:*

Transverse reinforcement in beams and columns was designed to meet the shear forces required by gravity loads analyses only. Such design criterion resulted in low amounts of shear reinforcement that was widely spaced throughout the length of columns and beams. Nonetheless, the shear reinforcement provided is enough to develop the flexural capacity of the members, even assuming that the flexural reinforcement will develop its yield strength. Therefore, shear failure of columns or beams is not anticipated.

d) *Joint Shear Strength:*

Transverse reinforcement at the beam-column joint was not required by the 1963 ACI code [2], and therefore it was not provided in the building. Despite the absence of shear reinforcement in the joint, the joint shear capacity should be sufficient to develop the flexural capacity of beams and columns.

4.2.2.2 Modeling Assumptions and Parameters

The previous evaluation of frame members indicated that the weak links of the structure are predominately related to poor anchorage of the flexural reinforcement in columns and beams. The anchorage failure mechanism was idealized using the modified model for reinforced concrete elements described in Chapter III. Shear failure of the reinforced concrete beams and columns was not anticipated and therefore it was not considered in the analyses.

The main modelling parameters for critical sections in columns and beams were estimated as follows:

a) *Moment - Rotation Envelopes - Beams:*

The relationship adopted to model the moment- rotation characteristics of the beam end sections is presented in Fig. 4.6. For "positive" bending, the peak moment capacity and corresponding curvature of the sections were determined as the moment that would cause failure in bond of the reinforcement in tension, as described in Chapter III. Slope of the softening segment following anchorage failure of bars was partly based on the work of Pessiki et al.[11]. Their research work included beam-column joint assemblies with beam reinforcing details that were very similar to those provided in the beams of the building under study.
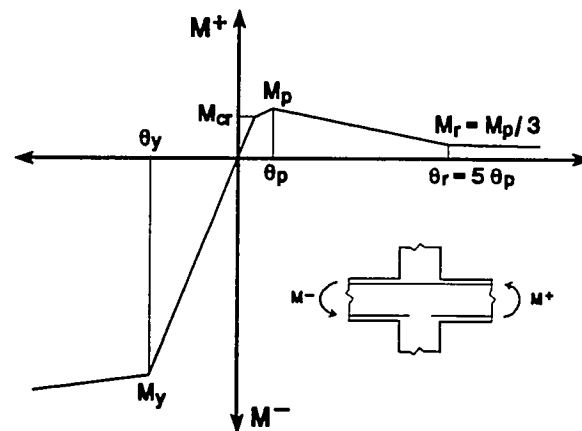
Figure 4.6 Moment - rotation envelope for beams. Both beam end sections.

For "negative" bending, it was assumed that the sections were able to develop yielding and strain hardening (this assumption was necessary to avoid a numerical instability of the solution algorithm of the program). The experimental evidence obtained by Pessiki et. al. actually showed some strength and stiffness degradation of the sections in "negative" bending after the pull-out of bottom beam reinforcement (see Chapter II). Since the observed degradation of strength and stiffness was relatively small compared to that observed for "positive" bending, the assumption indicated above will not significantly affect the overall response of the structure.

b) *Moment - Rotation Envelope - Columns:*

The results presented by Pessiki et al. regarding the behavior of short splices in columns were inconclusive (see Chapter II) and therefore they cannot be used directly to estimate the rate of strength degradation after a splice failure. Because of the sudden and brittle nature of such a failure, it is believed that a rather steep softening segment will follow column splice failure. On the basis of this assumption, the moment - rotation envelope shown in Fig. 4.7a was adopted to model column sections having a short splice (base of columns). The procedure to determine the peak moment capacity and corresponding curvature of these sections was the same as that used to estimate the pull-out failure of the bottom beam bars indicated above.

a) section at base of columns

b) section at top of columns
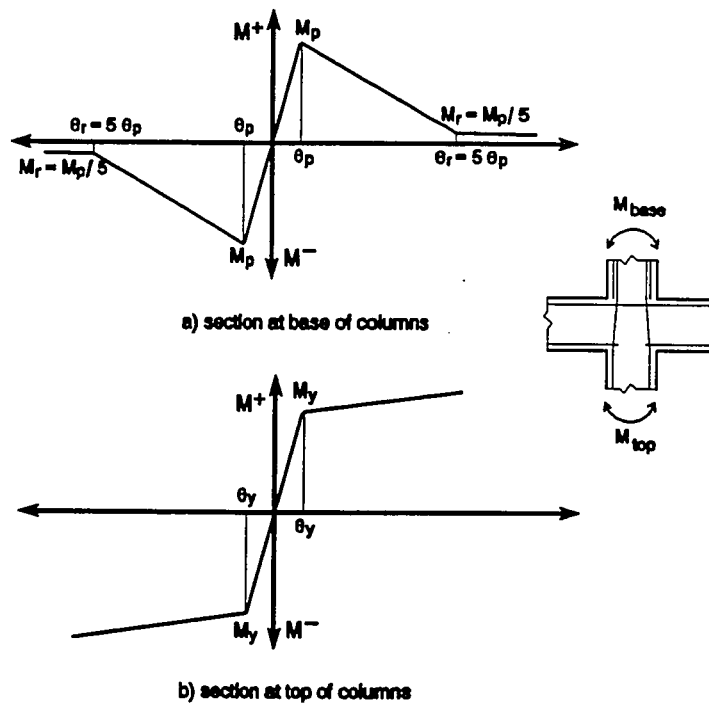
Figure 4.7 Moment - rotation envelopes for columns.

The top section of the columns was assumed to reach yielding and strain hardening in accordance with the continuity of the bars at those sections. The moment - rotation envelope adopted for these sections is shown in Fig. 4.7b.

4.2.2.3 Lateral Stiffness and Strength

Based on the assumptions indicated above, an estimate of the lateral strength of the building was obtained by applying a uniform lateral load distribution in the longitudinal direction. The results are presented in Fig. 4.8 as the base shear coefficient and the drift at the centroid of inertia forces (drift at effective height of building for motion in its first mode of vibration, see Eq. 3.14). The use of the drift at the centroid of inertia forces to plot the base shear and drift relationships will be discussed later in Chapter VII.
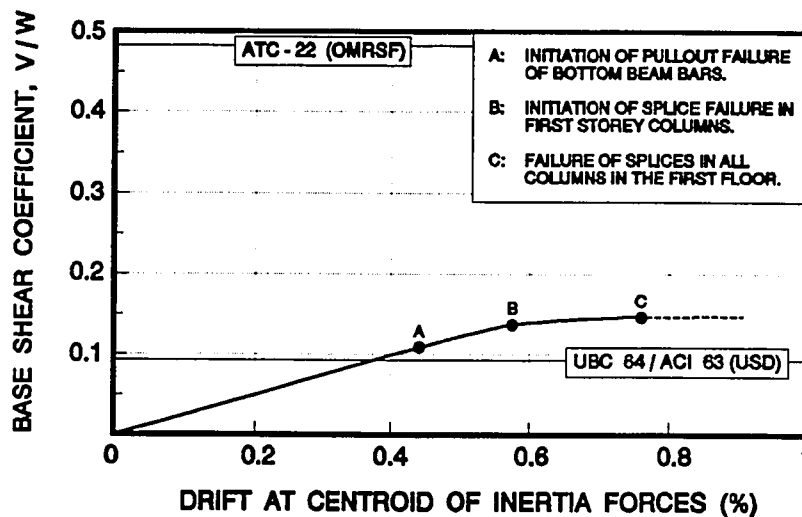
Figure 4.8 Base shear coefficient and drift at centroid of inertia forces relation for the three-story building in the longitudinal direction.

Three major events can be noted in the lateral response of the building. First, the behavior of the building is linear up to a value of a base shear coefficient of about 0.11. At this load level, pull-out of the bottom bars in first floor beams initiated, marking the departure from the assumed elastic behavior (inelastic behavior due to cracking is ignored by the computer model). However, lateral stiffness of the building did not decrease significantly until a base shear coefficient of about 0.13, when splices in first story interior columns began to fail. This second major event resulted in a sharp reduction in the lateral stiffness of the structure. First story displacements began to increase significantly with small increases in load after this event, and at a drift of about 0.76%, failure of splices in all first story columns

occurred. Shortly after this event, splice failure of second story columns began. Notice that even though local failure of splices caused strength degradation of the section at the base of the columns, the general failure of splices of column sections at a given floor did not result in an immediate reduction in the lateral strength of the structure. Due to redistribution of the bending moments from the base to the top of the column sections, column splice failure resulted in a gradual reduction of the lateral stiffness of the building.

The results shown in Fig. 4.8 indicate that for the given lateral force distribution, inelastic behavior is confined almost exclusively to the elements of the first story. Further increase of the lateral load beyond the failure of splices in the first story columns will have no significant impact on the lateral stiffness nor on the lateral strength of the building. Thus, the force level that would produce splice failure in all columns of the floor seemed a reasonable estimate of the lateral strength of the structure.

Also shown in Fig. 4.8 are the base shear coefficients as required by the 1964 UBC[6]. As can be seen, the computed ultimate strength of the building is about 1.5 times the lateral load level specified by the 1964 UBC (load factors and strength reduction factors included). This result was expected since the design of the building was governed by gravity loads and not by the lateral forces specified by the prevailing code.

The base shear coefficient required by ATC-22 [12] for an OMRSF is also shown in Fig. 4.8. Because lateral strength of the building is governed by failure of splices in columns, brittle elements were assumed to estimate the coefficient (see Appendix A). The figure shows that ATC-22 would require a lateral strength which is about three times larger than the computed ultimate strength for the building. This result clearly shows the enormous lack of lateral strength of the building implied by current standards.

4.3 PROTOTYPE STRUCTURE II - TWELVE-STORY BUILDING

4.3.1 General Description

The second structure selected for study was similar to a 12-story office building located in southern California. A plan view and typical elevation in the short direction of the building are shown in Figs. 4.9 and 4.10 respectively. The actual building consists of a 12 story office tower that rises above the street level and two lower levels of much larger area. Since the two lower levels of the building are below grade, the analyses were confined to the tower of the structure shown in Fig. 4.10. While the flexibility of the lower levels may influence the response of the real structure, the results that are obtained for the superstructure will be of general validity.
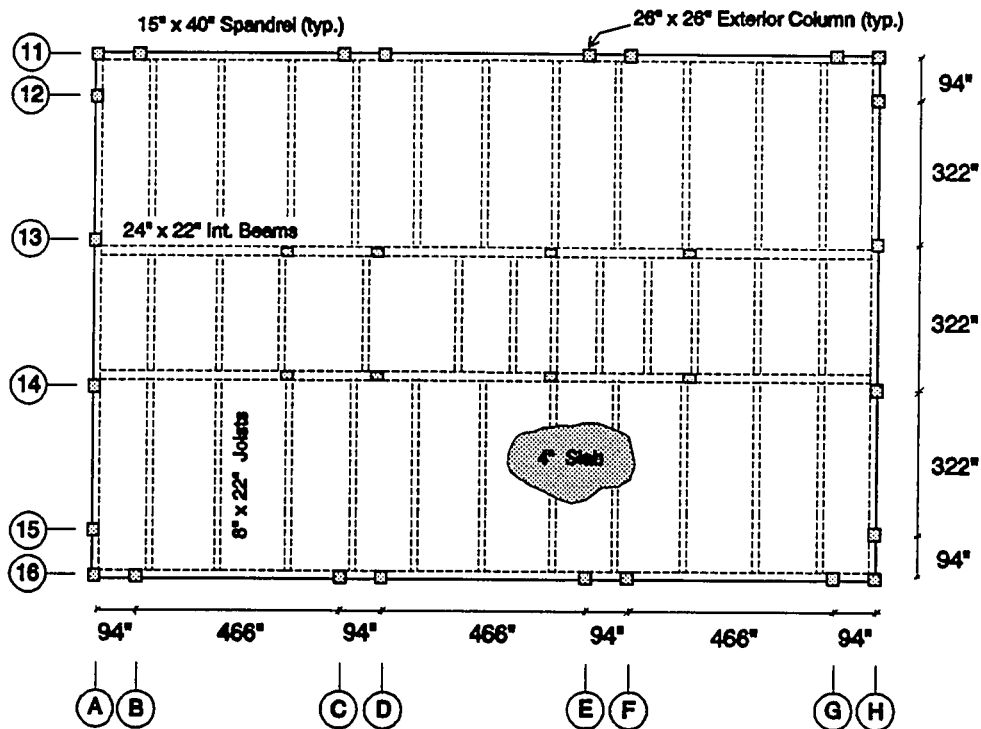
Figure 4.9 Plan view of 12 story building.
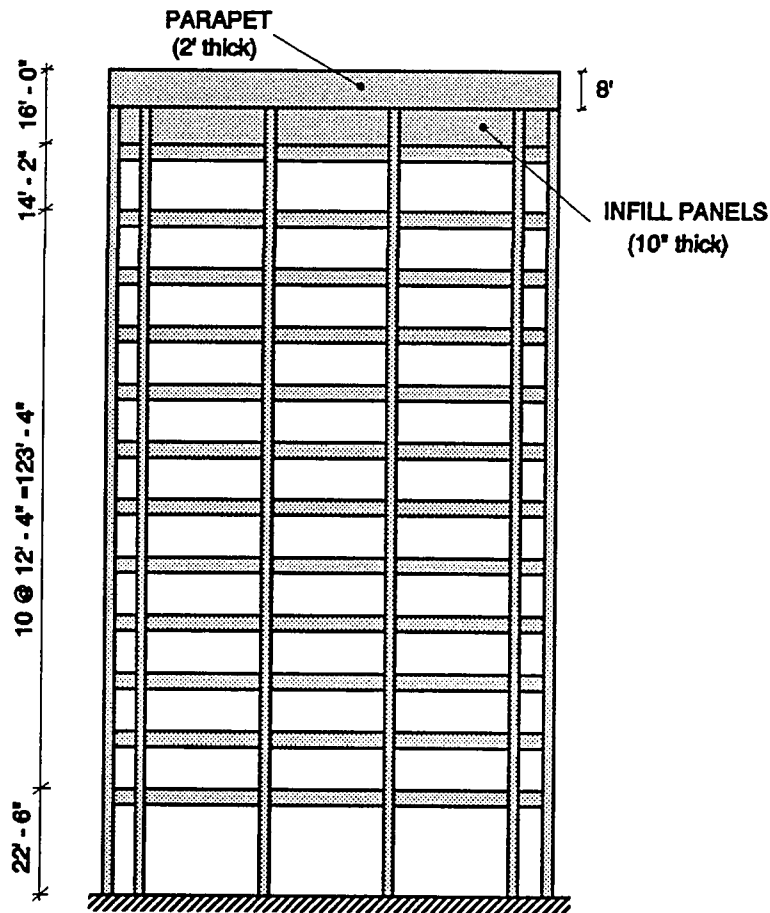
Figure 4.10 Typical elevation in the short direction of the 12 story building.

The primary lateral load resisting system of the building is provided by concrete moment frames located at the perimeter of the structure. In these perimeter frames, a double column configuration was used, probably to increase the lateral stiffness and overall redundancy of the structure. The perimeter frames have 26 in. by 26 in. columns and 15 in. by 40 in. deep spandrel beams over the entire building height. Slab thickness is 4 in. in all floor levels. Gravity loads are distributed by concrete joists that rest on the spandrel beams and on interior beams as shown in Fig. 4.9. All dimensions and reinforcing details of interior beams and interior columns were not available for the building. However, cross section

dimensions of interior columns, as scaled from the plans, were much smaller than those of the exterior columns. The smaller dimensions of interior columns and the relatively shallow interior beams and concrete joists make interior frames much more flexible than perimeter frames. It seemed reasonable to assume that perimeter frames will carry most of the lateral forces and, therefore, only perimeter frames of the building were considered for the lateral load analyses of the structure.

Normal weight concrete with a compressive strength of 5,000 psi was specified for columns. Beams and slabs were cast using light weight concrete with a compressive strength of 4,000 psi. Longitudinal reinforcement in beams and columns was specified as Grade 60, while transverse reinforcement in all members was specified as Grade 40.

4.3.2 Seismic Evaluation

The structure was constructed in the early 1970's and it was presumably designed according to the provisions of the 1967 UBC [5] for both lateral loads and member proportioning. Two main design configuration problems can be readily observed in this structure. First, the height of the first story is almost twice that of the upper stories (see Fig. 4.10), which creates a flexible "soft story" in the first floor. As discussed earlier in Chapter II, the "soft story" concept became rather popular in the late 1960's and it was not until after the 1971 San Fernando earthquake that soft stories were recognized to jeopardize the stability of the super-structure. Second, a massive parapet was provided at the roof level, presumably for architectural reasons. The parapet is partially supported on 10 in. thick infill walls which, in addition to adding extra mass, also provide an abrupt increase in the stiffness at the top story of the building.

4.3.2.1 Reinforcing Details and Member Strength

Typical cross section details and reinforcing schedule for columns and beams are presented in Figs. 4.11 through 4.15. Overall, this structure contained adequate detailing of the flexural reinforcement, especially around the hinging regions in columns and beams as shown in Figs. 4.12 through 4.14. Longitudinal reinforcement in columns was typically spliced in the midlength region with a 40 bar diameter lap (See Fig. 4.12), and therefore failure of splices in columns is not likely to occur. Special problems identified upon

	COLUMN LINE		
Story Level	A - 11, 12, 15, 16 H - 11, 12, 15, 16	A - 13, 14 H - 13, 14	11 - B, C, D, E, F, G 16 - B, C, D, E, F, G
1 st	16 # 11	4 # 18 + 12 # 14	12 # 11
2 nd to 5 th	8 # 9	12 # 11	8 # 9
6 th to 8 th	8 # 9	8 # 10	8 # 9
9 th to 11 th	4 # 9	8 # 9	8 # 9
12 th & Roof	4 # 9	8 # 9	4 # 9

16 Bar

12 Bar

8 Bar

26" (typ.)

[2" to face of main bar (typ.)

26" (typ.)

4 Bar
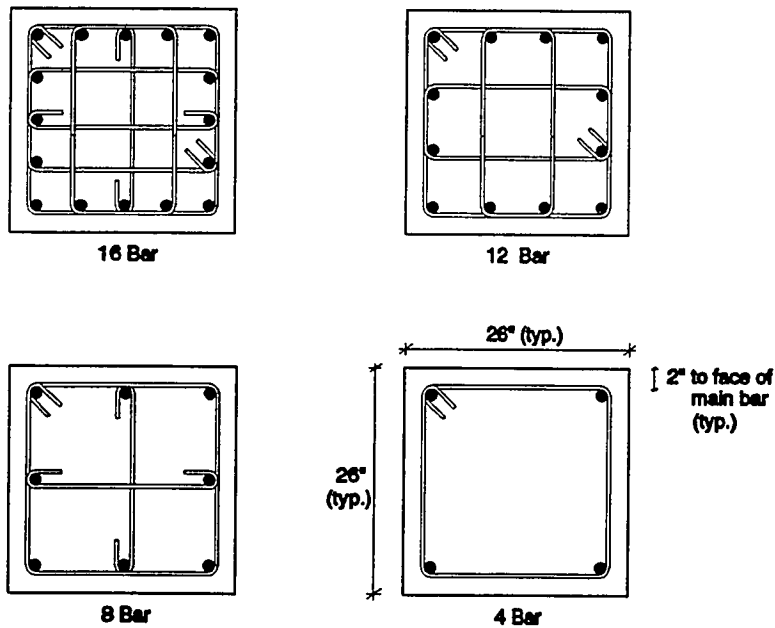
Figure 4.11 Column reinforcement details and schedule for the 12 story building.

evaluation of the reinforcement layout are summarized below:

a) *Transverse Reinforcement in Columns:*

Typical transverse reinforcement distribution in columns is shown in Fig. 4.12. As can be seen, the regions directly above and below the beam-column joint are
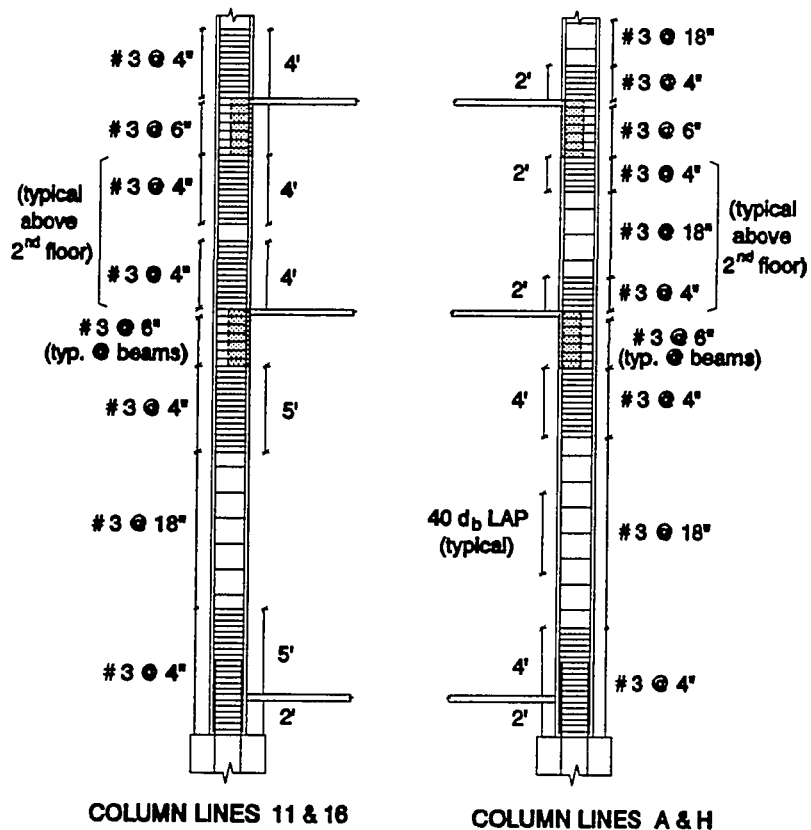
Figure 4.12   Tie configuration for perimeter frame columns of the 12 story building.

heavily reinforced with closely spaced ties at 4 in. Spacing of the ties and the length over which this reinforcement is distributed are both in accordance with current ACI specifications for hinging regions. Also, even though the size of the ties (# 3 bar) used to enclose # 11 bars and larger sizes does not meet current standards (a # 4 bar is presently required), the detailing of hoops and cross ties seems adequate. For the present study, it will be assumed that hoops and crossties provide adequate confinement to the concrete and lateral support to the longitudinal reinforcement.

Shear reinforcement was probably designed for the shear forces obtained directly from analyses using *design* lateral forces and not to ensure the

development of plastic hinges at the member ends. This would explain the abrupt increase in tie spacing to 18 in. that was provided for the remainder of the column length, as shown in Fig. 4.12. As a result of this tie distribution, shear failure is highly likely to occur in columns, particularly in the first and second stories of column lines A and H. Detailed calculations of the shear capacity of members, including the effects of axial forces from gravity loads, showed that shear failure will preclude the development of the hinges at the column ends in most story levels.

b) *Transverse Reinforcement in Beams:*

As in columns, beams were, in general, heavily reinforced around the joint area which provides adequate confinement of the hinging region. Nonetheless, transverse reinforcement within the central portion of the longer spandrel beams is typically spaced at 18 in. (See Figs. 4.13 and 4.14) and it is insufficient to develop the flexural capacity of the end sections in the lower stories of the structure. Similarly, the short spandrel beams defined by the double column configuration will probably fail in shear, despite the large amount of transverse reinforcement that was provided within the entire span as shown in Figs. 4.13 and 4.14.

c) *Anchorage of Bottom Reinforcement in Beams:*

Development length for beam reinforcement was specified as 30 bar diameters for all bar sizes. Such anchorage length is adequate to develop the yield strength of the bars, even for a #10 bar, the largest bar size that was used in the building. However, these bars will not be able to reach their ultimate strength with the provided development length. Bond failure could occur soon after reaching strain hardening. Anchorage failure of the bars after yielding will allow for some ductility of the section and for some force redistribution in the structure, but the performance of these sections under a strong ground motion will depend upon the ductility demands imposed by the earthquake loads.
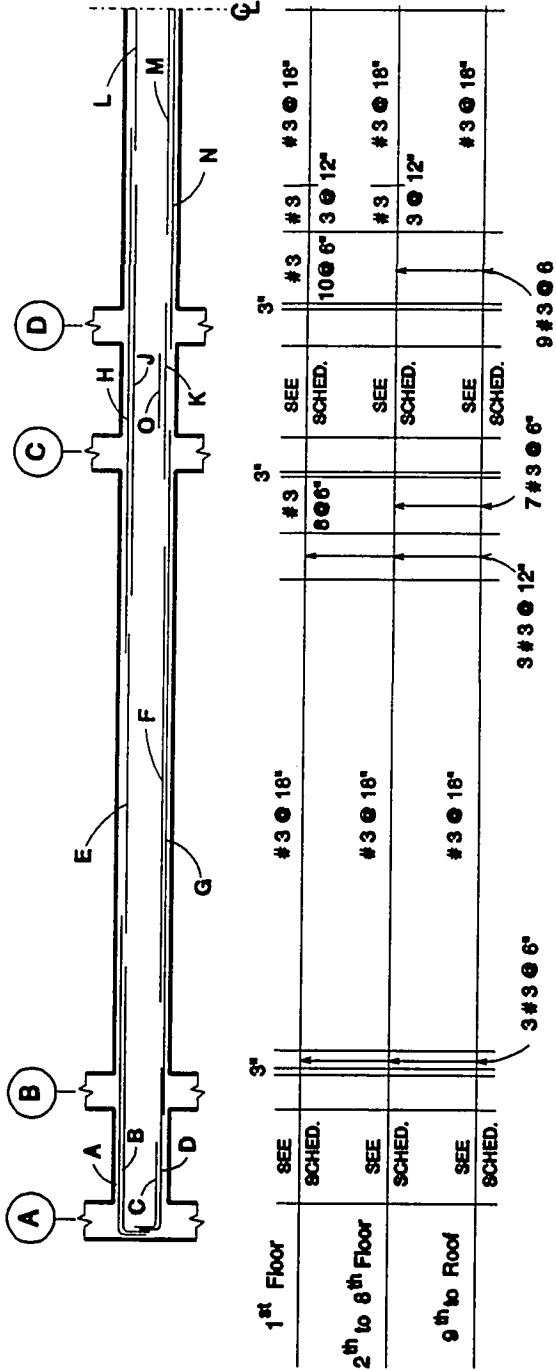
STIRRUP SCHEDULE

Floor #	SPANS A - B & G - H	SPANS C - D & E - F
1st	2#4@5"	#4@3"
2nd	#4@4"	#4@5"
3rd to 5th	#4@5"	#3@5"
6th to 8th	#3@5"	#3@5"
9th to Roof	#3, 1@3 Bal. @6"	#3, 1@3 Bal. @6"

1st Floor: SEE SCHED.   3#3@6"   #3@18"   3"   #3   8@6"   #3   3"   #3   10@6"   #3 3@12"   #3   #3@18"

2nd to 8th Floor: SEE SCHED.   #3@18"   3#3@12"   7#3@6"   SEE SCHED.   SEE SCHED.   #3 3@12"   #3@18"

9th to Roof: SEE SCHED.   #3@18"   9#3@6"   SEE SCHED.   #3@18"

Figure 4.13   Spandrel beam reinforcing schedule for the 12-Story building. Span A - H.
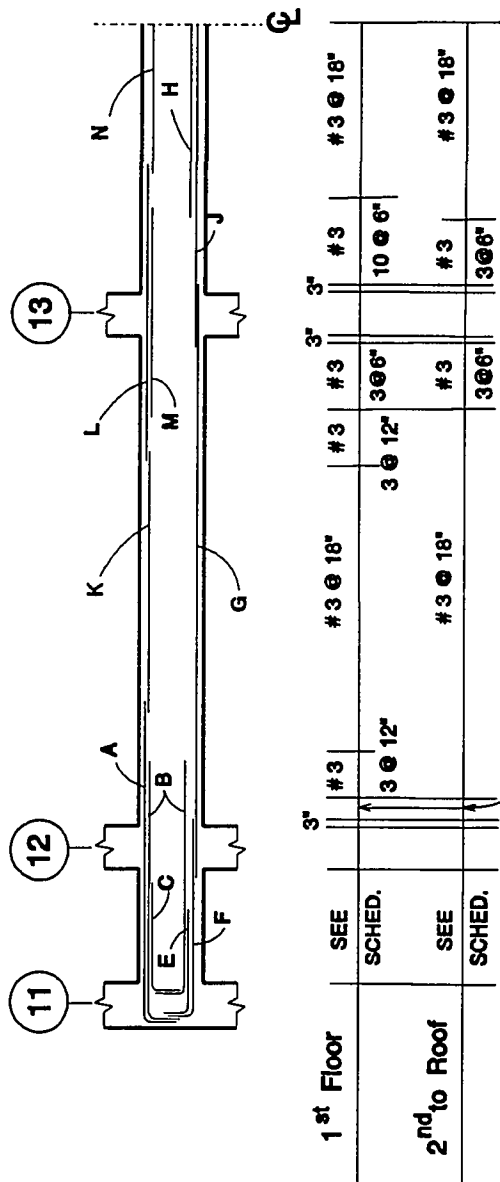
STIRRUP SCHEDULE	
Floor #	SPANS 11 - 12 & 15 - 16
1st	2 # 4 @ 4"
2nd	# 4 @ 5"
3rd to 5th	# 4 @ 3½"
6th to 8th	# 3 @ 5½"
9th to Roof	# 3, 1 @ 3 Bal. @ 6"

Figure 4.14 Spandrel beam reinforcing schedule for the 12-Story building. Span 11 - 16.

SPANDREL BEAM REINFORCING SCHEDULE - SPAN A - H

Floor #	A	B	C	D	E	F	G	H	J	K	L	M	N	O
1st	2#8	2#10	-	2#10 2#9	2#6	1#8	2#7	2#10	2#10	3#9	2#6	1#8	2#7	-
2nd	2#9	2#8	1#8	2#9	2#5	1#8	2#7	2#9	2#8	2#7 1#8	2#5	1#8	2#7	-
3rd to 5th	2#8	2#8	1#9	2#8	2#5	1#8	2#7	2#8	2#8	2#7 1#8	2#5	1#8	2#7	-
6th to 8th	2#8	2#7	-	2#8 1#7	2#5	1#8	2#7	2#8	2#8	2#7 1#8	2#5	1#8	2#7	-
9th to 11th	2#8	2#7	1#8	2#7	2#5	1#8	2#7	2#8	2#8	2#7	2#5	1#8	2#7	1#8
Roof	2#8	1#8	1#8	2#7	2#5	1#8	2#7	2#8	2#8	2#7	2#5	1#9	2#8	1#8

SPANDREL BEAM REINFORCING SCHEDULE - SPAN 11 - 16

Floor #	A	B	C	D	E	F	G	H	J	K	L	M	N	O
1st	2#8	2#10	2#10	2#10	2#10	2#9	3#9	1#9	2#10	2#6	3#9	2#9	2#6	-
2nd	2#9	2#10	-	-	-	2#9 2#10	3#8	-	3#8	2#6	2#9	3#8	2#6	-
3rd to 5th	2#8	2#8	1#8	-	1#8	1#8	3#8	-	3#8	2#6	2#9	2#8	2#6	-
6th to 8th	2#8	2#8	-	-	-	1#8	2#8 1#7	-	2#8 1#7	2#7	2#9	1#9	2#7	-
9th to 11th	2#8	1#8	-	-	1#8	2#7	2#8 1#8	-	2#7 1#8	2#6	2#8	1#8	2#5	-
Roof	2#7	1#8	-	-	1#8	2#7	2#7 1#8	1#8	2#7	2#6	2#8	1#9	2#5	-

Figure 4.15 Spandrel beam reinforcing schedule for the 12-story building.

d) *Joint Shear Strength:*

Transverse reinforcement details within the joint region is shown in Figs. 4.11 and 4.12. The provided amount of transverse reinforcement will help increase the joint shear strength but it is insufficient to supply adequate confinement to the joint region as required by current standards. Because column and beam members are expected to fail in shear rather in flexure, a shear failure of the joint is not anticipated in the original structure. However, should column and beam elements be able to develop their flexural capacity, shear strength of the beam-column joints would be inadequate in most cases.

4.3.2.2 Modeling Assumptions and Parameters

The previous evaluation of the building suggested that shear failure will most likely preclude the development of the flexural strength of most members in the structure. Thus, the shear model option for reinforced concrete elements was included in the analyses in addition to the moment softening feature (see Chapter III). Modeling parameters for critical sections of column and beam members were calculated as follows:

a) *Moment - Rotation Envelopes - Beams:*

These were obtained following the same procedure outlined in section 4.2.2.2 a) for the beams of the three-story building. However, because bottom reinforcing bars were expected to develop their yield strength, linear behavior was assumed for "positive" bending until flexural yielding of the section, as shown in Fig. 4.16. Strain hardening of the section was then assumed to occur until the bottom reinforcing bars pulled out at the estimated peak moment capacity. The peak moment capacity was estimated the using the approach described in Chapter III. Slope of the softening branch following peak moment capacity was arbitrarily assumed as shown in Fig. 4.16. The assumed rate of strength degradation after bond failure is more rapid than that adopted for the beams of the three-story building, mainly because failure occurs at higher stresses in the reinforcement. Beam sections in "negative" bending were assumed to reach yielding and ultimate strength as shown in Fig. 4.16.
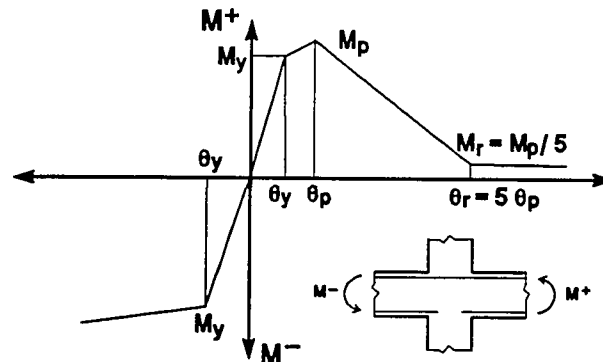
Figure 4.16 Moment - rotation envelope adopted for beam elements.

b) *Moment - Rotation Envelopes - Columns:*

Because splices of the longitudinal reinforcement were located in the mid-length of columns and because of the good confinement of the hinging regions, column end sections were assumed to develop yielding and ultimate strength. Thus, moment- rotation envelopes for all columns followed the same relationship indicated in Fig. 4.7 b).

c) *Shear Strength - Columns & Beams:*

In columns, the shear force distribution induced by earthquake loadings will typically be uniform along the length of the member, even under the combined action of the gravity loads. Therefore, the shear failure of such a member can be reasonable well predicted by comparing the shear force at the member ends with its estimated shear capacity.

In beams, however, the presence of gravity loads will normally result in a non-uniform shear force distribution, with shear forces that are maxima at the member ends as shown in Fig. 4.17. When the shear forces induced by earthquake loadings are comparable in magnitude to those induced by gravity loads, the combined shear force distribution will remain non-uniform and maximum shear forces will occur only at one of the member ends (See Fig. 4.17). The shear resisting mechanisms of a reinforced concrete member

subjected to combined flexure and shear involve the participation of the entire member, or at least an important portion of it. Thus, a shear failure criterion based solely on the comparison between the beam shear capacity and the shear force acting at the member end sections seemed unrepresentative of the expected behavior and also too conservative. Shear failure of a beam element was then determined using a different criterion as follows: a beam element was considered to have failed in shear when the average value between the maximum shear force at the member end and that at mid span exceeded the estimated shear capacity of the beams, as shown in Fig. 4.17.

SHEAR FORCE DISTRIBUTION
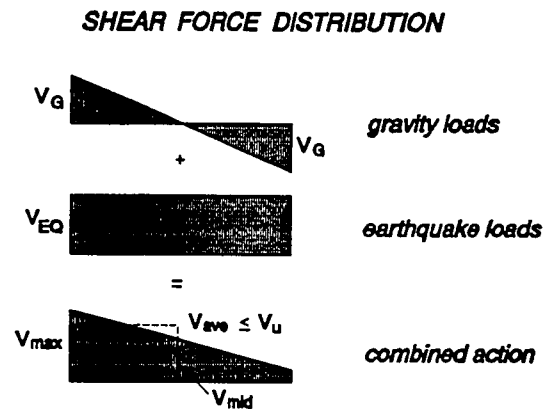
Figure 4.17 Shear force distribution and failure criterion for beam elements.

To account for the non-uniform shear force distribution in beams and also to provide adequate confinement to the hinging regions, a smaller stirrup spacing is usually provided at the end beam sections. Consequently, a larger shear capacity can be obtained at the end sections of the beam. In this study, shear strength of beam elements was estimated using the shear reinforcement provided within the central portion of the member, thus obtaining a lower bound for the shear capacity. This approach is conservative and it is consistent with the shear failure criterion adopted for beams which will allow higher shear forces at the member ends prior to establishing the shear failure of the member.

4.3.2.3 Lateral Stiffness and Strength

Evaluation of the lateral strength of the structure was obtained by applying a uniform lateral load distribution throughout the height of the building. To evaluate the impact of the potential shear failure of columns and beams on the lateral strength of the structure, three different member failure modes were considered. First, an analysis was conducted on the original structure with the estimated shear and flexural strengths for the members allowing for the potential shear failure of columns and beams (Case 1). A second analysis was carried out on a modified structure in which column shear failure was prevented, but it was allowed to occur only in beams (Case 2). The third analysis was conducted for the same structure, but shear failure was prevented in all column and beam members (Case 3).

In Fig. 4.18, the results obtained for the first two cases studied are presented for the analysis in the short direction of the building. In this figure, the response of the building is represented as the relationship between the base shear coefficient and the drift at the centroid of the inertia forces. In case 1, the behavior of the structure is almost linear until shear failure of two of the short spandrel beams in the first floor. This event is indicated as point A in Fig. 4.18. The redistribution of the forces carried by the failing element caused a sudden and significant increase in the lateral displacement of the structure (Segment A-B in Fig. 4.18). In addition, and most important, failure of this element triggered the progressive shear failure of the second, third and first story columns respectively. The abrupt and sequential collapse of these elements lead to the local collapse of the first and second stories and eventually to the collapse of the overall structure.

Behavior of the building when shear failure was prevented in columns (case 2) was very similar to that observed in the previous case until a drift of about 0.6% (Point B in Fig. 4.18). At this drift level, the building regained some of its original stiffness and continued carrying some additional load until shear failure of the remaining short spandrels in the first floor. Failure of the latter elements induced the progressive shear failure of the short spandrel beams in the upper floors as well as induced the shear failure of the longer span beams. As a result, the lateral stiffness of the building was significantly reduced, which led to extremely large displacements, as shown in Fig. 4.18. While the successive shear failure of beams may not cause the immediate collapse of the building, it will compromise the overall lateral stability and strength of the structure. This behavior is indicated as a dashed
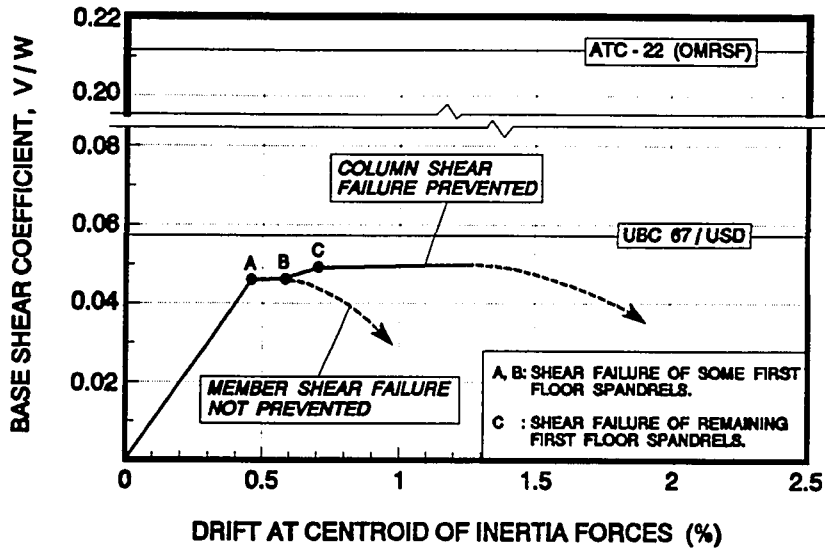
Figure 4.18 Base shear coefficient and drift at the centroid of inertia forces relationship for the twelve-story building in the short direction. Case 1: member shear failure not prevented. Case 2: shear failure prevented only in columns.
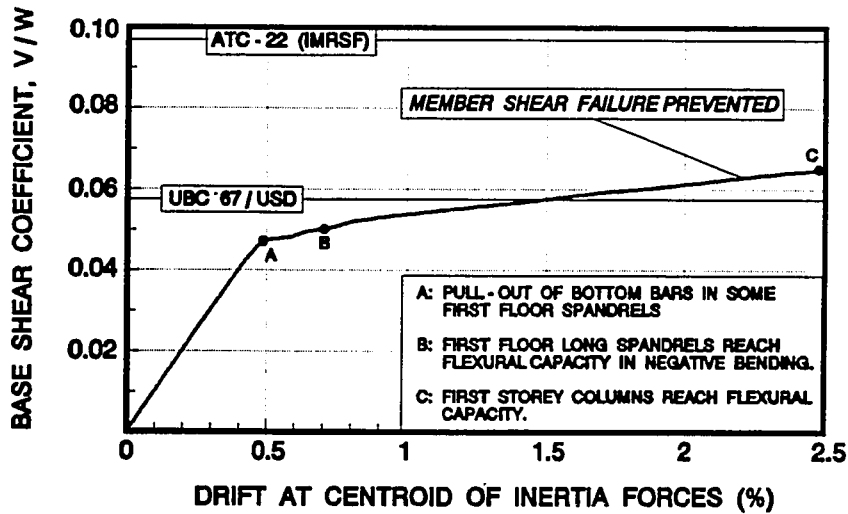
Figure 4.19 Base shear coefficient and drift at the centroid of inertia forces relationship for the twelve-story building in the short direction. Case 3: shear failure prevented in all members.

line in Fig. 4.18. It must be indicated that any restraining action provided by the slab after shear failure of the beams has been ignored in the analysis. This restraining action will help increase the overall stiffness and strength of the building and, therefore, the actual strength and stiffness reduction of the structure may not be as large as that implied by the results shown in Fig. 4.18.

Also shown in Fig. 4.18 are the required base shear coefficients for the structure according to the ultimate strength provisions of the 1967 UBC [5] and the recommendations of the ATC-22 [12] for an ordinary moment resisting space frame (OMRSF) with brittle elements. Since shear failure of columns and beams was not anticipated in the original design of the building, actual lateral strength of the structure does not meet the required strength by the 1967 UBC. Furthermore, the required lateral strength by the provisions of the ATC-22 is several times larger than that obtained when shear failure of members is included in the analyses.

Fig. 4.19 shows the base shear coefficient and drift relationship for case 3. In this case, the building stiffness changes at a drift of about 0.5 %, indicated as point A in Fig. 4.19. The sharp reduction of stiffness at this load level is mainly due to the anchorage failure of bottom beam bars in some of the spandrels of the first floor. Soon after this event, at a drift level of about 0.7% (point B), the longer spandrels of the first floor reached their estimated ultimate moment capacity in "negative" bending. Also at this drift level, yielding at the base of first story columns commenced. The building continued to carry additional load through yielding and strain hardening of the column sections until a drift of about 2.5%. At this drift level, some of the first story columns reached their estimated ultimate bending moment capacity (point C).

The results obtained above for case 3, indicate that while columns would be able to undergo large drift levels before reaching their flexural capacity, beams are relatively weak in comparison to the columns and would experience significant damage and loss of strength beyond the 0.7% drift level. On the basis of these results, ultimate strength of the building was conservatively defined as the base shear coefficient corresponding to a drift level for the centroid of inertia forces of 1%. However, the curve is fairly flat and the strength would not be much larger at a drift value of 2.5%.

Also shown In Fig. 4.19 is the required lateral strength by the ultimate strength design provisions of the 1967 UBC [5] (load and strength reduction factors included). The estimated lateral strength of the building (as define above) is slightly lower than that required by the 1967 UBC. One possible explanation of this result is the unexpected premature anchorage failure of bottom bars in the spandrel beams which is the main cause of the sharp reduction in the stiffness of the building as described above.

Similarly, the lateral strength of the building is compared in Fig. 4.19 to that required by the ATC-22 [12] for an intermediate moment resisting space frame (IMRSF, i.e.; frames with some degree of ductile detailing). The lack of adequate lateral strength of the building implied by the provisions of ATC-22 is apparent. Notice, however, that the required strength in this case is approximately half of that required for cases 1 and 2 in which column shear failure was the governing mode of failure of the building.

Also, notice that the lateral strength of the structure for the flexural dominated behavior (case 3), is only slightly higher than that obtained for the shear dominated behavior (cases 1 and 2). This result suggests that only a small increase in the shear capacity of beams and columns would be required to change the brittle mode of failure of cases 1 and 2, to a more ductile and reliable building response as obtained for case 3. Further, it appears then that shear strengthening of columns and beams should be considered as part of a retrofit scheme.

4.4 PROTOTYPE STRUCTURE III - SEVEN-STORY BUILDING

4.4.1 General Description

The third building chosen for study is representative of residential and office buildings constructed during the mid 1950's. The prototype structure is a seven story reinforced concrete structure. Typical plan view and elevation in the longitudinal direction of the building are presented in Fig. 4.20. The lateral load resisting system consists of six structural walls (8" thick) in the short direction and moment resisting frames in the longitudinal direction. Exterior frames have 8 in. by 72 in. deep spandrel beams and 18 in. by 24 in. rectangular columns over the entire height of the building. Corner columns are 18 in. by 18 in. and form part of the boundary element for the outer structural walls. Spandrel beams are eccentric with respect to the column axis; flush with the interior face of the
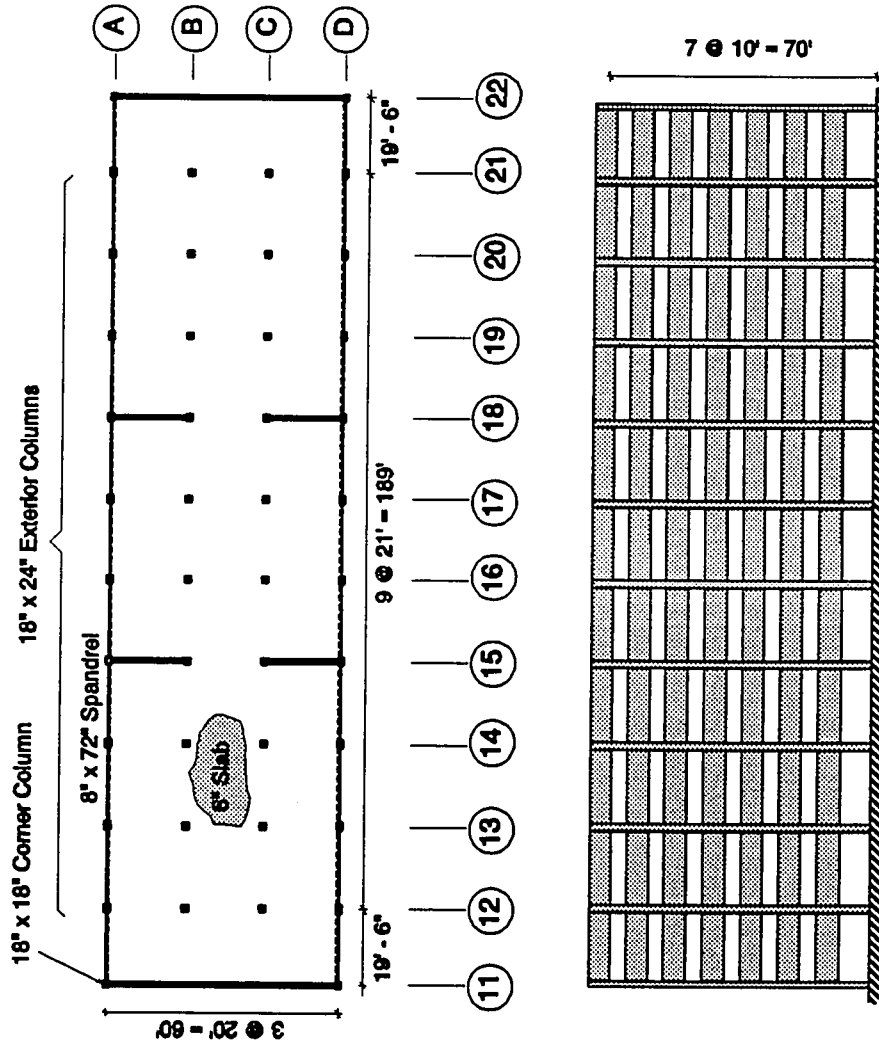
Figure 4.20 Plan view and longitudinal elevation of the 7 story building.

columns. A one-way floor slab, 6 in. thick, spans between the spandrels and interior shallow beams (the latter are not shown in Fig. 4.20 for clarity). Concrete type was specified as normal weight, with a compressive strength of 3000 psi. All reinforcing steel was specified as Grade 40, except for the column vertical steel which was specified as Grade 50.

4.4.2 Seismic Evaluation

Seismic design of the building followed the provisions of the 1955 UBC [9], while design of the reinforced concrete members was based on the working stress design provisions of the 1956 ACI code [10]. In the short direction of the building, the structural walls provide a very stiff and strong lateral load resisting system which will be assumed to have adequate lateral strength. In the longitudinal direction, the presence of the deep spandrel beams in the perimeter frames produce "captive" columns of only 4 ft. height. Flexural stiffness of these "captive" columns is almost six times larger than that of interior columns. Thus, interior frames are much more flexible than perimeter frames and it is reasonable to assume that perimeter frames will carry most of the lateral forces. Based on this assumption, only the perimeter frames were considered in the evaluation and in the subsequent analyses of the building.

Notice also that the clear length of the columns in the first story is almost twice that of the columns on the upper floors which essentially creates an unintended "soft" first story.

4.4.2.1 Reinforcing Details and Member Strength

Typical cross section details and reinforcing schedule for beams and columns of the perimeter frames are presented in Figs. 4.21 and 4.22 respectively. Based on the evaluation of the reinforcing layout, the main deficiencies found in this structure are summarized below:

a) *Lap Splices in Columns:*
Prior to the development of the ductility provisions for buildings in seismic zones, column splices were commonly designed as compression splices and located just above the slab floor level. This building was not an exception to this practice as can be seen in Fig. 4.22. Assuming a 20 bar diameter lap, as required by the 1956 ACI code [10], splice failure prior to yielding of the bars is expected in all sections at the base of first story columns. Because of the

Typical @ interior spans

STIRRUP SCHEDULE

1.5" (clear)   ¾" (clear)

#4 @ 18"

3' - 6"

6" slab

2' - 0"

8"

Typical beam cross section
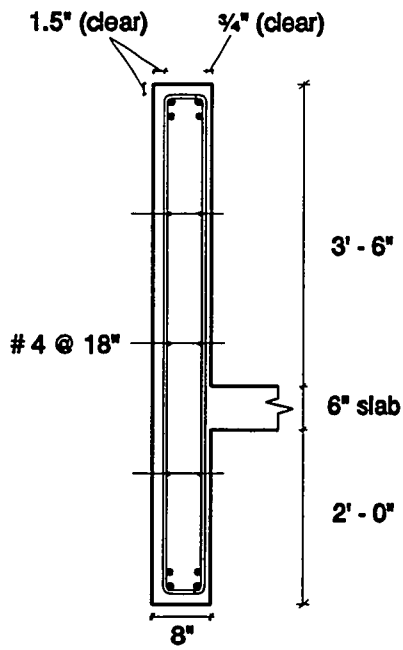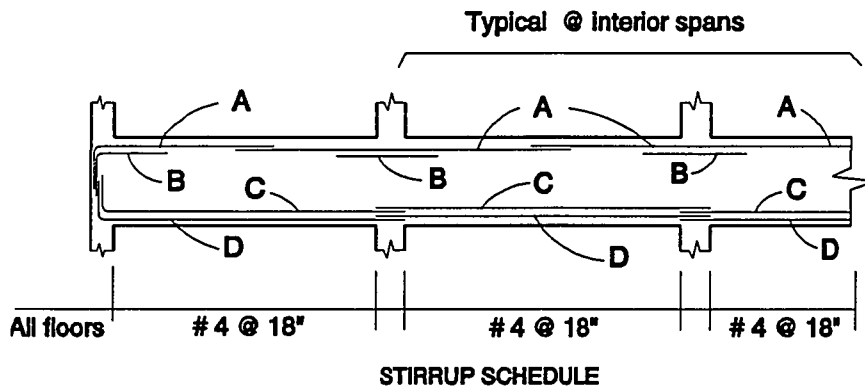
BEAM REINFORCING SCHEDULE				
Floor #	A	B	C	D
1ˢᵗ to 2ⁿᵈ	2#8	2#8	2#7	2#8
3ᵃ to Roof	2#8	2#7	2#7	2#8

Figure 4.21 Beam reinforcing details and schedule for the 7 story building.

	MAIN REINFORCEMENT	
Story Level	A - 12 through A - 21 D - 12 through D - 21	A - 11 & A -22 D - 11 & D - 22
1ST to 3RD	8 # 11	4 # 9
4TH to Roof	4 # 10	4 # 9
	TIES	
1ST	# 4 @ 12"	# 3 @ 15"
2ND	# 4 @ 16"	# 3 @ 18"
3RD	# 3 @ 15"	# 3 @ 18"
4TH	# 3 @ 16"	# 3 @ 18"
5TH to Roof	# 3 @ 18"	# 3 @ 18"
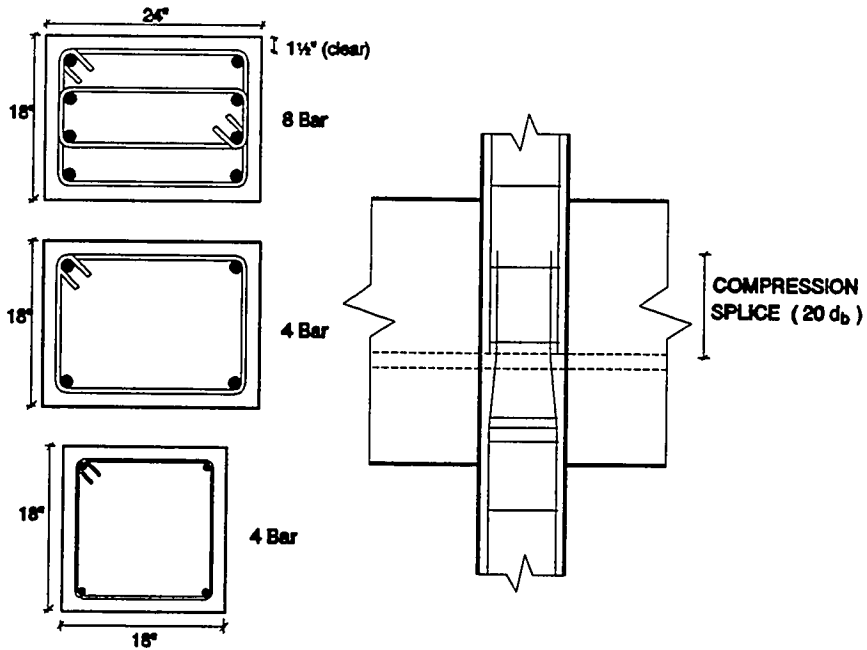
Figure 4.22 Column reinforcing schedule and details for the 7 story building.

presence of the deep spandrels that extend above the floor level in the second and upper stories, the section of maximum stresses for the column reinforcement was assumed to be at the top face of spandrels. The development length of the reinforcement is assumed equal to the height of the spandrels above the floor level; i.e. 42 in.(see Figs. 4.21 and 4.22). Such a development length is insufficient to prevent a splice failure of the reinforcement in the second and third stories, but is adequate to develop yielding of the bars in the fourth and upper stories. For sections located at the top of columns, the reinforcement was assumed to develop the yield strength in all stories.

b) _Anchorage of Bottom Reinforcement in Beams:_

In spite of the low level of lateral forces used to design the building, moment reversals at the beam ends due to earthquake loads were expected and therefore, the anchorage of bottom reinforcement was designed as "negative" reinforcement. The provisions for development length of reinforcement of the 1956 ACI code [10] do not meet the present requirements of the 1989 ACI [4] code, but because of the lower yield strength of the steel reinforcing bars utilized in beams (40 ksi), all bottom reinforcement will develop yielding. Nonetheless, these bars will not be able to reach their ultimate strength and anchorage failure is anticipated soon after reaching strain hardening.

c) _Transverse Reinforcement in Columns:_

Following common practice of the 1950's, transverse reinforcement was designed to meet the shear forces as obtained from the 1955 UBC [9]. Consequently, the transverse reinforcement provided in the columns does not ensure the development of the flexural capacity of the columns. Therefore, column shear failure prior to column hinging is expected in all floor levels.

d) _Transverse Reinforcement in Beams:_

Because of the large cross section of the spandrel beams, the design shear forces can be resisted with a small amount of transverse reinforcement. In fact, rigorous application of the provisions of the 1956 ACI code [10] would have called for a 36 in. spacing (half of the depth of the member) instead of the 18 in. spacing that was actually provided in the beams, as can be seen in Fig. 4.21.

This smaller spacing of the web reinforcement was probably provided to simplify the construction process, and it will enhance the shear behavior and strength of the spandrels. Detailed calculations using current design provisions indicated that the flexural strength of the beam ends will be developed prior to a shear failure.

e) *Joint Shear Strength:*

Transverse reinforcement through the joint region was probably not provided at all. In spite of the lack of confinement in the joint region, maximum computed shear stresses at the joint were much lower than the expected capacity of the connection. Thus, joint shear failure is unlikely to occur, even in the case that columns develop their flexural strength prior to failing in shear.

4.4.2.2 Modeling Assumptions and Parameters

The previous evaluation of the building indicates that the critical modes of failure of the members are column shear failure and/or splice failure of reinforcement of sections at the base of columns. Column shear failure was modeled following the same procedure described in section 4.3.2.2 c). Moment - rotation envelopes for column end sections were modeled as described in section 4.2.2.2 b) (See Fig. 4.7). Beam shear failure was not anticipated and therefore it was not considered as a possible mode of failure in the analyses. Anchorage failure of bottom beam bars is expected after yielding of the reinforcement and it was modeled as described in section 4.2.2.2 a). The moment - rotation envelopes adopted for the beam end sections are therefore similar to those shown in Fig. 4.16.

4.4.2.3 Lateral Stiffness and Strength

Estimation of the lateral strength of the structure followed the same procedure outlined for the previous two buildings studied; applying a uniform lateral load distribution over the height of the building. Two possible modes of failure were considered in the evaluation. First, shear failure of columns was included as one possible failure mechanism for the building, in addition to potential anchorage failure of reinforcement in columns and beams. The second mode of failure included failure of column splices and anchorage failure in beams as above. However, shear failure of columns was prevented in the second case.

The response of the building for the two cases studied is presented in Fig. 4.23 as the relationship between the base shear coefficient and the drift at the centroid of the inertia forces. The results indicate that shear failure of the columns initiated at the second story and propagated rapidly to the third and first story columns respectively. The sudden failure of these elements resulted in an abrupt reduction of the lateral stiffness of the building and led to the sudden collapse of the structure, as shown in Fig. 4.23. Because of the low shear strength of the "short" columns in the building, shear failure begins at relatively small lateral drifts (≈ 0.1 %).
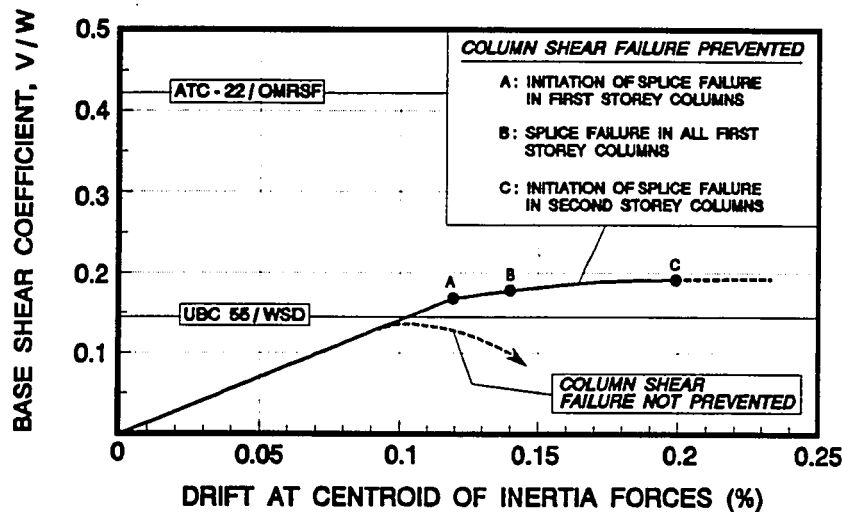
Figure 4.23   Base shear coefficient and drift at centroid of inertia forces relationship for the seven-story building in the longitudinal direction.

For the second failure mechanism studied, in which column shear failure was prevented, the building exhibited linear behavior until failure of the splices in the first story columns. At this load level, the lateral stiffness of the building was reduced considerably as shown in Fig. 4.23. At a drift level of about 0.14%, failure of the splices in all first story columns was reached. The latter event, however, did not have a significant impact on the lateral stiffness of the building. A probable explanation of this result is the large number of columns present in the longitudinal direction of the building which allowed for a gradual redistribution of forces within its members. Subsequent stiffness degradation of the building

is mainly due to the yielding of beams of the first floor. Peak lateral capacity for the building is assumed to be reached at about a drift level of 0.2% when splice failure of the second story columns initiated.

A comparison between the required base shear coefficient by the 1955 UBC [8] code and that predicted for the two cases studied above is presented in Fig. 4.23. In spite of the premature shear failure of columns considered in the first case, the estimated lateral strength of the building is only 10% smaller than that required by the prevailing code. If shear failure is prevented in columns as in the second case studied, the predicted lateral strength of the building is approximately 20% larger than that required by the 1955 UBC.

On the other hand, the current provisions of the ATC-22 [12] for an OMRSF would require at least twice as much lateral strength as that estimated, even for the case in which column shear failure was prevented in the analysis.

4.5 GROUND MOTIONS

4.5.1 Selected Earthquake Records

The ground motion selection criterion used in this study was based on major possible earthquakes that could be expected in a zone of high seismic risk, on firm and soft soil conditions. Accordingly, five earthquake records were used as input motion for the evaluation of the dynamic response of the existing and retrofitted buildings. These records correspond to four earthquakes: El Centro 1940, U.S.A., Chile 1985, Mexico 1985 and Loma Prieta 1989, U.S.A. Table 4.1 shows information regarding the seismic events and soil characteristics for the selected ground motions. Ground acceleration time histories for the records are presented in Figs. 4.24 and 4.25. The El Centro, Viña del Mar and Corralitos records possess a predominant high frequency content, typical of "near-fault" earthquakes and represent an extreme event on firm soil conditions. The Mexico City - SCT1 and Oakland records were both measured on soft soil sites, as shown in Table 4.1. The characteristics of the Mexico City - SCT1 record and its influence on the dynamic response of structures have been well studied and clearly represents one of the most severe

Table 4.1 Earthquake data and site information for ground motions selected for study.

Location	Richter Magnitude	Epicenter Distance (km)	Station & Component	Peak Ground Acceleration	Soil Type
Imperial Valley, California, U.S.A. (May 1940)	6.5	11.5	El Centro N00E	0.35 g	Alluvium
CHILE (March 1985)	7.8	110	Viña del Mar S20W	0.36 g	Alluvium
MEXICO (Sept. 1985)	8.1	400	Mexico City- SCT1 N90E	0.17 g	Silty Clay deposits
Santa Cruz Mtns., California, U.S.A. (October 1989)	7.1	5	Corralitos N00E	0.63 g	Rock
		76	Oakland (Outer Harbor Wharf) N55W	0.27 g	Bay Mud
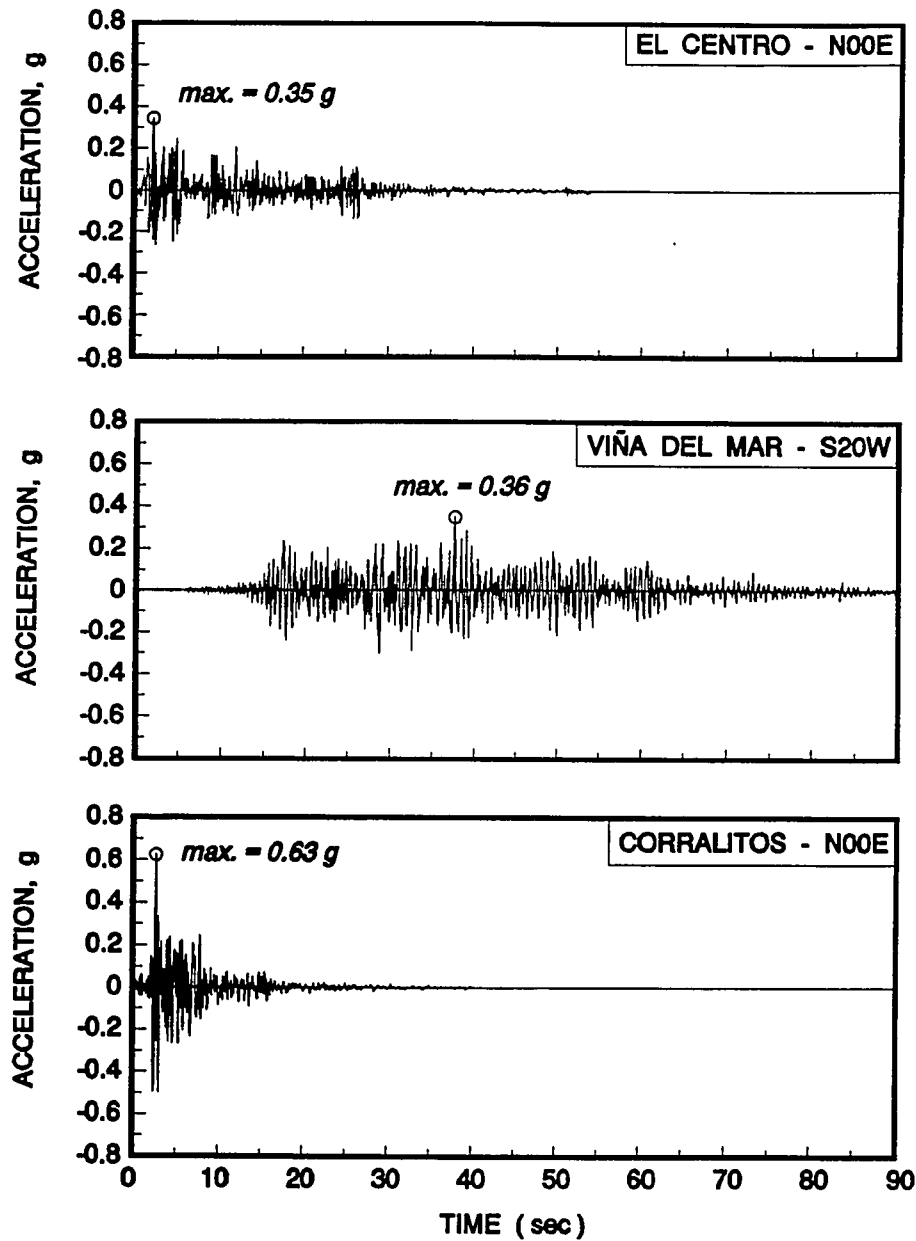
Figure 4.24 Ground acceleration for the earthquake records measured on firm soil sites. El Centro (N00E), Viña del Mar (S20W) and Corralitos (N00E).
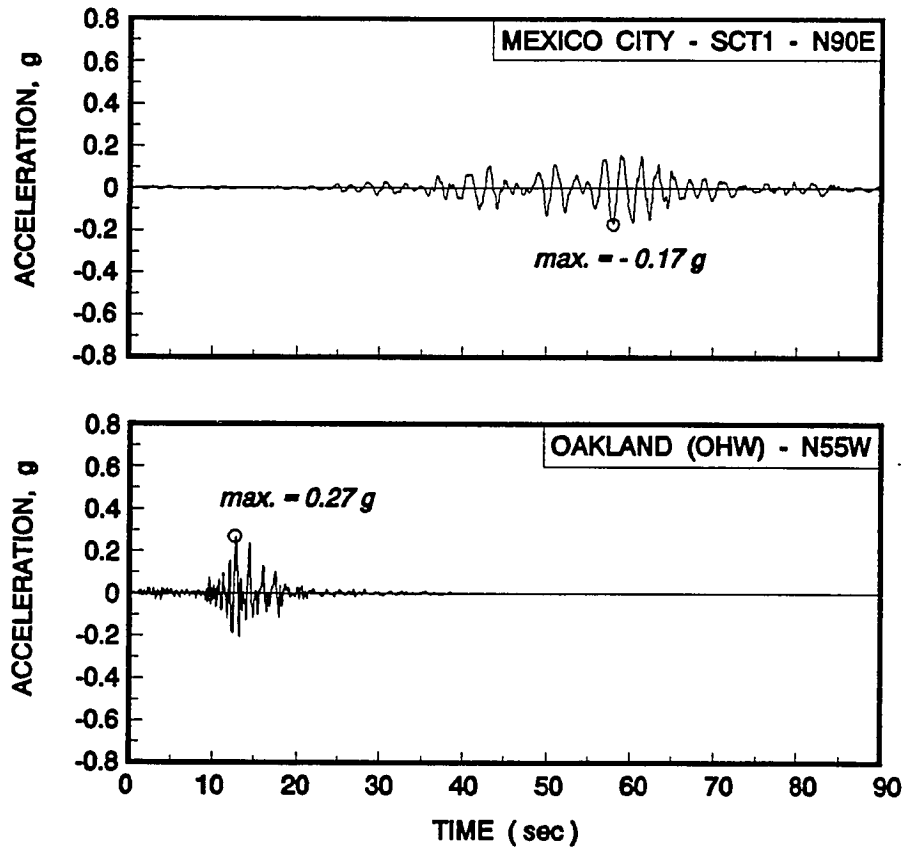
Figure 4.25 Ground acceleration for the earthquake records measured on soft soil sites. Mexico City - SCT1 (N90E) and Oakland (Outer Harbor Wharf - N55W)

recorded events on soft soil conditions. The Oakland record is interesting because it is one the strongest components measured on soft soils during the Loma Prieta earthquake. In addition, it was recorded on the same type of soil and within a few miles of the collapsed section of the Cypress viaduct [16]. The Mexico City - SCT1 and Oakland records will be used to study the soil-structure interaction effects using the procedure and the soil properties described in Chapter III (Table 3.1).

4.5.2 Elastic Response Spectra

The elastic pseudo-acceleration response spectra corresponding to a 2% damping for the ground motions measured on firm soil sites are presented in Fig. 4.26. The highest spectral value is obtained for the Corralitos record with a peak value of 2.8 g at about 0.3 seconds. This spectral ordinate largely exceeds the peak spectral values for the rest of the selected ground motions on firm soil. On the other hand, the spectral ordinates for the El Centro record are not as high as those of the Viña del Mar and Corralitos records. However, the record for El Centro has the advantage of having a significant low frequency content that is unusual for a record measured on firm soil. Thus, the El Centro record scaled to a peak ground acceleration of 0.5 g was included as input motion in addition to the original record. The scaled El Centro record represents a more severe event on firm soil conditions while at the same time it maintains the frequency content characteristics of the original record. The response spectrum corresponding to the scaled version of the record for El Centro is also shown in Fig. 4.26.

Overall, the spectral ordinates for the records measured on firm soil reveal the predominant high frequency content of these components and define a response spectrum envelope with ordinates ranging from 1 to 2.7 g in the period range of 0.1 to 1 seconds. For the period range of 1 to 1.5 seconds, the scaled El Centro and the Viña del Mar records have the largest spectral ordinates with almost identical values. The rest of the period range is clearly dominated by the scaled El Centro record.

The elastic pseudo-acceleration response spectra corresponding to a 2% viscous damping for the two records measured on soft soil sites are presented in Fig. 4.27. Both records exhibit similar peak spectral ordinates. However, the predominant frequency content of these two records is completely different. Maximum response for the Mexico City - SCT1 record is obtained at a natural period of about 2 seconds, while maximum response for the Oakland record occurs at a natural period of about 0.6 seconds.

Elastic displacement response spectra for a 2% viscous damping are presented in Figs. 4.28 and 4.29 for the ground motions on firm and soft soil sites respectively. As can be seen in Fig. 4.28, the displacement spectral ordinates for the records on firm soil are primarily dominated by the Scaled El Centro record, particularly in the long period range.
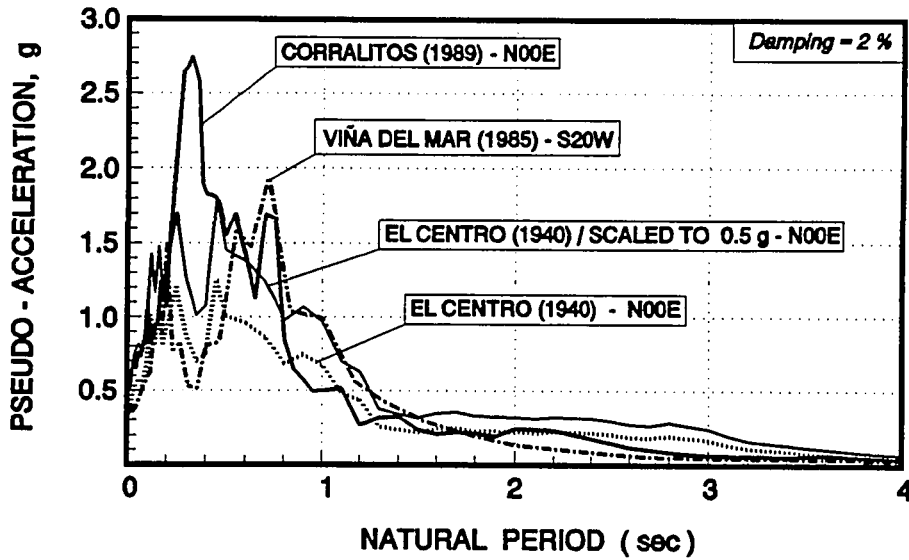
Figure 4.26 Elastic response spectra (Pseudo-Acceleration) for selected ground motions on firm soil sites.
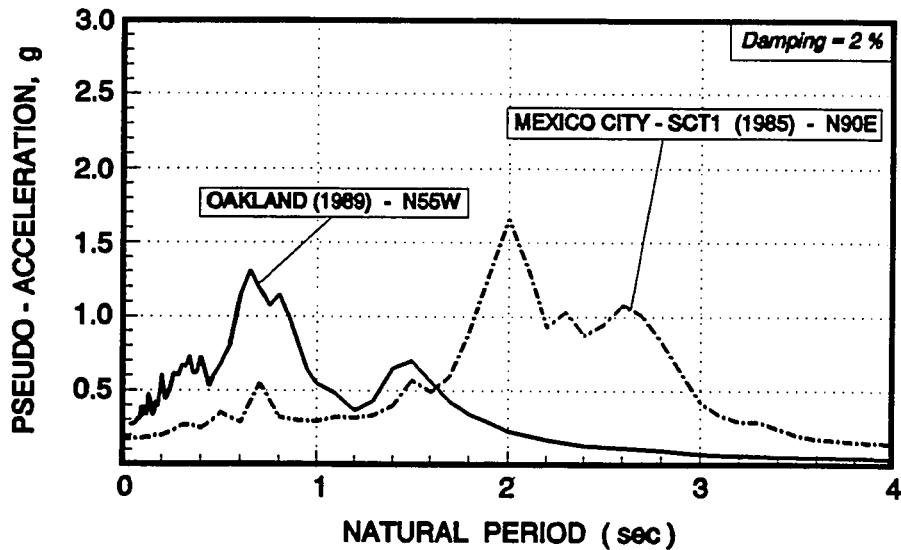
Figure 4.27 Elastic response spectra (Pseudo-Acceleration) for selected ground motions on soft soil sites.
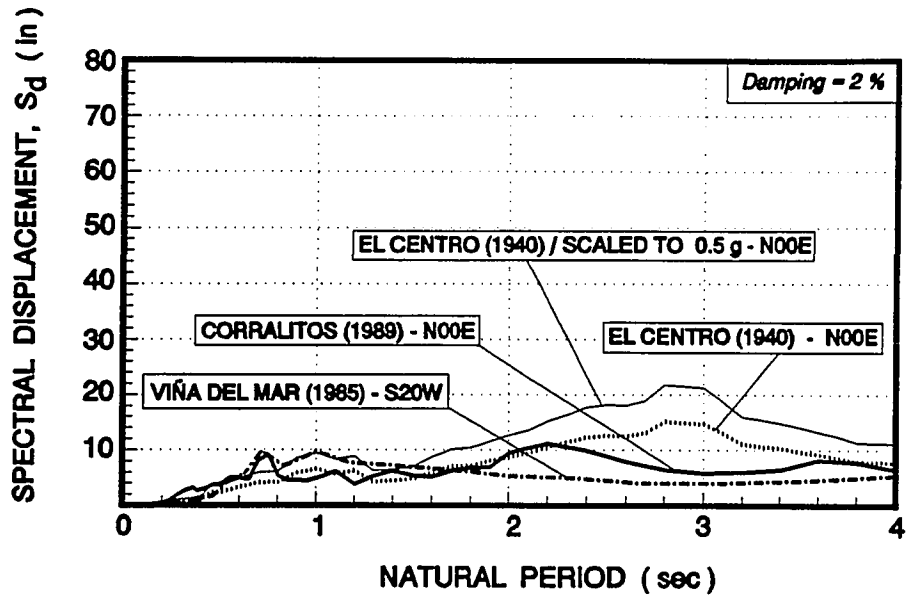
Figure 4.28 Elastic response spectra (Displacement) for selected ground motions on firm soil sites.
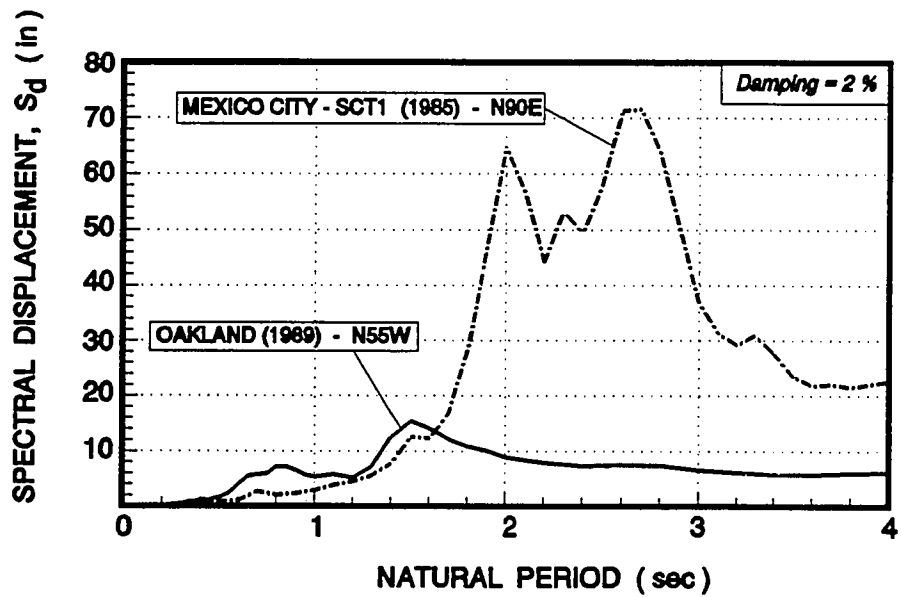
Figure 4.29 Elastic response spectra (Displacement) for selected ground motions on soft soil sites.

• For the records measured on soft soil sites, the spectral ordinates are quite similar in the short period range until a period of about 1.6 seconds, but then are largely dominated by the Mexico City - SCT1 record in the long period range. Notice the extremely high displacement requirements imposed by the latter record when this is compared to the rest of the records considered in this study on firm and soft soils.

4.5.3 Inelastic Ductility Displacement Spectra

In order to evaluate the effects of inelastic behavior on the dynamic response to the selected ground motions, displacement ductility demands were calculated using a bi-linear, stiffness degrading, fixed-base SDOF model. Three yield strength levels, C_y, were considered in the analyses: 10, 30 and 50% of the weight of the oscillator. Strain hardening was arbitrarily assumed as 15 % of the initial stiffness and viscous damping was assumed to be 2 % of the critical damping value. The results are presented in Figs. 4.30 and 4.31 for the ground motions on firm and soft soil conditions respectively. As can be seen in Fig. 4.30, the highest displacement ductility demands for the records on firm soil are obtained for the Corralitos and the scaled El Centro records. Notice that the ductility demands for the scaled El Centro, Viña del Mar and Corralitos records are practically the same in the period range of 0 to 1 second for a low yield level (C_y = 10%). However, when the yield level is increased to 30 %, the reduction in the ductility demands is much higher for the Viña del Mar and El Centro records than for the other two records. Notice the high ductility demands required by the Corralitos record in the short period range, even for a yield strength of 50 % of the weight of the structure. For low yield strength levels (C_y = 10 %), the scaled El Centro exhibits ductility demands that are as high as the rest of the records on firm soil for the period range up to 1 second, and are higher in the long period range.

Analyses of the displacement ductility demands for the records on soft soils revealed the following results. Both records exhibit very high ductility demands for a structure with a relatively low yield strength (C_y = 10%). Nonetheless, these demands are drastically reduced over the entire period range upon increasing the yield strength to 30%, particularly for the Mexico City - SCT1 record. Notice also that for a yield strength of 10% and for periods larger than 0.6 seconds, the Mexico City - SCT1 record shows higher ductility demands than the Oakland record. However, when the yield strength is increased to 30 %
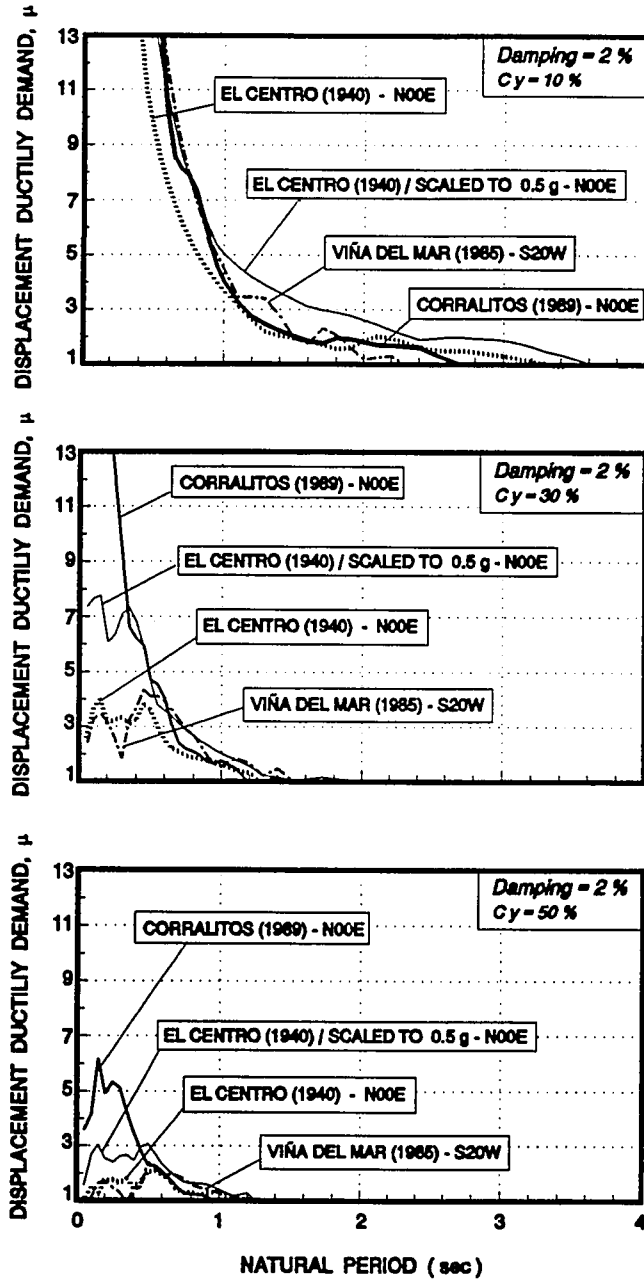
Figure 4.30 Displacement ductility demands for selected ground motions on firm soil sites. Stiffness degrading model and 15% strain hardening. Yield strengths of 10, 30, 50% of the weight of the oscillator.
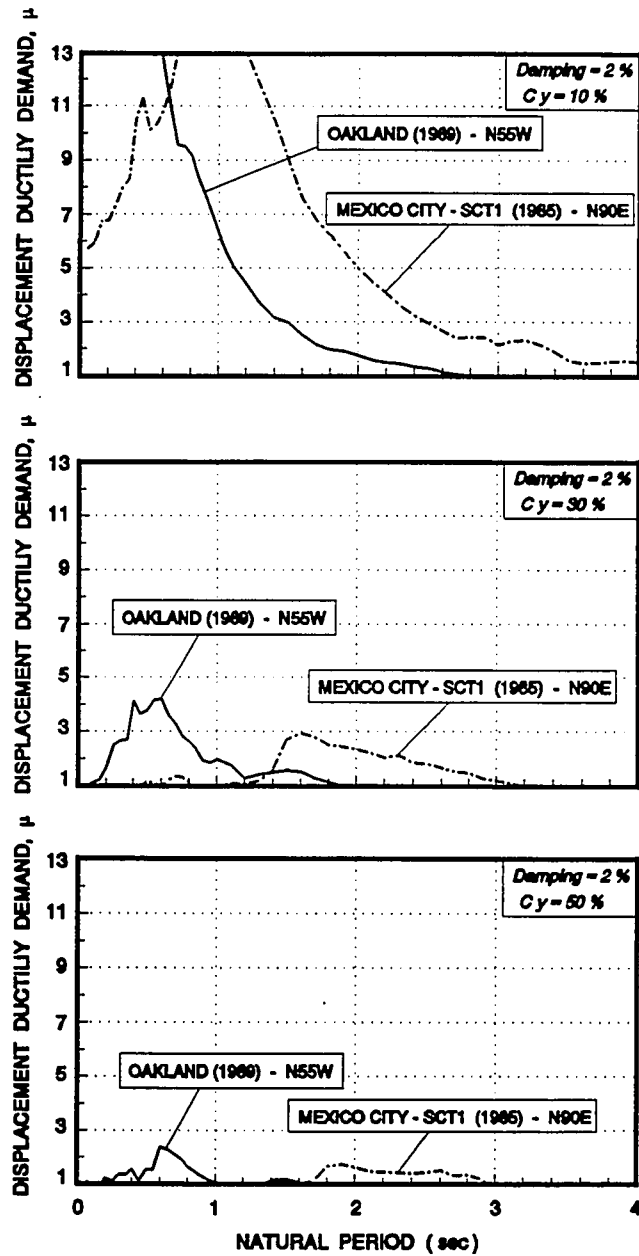
Figure 4.31   Displacement ductility demands for selected ground motions on soft soil sites. Stiffness degrading (fixed-base) model and 15% strain hardening. Yield strengths of 10, 30, 50% of the weight of the oscillator.

or higher, this situation is reversed and it is the Oakland record that imposes higher ductility demands for periods up to about 1.4 seconds.

It must be emphasized that the displacement ductility demands obtained above for the records on soft soil sites do not include the foundation flexibility nor the interaction between the soil and the super-structure. Previous studies [17] suggest that ductility demands tend to increase when soil-structure interaction effects are considered and therefore the demands shown in Fig. 4.31 are likely to be higher when these effects are considered.

The results presented above suggest that a retrofit scheme for short period structures (T < 1 second) on firm soil, must be able to supply a considerable amount of ductility in addition to a high level of strength (see Fig. 4.30). These high ductility demands may impose a tough requirement on the retrofit schemes for structures on firm soil sites. While it is relatively simple to increase the strength of an existing structure, it is not as easy to provide it with adequate ductility. In addition, most strengthening schemes produce an increase in stiffness and consequently shorten the period of the structure, which will call for even higher ductility demands on the retrofitted structure. On the other hand, a similar strengthening scheme used on soft soil sites, will have to satisfy lower ductility demands for an equivalent strength level (see Fig. 4.31).

For long period structures (T > 1.5 seconds), the ductility demands are relatively low for all records measured on firm soil sites and also for the Oakland record. For the Mexico City - SCT1 record, however, a similar retrofit scheme must satisfy higher ductility demands, unless the retrofitted structure is stiffened to such a degree that its natural period is shortened to a value of about 1 second or smaller.

CHAPTER V

ON THE BEHAVIOR OF POST-TENSIONED BRACING SYSTEMS

5.1 GENERAL

Concentric bracing systems with medium to short slenderness ratio braces (braces that carry tension and compression) have been the subject of numerous studies and their behavior under static and dynamic loads is relatively known and understood. In contrast, the use of slender braces (braces that carry tension only) with initial prestress is uncommon and its behavior unfamiliar.

The present Chapter reviews basic behavior of post-tensioned bracing and identifies main parameters that significantly influence the behavior of the system. The study focuses on the effects of initial brace prestressing and material strength on the lateral stiffness and strength of the structure, and on the ability of the system to dissipate energy under reversed cyclic loading. The results obtained are used to establish the design and performance criteria of the post-tensioned bracing as a retrofit scheme.

5.2 SINGLE-STORY BUILDING

Consider the single-story - single-bay reinforced concrete frame shown in Fig. 5.1. The frame represents a portion of a frame structure that is in need of seismic retrofit. For simplicity, the original frame structure was selected to have ductility, but a lack of adequate strength. Member yielding was selected to occur prior to reaching an inter-story drift of 1 %; behavior believed to be representative of structures requiring seismic retrofit. To strengthen the existing frame, two high strength steel rods were provided as X-bracing, as shown in Fig. 5.1. Brace size was selected as the smallest possible size available for this type of material. Modeling and material properties used to emulate the behavior of steel rods followed the procedure outlined in Chapter III.

As indicated in Chapter II, one of the advantages of post-tensioned bracing systems is that braces can be initially prestressed, which will, in general, improve the performance of the braces and that of the braced structure. The effect of initial prestressing on the steel

120
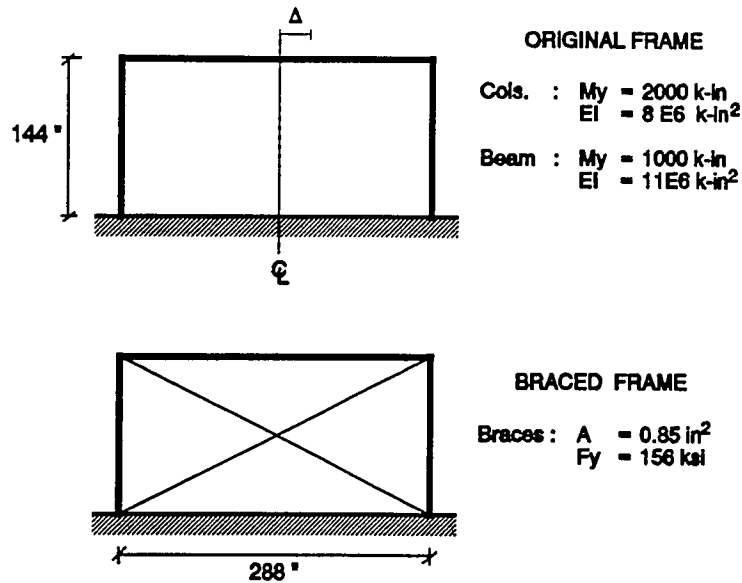
Figure 5.1   Single-story - single-bay reinforced concrete frame. Original bare frame and braced frame with high-strength slender braces.

braces is to produce a shift in the axis of the axial load - elongation relationship for the braces, as illustrated in Fig. 5.2. The shift results in an apparent compression strength of the brace equal to the prestressing force, F_p, and in apparent yield strength in tension equal to the yield strength of the brace, F_y, minus the initial prestress force, F_p. Brace initial stiffness for the brace which elongates and for the brace that shortens is the same, and therefore both braces will contribute to the initial lateral stiffness of the structure. If no initial prestress is provided, only the brace which elongates contributes to the lateral stiffness of the structure (tension-only-brace system). In the latter case, the brace that shortens begins to sag as soon as the lateral load is applied.

Initial brace prestressing will also generate additional internal forces on the existing structure, axial forces and bending moments in beams and columns. For clarity, however, it will be assumed that the beam has infinite axial stiffness. Therefore, bending moments in columns due to shortening of the beam when braces are initially prestressed will be neglected for the single story structure. The effects of initial brace prestressing on the distribution of initial forces in frame members is discussed in the following section for the
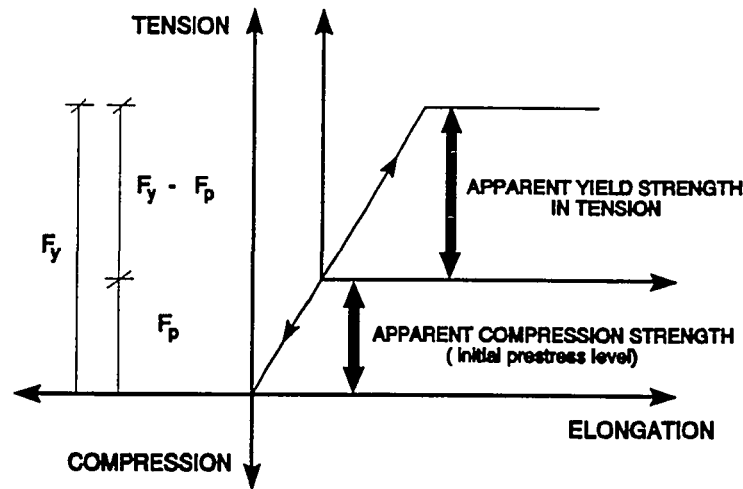
Figure 5.2 Effects of initial prestress on high slenderness ratio braces.

analysis of multi-story buildings.

5.2.1 Lateral Stiffness and Strength

To evaluate and compare the stiffness and strength of the original and braced structure, the single-story structure was subjected to a monotonically increasing lateral load until a lateral drift of 2%. For the braced structure, four different levels of initial brace prestressing were investigated, mainly to include various alternatives for the retrofit scheme. The selected prestressing levels were: 0, 25, 50 and 75% of the brace yield strength. Fig. 5.3 shows the lateral load and inter-story drift relationship obtained for the original and braced structures. In this figure, the lateral load is normalized with respect to the strength of the original frame at an inter-story drift of 2%.

The increase in lateral stiffness provided by the bracing system is apparent in all cases. The minimum increase in initial stiffness is obtained when braces are not initially prestressed because only the brace which elongates contributes to the lateral stiffness of the structure. The maximum increase in the initial lateral stiffness is obtained when some initial prestress is given to the braces because both braces contribute to the lateral stiffness of the frame, as discussed above.
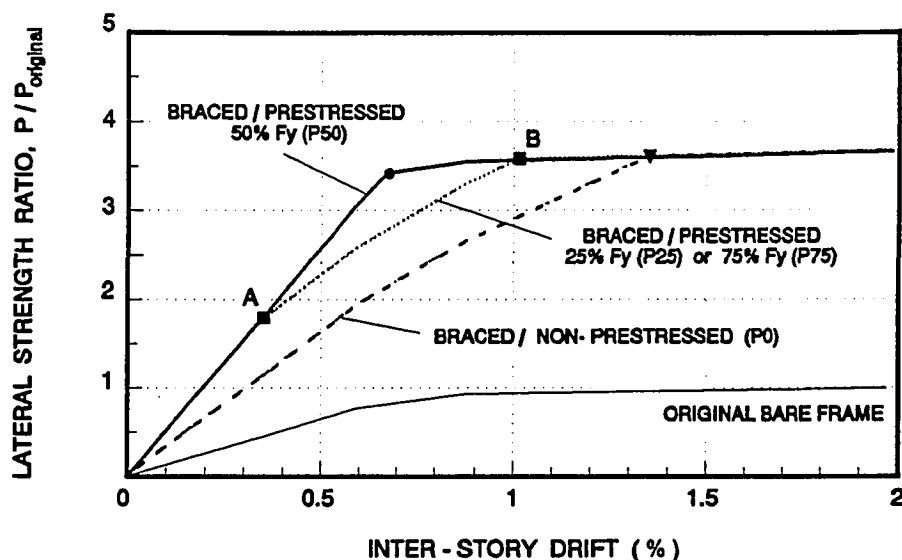
Figure 5.3 Lateral load and inter-story drift relationship for the original bare frame and braced frame with different levels of initial prestress for the braces.

For the structure with braces without initial prestressing (structure P0), the brace that elongates remains within the elastic range until a drift level of about 1.35% when this brace reaches its yield strength. The non-linear behavior exhibited by the structure prior to yielding of the brace is due solely to yielding of the beam and the columns of the existing frame. As described above, the brace which shortens has no contribution to the lateral behavior of the structure. Clearly, the lateral resistance provided by the bracing system is given by yield strength of the brace that elongates.

For the structure with braces with an initial prestress of 50 % of the brace yield strength (structure P50), the *apparent compression strength* and the *apparent yield strength in tension* of the braces (see Fig. 5.2) is the same; i.e. 50% of the material yield strength. In this case, both braces will contribute to the lateral stiffness of the frame (i.e. remain elastic) until the brace which shortens begins to sag at the same time that the brace which elongates reaches its yield strength. Such a behavior is observed in Fig. 5.3 at a drift level of about 0.68%. As above, the lateral resistance of the bracing system is provided by the

yield strength of the brace which elongates. The additional increase in lateral strength beyond the 0.68% drift is provided by the existing frame alone.

For initial brace prestressing levels of 25 and 75 % of the brace yield strength, the resulting lateral load and drift relationships are identical, as shown in Fig. 5.3. However, the sequence of events in the bracing system is different. Fig. 5.4 shows the loading paths followed by the braces with these two levels of initial prestress, which will help explain the behavior observed in Fig. 5.3. For the structure with braces with initial prestressing of 25% of the material yield strength (structure P25), the *apparent compression* strength (or initial prestress level) of braces is 25% of the material yield strength. At the same time, the magnitude for the *apparent compression strength* in structure P25 is exactly the same as that of the *apparent yield strength in tension* for braces with initial prestress of 75% of brace yield strength in structure P75 (see Fig. 5.4). It is clear then that the brace which shortens in structure P25 will begin to sag at the same load and drift level as that required to yield the brace which elongates in structure P75 (path O - A in Fig. 5.4). Such behavior occurs at a drift level of about 0.35%, point A in Figs. 5.3 and 5.4. Because an elasto-plastic relationship (no-strain hardening) was assumed for the behavior of the braces in tension, the lateral stiffness of the frame is reduced in the same proportion for both structures, P25 and P75, as shown in Fig. 5.3. Beyond the 0.35% drift, only one brace continues to provide lateral stiffness to the frame (brace which elongates in structure P25 and brace which shortens in structure P75). At a drift of about 1% (point B in Figs. 5.3 and 5.4), the sequence of events just described is reversed. The brace which shortens in structure P75 begins to sag at the same load and drift level as that required to yield the brace which elongates in structure P25 (path A - B in Fig. 5.4). Similar to the two cases presented above for braces without prestressing or for braces with initial prestressing of 50% of the brace yield strength, the lateral resistance of the bracing system is provided by the yield strength of only the brace that elongates (brace that shortens reaches its apparent compression strength in every case).

While the lateral load and drift relationship of the two systems (structure P25 and P75) under monotonic load is identical, the energy dissipation characteristics are quite different, as will be shown in the following section.

BRACE WHICH ELONGATES   BRACE WHICH SHORTENS

INITIAL PRESTRESS : 25% Fy (P25)

BRACE WHICH ELONGATES   BRACE WHICH SHORTENS

INITIAL PRESTRESS : 75% Fy (P75)
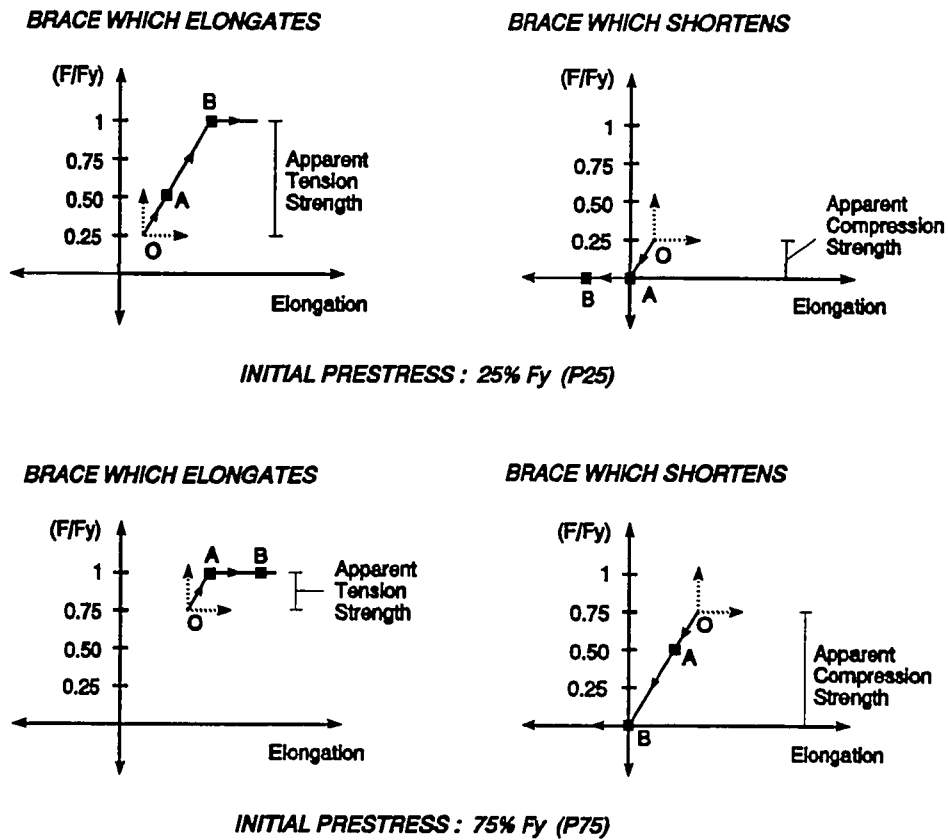
Figure 5.4   Loading paths for braces with initial prestress levels of 25 and 75% of the yield strength.

Note that maximum strength of the bracing system of structures P25 or P75 is reached at a drift level that falls between those obtained for braces with 50 % of initial prestressing and no initial prestressing (see Fig. 5.3). Because of the larger initial stiffness, maximum strength of a bracing system with prestressed braces will always develop at a smaller drift than that of a bracing system with non-prestressed braces. Also note that minimum drift for maximum strength of the bracing system is obtained when braces are initially prestressed to 50 % of yield strength.

Because of the relatively high yield strength of the rod braces, the additional strength provided by the braces to the original frame is substantial ($\approx$ 3.5 times). Notice

that, as in any prestressing system, the level of initial prestressing has no influence on the ultimate strength (strength at 2% drift) of the braced structure. The latter depends exclusively on the available strength of the existing structure and on the strength of the braces.

5.2.2 Hysteretic Behavior

To evaluate the hysteretic characteristics of the bracing system, the single-story braced frame was analyzed under reversed cyclic static loading for all four levels of initial brace prestressing. The selected loading pattern consisted of four full cycles, each one corresponding to a predetermined drift level. The selection of the drift levels was based on the observed behavior under monotonic load and corresponded to particular events in the response of the bracing system. In addition, a final cycle corresponding to a 2% drift was also included as part of the loading pattern. Table 5.1 presents the selected drift levels and the corresponding state of the braces at each drift level. The cyclic loading pattern used in the analyses was the same for all four levels of initial brace prestressing.

The resulting hysteresis cycles for the four levels of initial brace prestressing levels are presented in Fig. 5.5. The hysteretic behavior of the structure is presented in terms of the lateral load ratio (normalized as above) and the inter-story drift ratio. Each full cycle is presented separately for clarity and for the purpose of comparison. Overall, the main effect of initial brace prestressing is to provide the bracing system with the ability to dissipate energy at low deformation cycles due to the yielding of braces in tension. In the first cycle, braces remain within the elastic range for all levels of initial brace prestressing, except for the case with 75 % initial prestress (P75) in which the brace which elongates reaches yielding in tension (see Table 5.1). Notice the difference in behavior of this case with that in which braces are initially prestressed to 25 % of the yield strength (P25). In the latter case, the brace which shortens becomes slack (see Table 5.1) and non-linear elastic behavior is observed with no hysteretic behavior.

In the second cycle, small hysteretic behavior is observed for braces with no initial brace prestressing (P0) and for braces with 25 % initial prestress (P25). The hysteretic behavior is mostly due to the hinging of the beam and columns of the reinforced concrete

Table 5.1 Selected drift levels and corresponding state of braces.

Cycle No.	Drift Level (%)	Brace	State of Brace			
			$P0^*$	$P25^*$	$P50^*$	$P75^*$
1	0.65	Elong.	elastic	elastic	reach yielding	yielded
		Short.	slack	slack	begin to sag	elastic
2	1.01	Elong.	elastic	reach yielding	yielded	yielded
		Short.	slack	slack	slack	begin to sag
3	1.35	Elong.	reach yielding	yielded	yielded	yielded
		Short.	slack	slack	slack	slack
4	2	Elong.	yielded	yielded	yielded	yielded
		Short.	slack	slack	slack	slack

* Initial brace prestress level

frame, because yielding of braces is either non-existent or just developing (see Table 5.1). For braces with 50% (P50) and 75 % (P75) of initial prestress, braces reach yielding in tension and therefore the energy dissipated during the second cycle is higher than that dissipated for braces with lower levels of initial prestress.

In the third cycle, yielding of braces is observed in all cases in which braces are initially prestressed, which allows more dissipation of energy than for the case in which braces are non-prestressed (see Fig. 5.5). In the fourth cycle, yielding of braces in tension is reached in all cases (see Table 5.1) and dissipated energy of the system is significantly increased with respect to that of the previous cycle. However, the hysteresis loop shows significant pinching near the origin in this last cycle.
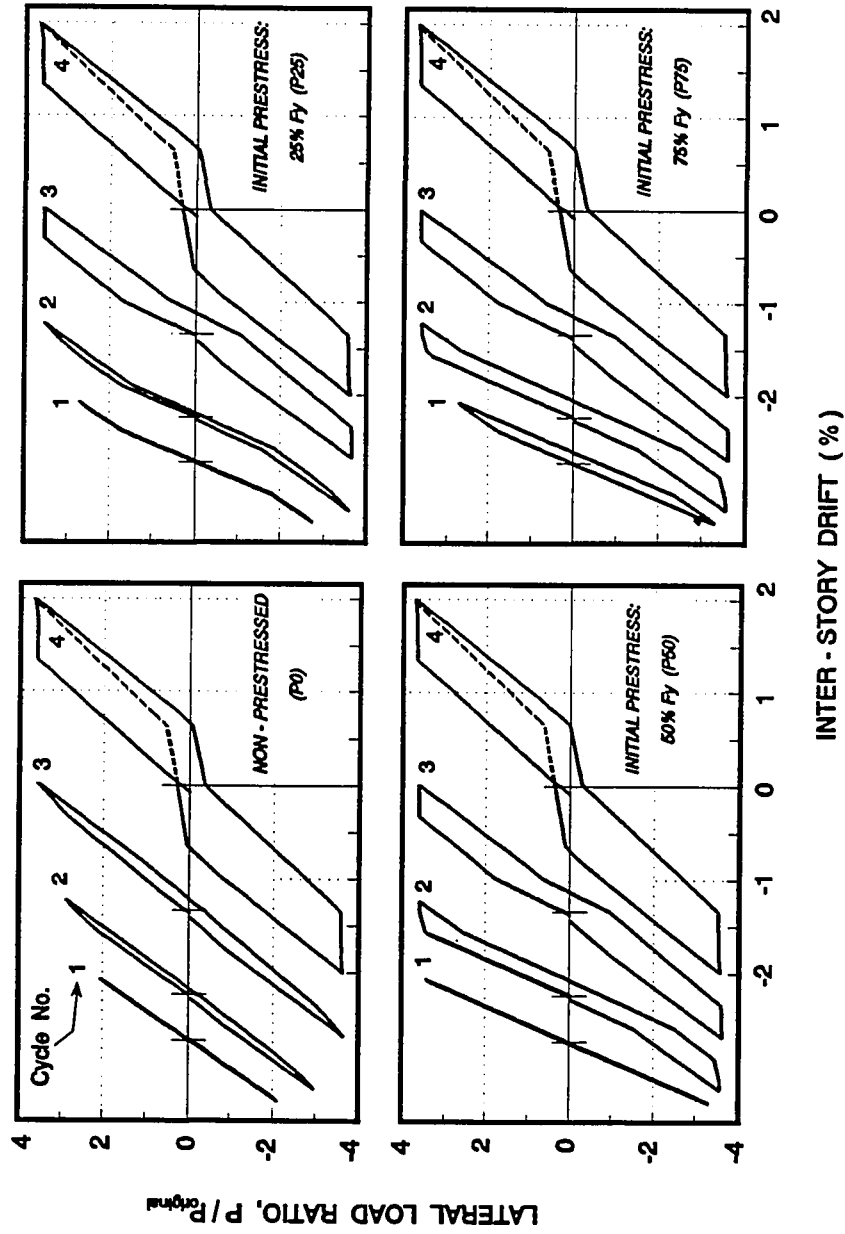
Figure 5.5 Hysteresis cycles for the single-story single-bay braced structure with different levels of initial brace prestressing.

The latter results presented above can be better understood by looking at the variation of the axial force level in the braces at each load cycle. This relationship is presented in Fig. 5.6 for braces with an initial prestress level of 75 % of the yield strength (P75). In addition, the corresponding hysteresis cycles have been reproduced again in this figure, in which particular events are indicated for each load cycle. Because of the high initial prestress level, both braces reach yielding during the first cycle, as shown in Fig. 5.6. Upon reversal of the load, braces unload but they never become slack in this cycle (points 2 & 4). Notice that even though both braces reach yielding, the remaining axial force in the braces upon completion of the first cycle is 50 % of the brace yield strength (point 5). Further, note that the maximum drift level reached during this first cycle corresponds to that in which braces reach yielding and begin to sag simultaneously under monotonic load when braces are initially prestressed to 50% of the yield strength (See Table 5.1). At the beginning of the second cycle, both braces have an initial prestress level of 50 % of the yield strength. Therefore, the behavior of the frame for braces with initial prestress of 75% in the second cycle is the same as that with braces with 50 % of initial prestress. The hysteresis loops are for these two cases are the same, as can be seen in Fig. 5.5.

During the second cycle, both braces yield in tension and become slack. However, by the end of the second cycle there still remains a prestress force of 25 % of the yield strength in the braces (point 13). As above, notice that the maximum drift level imposed on the frame during the second cycle corresponds to that in which braces with 25 % of initial prestress reach yielding in tension under monotonic load (See Table 5.1). The initial state of the structure is then the same as that with braces with 25 % of initial prestress. The hysteresis loop for the third cycle is therefore the same for braces with initial prestress of 25, 50 and 75% of the yield strength, as can be seen in Fig. 5.5. During the third cycle, braces yield and become slack, and by the end of this cycle the initial prestress level is lost (point 21). The maximum inter-story drift imposed on the structure in the third cycle (point 16) is that corresponding to yielding of the braces when no initial prestress is provided (see Table 5.1). The hysteresis loop corresponding to the fourth cycle is thus the same for all prestressing levels examined, as shown in Fig. 5.5.

Due to the absence of initial prestressing, yielding of the braces during the fourth cycle causes the braces to become slack upon unloading of the frame (point 24 for brace A and point 28 for brace B). As a result, there exists a deformation range over which the
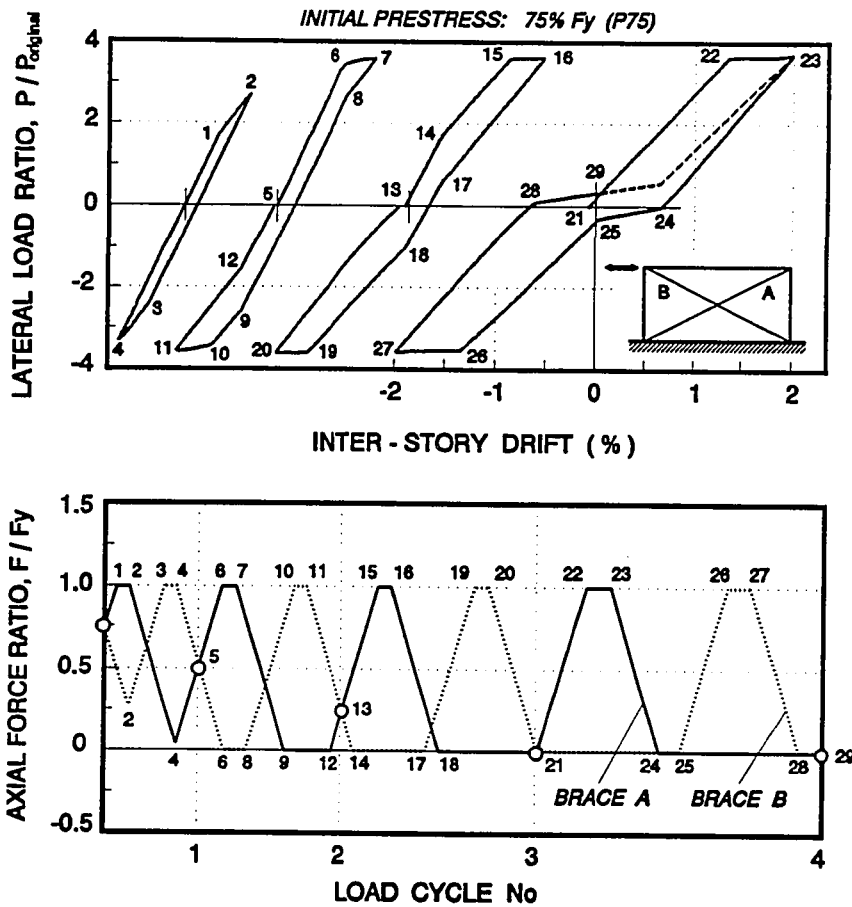
Figure 5.6 Variation of the axial force level with the load cycle for braces with an initial prestress level of 75 % of the yield strength.

braces carry no load and provide no lateral stiffness to the frame. Such behavior is typical of tension-only-brace systems and is illustrated by segments 24 - 25 and 28 - 29 in Fig. 5.6. The small stiffness of the hysteresis loop upon reloading of the frame in the opposite direction (slope of segments 24 - 25 and 28 - 29) corresponds to that of the reinforced concrete frame alone. Also note that when the structure reaches its undeformed position (point 25), stiffness of the frame changes abruptly when the opposite brace begins to carry tension.

The behavior described above is aggravated if braces reach yielding in following cycles, because each time that braces yield in tension a larger deformation is required for the braces to carry tension upon reversal of the load. Therefore, the ability of the system to dissipate energy decreases for each cycle in which braces reach yielding. Such behavior is shown with a dashed line in Fig. 5.6.

It is important to realize that the initial prestress level is not always lost upon yielding of the braces. As described above, initial brace prestress is lost only when the structure is deformed beyond the drift level corresponding to that of yielding of the braces when no initial prestress is provided. The axial load - elongation relationship experienced by one of the braces with initial prestress of 75% of the yield strength under the cyclic loading is shown in Fig. 5.7. Maximum elongations developed by the brace at the end of each cycle are also shown in this figure. As can be seen in Fig. 5.7, the maximum elongation developed by the brace upon losing its initial prestress level (third cycle, point 16) is exactly equal to 1.75 times the yield elongation. In other terms, the maximum elongation that the brace can be allowed to develop in tension without losing its initial prestress, is equal to the yield elongation as measured from its deformation upon initial prestressing (undeformed position for the braced structure), as shown in Fig. 5.7. This result is general and it does not depend on the initial level of brace prestressing, as demonstrated by the sameness of the hysteretic loops after yielding of the braces with different levels of initial prestress. The maximum deformation that a brace can experience using the criterion described above is twice the elongation at yielding of the brace (for a theoretical initial prestress of "100%" of brace yield). Such maximum elongation is well below the elongation at ultimate for both rods and strands (see Fig. 3.11).

5.2.3 Summary

The results presented above show that, as in any other prestressing system, initial prestress of braces results in a higher lateral stiffness of the structure but it has no effect on its ultimate strength.

For static lateral loads, "optimum" behavior is obtained for an initial brace prestressing level equal to 50 % of the brace yield strength. With this initial level of prestress, the brace which elongates reaches yielding at the same time that the brace which
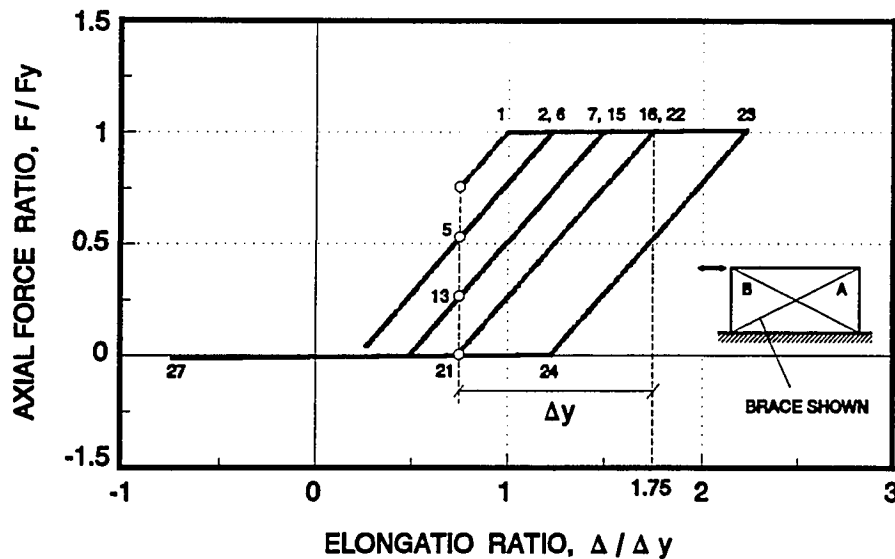
Figure 5.7   Brace force and elongation relationship for braces with an initial prestress level of 75% of the yield strength.

shortens begin to sag. Maximum strength of the bracing system is therefore reached at the smallest possible drift for the braced structure. For lower levels of initial prestress, the brace which shortens begins to sag prior to yielding of the brace which elongates. For prestress levels higher than 50% of the yield strength, the behavior of braces just described is reversed. As a result, the braced structure shows a reduction in its lateral stiffness, developing larger displacements, prior to reaching the maximum strength of the bracing system.

Under reversed cyclic loading, high levels of initial brace prestressing provide the system with the ability to dissipate energy at small drifts due to yielding of braces in tension. The higher the level of initial prestress, the smaller the lateral drift required to begin to dissipate energy.

Yielding of braces in tension reduces the amount of initial prestress, but it does not necessarily lead to the complete loss of prestress. Braces can be allowed to yield in tension without completely losing prestress provided that the maximum elongation of the brace after prestressing is limited to the yield deformation.

5.3 MULTI-STORY BUILDINGS

The behavior of a single-bay - single-story braced frame with slender braces under static loading was discussed in detail in the previous section. For multi-story buildings, a behavior similar to that of the single-story structure can be expected under static lateral loads. Since a static load analysis provides information only on stiffness and strength and not on the amount of deformation required during an earthquake, the behavior of the system requires even further evaluation. Under earthquake loads it might be desirable to provide an initial prestress level higher than 50 % of the brace yield strength and allow braces to yield at small lateral drifts. This condition encourages early dissipation of energy in the braced structure which will help reduce and thus improve overall response of the building. On the other hand, early yielding of braces in tension could lead to elongations larger than the maximum allowable (as defined in the previous section) and cause the braces to lose the initial prestressing force in the early stages of severe ground motion. Such behavior could be detrimental for the response of the braced structure because braces become slack upon unloading of the structure. While this behavior could be catastrophic for a single-story structure, it is unlikely that all braces lose the initial prestress level at the same time in a multi-story building, particularly if a large number of braces has been provided. Thus, the consequences of such an event in multi-story buildings are not expected to be as destructive as for a single-story structure, although large lateral displacements can be anticipated if all braces in a given story lose their initial prestress force.

In this section, an overview of the behavior for the post-tensioned bracing system in multi-story buildings under earthquake loading is presented. The effects of the level of initial brace prestressing and brace yield strength are the main parameters considered in the evaluation of the dynamic response of structure. In addition, the forces generated in a typical frame by initial brace prestressing are investigated. Based on the results obtained, general design criteria are developed (optimum level of initial brace prestress and brace yield strength).

5.3.1 Building Structure and Retrofit Schemes Selected for Evaluation

To evaluate the effects of initial prestressing and brace yield strength on the dynamic response of a multi-story structure, the three story building presented in section 4.2

was selected for study. The building was analyzed only in the longitudinal direction and was subjected to the El Centro 1940 record. Two different bracing configurations were selected as possible retrofit schemes, as shown in Fig. 5.8. In both cases, the bracing system is provided only to perimeter frames.

CONFIGURATION C1
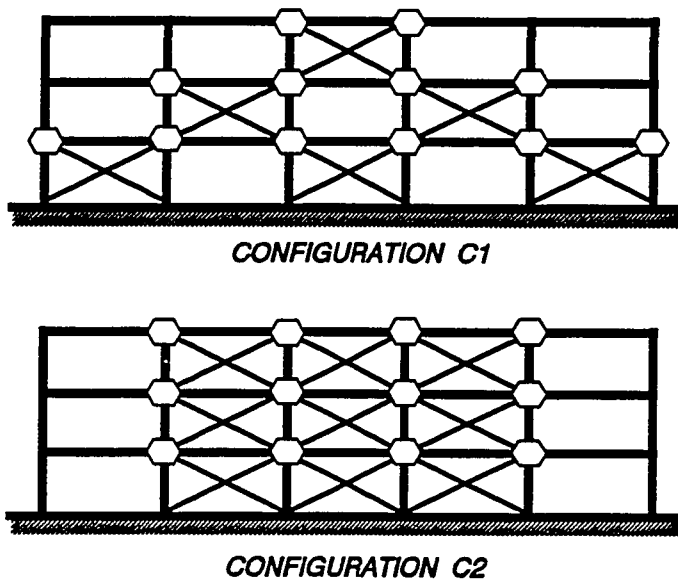
CONFIGURATION C2

Brace Area: 3.16 in^2 (Rods or Strands)

Figure 5.8 Bracing configuration patterns selected for evaluation.

Similar to the procedure followed for the single-story structure, four levels of initial brace prestressing were considered in the analyses: 0, 25, 50 and 75 % of the brace yield strength. In addition, the bracing system was evaluated for steel rods and for steel strands as possible post-tensioned materials for the braces. The material properties adopted for rods and strands, and the model used to emulate the behavior of these type of braces followed the procedure presented in section 3.2.5.1.

To help identify the different cases studied, i.e.: bracing configuration pattern, level of initial brace prestressing and material type used for braces (rods or strands), a particular nomenclature is used as follows:

C # - P # - α

R for rods

S for strands

configuration

pattern number

level of initial
brace prestressing (%)
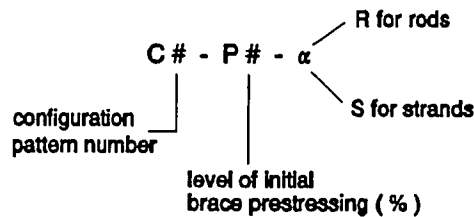
5.3.1.1 Effects of Initial Brace Prestress on Internal Force Distribution

As described above, initial prestress of braces generates internal forces in the existing structure which will modify the distribution and magnitude of internal forces due to gravity loads alone. Depending on the level of initial prestress, brace size and bracing configuration, internal forces due to prestressing of braces can be either beneficial or detrimental for the behavior of the existing reinforced concrete members. Compressive axial forces will be, in general, beneficial for the flexural and shear behavior of the members. In columns, however, compressive axial forces will add to those from gravity loads, and the resulting axial force may exceed the load at balanced strain conditions, which will reduce the flexural capacity and available ductility of the section.

In Fig. 5.9, the bending moment distribution in columns of perimeter frames due to gravity loads is compared to that obtained after brace prestressing with configuration C1 and initial prestress level of 75% of the brace yield strength. In computing internal forces in frame members it has been assumed that the forces due to brace prestressing are resisted by the perimeter frames alone. Also shown in Fig. 5.9 is the ratio between the acting moments and the estimated capacity of the sections. At the base of columns, the capacity of the section is given by the failure of splices, M_{sp} ; at the top the sections are assumed to develop flexural yielding, M_y .

Overall, the increase in the magnitude of bending moments, is in general, minimal. Maximum increase in moments occur in second story columns (from 18% to 26 %). However, the magnitude of the maximum moments developed after prestressing is of the same order as the maximum moments developed under gravity loads alone. Note that the
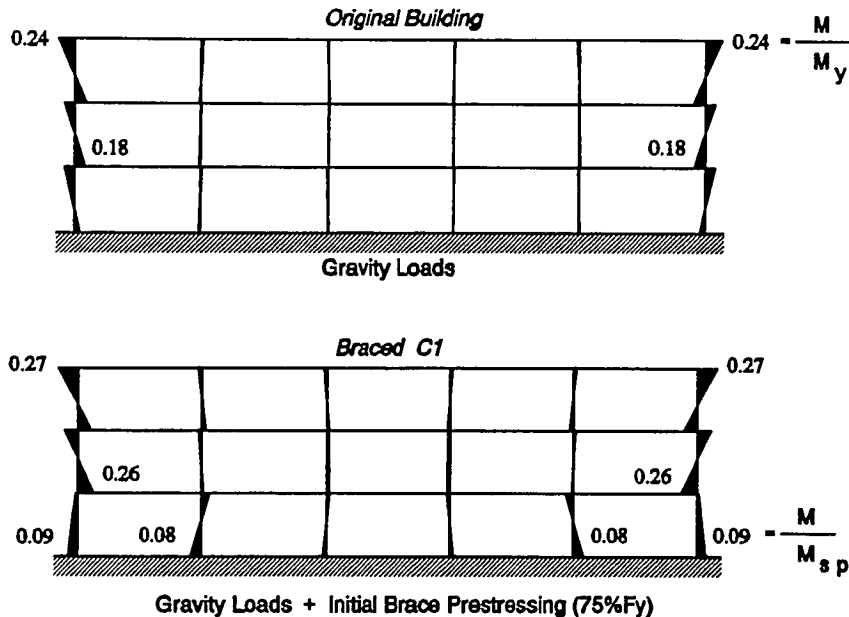
Figure 5.9 Effects of initial brace prestressing on the bending moment distribution in perimeter frame columns. Original building and braced structure, configuration C1 with initial brace prestressing of 75% of brace yield strength.

bending moment at the base of exterior columns is reversed with respect to that obtained under gravity loads alone. Also note that these columns are no longer in reversed curvature, but rather in single curvature with a small bending moment at the top. In beams, initial brace prestressing has only a minor effect on the distribution of bending moments.

In Fig. 5.10, the axial force distribution in columns and beams due to gravity loads is compared to that after brace prestressing for the same bracing configuration (C1) and prestress level considered above. As expected, axial forces in columns due to initial brace prestressing are all compressive forces. The resulting axial forces due to gravity loads and initial brace prestressing are, in average, three times as high as those under gravity loads alone. However, maximum axial forces in first story columns approach 28% of the maximum capacity in pure compression, P_c, and remain below the load at balanced strain conditions. The effects of brace prestressing will improve the flexural behavior of the column in this case.
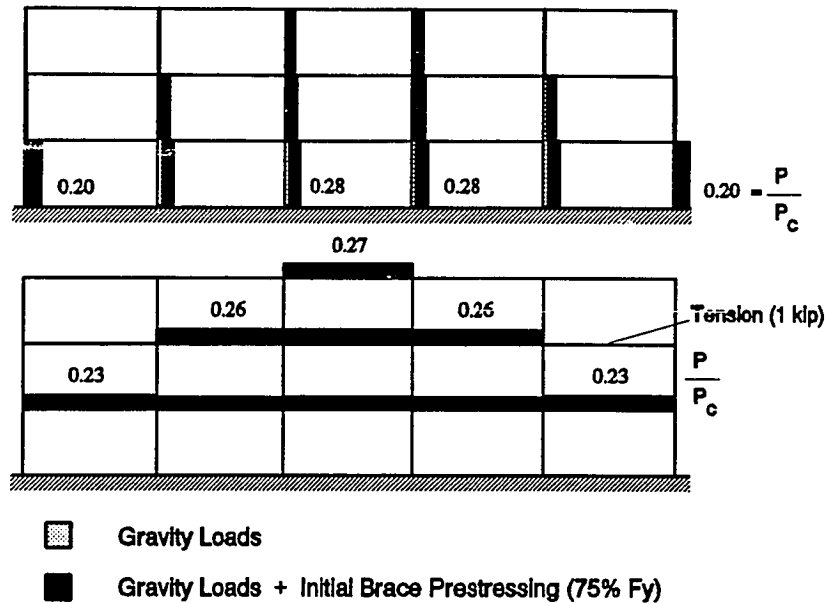
Figure 5.10 Axial force distribution in columns and beams for the braced structure with configuration C1 and initial brace prestressing of 75% of brace yield strength.

Axial force in beams due to brace prestressing are all compressive forces, except for the beams of exterior bays in the second floor level in which some minor axial tension is developed. The magnitude of the tensile forces in these beams is very small ($\approx$ 1 kip) relative to the scale used in Fig. 5.10. Maximum axial compression in beams approach 27% of the capacity in pure compression for the beam in the top story.

The level of forces induced by initial brace prestressing with configuration C2 is of similar magnitude.

The results presented above show that in general the level of forces induced by initial prestressing of the braces is beneficial for the behavior of the reinforced concrete members. Induced bending moments vary slightly from those under gravity loads alone and axial forces are mostly compressive forces with magnitudes that remain below the load at balanced strain conditions. It is clear, however, that these results will vary for each structure and for each bracing configuration, and therefore each case will have to be analyzed individually.

While the initial pre-compression forces due to brace prestressing will in general enhance the flexural behavior of existing members, the magnitude of these forces under earthquake loading may vary considerably, particularly for exterior columns. It was thus decided that compressive forces due to brace prestressing cannot be relied upon to improve the behavior of the reinforced concrete members and it was not included in the analyses. As stated in Chapter III, member capacity was based on axial forces due to gravity loads alone.

5.3.1.2 Lateral Stiffness and Strength

To compare the stiffness and strength of the original and retrofitted building, inelastic lateral load analyses were performed. Fig 5.11 shows a comparison of the relationship of the base shear coefficient and the drift at the centroid of inertia forces for the existing and braced building with steel rods using configuration C1. A uniform lateral load
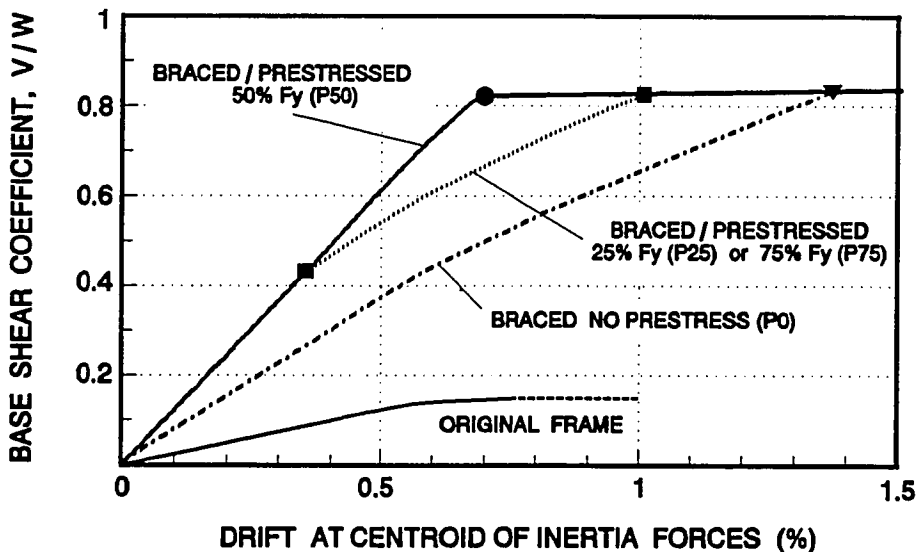
Figure 5.11 Base shear coefficient and drift relationship for the original and braced building with configuration pattern C1 (steel rods) and different levels of initial brace prestressing.

distribution was used to obtain the relationships shown in Fig. 5.11. Similar to the results obtained for the single-story structure, the increase in stiffness and strength provided by the bracing system is substantial. Notice the resemblance in the behavior of the braced structure for different levels of initial brace prestressing with that of the single story structure (see fig. 5.3). The main reason for this result is that lateral stiffness and strength of the braced building with configuration C1 is governed by the behavior of the braces in the first story. In Fig. 5.11, the reductions in stiffness of the building are due to yielding of the braces which elongate and/or sagging of the braces which shorten, as described for the single story structure for the different prestress levels.

The base shear strength of both bracing configurations (C1 and C2) is the same (same number and size of braces in the first story). However, because of the larger number of braces in the second and third stories, lateral stiffness of configuration C2 is somewhat larger than that of configuration C1 (load and drift relationship for configuration C2 is not shown in Fig. 5.11 for clarity).

The overall behavior described above for configurations C1 and C2 is similar when strands are provided instead of rods. However, due to the higher yield strength of steel strands, a higher ultimate strength is developed for the braced building.

5.3.1.3 Dynamic Response Analyses

Dynamic Properties

The dynamic properties of the existing and retrofitted buildings are presented in Table 5.2. Because cracking of the reinforced concrete elements is expected to take place in the early stages of the response of the building during severe ground motion, natural periods of vibration were computed assuming all members to be initially cracked. As can be seen, the stiffness provided by the bracing configurations (C1 and C2) result in a significant reduction in the fundamental period of vibration of the building, particularly when braces are initially prestressed. Based on the response spectra obtained for the El Centro 1940 record, it can be anticipated that shortening in the period of vibration will result in an increase in response and in higher displacement ductility demands for the braced structure (See Figs. 4.26 and 4.30). This result will be typical for most buildings located on firm soil sites and correspond to the most severe condition for the retrofit scheme from the

standpoint of dynamic response of the retrofitted building. Notice that the addition of the bracing system has minimal influence in the modal participation factors (see Table 5.2).

Table 5.2 Dynamic properties of original and braced buildings.

Building	Period (sec)		Modal Mass Ratio	
	1st Mode	2nd Mode	1st Mode	2nd Mode
Original	1.11	0.36	0.87	0.10
Config. C1 w/o prestress	0.66	0.25	0.84	0.12
w/ prestress	0.52	0.21	0.83	0.13
Config. C2 w/o prestress	0.60	0.21	0.90	0.09
w/ prestress	0.46	0.17	0.90	0.08

Dynamic Response

In this section, the performance of the post-tensioned bracing system is evaluated by examining the response of the braced building to the El Centro record. In addition, variables that have a substantial influence in the overall behavior of the retrofitted building are identified and minimum criteria for the design of the post-tensioned bracing system are established.

a) *Maximum Displacements and Inter-story Drifts*

A comparison of the time history responses obtained for the original and braced buildings with steel rods for the four levels of initial brace prestressing is presented in Fig. 5.12. As can be seen, maximum roof displacement is reduced with respect to that obtained for the original structure in all cases, except in the case in which no initial brace prestressing was provided. Notice that maximum roof displacement is decreased as the level of initial brace prestressing is increased. Also note that initial brace prestressing has a significant influence in limiting the number of large amplitude cycles, which will help reduce the level of cumulative damage in the structure. Even for a 25 % initial prestress, the number of large amplitude cycles is confined to approximately the first 6 seconds of the record. When no
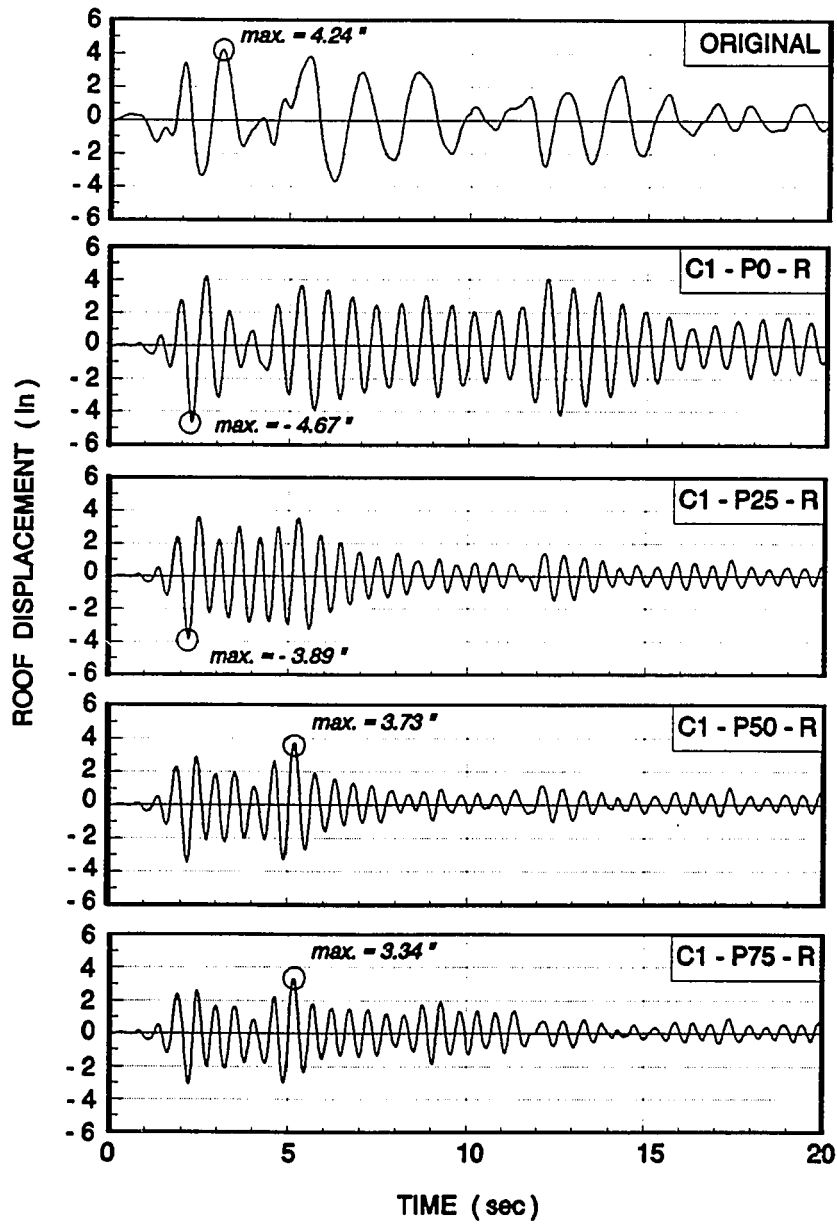
Figure 5.12 Time history response of original and braced building with configuration C1 subjected to El Centro record. Comparison of response for different levels of initial brace prestressing.

initial brace prestressing is provided, large amplitude cycles are obtained over most of the response. Although not presented here, the same trend is observed for steel strands and for bracing configuration C2.

Maximum inter-story drifts ratios obtained for each story level for the original and braced structure with steel rods and strands are shown in Fig. 5.13. The relationships are shown for all four levels of initial brace prestressing, but only for bracing configuration C1. Because configuration C1 provided a story stiffness that is gradually reduced with height, maximum inter-story drift distribution with height differs from that obtained for the original structure. While inter-story drift maxima for the braced structure does not always occur in the first story (as in the original structure), the braced structure shows a reduction in the maximum inter-story drifts for all levels of prestress, including the case when no initial prestress is provided. The results also show that, in general, a higher level of initial brace prestressing leads to smaller inter-story drifts for both steel rods and strands. The same conclusion holds true for bracing configuration C2. Notice that for a given initial level of brace prestressing, maximum inter-story drifts are, in general, very similar for both rods and strands.

While maximum roof displacement for bracing configuration C1 with steel rods without initial prestress (C1-P0-R) increased with respect to that of the original building (see Fig. 5.12), inter-story drift maxima were in fact reduced (Fig. 5.13).

b) *Performance of Braces*

Overall, using either steel rods or steel strands, there were a limited number of braces that reached yielding or that became slack for both bracing configurations. Although a few steel rods reached yielding for initial prestress levels of 25% and higher, initial brace prestress was reduced but it was never lost. Strands reached yielding only when initially prestressed to 75 % of the yield strength and became slack on fewer instances than steel rods.

In Fig. 5.14, the axial force and elongation relationship for one of the most stressed rod braces of configuration C1 is presented. Also shown in this figure is the axial force time history for the same brace. The relationships are shown for 25, 50 and 75% of initial prestress. While this brace reached yielding during maximum response of the building when initially prestressed to 50 and 75% of the brace yield strength, its initial prestress level was
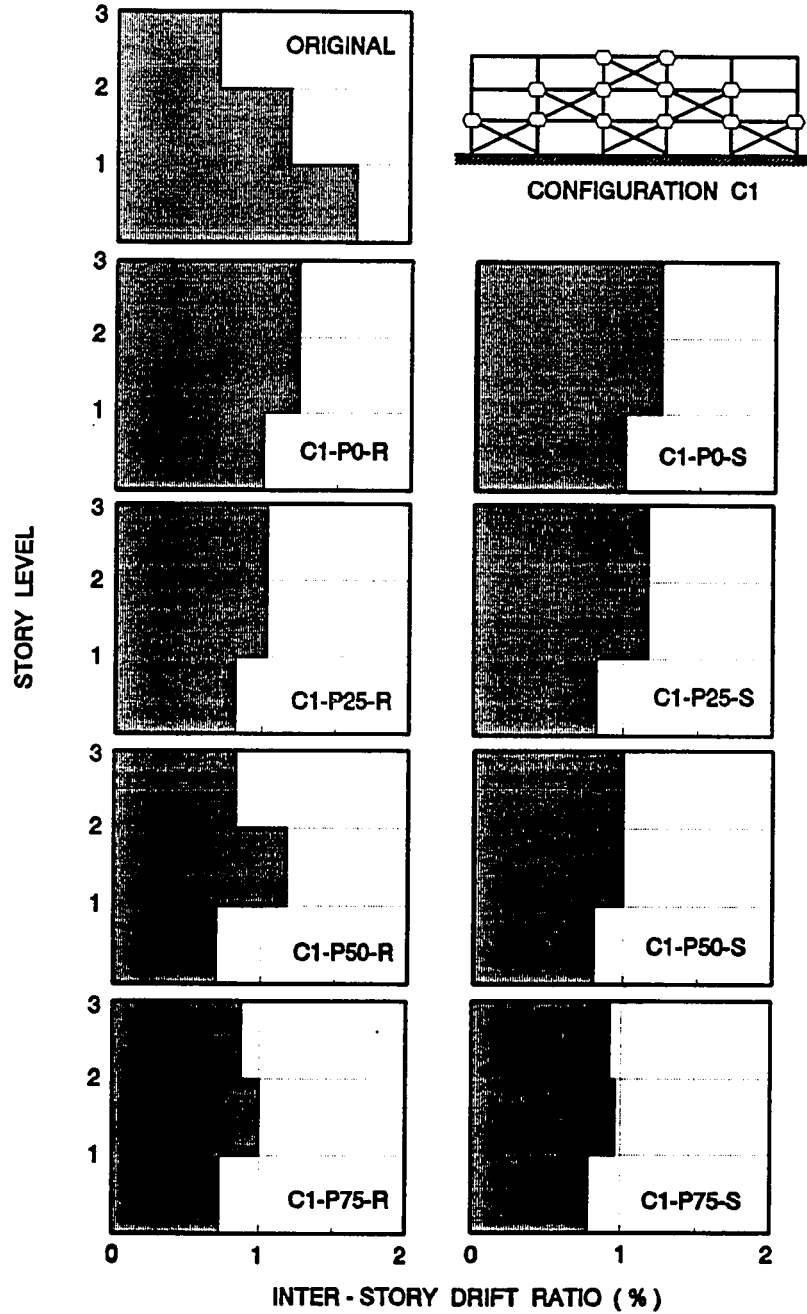
Figure 5.13   Comparison of maximum inter-story drift ratios obtained for the original and braced building with rods and strands using configuration C1, subjected to El Centro.
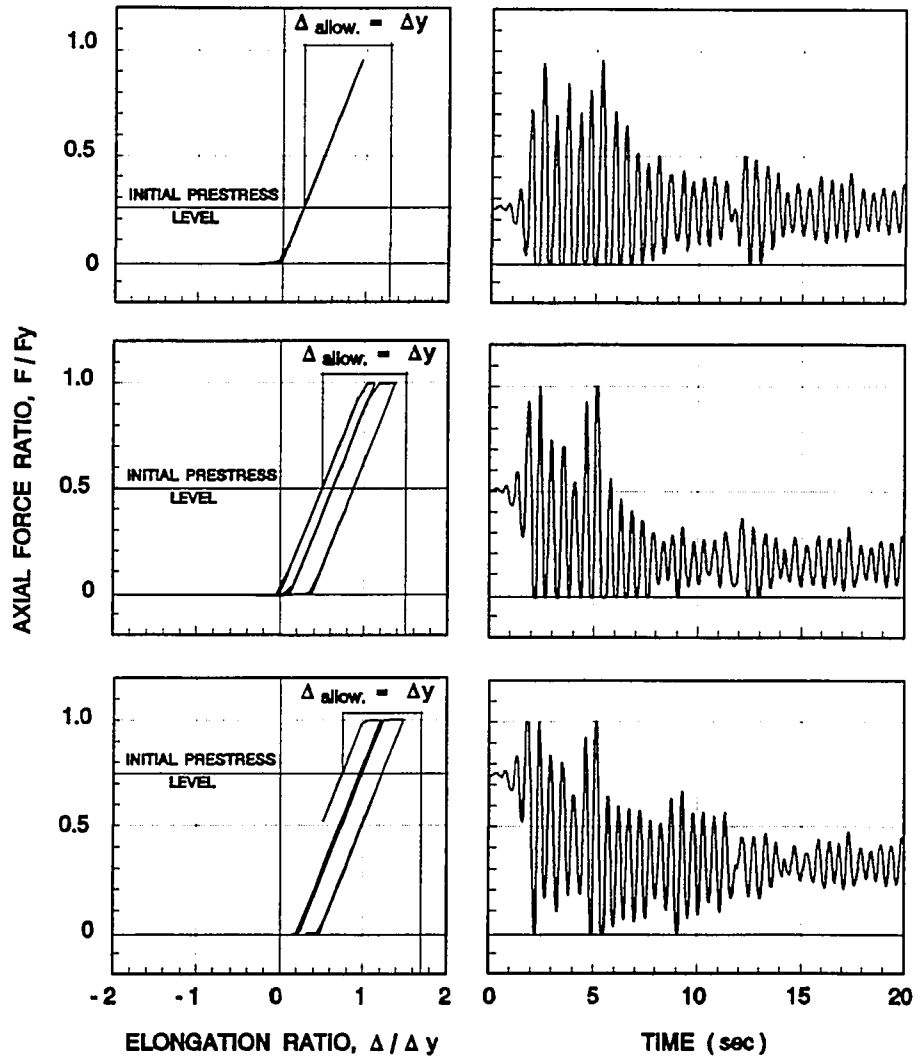
Figure 5.14 Comparison of brace force and elongation relationship for different levels of initial prestress. Braced structure with configuration C1 subjected to El Centro record.

only partially reduced. Thus, this brace never lost prestress and always became taut upon reversal of the load. It should be remembered that in order for a brace to lose the prestress level completely and become slack upon unloading, the brace has to undergo an elongation equal to the yield elongation ($\Delta_{allow.}$ in Fig. 5.14), regardless of the level of initial prestress force (see section 5.2.2). It must be emphasized that the relationships shown in Fig. 5.14

correspond to one of the most stressed braces during the seismic event. The rest of the rod braces were subjected to smaller elongations and became slack in fewer instances.

The reduction in maximum response and inter-story drift ratio observed for higher levels of initial brace prestress, and the adequate performance of the braces described above, indicate that early yielding of braces is beneficial for the overall response of the structure. Thus, yielding of braces should be allowed during an extreme event, provided that maximum brace elongation remains below the allowable level described earlier.

c) *Performance of Reinforced Concrete Frame Members*

The analyses indicate that for the original structure splice failure occurred in all first story columns, with extensive damage and loss of strength and stiffness of the failing column sections. Pull-out of bottom beam bars is also observed, with almost total loss of capacity in positive moment. Yielding in "negative" moment is observed in all beam sections but with minor inelastic excursions.

For the braced structure, the performance of beams and columns vary depending on the level on initial level of brace prestress. Overall, the higher the level of initial brace prestress the better the performance of reinforced concrete members. When braces are not initially prestressed, the improvement in the behavior of existing members is minimal, if any. The behavior described above is observed for both bracing configurations, C1 and C2.

To illustrate the effects of initial brace prestressing on the behavior of the existing reinforced concrete members, the moment - rotation relationship obtained at the base for a first story column is presented in Fig. 5.15. In these figures, the moment - rotation relationships of the members obtained for the original structure is compared with that of the braced structure using configuration C2. Since lower levels of initial brace prestressing do not improve the performance of members significantly, the relationships are shown only for prestress levels of 50 and 75 % of the brace yield strength. The results for both rods and strands are presented. The acting moment and corresponding rotation are shown as a fraction of the values that would produce a splice failure of the column section. The member shown corresponds to the column with the largest rotational demands in both the original and the braced structure.

Figure 5.15 Comparison of moment-rotation relationship for a column of the three-story building (El Centro record). Original and braced building, Config. C2, rods and strands, initial prestress of 50 and 75% of brace yield strength.

As can be seen, splice failure in this element was not prevented with bracing configuration C2. However, the bracing system was able to limit the strength and stiffness degradation of the element. While the reduction in moment capacity of the section is as much as 75 % of its maximum strength in the original structure, the same moment reduction is at most 40 % when rod braces with 50 % initial prestress were provided. The rest of the cases examined in Fig. 5.15 exhibit even lower reductions in strength. It should be emphasized that the column section shown in the figure corresponds to the element with the largest rotational demands and that the rest of the column members showed reductions in strength that are even smaller or non-existent (splice failure prevented). The smallest reductions in strength are obtained for braces (rods or strands) with 75 % of initial prestress. The use of strands results in only marginal improvements in the behavior of the column section. Overall, the results show that the bracing system can be designed to prevent or at least reduce strength and inelastic rotation demands in columns.

In Fig. 5.16, the moment - rotation relationship for the end section of an exterior beam in an interior frame is presented. The relationships are shown for the same bracing configuration pattern and levels of initial brace prestressing as those of the column element presented above. The acting moment and corresponding rotation are shown as a fraction of the values that would cause yielding of the section in "negative" moment. As above, the beam section shown corresponds to the element with the largest rotational demands in the original and in the braced structure. Notice the resemblance of the overall shape of the hysteresis loops with those obtained from experimental studies (see Fig. 2.7).

The results of Fig. 5.16 indicate that the bracing system was not able to prevent anchorage failure of bottom reinforcing bars, although it always helped reduce the extent of inelastic excursions and, thus, reduce the level of damage of the sections. In general, pull-out of bottom reinforcing bars in beams was not prevented with any of the two bracing configurations considered. In addition, the effectiveness of the bracing system (C1 or C2) to reduce the loss of strength that follows anchorage failure of bottom bars is minimal, regardless of the level of initial prestressing considered for the braces. Because pull-out of bottom reinforcing bars commences at smaller drifts than those required to produce splice failure in columns (See Fig. 4.8), it appears that in order to prevent such a failure a very stiff bracing system would be required. This result imposes a severe requirement on the post-tensioned bracing system if pull-out of bottom beam bars is to be prevented.
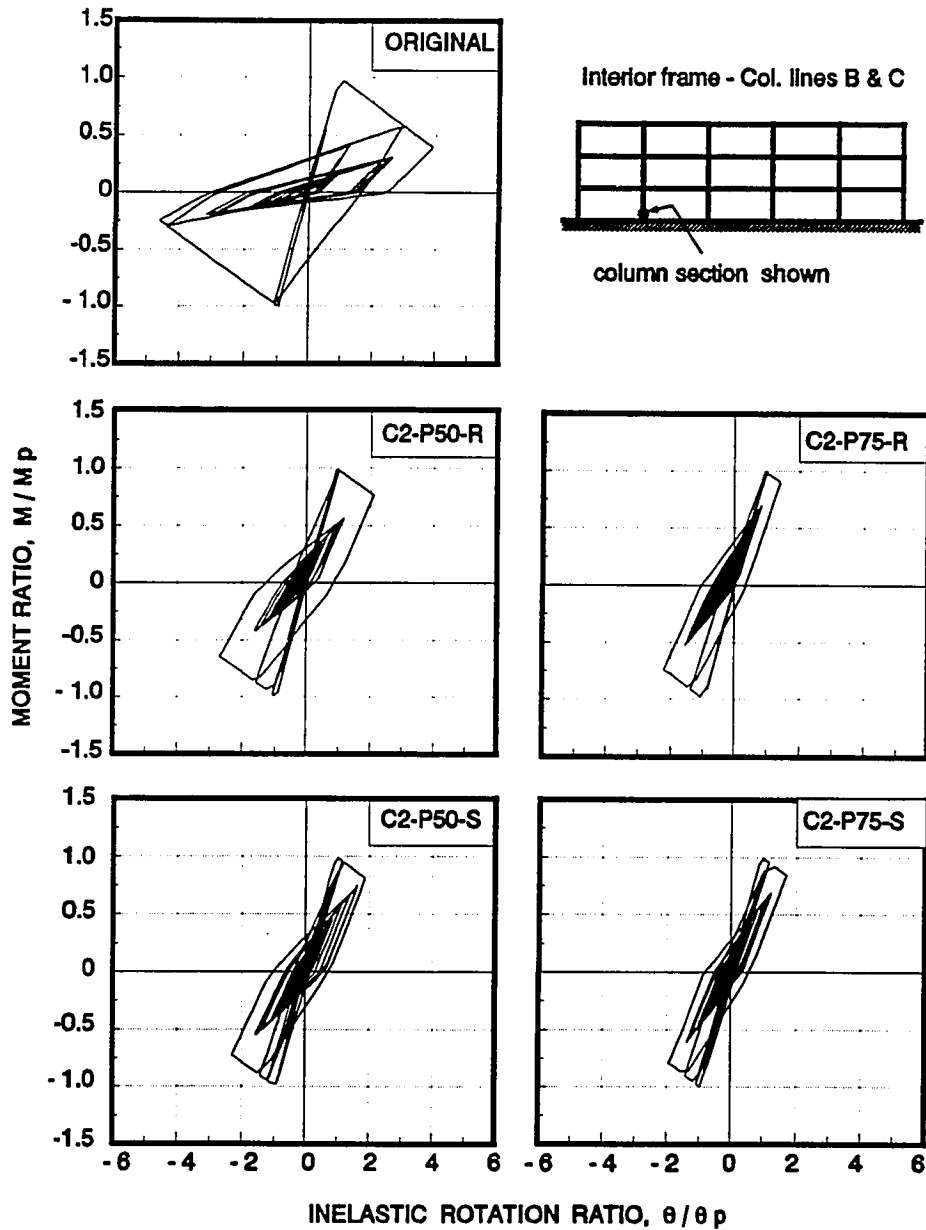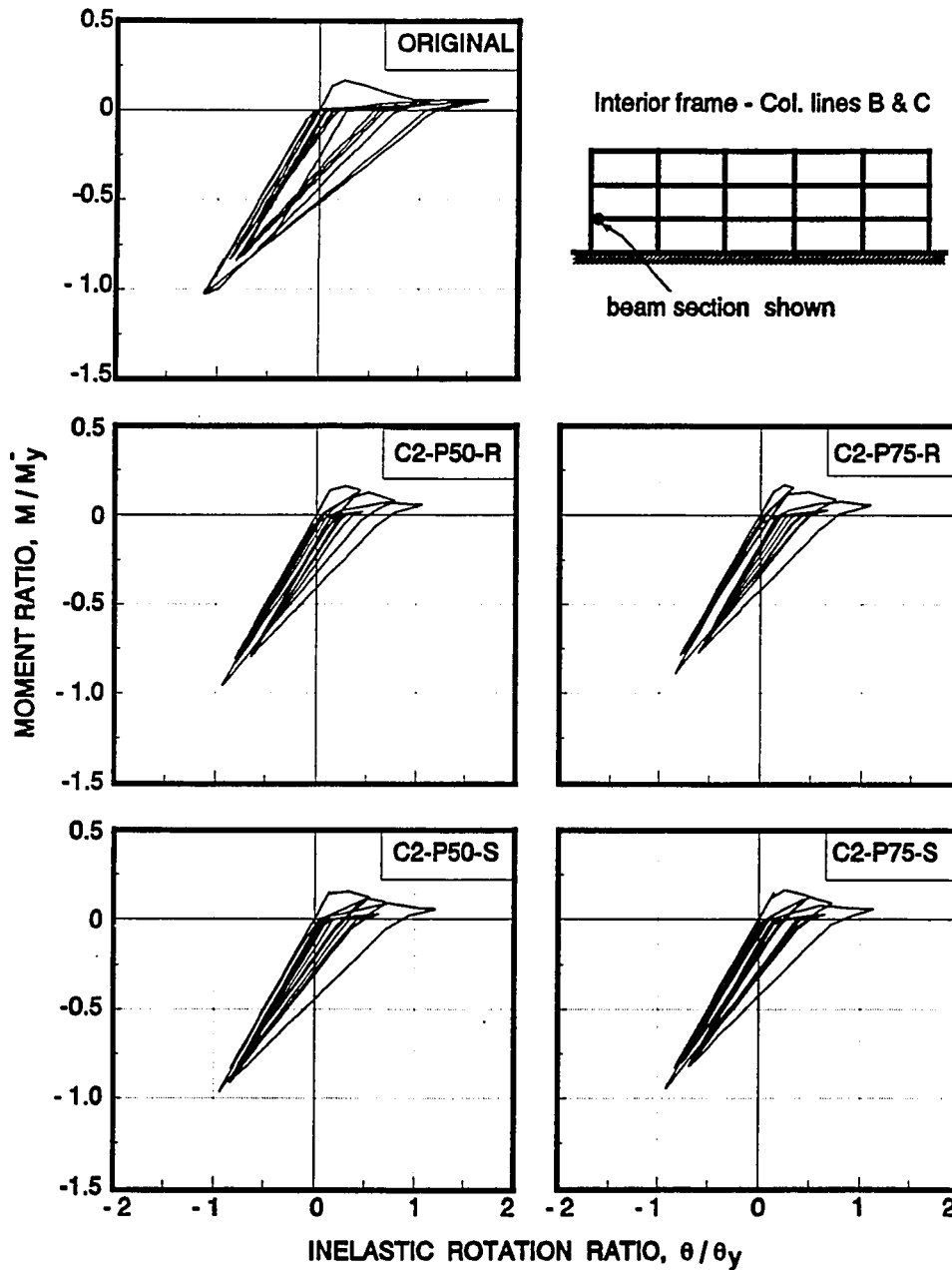
Figure 5.16 Comparison of moment-rotation relationship for a beam of the three-story building (El Centro record). Original and braced structure, config. C2, rods and strands, initial prestress levels of 50 an 75% of brace yield strength.

d) Story Shear

To examine the behavior of the braced structure further, the story shear developed in the original and braced structure is studied. Fig. 5.17 shows the story shear and inter-story drift ratio relationship for the original building. As can be seen, most of the inelastic behavior is concentrated in the first story which is consistent with the level of damage described above for this story level. Shear strength is reached in the first story and, despite the generalized splice failure in the columns in this story, only marginal reductions are observed in the base shear capacity. Such behavior is explained by the redistribution of bending moments from the base to the top of first story columns that follows after failure of splices. On the other hand, story stiffness showed a significant reduction after failure of splices and the drift in the first story reached about 1.7%. The inelastic behavior that is observed in the upper two stories is due exclusively to the anchorage failure of bottom beam bars and yielding of the end sections of beams as splice failure in second and third story columns was not observed.

A comparison of the story shear and inter-story drift relationships for the original and braced structures is presented in Fig. 5.18. In this figure, the relationships are shown for steel rods and strands, with bracing configuration C1. Based on the better performance of the braced structure with high initial brace prestressing, the story shear and inter-story drift relationships are compared only for braces with an initial prestress of 50 and 75% of the brace yield strength. A similar comparison is shown in Fig. 5.19 for bracing configuration C2.

Overall, both bracing configurations show a significant increase in story shear stiffness and strength, and a considerable reduction in the inelastic behavior of the building. For bracing configuration C1, most of the hysteretic behavior occurs at the second story level rather than at the first story, as it was anticipated from the maximum inter-story drifts obtained in Fig. 5.13. When steel strands with an initial prestress of 50 % of the brace yield strength are provided, braces do not reach yielding and therefore the hysteretic behavior observed is due only to that of the original reinforced concrete frame.

In bracing configuration C2, the shear strength provided by the bracing system is essentially the same for every story (see Fig. 5.8), and since maximum shear demands for
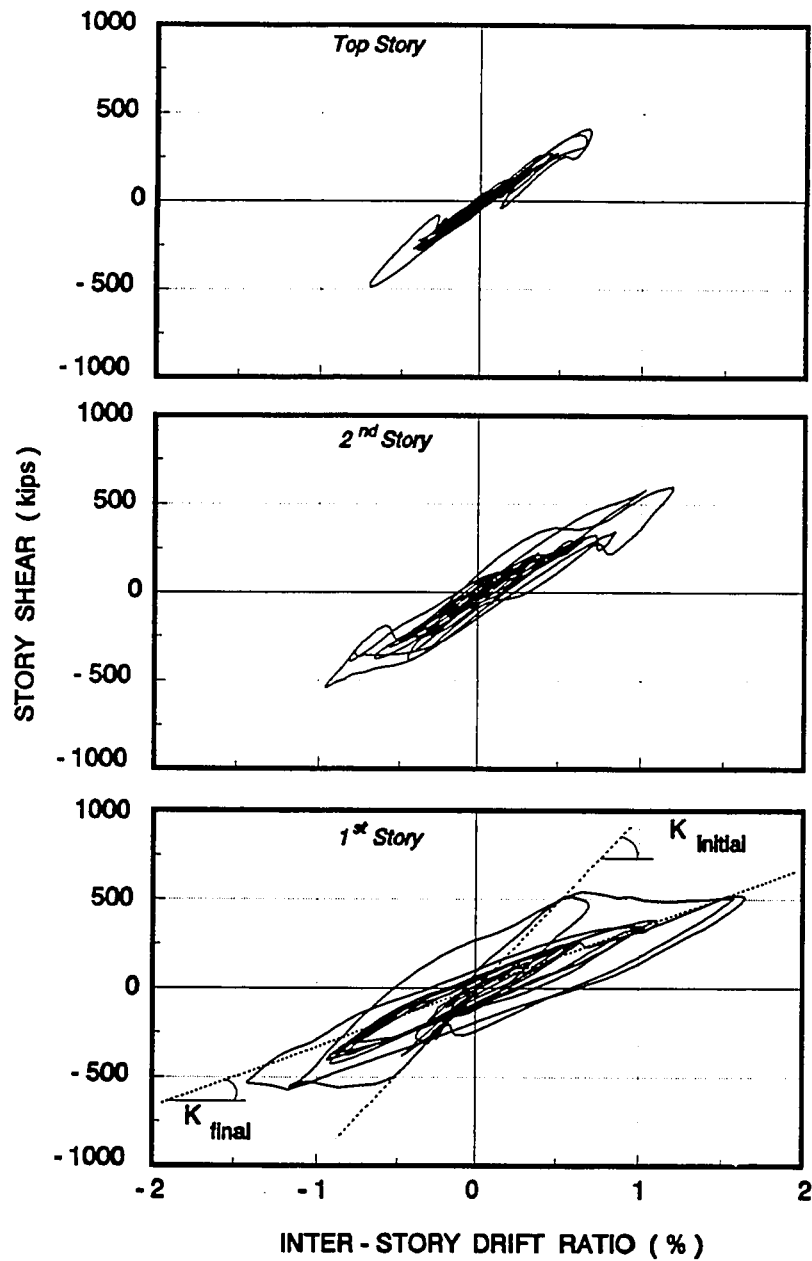
Figure 5.17 Story shear and inter-story drift ratio relationship for the 3-story building subjected to El Centro 1940.

151
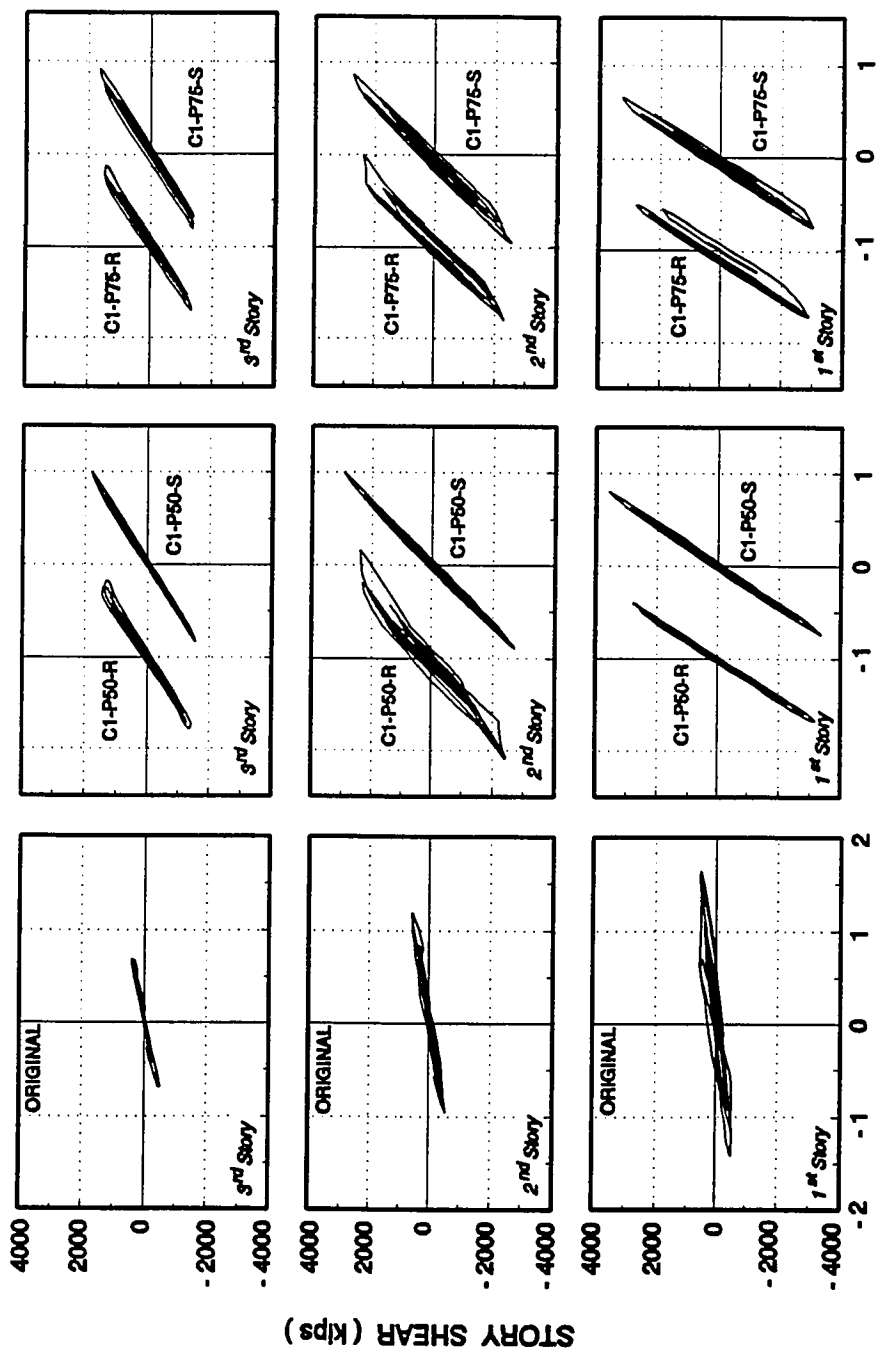
Figure 5.18 Comparison of story shear and inter-story drift relationship for the three-story building (El Centro record). Original and braced structure, config. C1, rods and strands with initial prestress of 50 and 75% of brace yield strength.
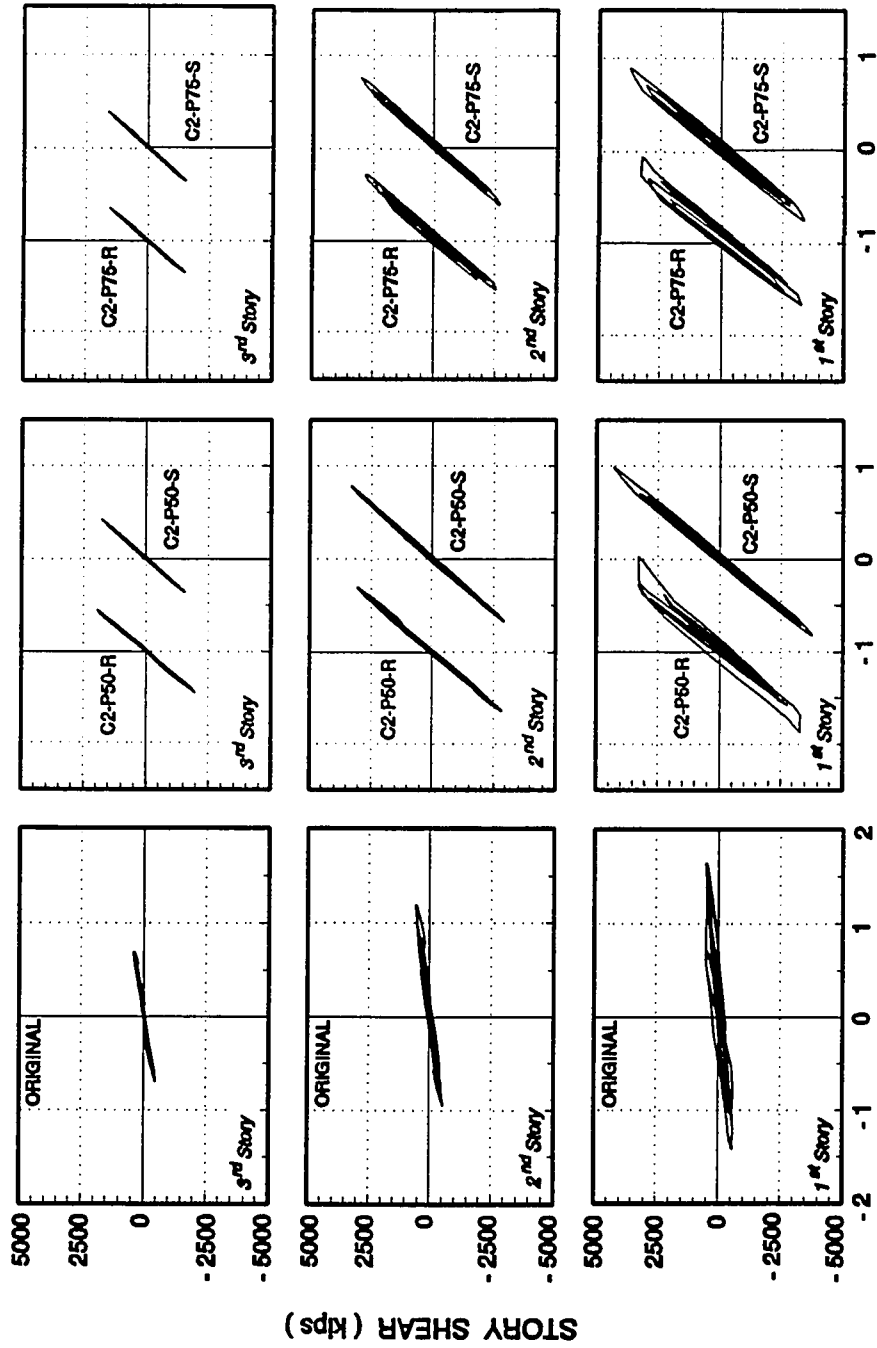
Figure 5.19 Comparison of story shear and inter-story drift relationship for the three-story building (El Centro record). Original and braced building, config. C2, rods and strands with initial prestress of 50 and 75% of brace yield strength.

the building occur in the first story, inelastic behavior initiated and is concentrated in the first story. As a result, story shear and inter-story drift maxima always occur in the first story, regardless the level of initial brace prestressing, as shown in Fig. 5.19.

The level of initial prestress has only a moderate influence on the behavior and distribution of the story shear of the building. As discussed in previous sections, when braces, steel rods or strands, are initially prestressed to 75 % of the yield strength, braces reach yielding at smaller drifts than those required to yield braces with lower levels of initial prestress. Thus, the system with high initial prestress (75% of brace yield strength) begins to dissipate energy in the early stages of a ground motion and results in a larger number of hysteresis cycles. Such behavior apparently results in a more even distribution of the inelastic behavior throughout the height of the structure, as can be seen in Figs. 5.18 and 5.19 for both configurations with braces with initial prestress of 75% of brace yield strength. Also note that maximum inter-story shears and inter-story drifts are slightly reduced with respect to those obtained for braces with initial prestress of 50% of brace yield strength.

e) Axial Forces in Columns and Beams

One aspect that is of concern in the use of a high strength post-tensioned bracing system is the level of axial forces (compression and tension) induced in the frame members, particularly in columns. Fig. 5.20 shows the maximum axial force level developed in the columns of the perimeter frames braced with configurations C1 and C2, for braces with initial prestress levels of 50 and 75% of the brace yield strength. Maximum compressive forces are presented as the ratio between the maximum axial force induced, P_m, and the axial load strength for balanced strain conditions, P_b. Also shown is the ratio between the maximum axial force, P_m, and the axial load strength of the column in pure compression, P_c. Tension forces are presented as fraction of the force that would produce failure of splices in the column in pure tension, T_{sp}.

As expected, because of the higher strength of steel strands, these type of braces always induce higher axial forces in the columns than steel rods. The level of initial brace prestressing has little effect on the maximum axial compressive forces induced in the columns, because most braces reach yielding for the prestressing levels considered in Fig. 5.20. On the other hand, maximum tension forces appear to be reduced when a higher level of initial brace prestressing is used.
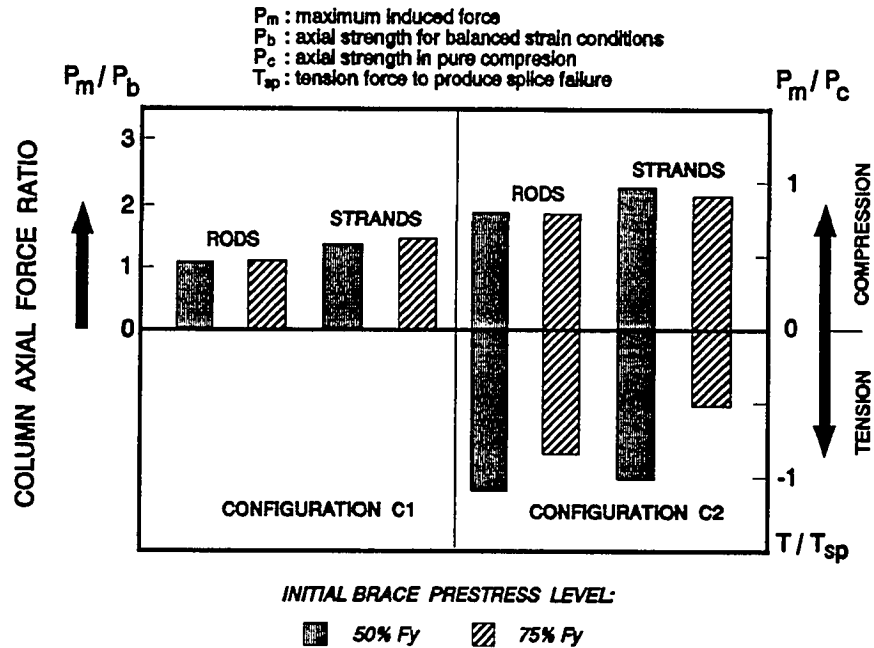
Figure 5.20 Comparison of maximum axial force in columns for bracing configuration C1 and C2, for rods and strands with initial prestress of 50 and 75 % of the brace yield strength.

Maximum compression forces for configuration C1 remained below the compression capacity of the columns, although they exceeded the load strength corresponding to balanced strain conditions. Compression forces from gravity loads were never exceeded in this case, and therefore axial tension forces in columns were never developed when bracing pattern C1 was used.

On the other hand, maximum compressive forces obtained for bracing configuration C2 are much higher than those obtained for configuration C1. In fact, the level of compressive forces developed for bracing pattern C2 far exceeded the axial strength corresponding to balanced strain conditions. Tension forces developed for bracing configuration C2 were quite high in general, and exceeded the predicted capacity in tension for braces with an initial prestress of 50 % of the brace yield strength.

While axial compression will, in general, help improve strength of columns, the level of axial forces observed for bracing configuration C2 is probably more harmful than beneficial for the strength and integrity of the columns. As shown above, compressive and tension forces were excessive and jeopardized the safety of the building. Nonetheless, bracing configuration C2 could be used as a possible retrofit scheme for the structure, provided that axial strength of the columns is increased to a safe level. Because maximum axial forces developed in columns remained within a reasonable level, the use of external jacketing or steel collector members are viable alternatives to improve the axial strength of the columns.

Axial compressive forces induced in beams remained below the axial member capacity, although they reached very high levels for some beams of the braced bays with configuration C2. For strands with an initial prestress of 75% of the brace yield strength, maximum compression forces in beams of braced bays (first and second floor levels) reached almost 80% of the capacity in pure compression. Axial tension in beams was observed in only a few members and was very small with both bracing configurations.

The results presented above suggest that while the axial force level in column and beam members may indeed be quite high and exceed the axial capacity of the existing members, the post-tensioned bracing system can be designed to provide an allowable axial load level. The level of axial load induced in columns is related to the proper selection of the bracing configuration rather than to the strength of the braces, as demonstrated by the significant difference in the axial force level obtained for bracing configurations C1 and C2. Overall, the level of axial forces induced is such that external strengthening of members is a feasible alternative.

The results obtained above indicate that using either rods or strands, the overall dynamic response and the magnitude of axial forces in existing members is, in general, very similar. There is, however, one aspect in which the material strength may be decisive in the design process of the post-tensioned bracing system. Because of the higher ultimate strength of steel strands, brace forces for a bundle of strands will be larger than those of a bundle of steel rods ($\approx$ 1.4 times larger). Thus, it can be anticipated that the design of anchor systems and modifications to foundations for steel strand braces will be both more cumbersome and expensive.

5.4 SUMMARY AND CONCLUSIONS

The post-tensioned bracing system as a retrofit scheme was studied by examining the behavior of a single-story single-bay structure and a three-story frame building. Both inelastic static and dynamic behavior were investigated. Main parameters studied included the level of initial brace prestressing and brace yield strength. Based on the analyses and the results obtained from the evaluation of the post-tensioned bracing system, the following conclusions were obtained:

a) Yielding in tension reduces the amount of initial prestress in the brace, but it does not necessarily lead to the total loss of prestress. Braces can be allowed to yield without completely losing the prestress force. The maximum allowable elongation of the brace beyond that at prestressing must not exceed the yield deformation.

b) Dynamic analyses indicate that high initial prestress levels help reduce the lateral response of the building. Initial prestress levels of 50% of the brace yield strength or higher should be used in design for the best performance of the system.

c) Initial brace prestressing can significantly modify the distribution of internal forces (bending moments and axial forces) of existing elements. Depending on the bracing configuration, brace size and initial prestress level, the magnitude of the induced forces due to prestressing may reach values that approach the capacity of the members, particularly in exterior columns of the building. Initial brace prestressing could become a disadvantage of the post-tensioned bracing system and may impose a limitation on the maximum brace size that can be safely prestressed without jeopardizing the integrity of the existing building.

d) Brace strength (steel rods versus steel strands) showed no significant influence on the overall dynamic response of the structure. At the same time, the higher strength of steel strands leads to compressive axial forces in columns and beams that are slightly higher than those obtained with steel rods. However, because of the lower strength of steel rods the design of anchor systems and modifications to foundations for steel rod braces may be more economical, and may represent a preferable alternative to steel strands in the design of a post-tensioned bracing system.

CHAPTER VI

RETROFIT SCHEMES - PERFORMANCE AND EVALUATION

6.1 GENERAL

The inelastic response of original and retrofitted buildings for the selected earthquake records is presented in this chapter. The results are presented individually for each of the prototype buildings considered in the present study. The selected retrofit schemes to improve the seismic behavior of the original building include post-tensioned bracing systems, concentric X-bracing and the addition of structural walls.

As discussed in Chapter II, solutions that confine retrofit operations to only the perimeter of the structure are often preferred because they expedite the rehabilitation process and minimize disturbance to the occupants. Accordingly, the retrofit schemes included in this study will be added only to perimeter frames of the buildings.

The performance of the original and retrofitted buildings is compared and evaluated by examining lateral displacements, maximum inter-story drifts, and the behavior of the existing reinforced concrete frame and that of the new elements incorporated by the retrofit scheme.

6.2 PROTOTYPE STRUCTURE I - THREE-STORY BUILDING

Analyses of the original and retrofitted buildings were conducted only in the longitudinal direction of the building. However, because structural properties and behavioral characteristics of frame members are similar in both directions, the results and conclusions obtained from analyses of the retrofit systems are believed to be applicable for the transverse direction as well.

6.2.1 Original Building

6.2.1.1 Dynamic Response Analysis

The lateral stiffness and strength characteristics of the original building have been presented in detail in Chapter IV. Table 6.1 shows the dynamic properties of the building

157

In terms of the fundamental period of vibration. Also shown in this table are the effective damping ratios corresponding to the different types of soil conditions selected for study. For firm soil conditions, effective damping was selected as 2% of critical in all cases as indicated in Chapter III. For soft soil conditions, effective damping of the soil-structure system was determined using the procedure outlined in section 3.3, and varied primarily depending upon the type of soil and, the ratio between the fundamental period of the flexible supported structure and that of the fixed-base structure (period lengthening ratio).

Table 6.1 Dynamic properties of original building.

Building	Fundamental Period (sec) [Effective Damping]*			
	Soil Type			
	Firm	Soft		
		Silty Clay Deposits (Mexico City)	San Francisco Bay Mud (California)	
			Case I	Case II
Original	1.11 [2.0 %]	1.13 [2.4 %]	1.12 [2.4 %]	1.13 [2.4 %]

* values are based on a h* / r ratio of 0.51 in accordance with the dimensions of the foundation.

Notice that the period lengthening of the building on soft soil sites is minimal. Consequently, effective damping ratios differ little from those of the building on firm soil sites.

Dynamic Response

a) Building Response on Firm Soil Sites

The time history response of the building for the earthquake records on firm soil is presented in Fig. 6.1. Roof displacement maxima is obtained for the Viña del Mar record, with a value of 7.51" which corresponds to 1.74% overall drift (roof displacement divided by the height of the building). Maximum roof displacement for the other two records is of the same order, as shown in Fig. 6.1. A comparison of maximum inter-story drifts for building subjected to the records on firm soils is presented in Fig. 6.2. Note that maximum inter-
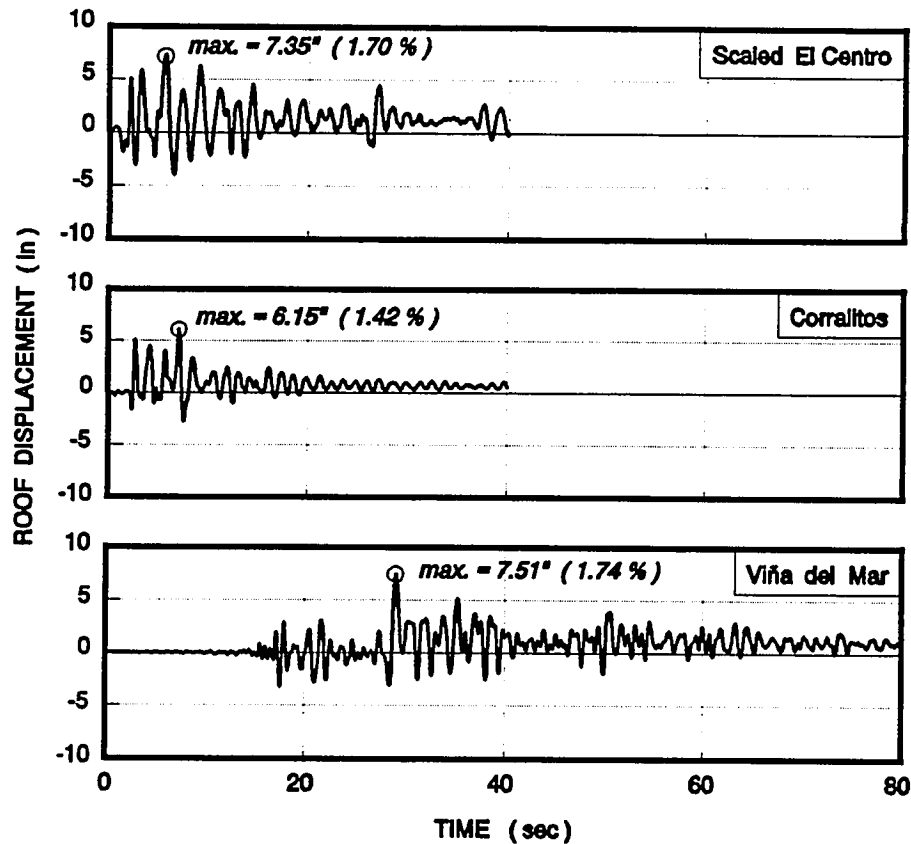
Figure 6.1 Time - history response of the original building obtained for the records on firm soil sites. (Scaled El Centro, Corralitos and Viña del Mar)

story drifts for the scaled El Centro and Viña del Mar records occurred in the first story, while for the Corralitos record maximum inter-story drift occurred in the second story. Inter-story drifts in the first story for the scaled El Centro and Viña del Mar records exceed a value of 3%. For the Corralitos record, maximum inter-story drift approaches 2% in the second story. In all three cases the values for the maximum inter-story drifts are large and may represent a threat to the overall stability of the building.

Overall, damage to frame members produced by the records on firm soils is severe. The analyses revealed that splice failure would occur in all columns of the first story and in some columns of the second story for all three earthquake records on firm soil sites.
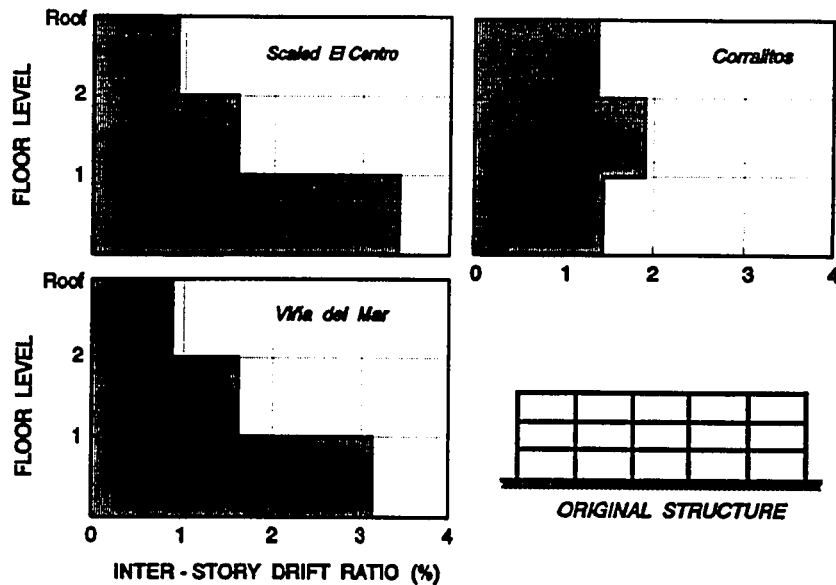
Figure 6.2 Maximum inter-story drift ratios for the original building subjected to the ground motion on firm soil sites. (Scaled El Centro, Corralitos and Viña del Mar)

Similarly, pull-out of bottom beam reinforcement is predicted in all beams of the first and second floor. Yielding in "negative" moment is observed in all beams in the first floor and in some beams of the second floor. Inelastic behavior of members in the top story was almost non-existent or minimal.

b) Building Response on Soft Soil Sites

The time - history response and the maximum inter-story drifts ratios obtained for the original structure subjected to the two records on soft soil conditions are presented in Fig. 6.3. The roof displacements shown in this figure consider soil-structure interaction effects and thus include the lateral displacements and rocking of the foundation. The latter is, however, negligible in this case. The drift values shown take due account of the lateral displacement and rocking motion of the foundation and correspond to the actual inter-story drift experienced by the building (Δ in Fig. 3.14). Also, the roof displacement and drift values shown in Fig. 6.3 for the Oakland record correspond to those obtained using soil
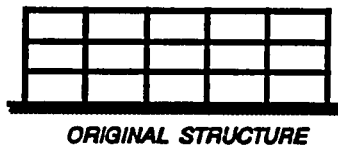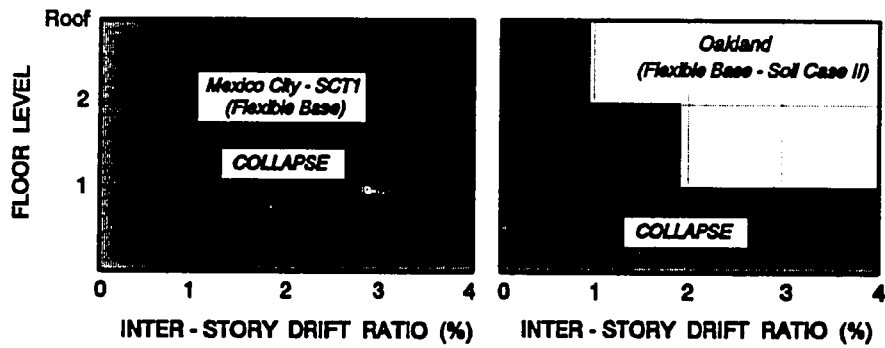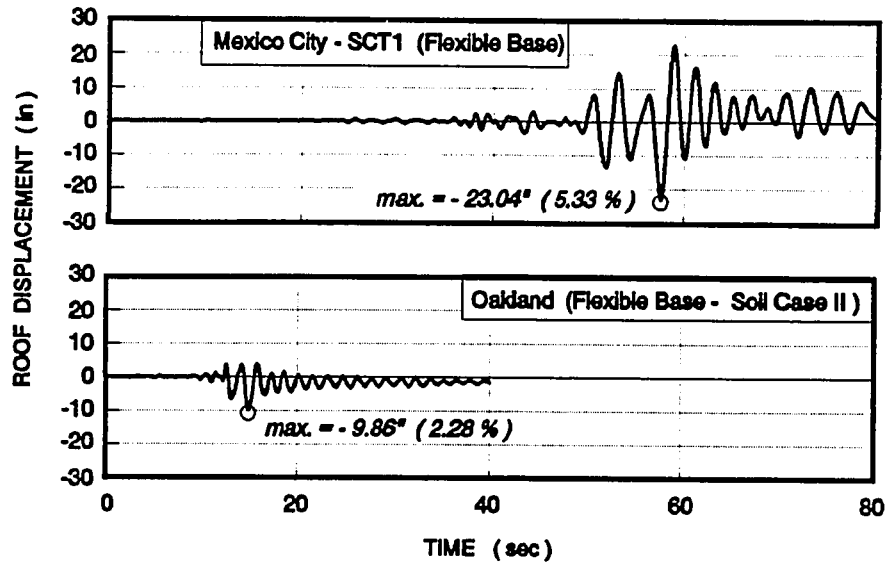
Figure 6.3 Time - history response and maximum inter-story drifts for the original building subjected to the records on soft soil sites. (Mexico City - SCT1 & Oakland (OHW))

case II, and differ little with those obtained for the fixed-base condition or using soil case I. In general, soil-structure interaction effects proved to be negligible and did not have any significant effects on the response of the original building.

The results shown in Fig. 6.3 suggest that the original building would probably have collapsed during these two ground motions. For the Mexico City - SCT1 record, the building exhibited lateral displacements far in excess of 4% drift in all three stories. For the Oakland record, only the first story exhibited a drift in excess of 4%. However, such an inter-story drift would most probably lead to the local collapse of the first story and that of the entire structure.

6.2.1.2 Summary

The behavior exhibited by the original building for the earthquake records on firm and soft soils is inadequate. For the buildings on firm soil, reinforced concrete members are expected to suffer extensive damage for the three earthquake records considered. Partial collapse of the structure is most probable, which combined with the lack of ductility of its members could lead to total collapse. For the buildings on soft soils, collapse of the building is anticipated for both records.

6.2.2 Retrofit Scheme I - Post-Tensioned Bracing Systems

Four bracing configurations were selected to evaluate the performance of the post-tensioned bracing system. Based on the results obtained in Chapter V, only steel rods were considered for braces and only two levels of initial brace prestressing were included in the analyses, namely: 50% and 75% of the brace yield strength. Figure 6.4 shows all four bracing configurations designed for study. Bracing configurations C1 and C2 are the same as those described in Chapter V, while bracing configurations C3 and C4 are new bracing schemes. As shown in Fig. 6.4, most braces consist of two 1 3/8" diameter steel rods, except for the braces of two bays on the third story of bracing configuration C3 which consider only one 1 3/8" diameter rod. The latter design configuration was adopted mainly to take advantage of the reduced stiffness and strength demands at the top story of the building. All bracing schemes were designed to provide different levels of stiffness and strength. Notice that for bracing configuration C4, braces have been anchored every other
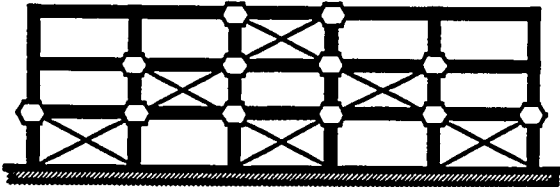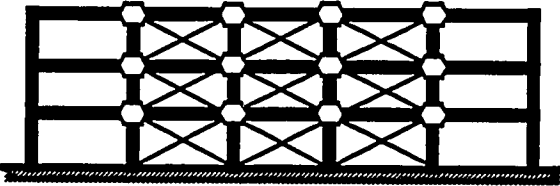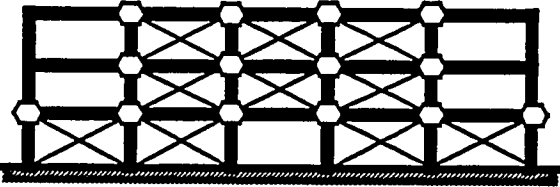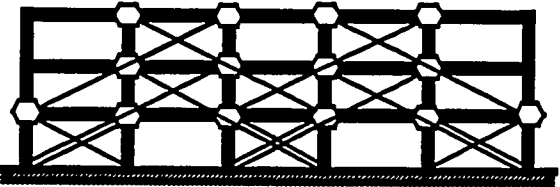
$2 - 1\frac{1}{4}" \phi$ Rods (G178) (Area = 3.16 in^2)

$1 - 1\frac{1}{4}" \phi$ Rods (G178) (Area = 1.58 in^2)

Figure 6.4 Bracing configurations for the three-story building with post-tensioned bracing system. (perimeter frames only)

floor, except at the first floor level where braces are anchored at each joint. The main reason for selecting such a scheme was to ease installation of anchor devices and reduce congestion of reinforcement at the joint.

A particular aspect of the post-tensioned bracing system is the addition of external forces to existing members due to the initial prestressing of braces. In Fig. 6.5, the bending moment distribution obtained in columns of perimeter frames due to gravity loads is compared with that obtained for the braced structure (scheme C4, braces with 75% of initial prestressing). Also shown in this figure is the ratio between the acting moments and the estimated capacity of the sections. At the base of columns, the capacity of the section is given by failure of splices, M_{sp} ; at the top, sections are assumed to develop flexural yielding, M_y. Forces due to prestressing of braces are assumed to be resisted exclusively by the perimeter frames. Bracing configuration C4 was selected to evaluate the effects of
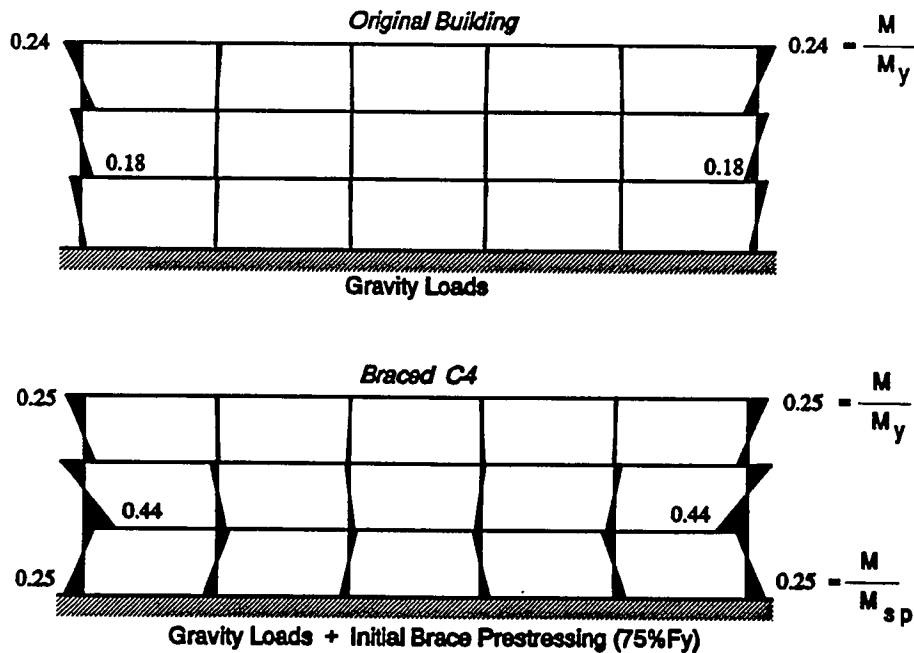
Figure 6.5 Effects of initial brace prestressing on the bending moment distribution in perimeter frame columns. Original building and braced structure, bracing config. C4 with initial brace prestressing of 75% of brace yield strength.

Initial brace prestressing because it produces some of the largest forces in the existing reinforced concrete members.

The increase in column bending moments due to initial brace prestressing is apparent, particularly for exterior columns. Notice that for first story exterior columns, bending moments are reversed with respect to those obtained under gravity loads alone. Maximum bending moments are obtained in first and second story exterior columns. The magnitude of these moments correspond to 25 and 44% of the splice capacity for the first and second story columns, respectively. In beams, initial brace prestressing had almost no effect on the bending moment distribution. The magnitude of the bending moments in columns due to brace prestressing does not pose a threat to the integrity of the structure, but will require special consideration to avoid serviceability problems.

The distribution of axial forces in columns and beams due to gravity loads and initial brace prestressing for the same bracing scheme (C4) is shown in Fig. 6.6. As expected, axial forces in columns are all compressive forces. Note that the magnitude of these forces is significantly increased with respect to those under gravity loads alone. For some interior
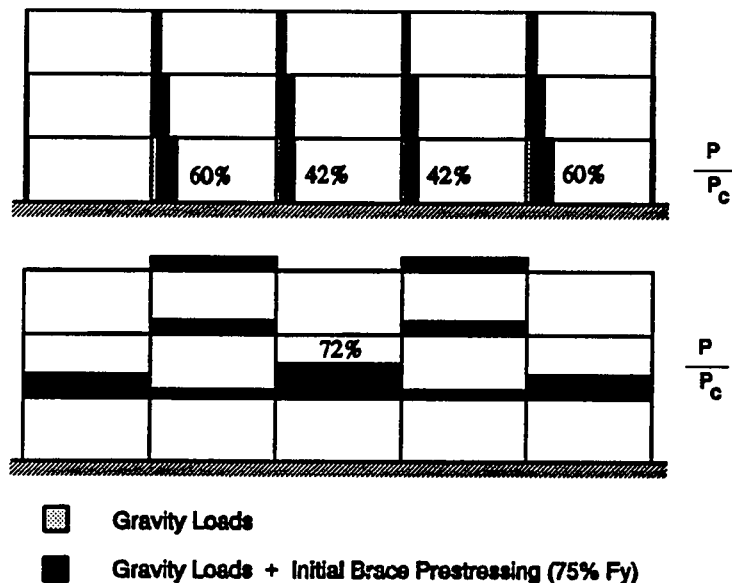
Figure 6.6   Axial force distribution in columns and beams for the braced structure with configuration C4 and initial brace prestressing of 75% of brace yield strength.

columns in the first story, the induced axial forces are greater than the load at balanced strain conditions, but remain below the estimated compressive capacity.

Axial forces in beams are all compressive forces. The level of the axial forces due to prestressing in beams remained, in general, within 40% of their capacity in pure compression. However, the axial force induced in the central beam of the first floor approached 72% of the capacity in compression and must be strengthened to carry these additional axial forces.

As indicated in Chapter V, the magnitude of the axial compressive forces due to brace prestressing may vary considerably during earthquake loading, and cannot be relied upon to improve the behavior of reinforced concrete members. Therefore, member capacity was based on axial forces due to gravity loads alone.

The forces induced by initial brace prestressing for the other bracing configurations are in general of the same magnitude or smaller. Axial forces induced in columns are always compressive forces for all the configurations studied. However, small initial tension forces are induced in some beam members for the other configurations. The techniques to help carry these tension forces or excessively high compression forces are discussed later in this Chapter.

6.2.2.1 Lateral Stiffness and Strength

In Fig. 6.7, the relationships for the base shear coefficient and the drift at the centroid of inertia forces for the existing (original) building and those for the braced building with the four configurations are compared. The relationships shown in Fig. 6.7 have been obtained using a uniform lateral load distribution over the height of the building. An initial prestress level of 75% of the brace yield strength is assumed for all bracing configurations.

As can be seen in Fig. 6.7, the increase in stiffness and strength for all bracing configurations is substantial. Because braces are initially prestressed to 75% of their yield strength, braces that elongate (lengthening braces) under the action of the lateral load reach yielding before braces that shorten (shortening braces) begin to sag. Maximum strength of the braced structure is reached when the shortening braces begin to sag in the first story. While bracing configuration C2 provides a larger initial stiffness than configuration C1, ultimate strength for both configurations is almost the same. This result is explained by the
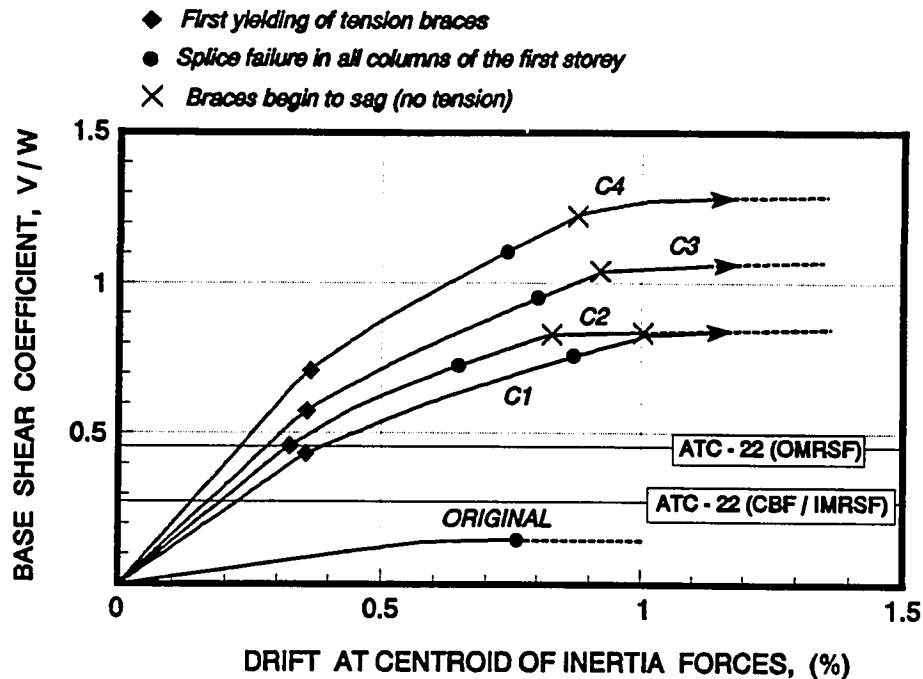
Figure 6.7 Base shear coefficient and drift at centroid of inertia forces relationship for the three-story building. Original and braced structure with post-tensioned steel rods (configurations C1, C2, C3 & C4; 75% initial prestressing).

fact that both bracing configurations have the same number and size of braces in the first story and that ultimate strength is primarily governed by inelastic behavior of the braces in that story.

Yielding of lengthening braces began at a drift level of about 0.35% for all bracing configurations, as shown in Fig. 6.7. In all cases, first yielding was observed for the braces of the first story. The drift level corresponding to failure of splices in all columns of the first story varied depending upon the bracing configuration considered. The most significant change is observed for bracing configuration C2, for which the drift corresponding to column splice failure is reduced with respect to that observed for the original building and for the other bracing configurations. Notice, however, that the base shear coefficient corresponding to failure of splices is almost the same for configurations C1 and C2. The reason for this result is that the lateral stiffness of the second and third stories of bracing

configuration C2 is larger than that of configuration C1 (see Fig. 6.4). Thus, for a given base shear coefficient, the drift at the centroid of inertia forces is smaller. On the other hand, the lateral stiffness and strength of the first story is the same for both bracing configurations, and therefore the base shear and the first story drift (not shown in the figure) at failure of splices is almost the same for both bracing configurations.

Overall, stiffness and strength of the braced structure is governed by the behavior of the bracing system. Notice that failure of splices in columns has no appreciable effect on the stiffness nor on the maximum strength of the structure.

Also shown in Fig. 6.7 are the base shear coefficients that would be required by ATC-22 for the original and the braced buildings. The higher coefficient shown corresponds to that of an Ordinary Moment Resisting Space Frame (OMRSF). The lower coefficient corresponds to a concentrically braced frame (CBF) with an intermediate moment resisting frame (IMRSF) capable of resisting at least 25% of the lateral loads. Since lateral strength of the building is governed by the bracing system rather than the failure of column splices, semi-ductile elements were assumed to calculate the coefficient for a CBF with an IMRSF. The building under study cannot be classified as an IMRSF because its reinforcing details are those of an OMRSF (ATC-22 does not include CBF with OMRSF). Also, the post-tensioned bracing system cannot be classified as a concentrically brace frame because the response modification factors embodied in the provisions of ATC-22 are intended for brace systems with structural steel sections. The latter bracing systems will, in general, higher energy dissipation capabilities than a post-tensioned bracing systems. Thus, a lower lateral load level can be allowed for concentrically braced frames. However, the required resistance for a CBF and an IMRSF can be considered, for comparison, as a lower bound for the required strength of a post-tensioned bracing system.

It is clear from Fig. 6.7 that all four bracing schemes meet the lower bound for strength defined above. Notice that if yielding of the braces is considered as the lateral resistance of the braced frame (as a possible design criterion in an elastic analyses procedure), all schemes would supply the required strength by ATC-22. The implications of these results are discussed later in Chapter VII.

6.2.2.2 Dynamic Response Analysis

Dynamic Properties

Table 6.2 shows the fundamental periods of vibration for the original and braced structures. Also shown in this table are the effective damping ratios corresponding to the different types of soil conditions selected for study. For the buildings supported on soft soils, the period lengthening ratio is larger for the braced buildings than for the original structure. Consequently, the resulting effective damping ratio is higher for the braced buildings (see Fig. 3.15), particularly for bracing configuration C4. This behavior is a direct result of the relative increase of the flexibility of the foundation medium with respect to that of the super-structure. Also note that the dynamic characteristics of the buildings supported on the clay deposits of Mexico City and those on the San Francisco Bay Mud - Case II are almost the same. The San Francisco Bay Mud - Case I is a stiffer soil type and has a smaller hysteretic damping ratio (see Table 3.1), and thus the effective damping ratios for case I are not as high as those for the other two types of soil.

Dynamic Response

The behavior of the braced structure subjected to all the selected earthquake records is presented in this section. For clarity, however, the response of the braced building on firm soil sites is presented separately from that on soft soils.

a) Building Response on Firm Soil Sites

Maximum inter-story drift ratios obtained for all four bracing configurations under the ground motions on firm soil sites are shown in Figures 6.8 through 6.10. In these figures, the maximum inter-story drifts are shown for the two levels of initial brace prestressing considered for study; 50 and 75% of brace yield strength. The results show that in most cases, the higher the initial brace prestressing, the lower the inter-story drift ratio, regardless of the bracing configuration or the ground motion considered. This result confirms the fact that early energy dissipation through yielding of braces leads, in general, to reduced overall response of the structure.

Notice that bracing configuration C1 shows, in general, very little improvement in the response with respect to that observed for the original structure (see Fig. 6.2). In this case, the increase in strength and ductility provided by the bracing system is offset by the

Table 6.2 Dynamic properties of the original and braced buildings with post-tensioned steel rods.

Building	Fundamental Period (sec) [Effective Damping]*			
		Soil Type		
	Firm	Soft		
		Silty Clay Deposits (Mexico City)	San Francisco Bay Mud (California)	
			Case I	Case II
Original	1.11 [2.0 %]	1.13 [2.4 %]	1.12 [2.4 %]	1.13 [2.4 %]
Config. C1	0.52 [2.0 %]	0.56 [3.8 %]	0.55 [3.2 %]	0.55 [3.4 %]
Config. C2	0.46 [2.0 %]	0.51 [4.4 %]	0.49 [3.8 %]	0.50 [4.3 %]
Config. C3	0.44 [2.0 %]	0.49 [4.6 %]	0.47 [3.9 %]	0.48 [4.5 %]
Config. C4	0.40 [2.0 %]	0.46 [5.6 %]	0.44 [4.0 %]	0.45 [5.6 %]

* values are based on a h^*/r ratio of 0.51 in accordance with the dimensions of the foundations

increase in demands due to shortening of the fundamental period of vibration of the building (see Fig. 4.26). Bracing configuration C2 does provide some improvement in the response of the building, particularly for the Viña del Mar record.

Bracing configuration C3 shows further improvement in limiting maximum inter-story drift ratios, but it still exhibits drift ratios that are quite high in the second story for the Corralitos record, as shown in Fig. 6.9. Configuration C4, reduces the response even more and for braces with an initial prestress of 75% of the yield strength, the maximum drift ratios remain below 1% for all three records on firm soil.

The performance of reinforced concrete members and steel braces for the records on firm soil sites is discussed in detail later in this section.
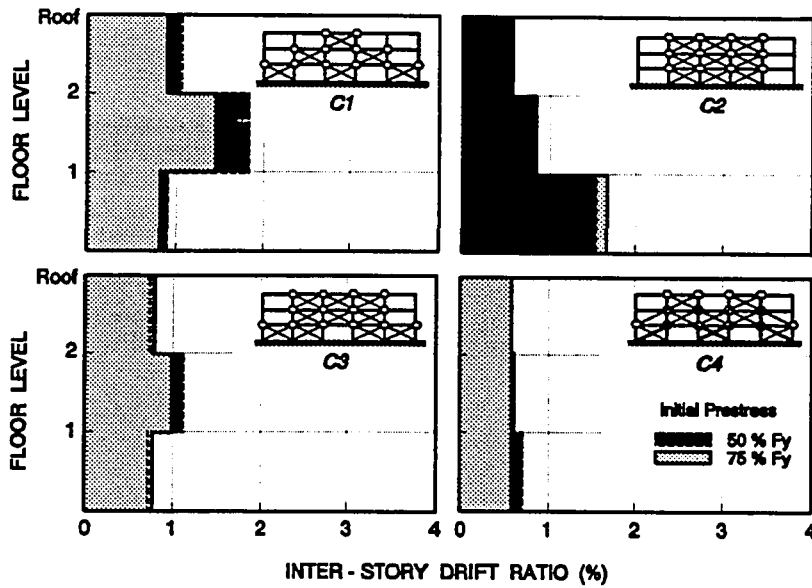
Figure 6.8 Maximum inter-story drift ratios for the braced building (bracing configurations C1, C2, C3 & C4) subjected to the scaled El Centro record.
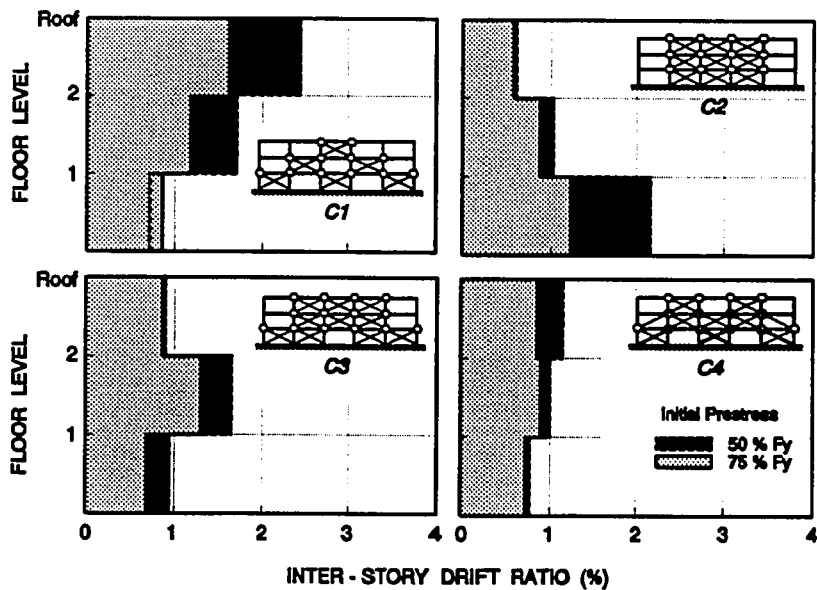
Figure 6.9 Maximum inter-story drift ratios for the braced building (bracing configurations C1, C2, C3 & C4) subjected to the Corralitos record.
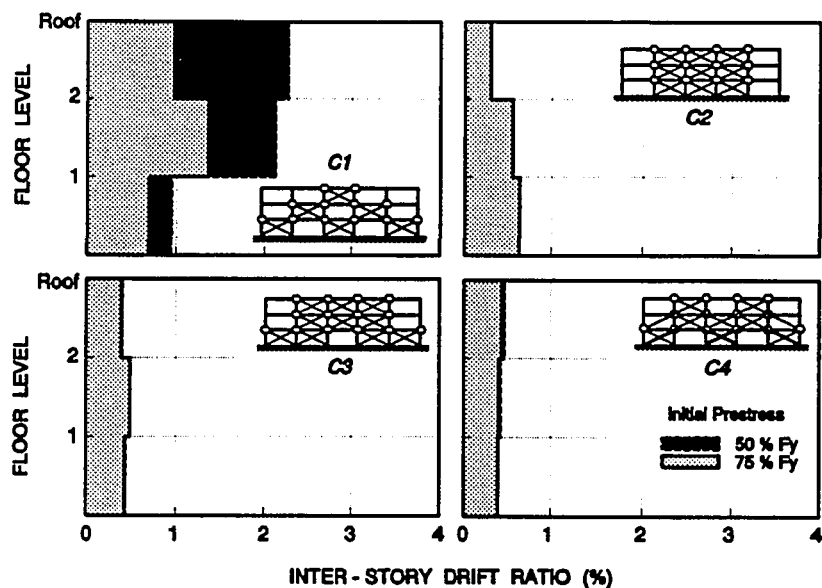
Figure 6.10 Maximum inter-story drift ratios for the braced building (bracing configurations C1, C2, C3 & C4) subjected to the Viña del Mar record.

b) Building Response on Soft Soil Sites

Maximum inter-story drifts for the braced building are presented in Figs. 6.11 and 6.12. The values shown in these figures correspond to the maximum drifts obtained from analyses of the building on a fixed or a flexible base, whichever was greater. For the Mexico City - SCT1 record, the flexible base condition always yielded the maximum inter-story drifts, as indicated in Fig. 6.11. For the Oakland record, a flexible foundation - soil case II yielded the maximum drifts for configurations C1, C2 and C3. However, for bracing configuration C4, the fixed-base condition yielded the largest inter-story drifts.

The results show a striking reduction in the response of the braced building (see Figs. 6.3 and 6.12). For the Mexico City - SCT1 record, inter-story drifts are less than 0.25% for all four bracing configurations. These results are very similar to those obtained for the fixed-base condition. Splice failure is prevented in all columns and pull-out of bottom beam reinforcement is observed in only a few beams with minimal inelastic behavior. Steel braces remained within the elastic range regardless of the level of initial prestress provided,
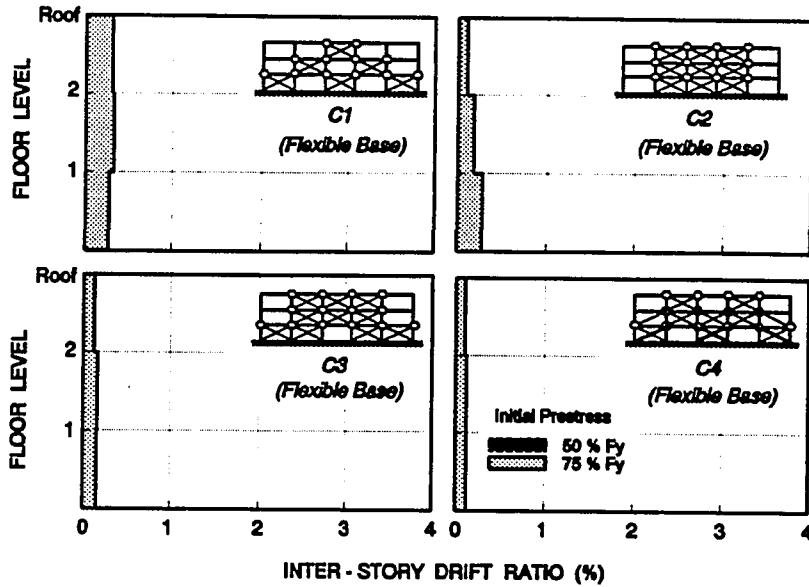
Figure 6.11 Maximum inter-story drift ratios for the braced building (bracing configurations C1, C2, C3 & C4) subjected to the Mexico City - SCT1 record.
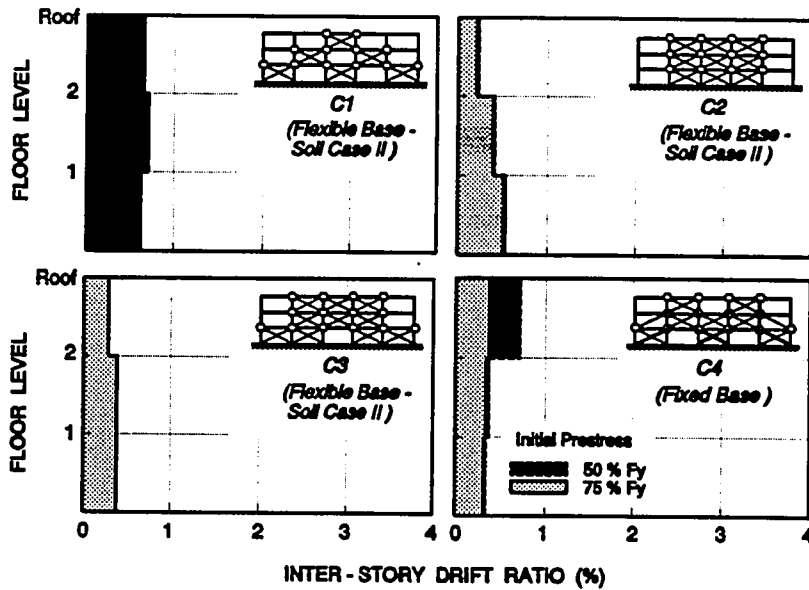
Figure 6.12 Maximum inter-story drift ratios for the braced building (bracing configurations C1, C2, C3 & C4) subjected to the Oakland (OHW) record.

for all bracing configurations. The use of a higher initial prestress level to dissipate energy through yielding of braces at small drifts did not have any influence in the response of the building in this case. It is clear, however, that initial brace prestressing must be provided to prevent the braces from becoming slack during the response of the building.

For the Oakland record, the response of the braced building is also significantly reduced. However, maximum inter-story drifts are in general larger than those observed for the braced structure under the Mexico City - SCT1 record. The level of initial brace prestressing has an appreciable effect only for bracing configuration C4, and similar to the results obtained for the braced structure on firm soil sites, a higher level of initial prestressing led to reduced inter-story drifts. Behavior of reinforced concrete members and steel braces vary with each bracing configuration, but their performance is improved in every case with respect to that of the original structure. Bracing configurations C3 and C4 with an initial prestress of 75% of the yield strength provide the largest reductions in the inter-story drifts.

Performance of Post-tensioned Bracing System

The results presented above for the braced structures on both firm and soft soil conditions indicate that the post-tensioned bracing can be used to reduce the response and improve the overall response of the three-story building under study. The effectiveness of the system to improve the response of the building depends, of course, on the bracing configuration. However, for the building under consideration, the post-tensioned bracing system is more effective for structures supported on soft soil sites than for those supported on firm soil sites.

Evaluation of the maximum inter-story drifts indicates that bracing configuration C4 with braces initially prestressed to 75% of their yield strength is the most effective for reducing the response of the building on both firm and soft soil sites. Also, from all of the earthquake records considered for study, the Corralitos record proved to impose the largest demands of strength and ductility on the braced structures. Thus, the results obtained for the braced building with bracing configuration C4 subjected to the Corralitos record were selected to evaluate the performance of the reinforced concrete members and steel braces.

a) Performance of Reinforced Concrete Members

In Fig. 6.13, the profile of plastic hinges developed in the perimeter frames of the original structure and those developed for the braced building with configuration C4 is compared. For the original structure, hinges are shown for the three records on firm soil, while for the braced building hinges are shown only for the Corralitos record. The amount of inelastic rotation developed by the hinges is indicated only for hinges developed at base of the columns. The numbers shown represent the ratio between the maximum rotation developed in the section and that of a splice failure. When failure is predicted for both directions of bending, the amount of inelastic rotation is shown for both cases. A similar comparison for the hinges developed in the members of interior frames is shown in Fig. 6.14.

The figures show a significant reduction in the inelastic behavior of the reinforced concrete members when the structure is braced with configuration C4; both, the number of hinges and the amount of inelastic rotation is reduced considerably. Splice failure in the columns of the perimeter frames is prevented in most cases or is just developing (or controlled). In the interior frames, failure of splices in first story columns is not prevented but the amount of inelastic rotation is reduced significantly, with only minor reductions in strength and stiffness (see typical moment-rotation relation for columns in Fig. 5.15). Note that for the braced structure failure of splices is also induced in some of the columns of the third story. Such a failure was not observed in any of the third story columns of the original building. Nonetheless, splice failure in these members is just developing in only a few columns of the perimeter frames. In interior frames the reductions in strength associated with the inelastic rotation are only about 20%.

Beam hinging is considerably reduced as well. However, the bracing system is unable to prevent the pull-out of the bottom beam reinforcement in most of the beams of the first and second floor levels. Yielding of beams in "negative" bending was developed in only a few sections.

Figure 6.15 shows the distribution of axial forces in columns and beams in the perimeter (braced) frames of the building. The axial force distribution is presented as the ratio between the maximum axial force developed in the member and the predicted capacity in pure compression or tension. Beams were treated as columns plus an effective slab

Original Building - Scaled El Centro

2.1

-9.1 4.1 -7.6 2.7 -7.6 2.7 -7.6 2.7 -7.5 2.7 -9.4 3.2

Original Building - Corralitos

-2.9 -2.8 -2.8 -2.7 -3.5

-2.7 2.1 -2.7 -2.7 -2.7 -2.7 -4.0

Original Building - Viña del Mar

-8.4 -7.1 -7.1 -7.1 -7.1 -8.8

Braced C4 - Corralitos

-1.0 -1.3

1.0 1.4
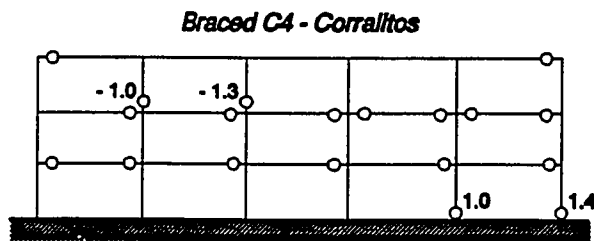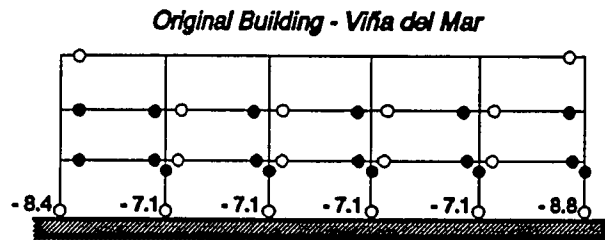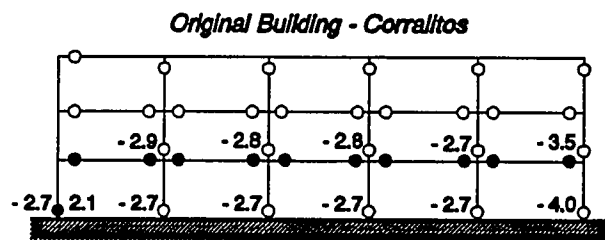
o   *hinge in only one direction of bending*

●   *hinge in both directions of bending*

+   -

Figure 6.13 Hinge location for the perimeter frames of the original and braced building with configuration C4. (Numbers indicate the ratio of inelastic rotation developed at the base of columns)
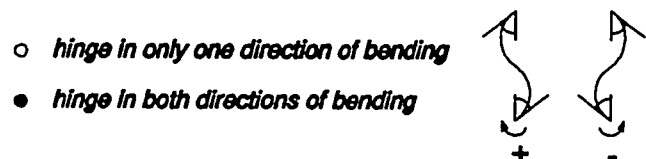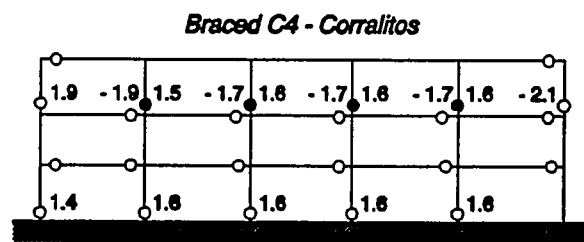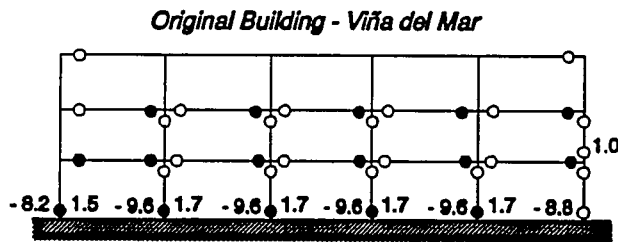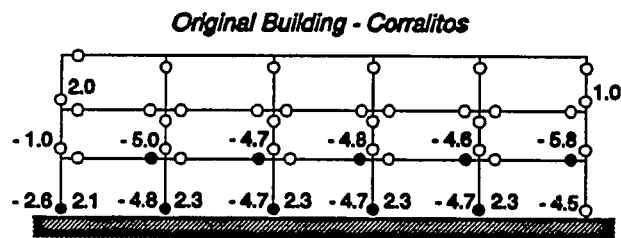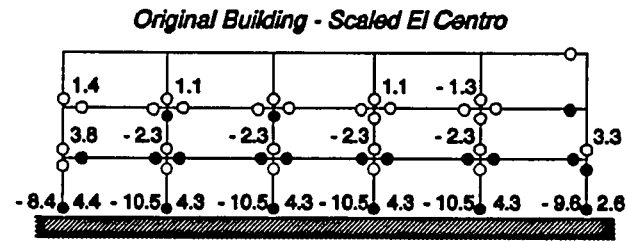
Figure 6.14 Hinge location for the interior frames of the original and braced building with configuration C4. (Numbers indicate the ratio of inelastic rotation developed at the base of columns)

width as discussed in Chapter III. As can be seen, axial forces in columns are primarily compressive forces, except for the exterior columns of the first story. The magnitude of these tension forces is significant and approach the maximum capacity of the columns in pure tension (≈ 211 kips). Clearly, tension forces are detrimental to the flexural capacity of the column members and will reduce the moment capacity associated with failure of splices. Similarly, the compression forces in some of the interior columns in the first story exceed the load at balanced strain conditions but remain below the capacity in axial compression. Notice, however, that maximum compressive forces during earthquake response do not differ significantly from the forces obtained upon initial brace prestressing (see Fig. 6.6).
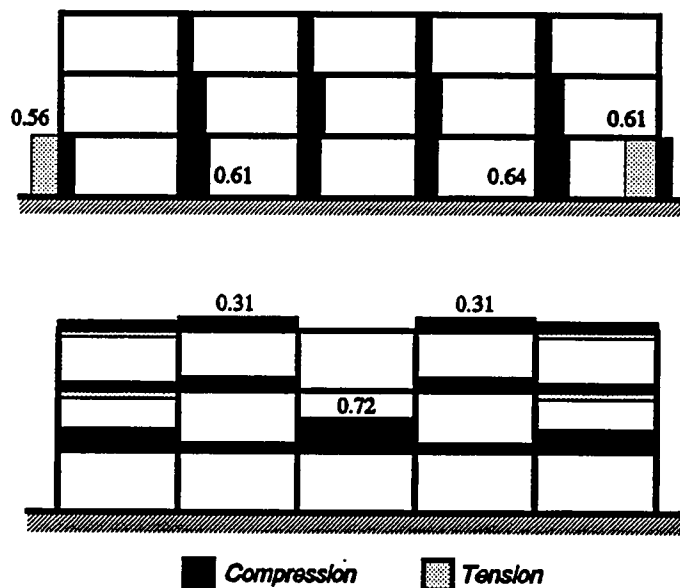
Figure 6.15 Distribution of maximum axial forces in perimeter frames of the braced building with configuration C4 subjected to the Corralitos record. (Axial force is shown as a fraction of the member capacity in pure compression or tension)

For beams, axial forces are mostly compressive forces, although some minor tension forces are observed for beams of exterior bays in the second and third stories. Maximum compressive force is observed for the first floor beam in the middle bay, approaching 72% of the beam capacity in pure compression. The level of axial forces in the rest of the beams remained within 50% of the compression capacity.

To help resist axial forces in the members, particularly tension forces, and to guarantee the effectiveness of the bracing system, it is likely that steel collector members will have to be provided along the length of the members. For the exterior columns, collector members need to be designed to resist the full magnitude of the tension forces. On the other hand, collector members to resist compression forces need to be designed to resist only a fraction of these forces to augment the compression capacity of the existing members. A detailed design of collector members is beyond the scope of the present study, however, the magnitude of the axial forces obtained for the braced structure is such that the design of collector members is feasible and relatively simple.

The addition of steel collectors to existing frame members may require a re-evaluation of the bracing scheme due to the changes in the relative stiffness of members in the structure. However, because the stiffness provided by the bracing system, will generally be much larger than that of the frame with strengthened elements, significant changes in the dynamic response (strength demands) are not anticipated. Therefore, the performance of the braced structure with strengthened elements is expected to be similar or better.

It should be reiterated that response obtained for bracing configuration C4 with the Corralitos record is the most critical case. The performance of the reinforced concrete members for the rest of the earthquake records considered in this study is even better than that presented above.
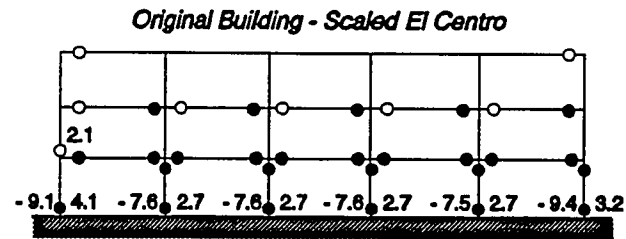
b) Performance of Steel Rod Braces

All braces reached yielding but none of them lost their initial prestress force. However, a few braces became slack during the response of the braced building, as shown in Fig. 6.16. Braces that became slack were on the second and third story of the building. First story braces yielded but never became slack. Maximum elongation of the braces approach 0.8% and correspond to about 1.4 times the yield displacement. This value for the elongation is below the 1.1% value at onset of strain hardening for steel rods, and therefore the elasto-plastic model assumed for the braces remains valid. The performance of the braces is satisfactory and consistent with the design criteria established in Chapter V for the post-tensioned bracing system.

○ *Brace reached yielding (never became slack)*

● *Brace reached yielding and became slack*
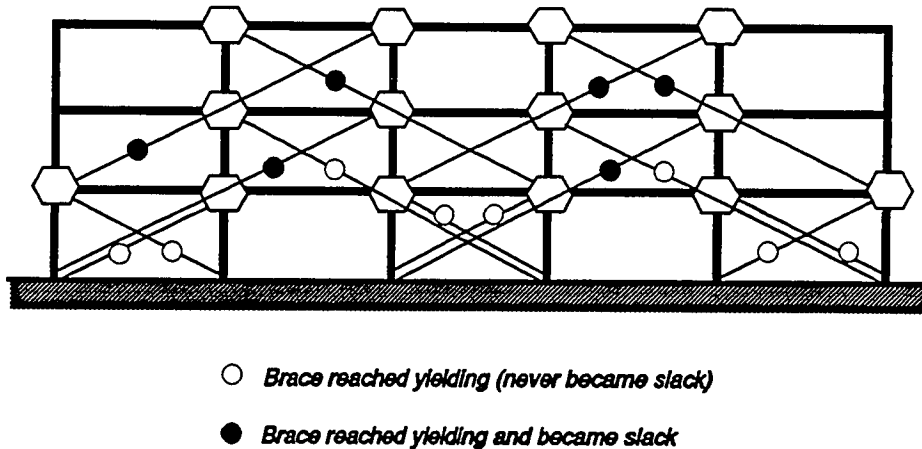
Figure 6.16 Braces that yielded and/or became slack during the response for the Corralitos record.

6.2.2.3 Summary

Four bracing configurations were studied. Each bracing configuration was designed to provide a distinct level of stiffness and lateral strength to the building. For the building on firm soil sites, all four bracing configurations improved the response of the building with respect to that observed for the original structure. Two of them can be considered to provide an adequate safety level against collapse (bracing configurations C3 and C4 with initial brace prestressing of 75% of their yield strength). However, only configuration C4 was considered to provide adequate protection to prevent severe damage of the existing reinforcing members (inter-story drifts of less than 1%, elimination of failure of splices in many columns and significant reduction of inelastic behavior in the reinforced concrete members).

For the buildings supported on soft soil sites, all four bracing configurations provided an adequate safety level against collapse and severe damage to the building. Furthermore, the results suggest that a smaller amount of bracing could be provided to the building without jeopardizing the level of safety against collapse.

An initial level of prestress of 75% of the brace yield strength proved to be the most effective in reducing the dynamic response of the building in all cases.

' 6.2.3 Retrofit Scheme II - X-Bracing (Structural Steel Braces)

Two bracing configurations were selected for evaluating the response of the structure, as shown in Fig. 6.17. Braces consisted of double angle sections and were selected to meet the slenderness requirements for seismic zones ($KL/r < 720/\sqrt{F_y}$) of the Load and Resistance Factor Design manual (LRFD) [45]. The slenderness ratio of braces varied from 82 (for 2L - 6 x 6 x 3/8) to 98 (for 2L - 5 x 5 x 5/16) for out-of-plane buckling, which governed the design of the braces. Yield strength of braces was 50 ksi in all cases.

2L - 5 x 5 x 5/16

2L - 5 x 5 x 5/16

2L - 6 x 6 x 3/8

DA1

2L - 5 x 5 x 5/16

2L - 6 x 6 x 3/8

2L - 6 x 6 x 3/8

DA2
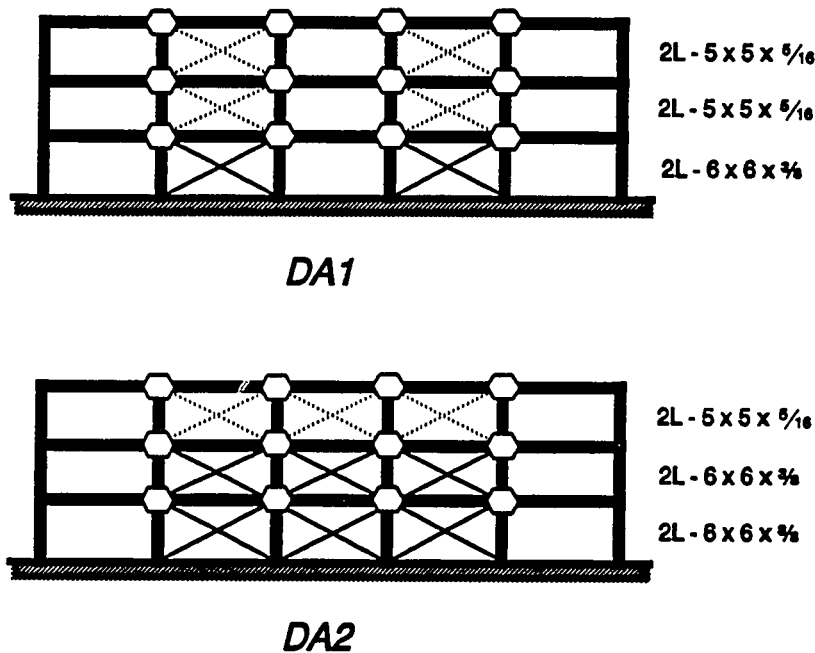
Figure 6.17 Bracing configurations for concentrically braced building with structural steel braces. (perimeter frames only)

6.2.3.1 Lateral Stiffness and Strength

In Fig 6.18, the relationships for the base shear coefficient and the drift at the centroid of inertia forces for the original and braced structures are compared. Also shown in this figure is the relationship for the post-tensioned bracing system obtained for configuration C4 (braces initially prestressed to 75% of the yield strength). As above, these relationships have been obtained using a uniform lateral load distribution over the height of

+ First buckling of braces in configurations DA1 & DA2
◆ First yielding of braces in tension
● Splice failure in all columns of the first storey
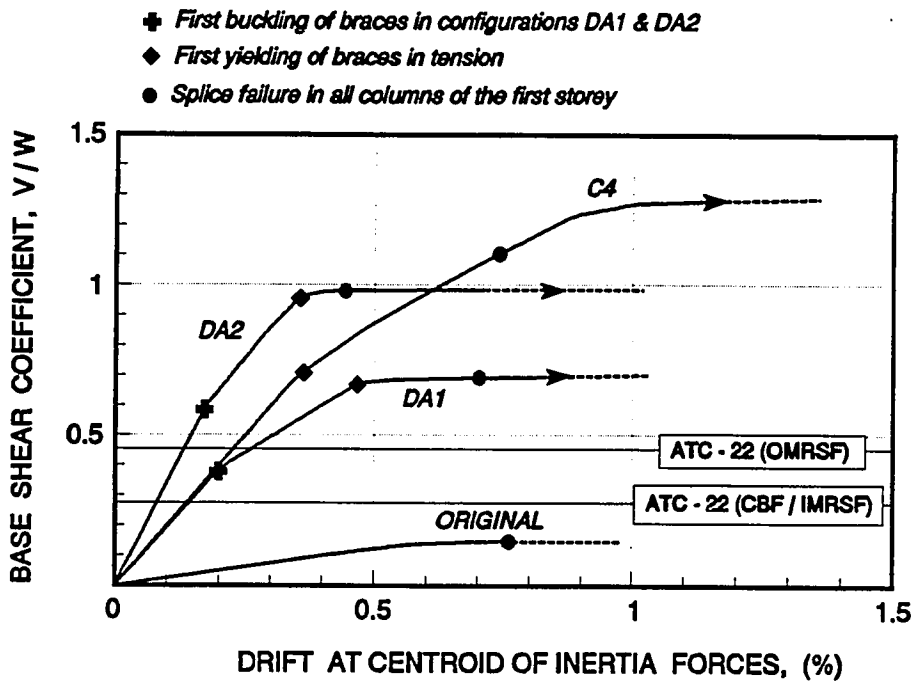
Figure 6.18 Base shear coefficient and drift at centroid of inertia force relationship for the three-story building. Original and braced structure with double angle sections (DA1 & DA2) and with post-tensioned rods (C4).

the building.

The increase in lateral stiffness and strength for configurations DA1 and DA2 is considerable. Notice that configuration DA1 was designed to provide the same initial stiffness as that of configuration C4. Such a design approach provides a basis of comparison of the energy dissipation capabilities of the two bracing systems without including the changes in strength demands due to different periods of vibration of the buildings (it is assumed that the dynamic response is governed primarily by the initial fundamental period of vibration of the structure). Because of the lower yield strength of the double angle sections, the ultimate strength of bracing configuration DA1 is much smaller than that of configuration C4. Bracing configuration DA2 provides higher initial stiffness to the building, but lower strength than configuration C4.

As shown in Fig. 6.18, buckling of double angle sections is predicted at a drift level of about 0.2% for both configurations DA1 and DA2. Reductions in stiffness due to buckling of braces are more pronounced for configuration DA1 than for configuration DA2. Yielding of braces in tension is observed at a about 0.48% for configuration DA1, while for configuration DA2 yielding of braces is predicted at about 0.36%. For both bracing configurations, buckling and yielding of braces initiated in the first story braces. Ultimate strength of the building is reached soon after yielding of braces in the first story for both configurations DA1 and DA2.

Also shown in Fig. 6.18 is the drift level that would cause failure of splices in all columns of the first story. As can be seen, yielding of first story braces preceded failure of column splices for both configurations DA1 and DA2; however, splice failure occurs soon after yielding of braces. As described above for the post-tensioned bracing system (configurations C1 and C2), the difference in drift level corresponding to the failure of column splices between DA1 and DA2 is merely a result of the different lateral stiffness and strength distribution of the two bracing configurations. The first story drift corresponding to failure of splices is similar with both bracing configurations.

The base shear coefficient required by the provisions of the ATC-22 for the *evaluation* of building structures is presented in Fig. 6.18. For comparison, two base shear coefficient levels are shown in this figure. The higher coefficient corresponds to that required for an ordinary moment resisting space frame (OMRSF) with brittle elements. The lower coefficient represents the strength required for a concentrically braced frame (CBF) and an intermediate moment frame (IMRSF) capable of resisting at least 25% of the lateral loads (semi-ductile elements were assumed to compute the coefficient because the stiffness and strength of the braced structure is governed by the bracing system). As noted earlier, the frame building under study cannot be classified as an IMRSF because its reinforcing characteristics are those of an OMRSF. However, it is reasonable to assume that the required strength for a CBF with an IMRSF is a lower bound for the lateral resistance of a CBF with an OMRSF.

The figure shows that the lateral resistance corresponding to yielding of braces for both bracing configurations DA1 and DA2 exceeds that required by the ATC-22 for a CBF with an IMRSF. Furthermore, the load corresponding to buckling of the braces is also

higher than that required by the ATC - 22, for both schemes. Implications of these results are discussed later in Chapter VII.

6.2.3.2 Dynamic Response Analysis

Dynamic Properties

The fundamental periods of the original and braced buildings with double angle braces are shown in Table 6.3. Also shown in this table are the effective damping ratios corresponding to the different types of foundation material selected for study. As expected, the period of vibration of the braced buildings is significantly reduced with respect to that of the original building, particularly for configuration DA2. For the building on soft soil sites, the resulting period lengthening ratio is significantly higher for the braced building than for the original structure. Consequently, the foundation damping factor ξ_0 (see Fig. 3.15) is considerably higher for the braced structure which results in high effective damping values for the soil-structure interaction system, as shown in Table 6.3.

Since the results obtained for the buildings with the post-tensioned bracing system on the San Francisco Bay Mud for cases I and II showed no significant differences in the response of the building, it was decided to base the evaluation of the concentric bracing system on only one of the two cases. For this purpose, case II was arbitrarily selected for study, as shown in Table 6.3.

Dynamic Response

As for the post-tensioned bracing system, the response of the building is first presented in terms of the maximum inter-story drift ratios for each one of the earthquake records, followed by a detailed examination of the performance of the members for the most critical condition. Maximum inter-story drifts obtained for the braced building, configurations DA1 and DA2, are presented in Figs. 6.19 and 6.20 for the records on firm and soft soils respectively. For the building on firm soil sites (Fig. 6.19), configuration DA2 effectively limits the response and inter-story drifts in the building, and provides an adequate safety level against collapse for all three earthquake records. Configuration DA1 is not as effective as configuration DA2, and for the Corralitos record, the building reaches high inter-story drifts

Table 6.3 Dynamic properties of the original and braced buildings with double angle sections.

Building	Fundamental Period (sec) [Effective Damping]*		
		Soil Type	
	Firm	Soft	
		Silty Clay Deposits (Mexico City)	San Francisco Bay Mud (California) Case II
Original	1.11 [2.0 %]	1.13 [2.4 %]	1.13 [2.4 %]
Config. DA1	0.40 [2.0 %]	0.46 [5.5 %]	0.45 [5.8 %]
Config. DA2	0.30 [2.0 %]	0.38 [9.8 %]	0.37 [9.9 %]

* values are based on h* / r ratios of 0.51 in accordance with the dimensions of the foundation.

that jeopardize the integrity of the building. Nonetheless, the overall response of the braced building is reduced with respect to that of the original building in all cases.

For the building on soft soil sites, the response of the building is appreciably reduced with both bracing configurations. Inter-story drifts for the Mexico City - SCT1 record are very small (less than 0.2%); the dynamic response of the braced structure is minimal. For the Oakland record, inter-story drifts are slightly larger than those obtained for the Mexico City -SCT1 record, but considerably smaller than those obtained for the original building. The results presented in Fig. 6.20 include the soil-structure interaction effects and because of the high effective damping obtained for the soil-structure system (Table 6.3), such a reduced response could have been anticipated. Nonetheless, additional analysis of the braced building on a fixed-base condition with an overall damping of 2% showed similar results. Indeed, the fixed-base condition analyses showed higher inter-story drifts for the Oakland record (about 15% higher), but did not alter the results presented above.
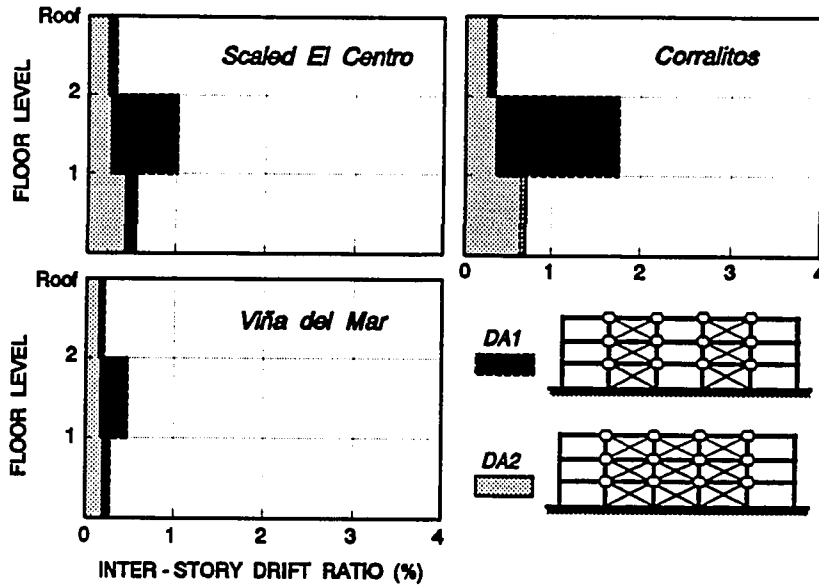
Figure 6.19 Maximum inter-story drift ratios for the braced building (bracing configurations DA1 & DA2) subjected to the records on firm soil sites (scaled El Centro, Corralitos & Viña del Mar).
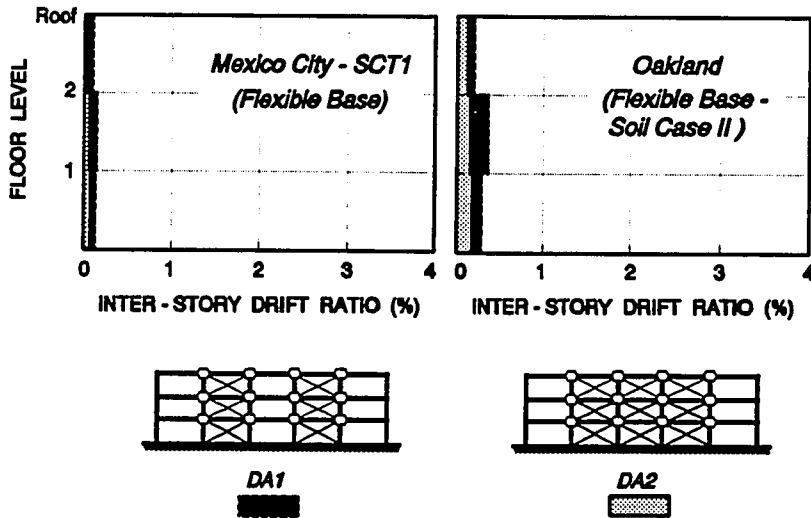
Figure 6.20 Maximum inter-story drift ratios for the braced building (bracing configurations DA1 & DA2) subjected to the records on soft soil (Mexico City - SCT1 & Oakland (OHW)).

Performance of X-Bracing System

The results indicate that the X-bracing can effectively reduce the response and improve the overall performance of the building under study. Similar to the results obtained for the post-tensioned bracing system, the X-bracing system is more effective for structures supported on soft soil sites than for those supported on firm soil conditions. Bracing configuration DA2, which has a larger number of braced bays and stronger braces, exhibited a better performance than configuration DA1.

To evaluate the performance of these two bracing configurations, a comparison of the behavior of the reinforced concrete members and steel braces is presented. Similar to the results obtained for the post-tensioned bracing scheme, the Corralitos record imposes the largest demands on the braced structures. Therefore, the evaluation of members will concentrate primarily on the results obtained for the Corralitos record.

a) Performance of Reinforced Concrete Members

A comparison of the number of plastic hinges developed in the perimeter and interior frames for configurations DA1 and DA2 is presented in Figure 6.21. The amount of inelastic rotation following a splice failure at the base of the columns is also shown in this figure. For configuration DA1, failure of splices is observed only in the second floor for the perimeter frames and, on the first and second stories for the interior frames. Beam hinging and particularly pull-out of bottom reinforcement is observed in many beams. While the number of plastic hinges in both perimeter and interior frames is reduced with respect to that obtained for the original building (see Figs. 6.13 and 6.14), the reductions in strength and stiffness associated with the inelastic rotation at the base of columns in the second story is still significant (see Figs. 5.15 and 6.21). This result suggests that local collapse of the second story is probable and therefore configuration DA1 does not provide an adequate safety level against collapse for the Corralitos record.

The behavior of reinforced concrete members with bracing configuration DA2 is significantly improved with respect to that with bracing configuration DA1. Column and beam hinging is practically eliminated in the perimeter frames. Failure of splices in columns is not prevented in the interior frames, but the amount of inelastic rotation, and thus the reduction in strength and stiffness (see Fig. 5.15), at the base of these columns is minimal.

Perimeter Frames

Interior Frames

BRACED DA1 - CORRALITOS

Perimeter Frames

Interior Frames

BRACED DA2 - CORRALITOS
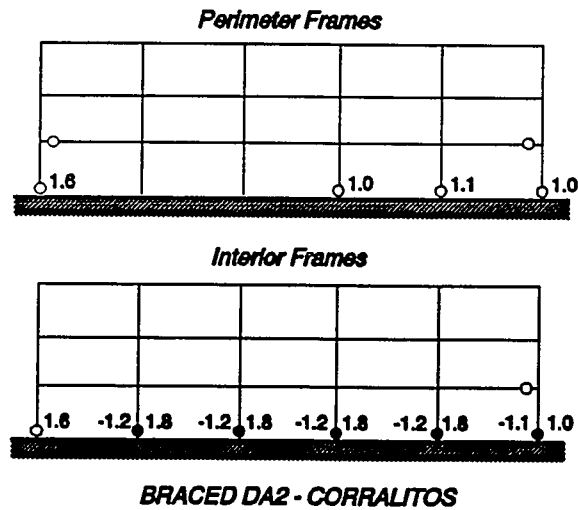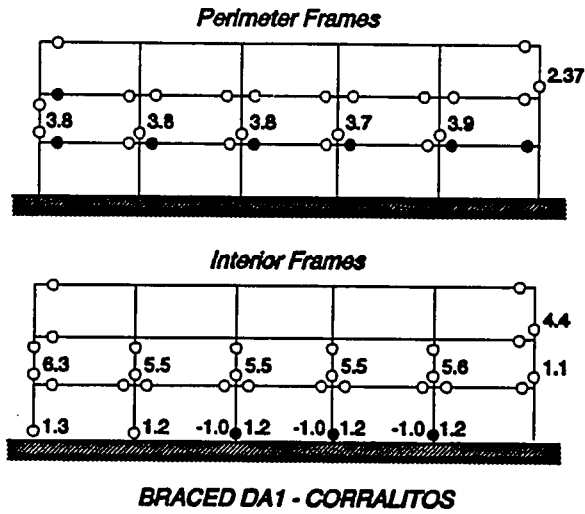
o   *hinge in only one direction of bending*

●   *hinge in both directions of bending*

+   -

Figure 6.21   Hinge location for perimeter and interior frames of the braced building with configurations DA1 & DA2. (Numbers indicate the ratio of inelastic rotation developed at the base of columns)

Beam hinging is almost non existent, as shown in Fig. 6.21.

The response of reinforced concrete members with configuration DA2 is improved with respect to that of configuration C4 (see Fig. 6.13 and 6.14). Bracing configuration DA2 is more effective in reducing hinging in beams, the number of hinges and amount of inelastic rotation in columns. However, both bracing configurations (DA2 and C4) are considered to provide adequate protection against severe damage in the reinforced concrete members. On the other hand, the behavior of reinforced concrete members with configuration C4 is better than that observed with configuration DA1. Considering that both systems, DA1 and C4, have the same initial stiffness (fundamental period), it is clear that the higher strength and the larger stiffness in the non-linear range of configuration C4 (see Fig. 6.18) are crucial for the better response of the building. Bracing configuration DA1 fails to protect the structure from severe damage and, perhaps, partial collapse, despite the higher energy dissipation characteristics of the structural steel bracing system.

The axial force distribution in columns is presented in Fig. 6.22 for both bracing configurations. The figure shows the maximum axial force developed in the members as a fraction of their corresponding capacity in pure compression or tension. It can be seen that significant tension forces are developed in the first and second story columns for both bracing configurations. Moreover, the estimated capacity in pure tension is exceeded in all the columns in the first story. Compression capacity was never exceeded, but maximum compression forces reached up to 65% of the estimated capacity. Note that the axial forces developed in columns with configuration C4 with post-tensioned rods (see Fig. 6.15) were smaller than those obtained in the present case, particularly tension forces. In addition, only two columns showed tension for configuration C4. This result is primarily attributed to the bracing configuration adopted for C4 and the initial pre-compression induced in columns due to initial prestressing of the rods.

Compressive axial forces in beams remained well below the compression capacity of these members for both bracing configurations, DA1 and DA2. Maximum compressive forces reached only 20% of the capacity in pure compression. However, axial tension exceeded the tension capacity in most of the first and second floor beams (computation of the tension capacity in beams neglected the possible contribution of the reinforcement of the slab).
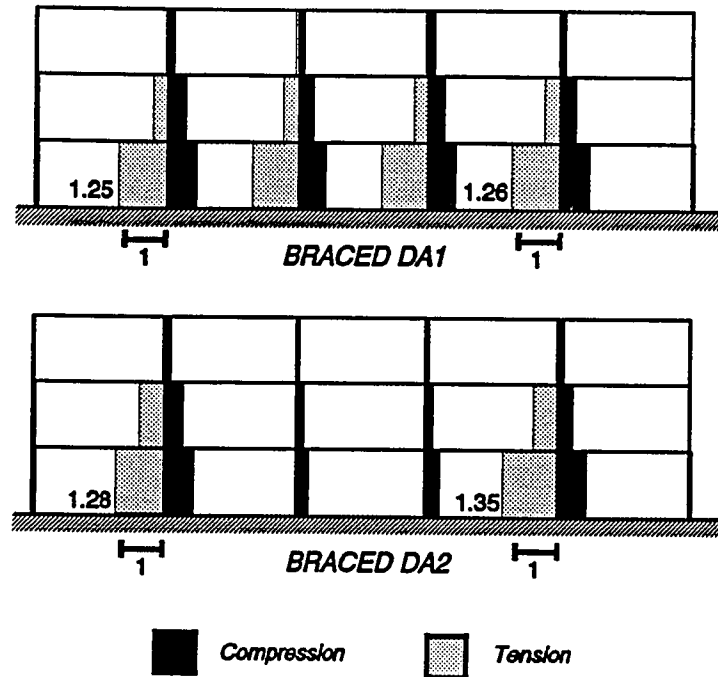
Figure 6.22   Axial force distribution in the perimeter frames of the braced building with bracing configurations DA1 & DA2. (Axial force is shown as fraction of the corresponding capacity of the member in pure compression or tension)

These results indicate that most interior columns and most beams of the first and second floor levels of both configurations must be strengthened to carry these high axial tension and compressive forces. High tensile forces in columns are particularly undesirable because they will expedite the failure of splices in columns. The addition of collectors members is crucial for the success of the X-bracing scheme as a retrofit scheme. As noted earlier for the post-tensioned bracing system, the addition of collector members may require a re-evaluation of the bracing scheme due to the changes in stiffness and thus in earthquake demands. However, because the stiffness provided by the bracing system is generally much larger than that provided by the addition of collector members, significant changes in earthquake demands are not anticipated.

b) Performance of Double Angle Braces

Brace yielding and buckling in configurations DA1 and DA2 for the Corralitos record are presented in Fig. 6.23. As can be seen, brace buckling was observed in all braces for both bracing configurations. For bracing configuration DA1, yielding was observed in all but the third story braces. Maximum elongations in tension and compression occurred for the second story braces; a result that is consistent with the maximum inter-story drifts obtained in Fig. 6.19 for the Corralitos record. For bracing configuration DA2, only first story braces reached yielding.

DA1

DA2
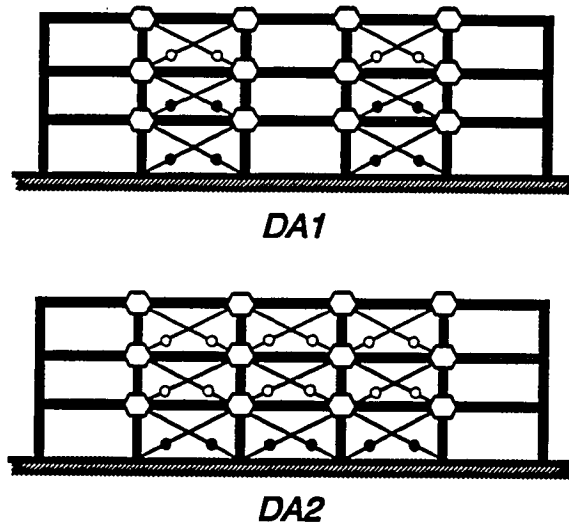
• *Brace yielded and buckled*

○ *Brace only buckled*

Figure 6.23 Yielding and buckling of braces of configurations DA1 and DA2 when subjected to the Corralitos record.

Typical hysteretic behavior of braces for these two bracing configurations is presented in Fig.6.24. In this figure, axial forces are shown as a fraction of the tensile yield strength. Similarly, elongations are shown as a fraction of that corresponding to yielding of the braces. The braces shown correspond to those that developed the maximum elongations in tension.
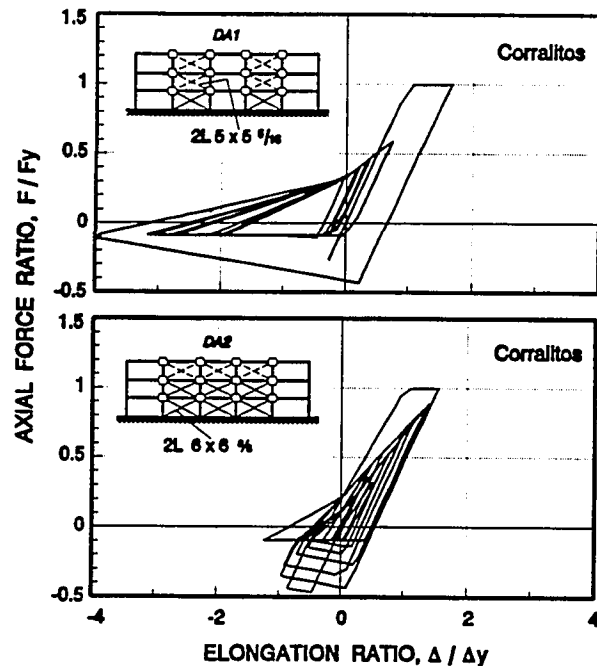
Figure 6.24 Typical hysteretic behavior of most stressed braces of configurations DA1 and DA2 for the braced buildings subjected to the Corralitos record.

For the brace in configuration DA1, inelastic excursions are extensive, particularly when the member buckles. However, for the brace in configuration DA2 inelastic excursions in compression are significantly smaller. The extension of inelastic excursions in tension are similar for both braces. Notice that for both braces shown, the members reach the yield load only once during the entire loading history. Buckling, however, is observed several times during the entire response of the building. Also note that both members reach their residual buckling capacity (P_r in Fig. 3.13), and that the reductions in strength relative to their corresponding initial buckling capacity is similar. Nonetheless, the loading paths to achieve the residual buckling capacity are totally different. The brace in configuration DA1 shows a sudden and extensive reduction of the buckling capacity in almost one cycle; the brace in configuration DA2 shows a gradual reduction of its buckling capacity through several small extensions in compression. As a result, stiffness degradation of braces is much smaller for the braces in configuration DA2, which led to smaller lateral displacements and consequently to a better performance of the reinforced concrete members.

6.2.3.3 Summary

Two bracing configurations were considered for study as retrofit schemes for the three-story building. The configurations were designed to provide two different levels of lateral strength and initial stiffness. For the purpose of comparison, one of the bracing configurations was designed to provide the same initial stiffness as that of bracing configuration C4 with post-tensioned steel rods.

For structures supported on soft soils, both bracing configurations provided an adequate safety level against collapse. Further, the expected level of damage in these instances is minimal. For structures supported on firm soils, only one bracing configuration, configuration DA2, provided adequate protection against severe damage and against collapse. The effectiveness of bracing configuration DA2 to protect the integrity of the reinforced concrete members was found to be similar to that provided by bracing configuration C4 with post-tensioned rods. Bracing configuration DA1, showed excessive damage at the second story level which jeopardized the overall integrity of the structure.

6.2.4 Retrofit Scheme III - Structural Wall

The third retrofit scheme consisted of the addition of a structural wall (shear wall) to the central bay of the perimeter frames, as shown in Fig. 6.25. Typical dimensions and reinforcing details of the selected structural wall are also presented in this figure. The design consists of an 8 in. thick eccentric reinforced concrete wall connected to the existing frame by a concrete jacket around the existing columns. The eccentric wall design was preferred to an infill panel, mainly to reduce the shear transfer problems that are encountered at the beam - infill wall interface (see Chapter II). In addition, eccentric walls are easier to erect and provide less disruption to the function of the building during retrofit operations. Also, an eccentric wall was particularly attractive in this case because spandrel beams leave enough space to build the wall on the outside of the frame, flush with the exterior face of columns, as shown in Fig. 6.25.

The column jacket consisted of four # 8 reinforcing bars, the addition of new #4 ties spaced at 4 in., and a 5 in. concrete cover, as shown in Fig. 6.25. Column jacketing was provided to prevent the failure of splices in these members and to allow columns to act as boundary elements for the wall [46]. Flexural reinforcement in the web consisted of #6

STRUCTURAL WALL
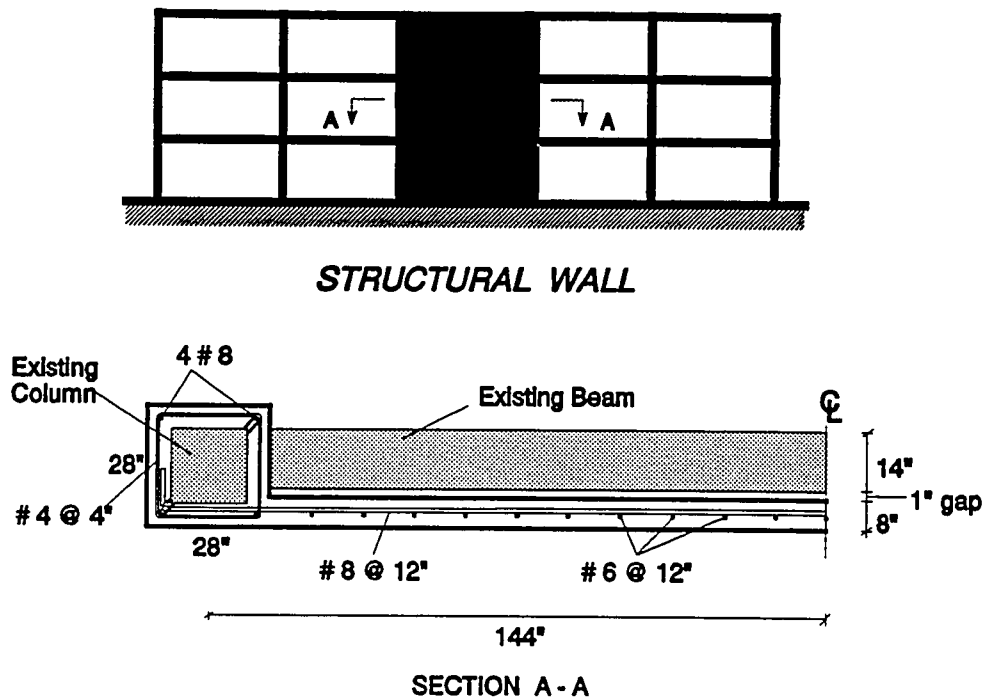
SECTION A - A

Figure 6.25 Cross section dimensions and reinforcing details of structural wall for the three-story building.

reinforcing bars spaced at 12 in. Shear reinforcement consisted of one curtain # 8 bars spaced at 12 in. as well. Design of the horizontal reinforcement followed capacity design principles to avoid a shear failure prior to developing the flexural capacity of the wall.

6.2.4.1 Lateral Stiffness and Strength

A comparison of the relationships for the base shear coefficient and the drift at the centroid of inertia forces for the original and braced building is presented in Fig. 6.26. The relationships have been obtained using a uniform lateral distribution over the height of the building. Also shown in this figure are the relationships obtained for the post-tensioned bracing system with configuration C4 (75% of initial prestress) and for the X-bracing system with configuration DA2.

It is clear from this figure that the structural wall increases the initial stiffness of the building substantially and provides the largest increase in stiffness of the three bracing
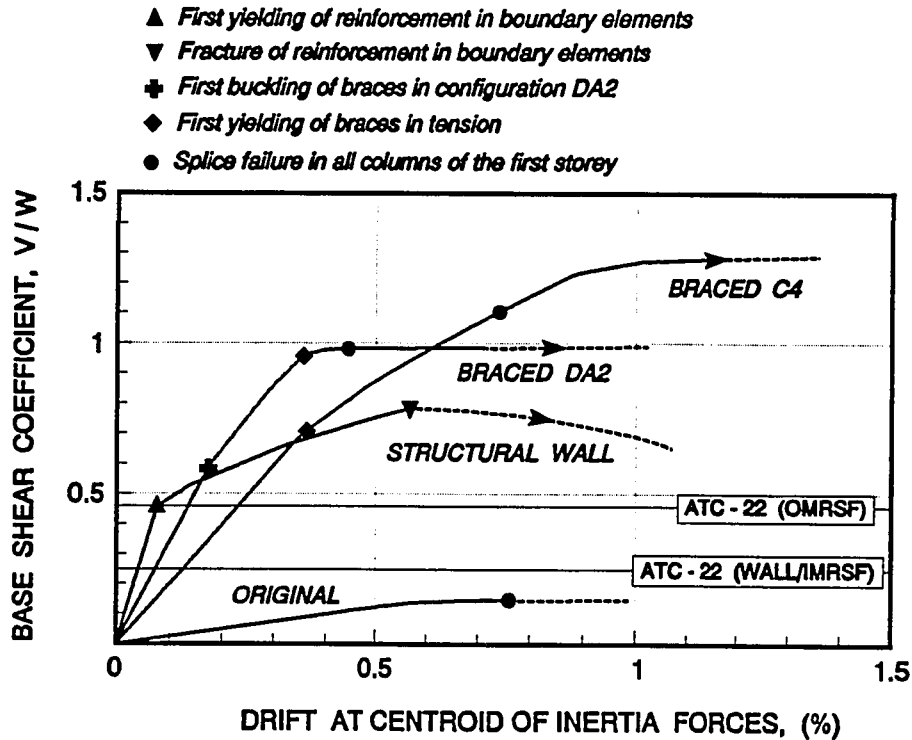
Figure 6.26 Base shear coefficient and drift at centroid of inertia forces relationship for the original and braced structure with a structural wall, with post-tensioned rods C4 and with double angle sections DA2.

schemes shown. However, the increase in ultimate strength of the wall - frame system is not as high as the other two bracing systems. Yielding of the wall in flexure is predicted at a base shear coefficient of about 0.46 and a drift of about 0.08%. A sharp decrease in the lateral stiffness of the building is observed after yielding of the wall as shown Fig. 6.26. Failure of the wall is predicted at a drift of about 0.6% by fracture of the longitudinal reinforcement in the boundary elements. Note that the wall fails in flexure prior to the failure of any of the columns splices, probably because of the high initial stiffness and the change in the deflected shape of the structure introduced by the addition of the structural wall.

For comparison, the base shear coefficient required by ATC-22 for a dual system consisting of a intermediate moment resisting space frame (IMRSF) capable of resisting at least 25% of the lateral forces and a reinforced concrete structural (shear) wall is shown in

Fig. 6.26. Because the structural wall is expected to behave in a ductile manner, response coefficients for semi-ductile elements were adopted to compute the coefficient, even though the existing frame is a OMRSF. Also shown in the figure is the required strength for an OMRSF. The building under study does not satisfy the requirement of a IMRSF (ATC-22 does not consider a wall with an OMRSF); however, it is reasonable to assume that the coefficient for a structural wall with an OMRSF should be at least that of a wall with an IMRSF. The figure shows that both yielding and ultimate strength of the wall are much higher than what it would be required by the ATC-22.

6.2.3.2 Dynamic Response Analysis

Dynamic Properties

The fundamental period of vibration for the original and the braced structure are presented in Table 6.4 for firm and soft soil conditions. The values for the fundamental period of the wall - frame system correspond to uncracked properties of the wall, except for the building on firm soil conditions, where values are shown for both uncracked and cracked properties of the wall. As discussed in Chapter III, flexural stiffness of wall elements was determined on the basis of the maximum level of moment attained during a given seismic event. For the buildings supported on soft soil sites, the behavior of the wall was found to be within the elastic range (uncracked stage). However, for the buildings supported on firm soils, cracking and yielding were observed at the base of the wall (cracked stage).

The reductions in the fundamental period of vibration of the structure are apparent. This result was expected because of the large initial stiffness provided by the wall, despite the addition of mass due to the self-weight the wall (wall increased total mass of building by only 4%). Notice the significant increase in the period of vibration due to cracking of the wall ($\approx$ 67% increase) for the wall - frame system on firm soil. A similar increase in periods obtained when soil-structure interaction effects are included. Because of the large increase in the period lengthening ratio ($\tilde{T}$ / T $\approx$ 1.8 for both soft soil types), effective damping values are unusually high.

Table 6.4 Dynamic properties of the original and braced buildings with a structural wall.

Building	Fundamental Period (sec) [Effective Damping]*		
	Soil Type		
	Firm	Soft	
		Silty Clay Deposits (Mexico City)	San Francisco Bay Mud (California) Case II
Original	1.11 [2.0 %]	1.13 [2.4 %]	1.13 [2.4 %]
Structural Wall	0.15 (0.25) † [2.0 %]	0.27 [25 %]	0.26 [24 %]

* values are based on a h* / r ratio of 0.51 in accordance with the dimensions of the foundations
† value in parenthesis corresponds to cracked wall at the base.

Dynamic Response

Maximum inter-story drifts obtained for the wall - frame system for the records on firm soil sites is presented in Fig. 6.27. As can be seen, the response is significantly reduced with respect to that observed for the original building, particularly for the scaled El Centro and Viña del Mar records. Further, the dynamic response of the wall -frame building for the scaled El Centro and Viña del Mar records is minimal. For the Corralitos record, maximum inter-story drifts approach only 0.5%. The latter drift values are smaller to those obtained for the post-tensioned bracing (configuration C4) and for the X-bracing (configuration DA2) systems (see Figs. 6.9 and 6.19 respectively).

The response of the wall - frame system for the records on soft soils was in both cases minimal with maximum inter-story drifts of about 0.03%. This result is in part attributed to the high damping ratio of the soil - structure system shown in Table 6.4. However, further analyses based on a fixed-base condition with 2% damping revealed similar or smaller lateral displacements. The lateral strength provided by the wall scheme is excessive and uneconomical for the retrofit of the building supported on soft soils. A smaller wall size or the addition of wing walls to existing columns instead of a full bay wall are more economical wall schemes that can be used for the building on soft soil sites.

Figure 6.27   Maximum inter-story drift ratios for the wall - frame building subjected to the records on firm soil sites (scaled El Centro, Corralitos & Viña del Mar).

Performance of Structural Wall System

The effectiveness of the structural wall system to reduce the response of the building on both firm and soft soils is apparent. Similar to the results obtained for the post-tensioned and concentric bracing schemes, the Corralitos record produces the largest demands on the building in terms of member forces and inelastic behavior. Thus, evaluation of member performance is based primarily on the results obtained for the Corralitos record.

Performance of Reinforced Concrete Members

Fig. 6.28 shows the profile of plastic hinges generated in the members of the perimeter frames during the response to the Corralitos record. The amount of inelastic rotation experienced at the base of the wall is also shown in this figure. As can be seen, column hinging, and most important failure of splices is completely eliminated in the perimeter frames. Beam hinging is almost non-existent as well, except for the hinges developed in the beams adjacent to the wall. These hinges in the beams correspond to pull-out of the bottom reinforcement. Yielding of beams in "negative" bending was not observed.

Perimeter Frames

WALL - FRAME SYSTEM - CORRALITOS

o   hinge in only one direction of bending

●   hinge in both directions of bending

+   -
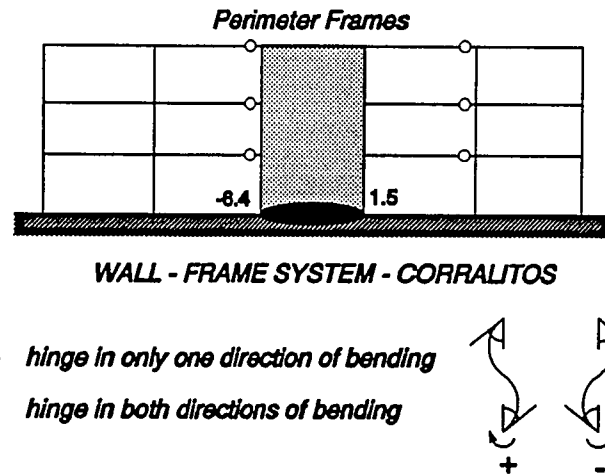
Figure 6.28   Hinge location for perimeter frames of the wall - frame system (Numbers indicate the ratio of inelastic rotation developed at the base of the wall)

For interior frames, column and beam hinging was non-existent.

The analyses predict the flexural yielding of the reinforcement at the base of the wall for the Corralitos record, as shown in Fig. 6.29. The plastic hinge extends for about 60% of the first story and wall cracking is observed up to the second story level. Maximum hinge rotation *(or rotational ductility demand)* at the base of the wall is significant ($\approx$ 6.4) but it is well below the rotation ductility capacity at ultimate ($\approx$ 15). Shear forces in the hinging region are quite high, approaching 87% of the estimated shear capacity of the wall. Web shear stresses in the hinge region are also high, but they are low enough to prevent crushing of the web due to large diagonal compressive forces (about 85% of the maximum recommended values for hinging regions [47]).

The performance of the wall - frame structure for the rest of the records on firm soils was even better. For the scaled El Centro record, the wall reaches yielding at the base, but the rotation ductility demands ($\mu_\theta \approx$ 3.7) are smaller than those for the Corralitos record. Column splice failure and pull-out of bottom beam reinforcement is prevented in every member in the structure. For the Viña del Mar record, the dynamic response of the building is minimal (see Fig. 6.27). Frame members show no inelastic behavior. The wall reaches flexural cracking at the base, but it never reaches flexural yielding.

6.2.4.3 Summary

The addition of a structural wall to the perimeter frames was studied as a retrofit scheme for the three-story building. The analyses showed that for the building on firm soil conditions, the structural wall system proved to be very effective in all cases, providing an adequate level of protection against collapse. Expected damage to the existing frame members is minimal. For the building on soft soil sites, the response of the building is minimal, and behavior of members is primarily in the elastic range. Moreover, the design of the wall was found to be too conservative when compared to the demands of strength and ductility imposed by the records on soft soil sites. Wall dimensions and reinforcement can be significantly reduced for the building on soft soil sites without jeopardizing the integrity of the wall - frame system.

6.3 PROTOTYPE STRUCTURE II - TWELVE STORY BUILDING

Analyses of the original and retrofitted buildings were conducted only in the transverse direction of the building. However, because of the similar properties and behavioral characteristics of the structure in both directions, the results and conclusions obtained of the retrofit systems are believed to be applicable for the longitudinal direction as well.

6.3.1 Original Building

6.3.1.1 Dynamic Response Analysis

Reinforcing details and lateral stiffness and strength characteristics of the original building were presented in detail in section 4.3. In Table 6.5, the fundamental periods of vibration and the effective damping ratios of the building corresponding to the different types of soil conditions selected for study are presented. For firm soil conditions, effective damping was selected as 2% of critical in all cases as indicated in Chapter III. For soft soil conditions, effective damping of the soil-structure system was determined using the procedure outlined in section 3.3.

Table 6.5 Dynamic properties of Twelve-Story building (short direction).

Building	Fundamental Period (sec) [Effective Damping]*		
	Soil Type		
	Firm	Soft	
		Silty Clay Deposits (Mexico City)	San Francisco Bay Mud (California)
			Case II
Original	3.52 [2.0 %]	3.63 [2.3 %]	3.60 [2.6 %]

* values were based on a h*/r ratio of 1.57 in accordance with the dimensions
of the foundation.

From Table 6.5, it can be seen that the period of vibration for the building is unusually long for a twelve story structure. There are two main factors that contribute to the

long fundamental period of the building. First, the building has an unusual first story height that is almost twice that of the upper stories (see Fig. 4.10). Second, the periods shown in Table 6.5 were obtained using cracked properties for the reinforced concrete elements. (For a similar building with a first story of the same height as that of the upper stories the fundamental period would be reduced to 3 secs. In addition, if gross properties are used for the reinforced concrete elements in the calculations, the fixed-base fundamental period of the building would only be 1.9 secs).

The lengthening in the period of the building on soft soil sites is minimal ($\tilde{T}/T = 1.03$ for Mexico City). Consequently, effective damping ratios for the building on soft soil sites and those on firm soil sites show little difference. Also note that for the structure supported on the San Francisco bay mud, only one case (Case II) is presented for study. The results presented here corresponds to the most unfavorable situation, and differ little from the results obtained for the structure supported on soil Case I (see Table 3.1) or on a fixed-base.

Dynamic Response

a) Building Response on Firm Soil Sites

In Fig. 6.29, the time history response of the original building for the scaled El Centro and the Corralitos records on firm soils is presented. Also shown in this figure are the maximum inter-story drifts obtained for all three earthquake records measured on firm soil sites. For the two Californian records (scaled El Centro and Corralitos), local collapse of the second story is anticipated due to shear failure of all the columns in that story. Failure of second story columns in shear leaves the building with no lateral stiffness at that story level. Because inertia forces continue to act on the upper stories after shear failure of the columns, lateral displacements in the second story increase without restraint until the upper structure becomes unstable and collapses on top of the first story (behavior of the structure is similar to that of a cantilever beam with a hinge at the base).

For the Viña del Mar record, the response of the building is quite different from that to the Californian records. Maximum inter-story drifts occurred in the tenth and eleventh story and reached only 1.4%. The lateral deformations in the tenth and eleventh stories are due exclusively to the shear failure of the short spandrel beams. In the first floor, the short spandrel beams also fail in shear and the long spandrels show anchorage failure of the
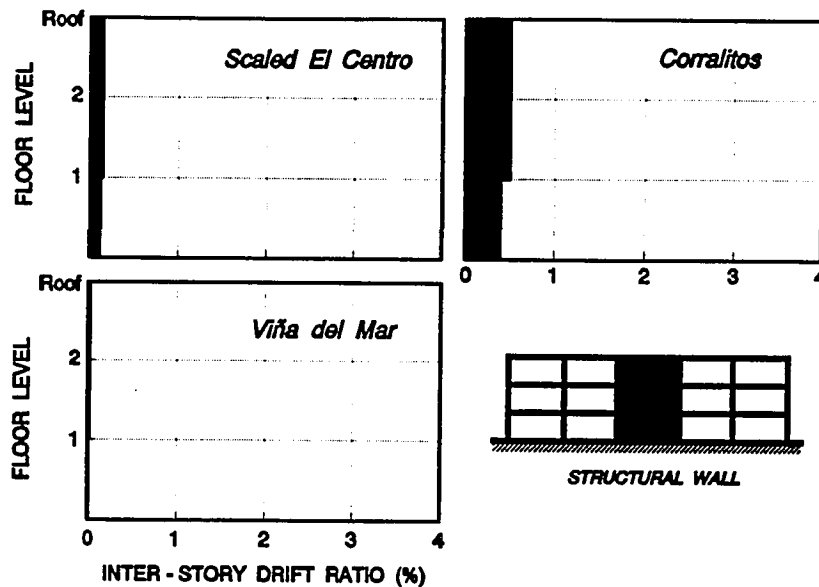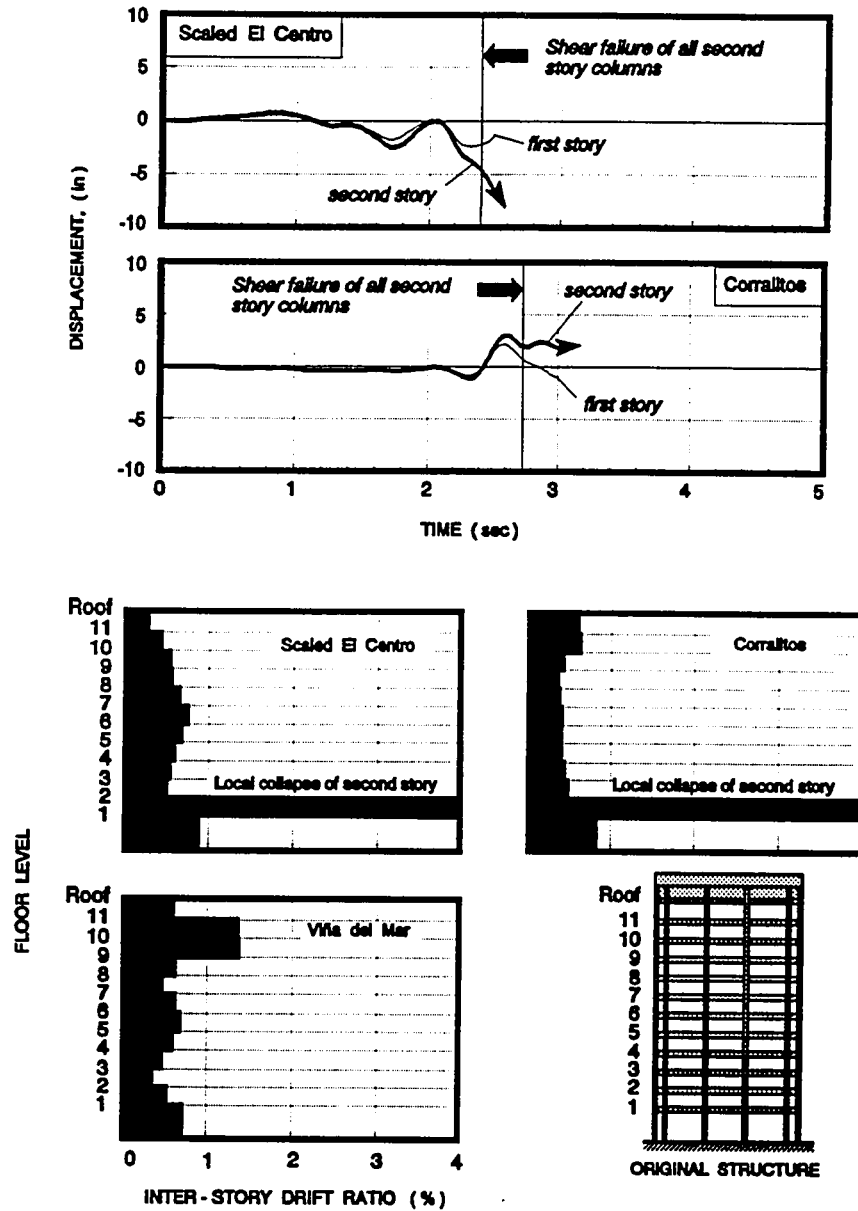
Figure 6.29   Time - history response and maximum inter-story drift ratios of original building subjected to the records on firm soil sites. (Scaled El Centro, Corralitos and Viña del Mar)

bottom reinforcement. However, column shear failure is not observed for the Viña del Mar record, probably because of the premature failure of the short spandrels in the tenth floor which modify the subsequent response of the building. Failure of spandrel beams and the maximum inter-story drift obtained for the Viña del Mar record do not jeopardize the integrity nor the stability of the building. Collapse of the building is not anticipated in this case.

b) Building Response on Soft Soil Sites

The maximum inter-story drifts ratios obtained for the original structure subjected to the two records on soft soil conditions are presented in Fig. 6.30. The drift values shown take due account of the lateral displacement and rocking motion of the foundation and correspond to the actual inter-story drift experienced by the building (Δ in Fig. 3.14).

ORIGINAL STRUCTURE
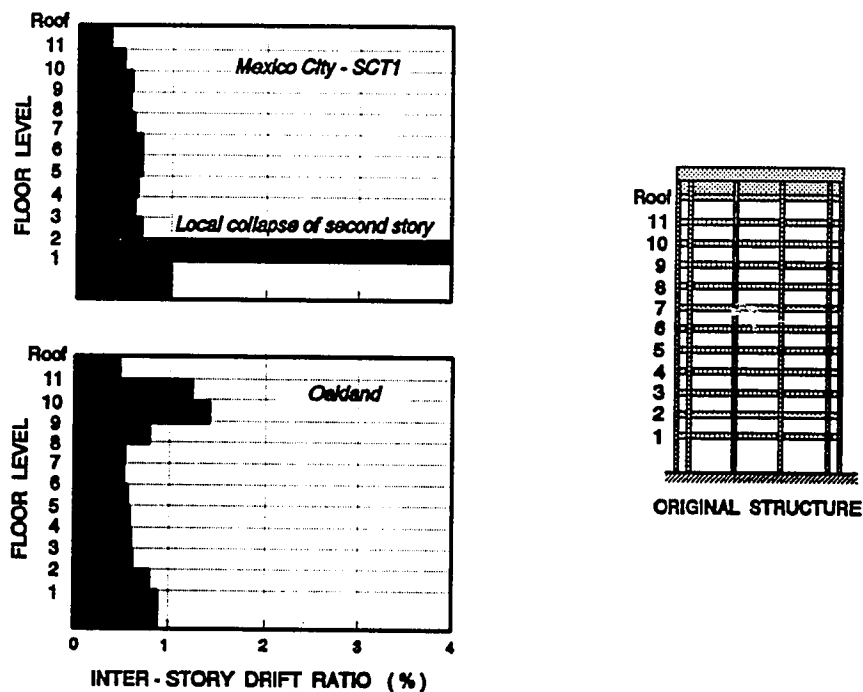
Figure 6.30   Maximum inter-story drift ratios for the original building subjected to the ground motion on soft soil sites. (Mexico City - SCT1 and Oakland)

Nevertheless, rocking motion of the foundation had only a minor influence in the overall lateral displacement of the building, and in general soil structure interaction effects had a minimal effect on the response of the original building (overall results obtained for the building on a fixed-base were similar).

It is clear from Fig. 6.30 that the original building would not have survived the Mexico City - SCT1 record. Similar to the behavior of the building for the records measured on firm soil sites, collapse of the second story is anticipated due to shear failure of all columns in that floor. Maximum displacements and story drifts in the second floor after the failure of the columns in shear far exceed 4% and would clearly lead to the collapse of the building.

Overall response of the building to the Oakland record is similar to that to the Viña del Mar record. Maximum inter-story drifts occur in the tenth and eleventh stories and are due to the failure of the short spandrels in those floor levels. The short spandrels in the first story fail in shear and anchorage failure of bottom reinforcement in the long spandrels is anticipated. Column shear failure is not observed, but moderate damage in the spandrels is expected. Collapse of the building is not anticipated for the Oakland record.

6.3.1.2 Summary

The behavior exhibited by the original building for some of the earthquake records on firm and soft soils is inadequate. For the building supported on firm soil sites, total collapse of the structure is anticipated for the scaled El Centro and the Corralitos record. For the Viña del Mar record, moderate damage in the spandrels is anticipated, but that does not jeopardize the overall integrity and stability of the building.

For the buildings on soft soils, collapse of the building is predicted only for the Mexico City - SCT1 record. For the Oakland record, the response is similar to that observed for the Viña del Mar record with moderate damage in spandrel beams of perimeter frames.

6.3.2 Retrofit Scheme I - Post-Tensioned Bracing Systems

Evaluation of the post-tensioned bracing system considered several different bracing configuration patterns and size of braces. Fig. 6.31 shows some of the configuration
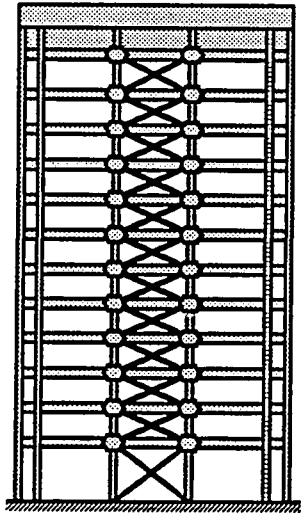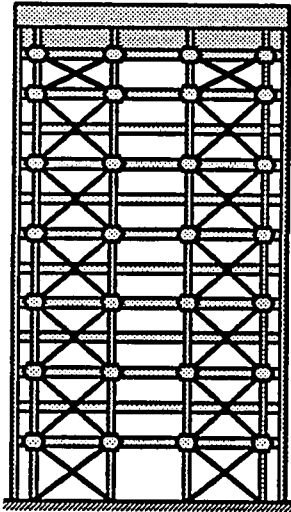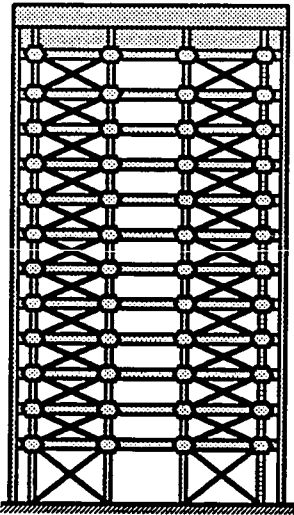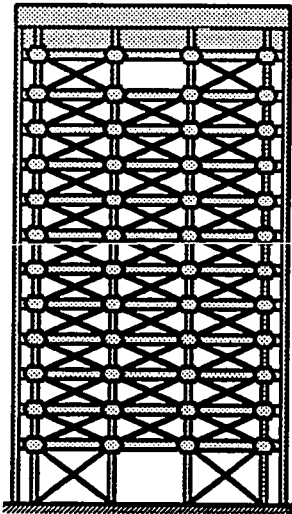
Figure 6.31 Bracing configurations for the twelve-story building with post-tensioned bracing system. (perimeter frames only)

patterns considered for study. In all configurations, brace size was selected so that story stiffness and strength was either uniform or gradually reduced with the height of the building. Each bracing scheme was designed to provide distinct levels of stiffness and strength.

Bracing configurations C1 through C3 failed to protect the building against collapse for most of the records on firm and soft soil sites, even with the largest brace size that could be anchored at an economic cost and from a practical viewpoint (maximum brace size was based on the maximum brace force that was feasible to transfer to the existing building). When a uniform brace size was provided throughout of the height of the building, the mode of failure of the building was the same as that of the original structure; i.e. shear failure of second story columns followed by large lateral deformations and instability of the story. On the other hand, when brace size was gradually reduced with height, column shear failure was, in general, shifted to the upper stories. With bracing configuration C2, column shear failure always resulted in large deformations of the unbraced floors and in the subsequent collapse of the building.

Bracing configuration C4, on the other hand, proved to protect the building from collapse for the records on firm soil and is treated in more detail in this section. Table 6.6 shows two alternate sizes and distributions of braces with height used with configuration C4, which represent two possible retrofit schemes for the building, C4A and C4B. Note that the brace size in the first and the second stories is the same for both configurations. The size

Table 6.6 Size and distribution of braces for schemes C4A and C4B.

Story Level	Brace Size [Area (in^2)]	
	C4A	C4B
3rd to Roof	2 - 1 3/8" ϕ rods [3.16]	3 - 1 3/8" ϕ rods [4.74]
2nd	3 - 1 3/8" ϕ rods [4.74]	3 - 1 3/8" ϕ rods [4.74]
1st	4 - 1 3/8" ϕ rods [6.32]	4 - 1 3/8" ϕ rods [6.32]

of braces in the first two stories corresponds to the largest brace that can be anchored from a practical and economical standpoint. Based on the results presented in Chapter V and in the previous section for the three-story building, only steel rods with only one level of initial brace prestress were considered for study; i.e. 75% of the brace yield strength.

Fig. 6.32 compares the bending moment distribution in columns for the original and braced structure with scheme C4B for an initial brace prestress level of 75% of the brace yield strength. Because the brace size in configuration C4A and C4B is similar, the distribution of internal forces with both schemes is also very similar. As can be seen in Fig. 6.32, bending moments after initial brace prestressing is significantly increased only in first and twelfth story exterior columns. Nonetheless, the magnitude of the bending moments induced is only a fraction of the yielding moment capacity of the columns ($\approx$ 7% My in the first floor and $\approx$26% My in the twelfth story). The shear demands associated with the

ORIGINAL   BRACED C4B
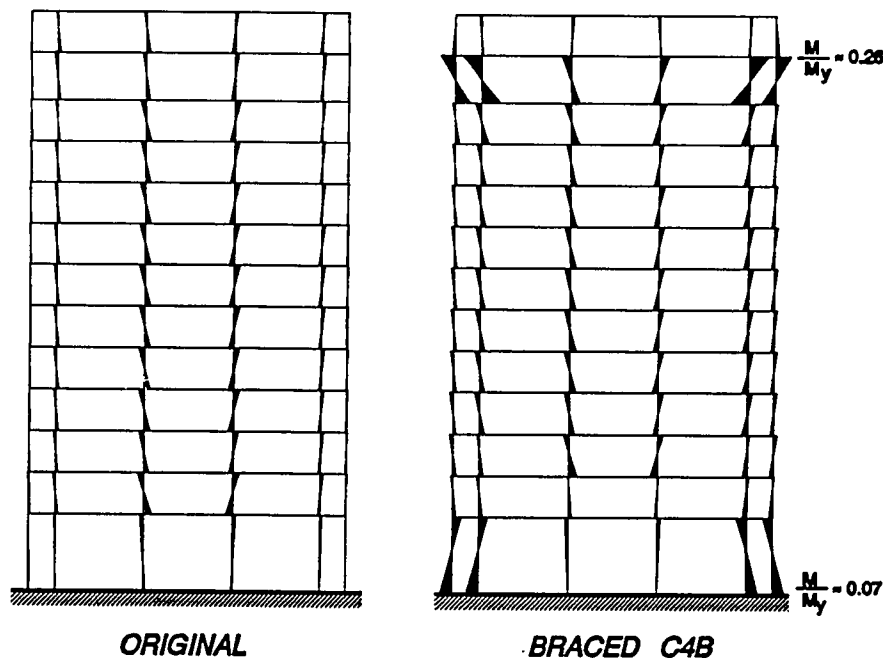
Figure 6.32   Effects of initial brace prestressing on the bending moment distribution in perimeter frame columns. Original building and braced structure, bracing config. C4 with initial brace prestressing of 75% of brace yield strength.

induced bending moments are also small approaching only 14% of the estimated shear capacity for the columns of the twelfth story. Bending moments and shear forces in beams are of the same order of magnitude, but represent an even smaller fraction of the capacity anticipated for the beams.

Axial forces in columns after prestressing are significantly increased with respect to those under gravity loads alone. The largest increases occurs for interior columns in the first story, where axial forces reach about 32% of the capacity of the column in pure compression. Axial forces in beams of braced bays induced by prestressing are of similar magnitude as those in columns, but because beams have smaller cross section dimensions compressive forces represent about 45% of the capacity in pure compression. In addition, the short spandrels of exterior bays show small tensile forces upon prestressing of braces. Thus, it is anticipated that collector elements may be required to augment the tensile capacity of beam members.

Overall, the level of forces induced by prestressing of braces with configuration C4B (and C4A) do not jeopardize the integrity of the existing structure. As discussed in previous sections, member capacity used in the analyses was based on axial forces due to gravity loads alone, mainly because the magnitude of the axial forces due to brace prestressing may vary considerably during earthquake loading.

6.3.2.1 Lateral Stiffness and Strength

The relationships for the base shear coefficient and the drift at the centroid of inertia forces for the existing and the building braced with configurations C4A and C4B are compared in Fig. 6.33. In this figure, the relationships have been obtained using a uniform lateral load distribution over the height of the building. As can be seen, the increase in stiffness provided by both bracing configurations is substantial and, as expected, the initial lateral stiffness of scheme C4B is slightly larger than that of configuration C4A. Because braces are initially prestressed to 75% of their yield strength, braces which elongate reach yielding before braces which shorten begin to sag. Yielding of first story braces began, with both schemes, at a drift of about 0.2%; an event that had only a minor influence in the overall lateral drift at the centroid of inertia forces, as shown in Fig. 6.33. Ultimate strength of the braced building is about four times larger than that of the original structure. The
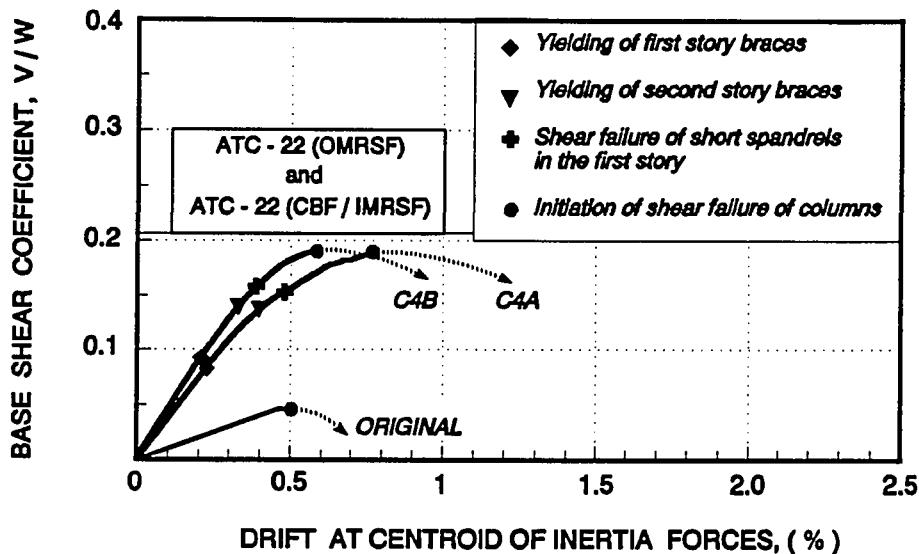
Figure 6.33 Base shear coefficient and drift at centroid of inertia forces relationship for the twelve-story building. Original and braced structure with post-tensioned steel rods (configurations C4A & C4B).

mode of failure of the braced building is similar to that of the original structure, and is due to shear failure of the columns in the first and second story. Because lateral strength provided by the bracing system is the same in these two stories (see Table 6.6), ultimate strength of the building is the same for both schemes. Note that prior to the shear failure of columns, second story braces reach yielding and the short spandrels of the first story fail in shear, as indicated in Fig. 6.33

Also shown in Fig. 6.33 are the base shear coefficients required by ATC-22 for an OMRSF and for a dual system consisting of a CBF with an IMRSF capable of resisting 25% of the lateral loads. Brittle elements were assumed in estimating the coefficients shown in the figure because columns remain susceptible to failing in shear even after bracing of the building. As discussed in section 6.2.2.1, the response modification factors embodied in the recommendations of ATC-22 for braced frames are intended for concentric bracing systems with structural steel sections. The factors are not considered appropriate for the evaluation of post-tensioned bracing systems. In addition, the building under study cannot be

classified as an IMRSF, because its reinforcing characteristics are those of an OMRSF (ATC-22 does not include provisions for a CBF and an OMRSF). However, it is reasonable to assume that the required lateral resistance for a CBF with an IMRSF is a lower bound for the strength required for an OMRSF with a post-tensioned bracing system. As can be seen, ultimate strength provided by both schemes is below the lower bound described above, which suggest the post-tensioned bracing system would be inadequate to protect the structure against collapse.

6.3.2.2 Dynamic Response Analysis

Dynamic Properties

Table 6.7 shows the fundamental periods of vibration and the effective damping ratios for the original and braced structure corresponding to the different types of soil sites selected for study. For the braced buildings (C4A and C4B) on firm soils, the reductions in the fundamental period of the building are substantial; about one-half of the fundamental period of the original structure. Note, however, that because the lengthening in the period of the braced buildings on soft soils is only moderate ($\bar{T}/T_{max} = 1.12$ for C4B in Mexico City) and the effective height to foundation ratio is relatively high ($h^*/r = 1.57$), the corresponding effective damping ratios of the system do not differ from those adopted for the structure on firm soils.

Also note that the resulting period of vibration for the braced buildings (C4A and C4B) is about 2 secs. For the Mexico City - SCT1 record, such period of vibration corresponds to maximum demands of strength (see Fig. 4.27) and therefore, a large response can be anticipated for the braced buildings.

Dynamic Response

Maximum inter-story drift ratios for the braced buildings, C4A and C4B, obtained for the ground motions on firm and soft soil sites are presented in Figs. 6.34 and 6.35, respectively. The results presented for the building located on soft soils take due account of the rocking motion of the foundation and correspond to the actual inter-story drifts for the building. For the three records on firm soils (Fig. 6.34), inter-story drifts remain below 1% in all stories, except for the first story drift obtained with configuration C4B subjected to the

Table 6.7 Dynamic properties of the original and braced buildings
with post-tensioned steel rods. (Twelve-Story Building)

Building	Fundamental Period (sec) [Effective Damping]*		
	Soil Type		
	Firm	Soft	
		Silty Clay Deposits (Mexico City)	San Francisco Bay Mud (California)
			Case II
Original	3.52 [2.0 %]	3.63 [2.3 %]	3.60 [2.6 %]
Config. C4A	1.87 [2.0 %]	2.07 [2.5 %]	2.02 [2.4 %]
Config. C4B	1.71 [2.0 %]	1.93 [2.9 %]	1.87 [2.5 %]

* values are based on a h^*/r ratio of 1.57 in accordance with the dimensions
of the foundation.

scaled El Centro record. The drift in the latter case approaches 1.25%. For the scaled El Centro record, shear failure is not prevented in all members, but it is confined to only a few columns and spandrels. On the other hand, for the Corralitos and Viña del Mar records, column shear failure is prevented in all column members. Notice that, in general, inter-story drifts tend to be more uniformly distributed with height in configuration C4A than in configuration C4B. With the latter scheme, deformations concentrate primarily in the first two stories. While this result could not have been anticipated, it can be simply explained by the larger stiffness and strength (larger brace size) in the upper stories of configuration C4B which help restrain the lateral displacements of the upper stories.

For the building on soft soils, the results for the building subjected to the Mexico City - SCT1 record are substantially different from those of the building subjected to the Oakland record, with both bracing configurations. For the Mexico City - SCT1 record, the bracing system is clearly unable to limit the lateral deformation of the building and collapse
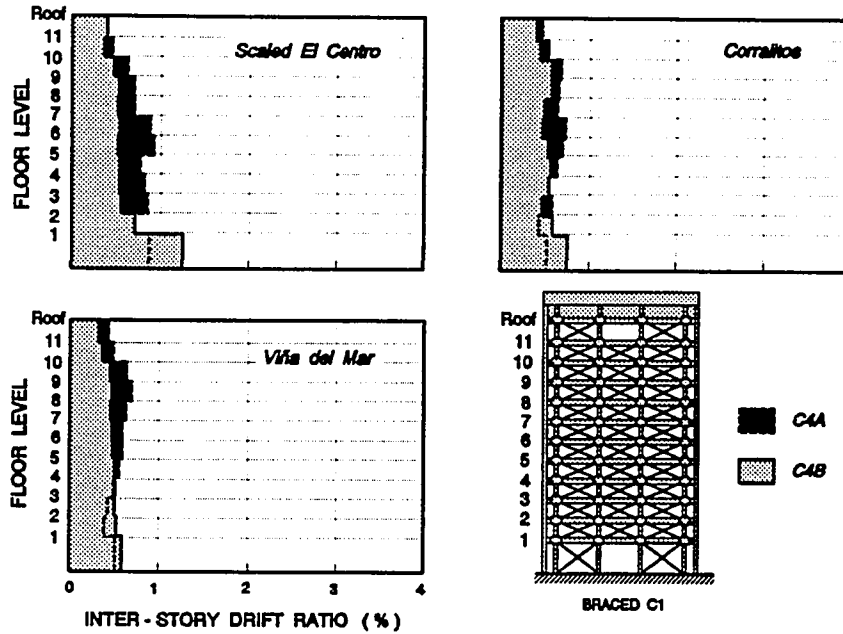
Figure 6.34 Maximum inter-story drift ratios for the braced buildings (C4A and C4B) subjected to the records measured on firm soil sites.
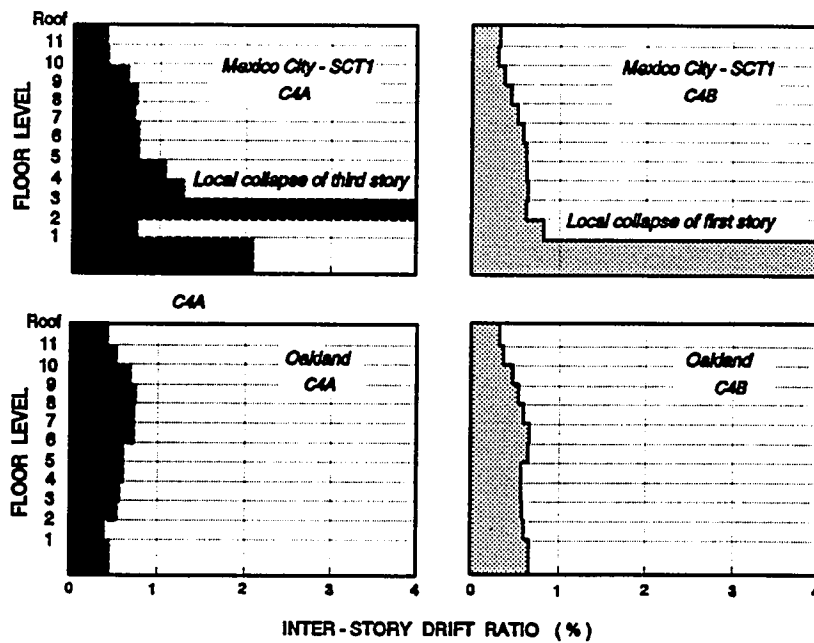
Figure 6.35 Maximum inter-story drift ratios for the braced building (C4A and C4B) subjected to the records measured on soft soil sites.

of the structure is anticipated due to column shear failure. The only difference between the response of the two bracing configurations studied is that with scheme C4A collapse of the building initiates in the third story, whereas with configuration C4B collapse of the building originates in the first story.

For the Oakland record, however, maximum inter-story drifts with both configurations remain below 1% and are reduced with respect to those obtained for the original building (see Fig. 6.30). Column shear failure is eliminated with configuration C4A. With configuration C4B shear failure is anticipated in only one column of the perimeter frames.

Performance of Post-tensioned Bracing System

The results presented above indicate that for buildings on firm soil sites the post-tensioned bracing system can be used to reduce the response and the lateral deformations of the twelve story structure selected for study. For the building on soft soils, the effectiveness of the bracing system varies depending on the ground motion considered. For the Mexico City - SCT1 record, the system is unable to prevent collapse of the building, while for the Oakland record lateral deformations are restrained and collapse of the building is prevented.

The following section presents an evaluation of the post-tensioned bracing system by comparing the performance of the reinforced concrete members for the original and retrofitted buildings. In addition, the expected behavior for the braces is also examined.

a) Performance of Reinforced Concrete Members

To evaluate the performance of the reinforced concrete members and that of the braces, the results obtained with scheme C4B with the scaled El Centro record will be used. Without including the Mexico City - SCT1 record, the scaled El Centro record imposes the largest demands on both the original and the braced buildings. In Fig. 6.36, the profile of plastic hinges developed in the perimeter frames of the original structure and those developed for the braced building is compared. Also shown in this figure are the members that exhibit shear failure during the response to earthquake record. (In Fig. 6.36, the length of the short exterior bays are shown larger than the actual scale)
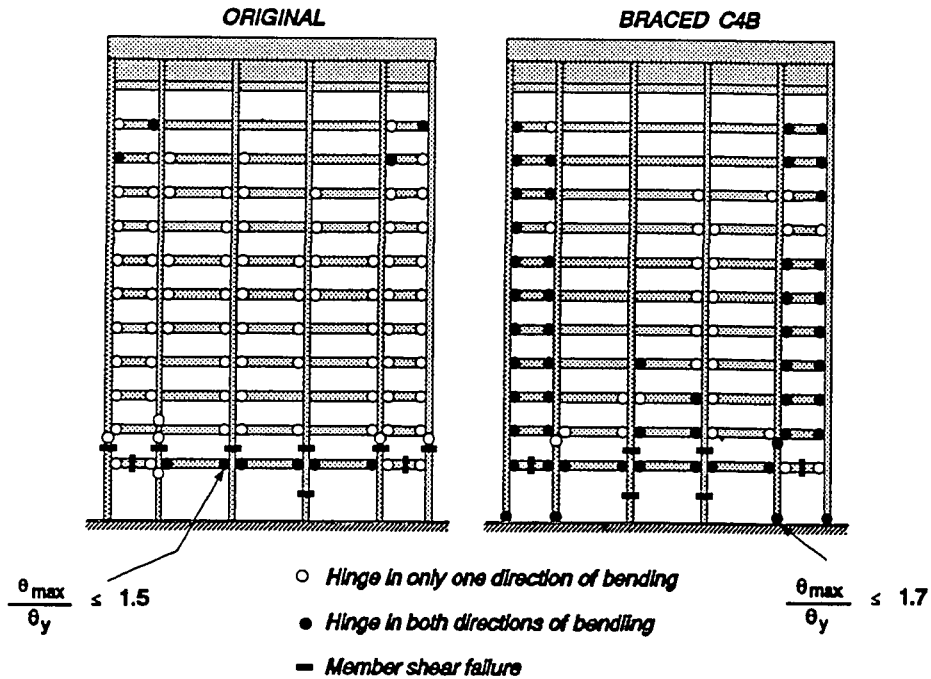
Figure 6.36 Hinge location for the perimeter frames of the original and braced building with configuration C4B. (Exterior bays are not drawn to scale for clarity)

In the original building, shear failure is anticipated in all second story columns. In addition, one column in the first story and the short spandrels of exterior bays of the first floor are also expected to fail in shear, as shown in Fig. 6.36. Failure of these elements lead to unrestrained lateral displacements in the second floor and ultimately to the collapse of the building. Because shear failure of columns and beams occurs in the early stages of the ground motion and at relatively small lateral drifts, the hinge rotation in long spandrels is relatively small ($\theta_{max} / \theta_y \leq 1.5$). In the short spandrels, the hinge rotation for negative moment is also small. For "positive" moment pull-out of bottom reinforcement is predicted in some of the first and second story spandrels with significant hinge rotation.

In the braced structure, column shear failure is confined only to the interior columns of the first and second story. The short spandrels of the first floor also fail in shear. However, maximum inter-story drifts in the braced structure are limited to 1.25% in the first story and therefore, the integrity of the structure is not considered to be at risk. In any

event, the columns could be encased using a steel jacket to help maintain the integrity of the concrete and prevent, or at least reduce, loss of axial capacity upon shear failure. The jacketing may have to be provided over the entire height of the building to prevent sudden interruptions in stiffness with height and induce a "soft story". In columns, plastic hinges develop only at the base of outer columns in the first story and at the top of some second story columns. Hinge rotations are small (Θ_{max} / Θ_y ≤ 1.7) and are below the available rotation of the section (Θ_u / Θ_y ≈ 6 to 7). In beams, plastic hinges develop primarily in the short spandrels, mainly because outer bays are not braced. In the short spandrels, pull-out of bottom reinforcement is predicted in many of the beams, with reductions in strength of about 80% in some elements. While anchorage failure could lead to significant large cracks opening in the hinging region of the spandrels, it does not threaten the integrity of the structure.

The distribution of axial forces obtained in columns with configuration C4B when subjected to the scaled El Centro record is presented in Fig. 6.37. In this figure, the level of axial forces is presented as the ratio between the maximum force developed in the member during the response and the capacity of the column in pure compression or tension. Axial forces are mostly compressive forces, except in the lower stories (first to sixth story) of the double column configuration where tensile forces are also generated. The axial tension forces are not exclusively due to the presence of the braces, but also due to overturning moments generated during the lateral deformation of the building, as revealed by examining the results for the unbraced structure. Maximum compressive forces occur in first and second story columns and approach the load at balanced strain conditions, which will help improve the flexure and shear capacity of the members. Tensile forces in the outer columns of the first story reach only 30% of the capacity in pure tension. However, due to the abrupt change in the amount of the longitudinal reinforcement between first and second story columns (see Fig. 4.11), tensile forces approach 92% of the column capacity in pure tension. Axial tension forces in the third and fourth stories are reduced, but they still represent an important fraction of the capacity in tension. On the basis of these results the need for steel collector elements is apparent to avoid distress of the columns in tension and/or significant reductions in the flexural and shear capacity of the columns.
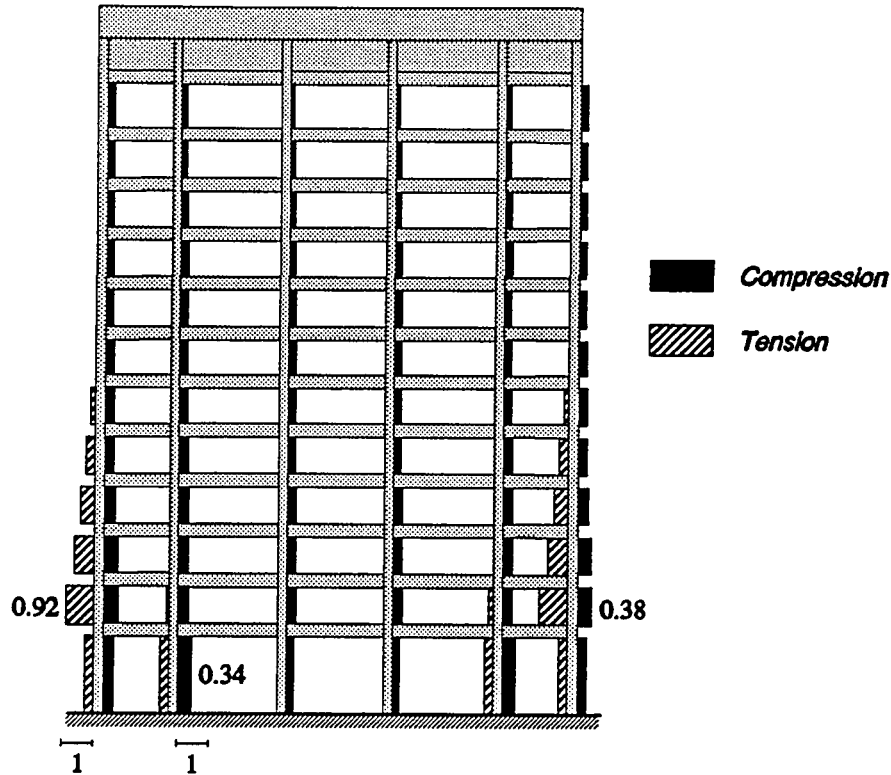
Figure 6.37 Distribution of axial forces in columns with configuration C4B for the scaled El Centro record. (Axial force is shown as a fraction of the member capacity in pure compression or tension; exterior bays not drawn to scale)

Long spandrel beams exhibit compressive forces throughout the height of the building. Maximum compressive forces approach, in general, 45% of the capacity of in pure compression. In the short spandrels, both tensile and compressive forces are developed during the response. The magnitude of compressive forces reached only 8% of the capacity in pure compression. However, using the minimum amount of longitudinal reinforcement provided in the spandrels (typically at mid-span) and neglecting the contribution of slab reinforcement, maximum tensile forces approach 35% of the capacity in pure tension in the lower stories. While failure in tension of the short spandrels is unlikely for the level of forces induced, tensile forces will reduce the flexural and shear capacity of the beams and they will probably have to be strengthened.

b) Performance of Steel Rod Braces

Fig. 6.38 shows the distribution of inelastic behavior in the braces for configuration C4B during the scaled El Centro record. Yielding is observed in most of the braces, particularly in the lower stories (first to sixth story). In the upper stories, only a few braces reach yielding, while the rest of the braces remain within the elastic range. As expected, the amount of plastic deformation is more extensive in the braces of lower stories and is gradually reduced for the braces in the upper stories. In the first floor, maximum brace elongations exceed the allowable elongation in tension (yield elongation), and therefore braces lose initial prestress completely. However, maximum elongations of braces in the

○ Brace reached yielding
   (never became slack)

▬ Brace reached yielding and
   became slack, with plastic
   elongations in tension
   exceeding maximum allowable.

Braced C4B - Scaled El Centro
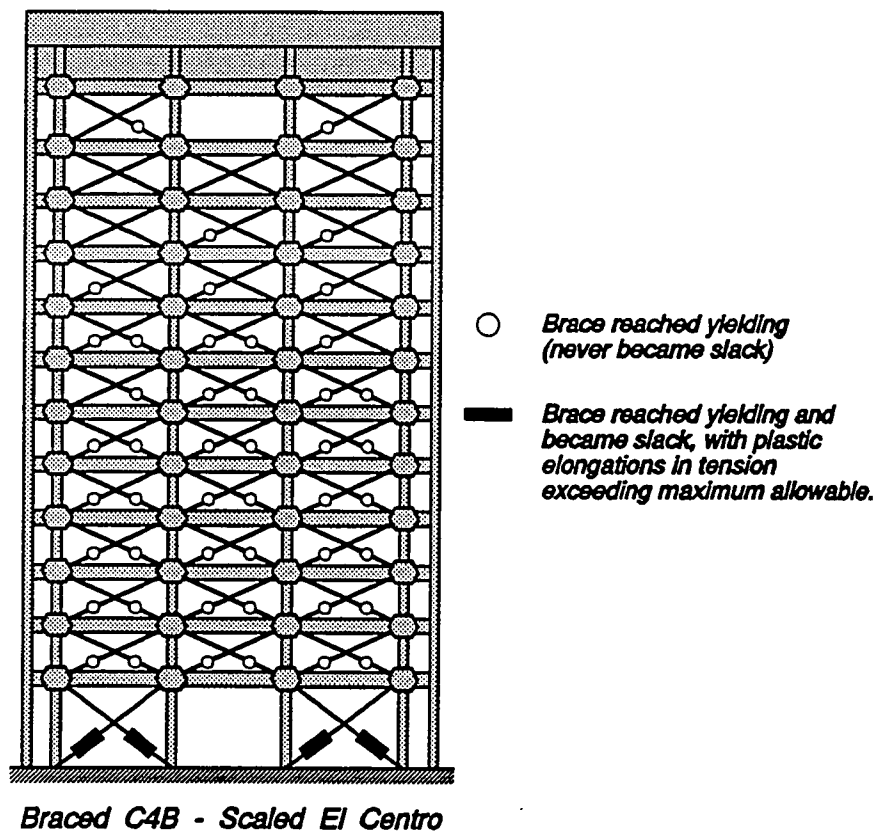
Figure 6.38 Braces that yielded and/or became slack during the response for the scaled El Centro record.

second story and in the upper stories, remain below the allowable elongation in tension. The residual prestress force in the latter braces is 45% of the brace yield strength or higher.

The performance of first story braces is inadequate and violates the performance criteria established for post-tensioned braces (see Chapter V). Even though maximum lateral drifts in the first floor are not considered to jeopardize the integrity of the building, the performance of first story braces raises serious questions regarding the ability of the system to limit lateral displacements in a larger or similar seismic events. Because braces in the first two stories in configuration C4B correspond to the largest brace that could be anchored at an economical cost, an increase in brace size is not economically feasible. However, configuration C4B could be used as part of the retrofit scheme for the building provided that columns in the first and upper stories be strengthened to avoid shear failure prior to flexural yielding of these elements. Possible strengthening schemes for the columns are reinforced concrete or steel jacketing of the members. As noted earlier, the addition of jacketing may require a re-evaluation of the bracing scheme due to the changes in stiffness, therefore in earthquake demands. However, because the stiffness provided by the bracing system is generally much larger than that provided by the jacketing, significant changes in earthquake demands are not anticipated.

The performance of braces with scheme C4A was better than that described above for scheme C4B. With scheme C4A braces reached yielding and became slack during the response to the scaled El Centro record. Despite significant yielding of braces, the prestress force was never lost completely and all braces became taut upon unloading of the frame. Either scheme represents a feasible retrofit alternative for the building, provided that columns are strengthened to prevent shear failure.

6.3.2.3 Summary

Several post-tensioned bracing configuration patterns with different sizes of braces were studied as possible retrofit schemes for the twelve-story building. Within each configuration, distinct levels of stiffness and strength were investigated. From the configurations studied, only one configuration pattern, C4, was able to protect the building from collapse when subjected to the records on firm soil sites. Nonetheless, shear failure was still observed in a few columns in the first and second story levels. The performance

of braces varied depending on the brace size and distribution. With scheme C4A, braces yielded and became slack during response, but never lost their prestress completely. However, with scheme C4B, braces yielded extensively in the first story and lost their prestress completely. Because the amount of bracing required in the lower stories correspond to the largest size of braces that can be anchored at an economical cost, an increase in the size of braces in these stories was not a viable alternative. In addition, increasing the size of braces does not guarantee better performance of the existing members or of the braces in similar events. To safeguard columns against a premature shear failure in the lower stories, it is suggested that the columns be encased with steel or reinforced concrete jacketing. The jacket of the columns should be designed to help carry the axial tensile forces developed in the columns of the outermost column lines. Similarly, the short spandrels of outer bays will probably require collector members to augment the tensile capacity of the spandrels.

For the Mexico City - SCT1 record, the post-tensioned bracing system was unable to protect the building against collapse, even for the largest possible size of brace that could be anchored at an economical cost. Due to the nature of the earthquake record and the dynamic characteristics of the braced building, the demands imposed by the record always offset the available strength and ductility in the braced building.

For the Oakland record, the performance of existing reinforced concrete members and that of the braces is similar to that observed for the records on firm soils. Consequently, recommended retrofit solutions for the Oakland event will be similar to those described above for the records on firm soils.

6.3.3 Retrofit Scheme II - X-Bracing (Structural Steel Braces)

Two bracing configurations were selected for evaluating the response of the structure, namely TS and DA-TS as shown in Fig. 6.39. Braces consisted of tubular or double angle sections, and were selected to meet the slenderness requirements for seismic zones ($KL/r < 720/\sqrt{f_y}$) of the Load and Resistance Factor Design manual (LRFD)[45]. In addition, tube sections followed the specifications for the flat width to thickness ratio of the LRFD manual ($b/t_w \le 110 / \sqrt{f_y}$) to avoid premature fracture of the tubes due to
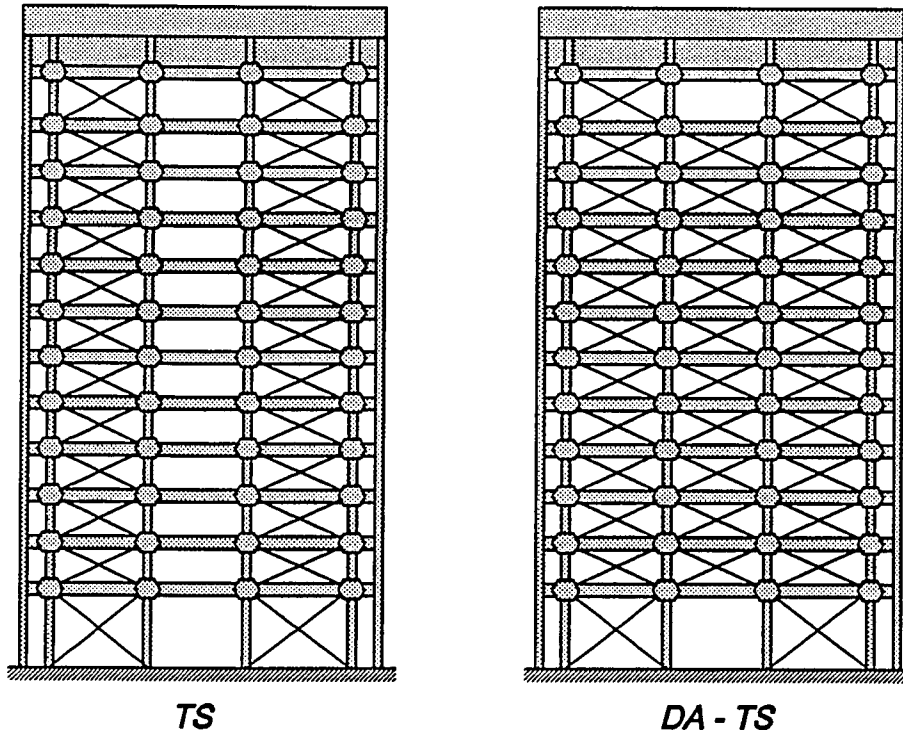
Figure 6.39 Bracing configurations for concentrically braced building with structural steel braces. (perimeter frames only)

Table 6.8 Size and distribution of braces for configurations TS and DA-TS. (Twelve-story building)

Story Level	Brace Size [Area (in^2)]		
	TS1	TS2	DA-TS
2nd to Roof	TS 6 x 6 x 5/16 [6.86]	TS 8 x 8 x 1/2 [14.40]	TS 10 x 10 x 5/8 [22.40]
1st	TS 7 x 7 X 3/8 [9.58]	TS 10 x 10 x 1/2 [18.40]	2L 8 x 8 x 1-1/8 [33.50]

repeated load reversals. Typical brace size and distribution of braces for both configurations are presented in Table 6.8. For bracing configuration TS, the response of the braced structure was studied for two different size and distribution of braces (configurations TS1 and TS2 in Table 6.8), and represented two distinct levels of stiffness and strength for the braced structure. Bracing configuration DA-TS was designed to meet the specific demands of the Mexico City - SCT1 record, which required large brace sections in the lower stories. Because there was no tube section that could meet the stiffness, strength and slenderness ratio required for the Mexico City - SCT1 record, double-angle sections were used in place of tubular sections in the first story. Braces used with scheme DA-TS exceed the maximum size that would be feasible to anchor at an economical cost and probably would not be a viable alternative. Nonetheless, the results for scheme DA-TS are included in the analyses mainly to illustrate unique behavioral characteristics of the braced building when subjected to the Mexico City - SCT1 record.

In all three bracing configurations, brace size was selected to provide, as closely as possible, a uniform distribution of lateral stiffness and strength throughout the height of the building. The resulting slenderness ratios of braces varied from 65 (heaviest braces) to 106 (lightest braces) for out-of-plane buckling, which normally governed the design of the braces (K = 0.67 as indicated in Chapter III). Yield strength was 50 ksi for double angle braces and 46 ksi for tubular sections.

6.3.3.1 Lateral Stiffness and Strength

In Fig 6.40, the relationships for the base shear coefficient and drift at the centroid of inertia forces for the original and braced structures are compared. Also shown in this figure is the relationship for the post-tensioned bracing system obtained for configuration C4B with braces initially prestressed to 75% of the yield strength. The relationships shown were obtained using a uniform lateral load distribution over the height of the building.

Configuration TS1 was designed to provide the same initial stiffness as that of configuration C4B, mainly to provide a basis of comparison for the two bracing systems without including the changes in the demands due to different periods of vibration of the buildings. Because of the lower yield strength of the tubular sections, ultimate strength of bracing configuration TS1 is smaller than that of configuration C4B. Bracing configuration
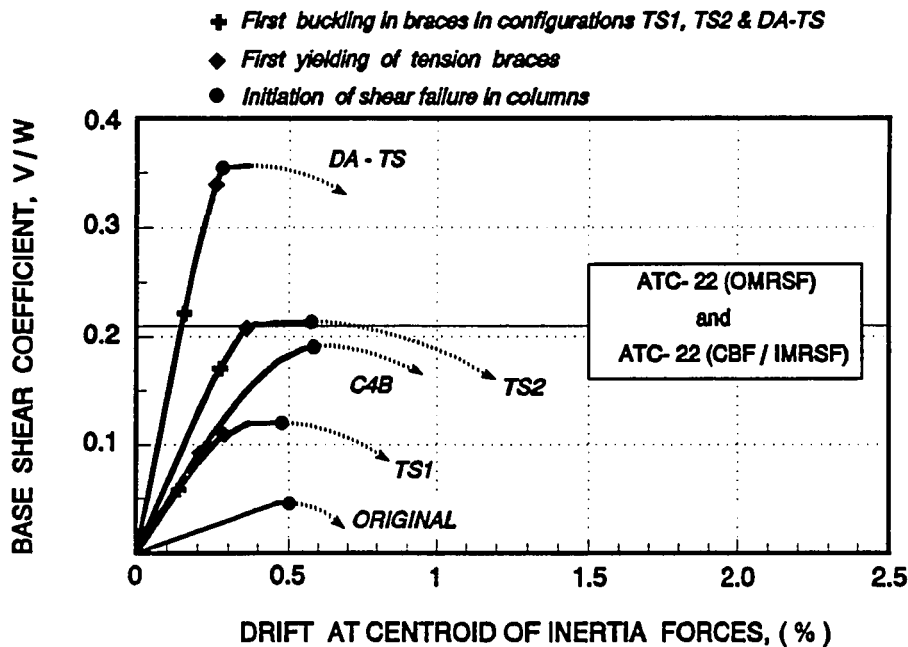
Figure 6.40   Base shear coefficient and drift at centroid of inertia force relationship for the twelve-story building. Original and braced structure with configurations TS1, TS2, DA-TS and C4B.

TS2 has both, higher initial stiffness and ultimate strength than configuration C4B.

The predicted mode of failure of the braced building is the same for all bracing configurations and is due to the shear failure of the columns in the second story. As shown in Fig. 6.40, shear failure of columns begins only after buckling and yielding of braces in the first story, for all three bracing configurations. Such behavior is welcome since it indicates that braces may begin to dissipate energy and reduce the response of the building prior to shear failure of columns. In configuration DA-TS, shear failure of second story columns begins soon after yielding of first story braces, and it occurs at a smaller lateral drift than for the building braced with the other configurations. Because lateral stiffness and strength of configuration DA-TS is much higher than those of the other configurations in every floor level, the lateral deformations measured at the centroid of inertia forces (seventh floor) are

smaller. However, lateral drift in the second story, where column shear failure initiates, is similar for all bracing configurations.

The base shear coefficient required by the provisions of the ATC-22 for the *evaluation* of building structures is also presented in Fig. 6.40. The coefficients are shown for an OMRSF and for a concentrically braced frame (CBF) with an intermediate moment frame (IMRSF) capable of resisting at least 25% of the lateral loads. Brittle elements were assumed for estimating both coefficients. For the braced building the use of modification factors associated with brittle elements is justified because columns remain susceptible to a shear failure even after bracing of the building. As noted earlier, the building under study does not correspond to an IMRSF because its reinforcing characteristics are those of an OMRSF (ATC-22 does include provisions for a CBF with an OMRSF). However, the required lateral strength for a concentrically braced frame with an IMRSF represents a lower bound for a building with CBF and an OMRSF.

Assuming that the design lateral resistance of the braced building is given by the buckling capacity of the braces (as assumed in the elastic design procedure of CBF systems), it can be seen that all three bracing schemes would have inadequate strength in light of the requirements of ATC-22. However, ultimate strength of configuration DA-TS is larger than the required strength for a CBF with an IMRSF. Because of the relatively high strength of scheme DA-TS, it is likely that the performance of configuration DA-TS will be adequate.

6.3.3.2 Dynamic Response Analysis

Dynamic Properties

The fundamental periods of vibration and effective damping ratios for the original and the building with X-bracing are shown in Table 6.9. Because of the relatively heavy braces in all three configurations, the period of vibration is significantly reduced with respect to that of the original building, particularly for configuration DA-TS. For the buildings located on firm soil sites, the shortening in the fundamental period of vibration will probably result in increased strength demands (see Fig. 4.26). For the buildings subjected to the Mexico City - SCT1 record, pseudo-accelerations are increased for all three bracing configurations

Table 6.9 Dynamic properties of the original and buildings with X-bracing.

Building	Fundamental Period (sec) [Effective Damping]*		
	Soil Type		
	Firm	Soft	
		Silty Clay Deposits (Mexico City)	San Francisco Bay Mud (California) Case II
Original	3.52 [2.0 %]	3.63 [2.3 %]	3.60 [2.6 %]
Config. TS1	1.74 [2.0 %]	1.96 [2.9 %]	1.90 [2.5 %]
Config. TS2	1.42 [2.0 %]	1.67 [3.2 %]	1.60 [2.8 %]
Config. DA-TS	0.95 [2.0 %]	1.30 [5.8 %]	1.21 [4.8 %]

* values are based on a h^*/r ratio of 1.57 in accordance with the dimensions of the foundation

due to shortening of the fundamental period of the buildings. Furthermore, the fundamental periods of the braced buildings are located to the left of the peak spectral response (configurations TS2 and DA-TS) or at the peak of the response (configuration TS1), as can be seen in Fig. 4.27. It is anticipated that the demands on the building with configuration TS1 (and possibly configuration TS2) will be significantly higher than those imposed on the original building by the same record. For the Oakland record, the demands of strength (pseudo-acceleration) are increased for all three bracing configurations.

Effective damping ratios for configurations TS1 and TS2 located on soft soil conditions do not differ significantly from those adopted for the buildings on firm soil sites. The reason is that the lengthening in the fundamental period of vibration of the braced buildings with TS1 and TS2 is relatively small and consequently, foundation damping factors are also relatively small. For configuration DA-TS, however, the lengthening in the period

is larger than that observed for the other bracing configurations, and effective damping ratios are substantially larger, particularly for the clay deposits of Mexico City.

Dynamic Response

Maximum inter-story drifts for the braced building with the three bracing configurations obtained for the records measured on firm soil sites is presented are Fig.6.41. For the Corralitos and Viña del Mar records, lateral deformations remain below 1% drift with all three bracing schemes. For the Corralitos record, column shear failure is prevented only with configurations TS1 and TS2. With scheme DA-TS, shear failure is predicted in interior columns of the first story, but maximum drifts remain below 1%. For the Viña del Mar record, shear failure of columns is prevented in all cases.

For the scaled El Centro record, the response of the building varies significantly with each bracing configuration. Bracing configuration TS1 fails to protect the structure from collapse; shear failure is predicted in all second story columns and lateral drifts reach 2.5% in that story. On the other hand, bracing configuration TS2 limits inter-story drifts to values that remain below 1% and prevents the shear failure in all but one interior column in the second story. The behavior described above can be partly explained by the fact that strength demands imposed by the scaled El Centro record on structures TS1 (1.74 secs.) and TS2 (T=1.42 secs.) are essentially the same (see Fig. 4.26). At the same time, lateral strength provided by configuration TS2 is larger than of TS1 (see Fig. 6.40). Therefore, an improved performance can be expected with scheme TS2.

When the building is braced with configuration DA-TS, the performance of the bracing system is not as effective as that with scheme TS2. Lateral drift in the first story reaches 1.25% and shear failure of some columns in the first and second floor is observed. In the latter case, strength demands for the scaled El Centro record increase significantly for configuration DA-TS (see Fig. 4.26) and probably offset the available strength of configuration DA-TS. Similar behavior is also observed for the other two records on firm soil sites.

In summary, lateral drifts obtained with bracing configurations TS2 and DA-TS for the records on firm soil sites do not jeopardize the integrity nor the stability of the structure and can be considered to provide an adequate safety level against collapse of the building.
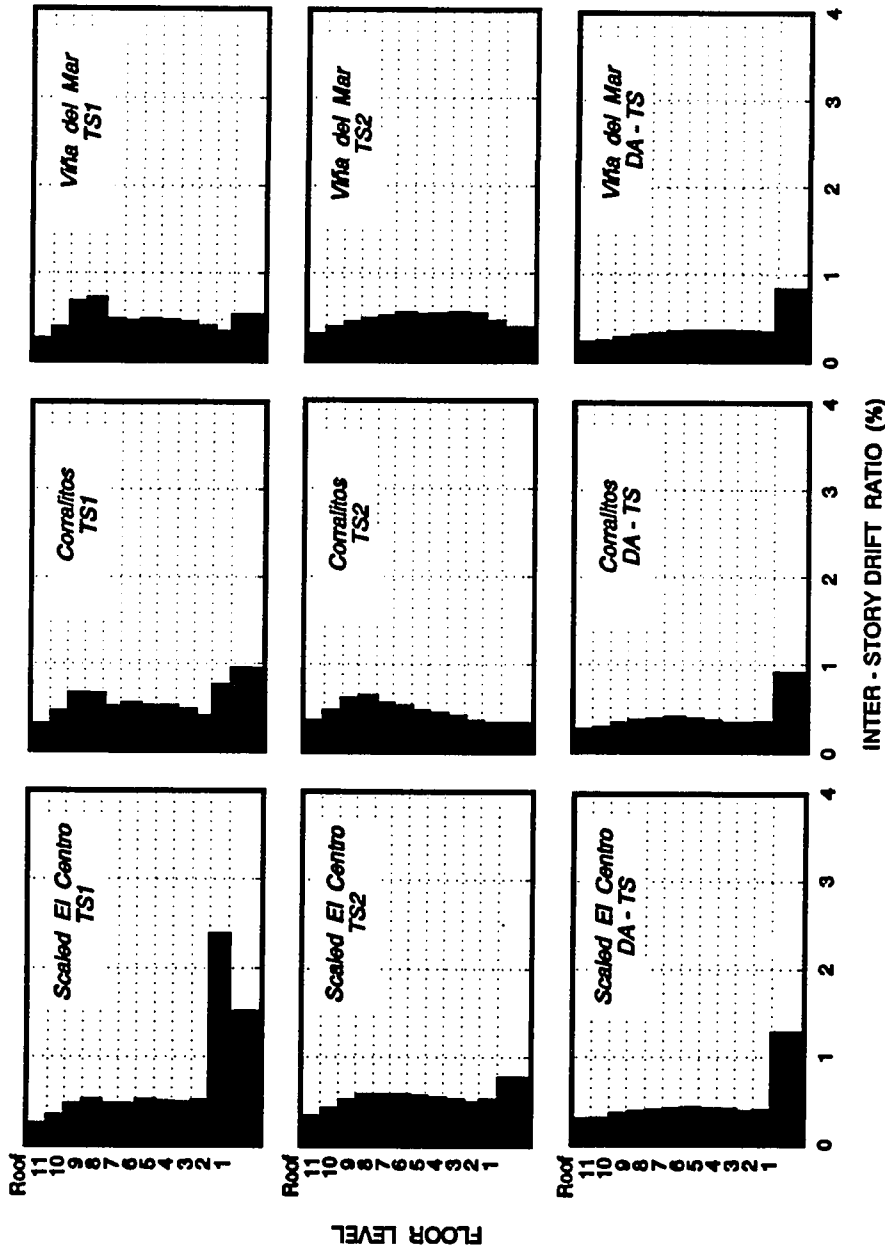
Figure 6.41 Maximum inter-story drift ratios for the braced building (configurations TS1, TS2 & DA-TS) subjected to the records on firm soil sites (scaled El Centro, Corralitos & Viña del Mar).

Maximum inter-story drifts for the buildings located on soft soil sites are presented in Fig. 6.42. As anticipated, bracing configurations TS1 and TS2 are unable to prevent collapse of the building when subjected to the Mexico City - SCT1 record. Shear failure is developed by all second story columns. On the other hand, the response of the building with configuration DA-TS is significantly reduced, with maximum inter-story drifts that are below 0.5%. Except for a few plastic hinges in some of the short spandrels and the buckling of braces in the first story, the behavior of the structure is essentially in the elastic range. The improved performance of the building with the latter configuration is due primarily to the decrease in the strength demands due to shortening of the period of braced building DA-TS (see Fig. 4.27 and Table 6.9). The potential energy dissipation characteristics of the bracing system do not play a role in the reduced response of the building (braces never reach yielding, only reach buckling in the first story).

For the Oakland record, configurations TS1 and DA-TS effectively reduce the response of the building and result in maximum drift ratios which are below 1% in all stories. Column shear failure is not observed in any of these two bracing configurations. However, when the building is braced with configuration TS2, most of the second story columns fail in shear with lateral drifts that reach 1.25% in the second story. Since the majority of second story columns fail in shear, configuration TS2 cannot be considered to provide an adequate safety level against collapse. The latter configuration could be used as a retrofit scheme provided that columns are encased with an external jacketing to permit the development of the flexural capacity of the columns in the lower stories.

Performance of X-Bracing System

The results presented above indicate that X-bracing can be designed to reduce the response and control lateral drift of the building under study. Contrary to the results obtained for the three-story building analyzed in the previous section, there is no unique solution that satisfies the demands of the records on firm soil and soft soil sites at the same time. Following is an evaluation of the behavior of the reinforced concrete members and steel braces for the configurations that led to an adequate performance of the structure.
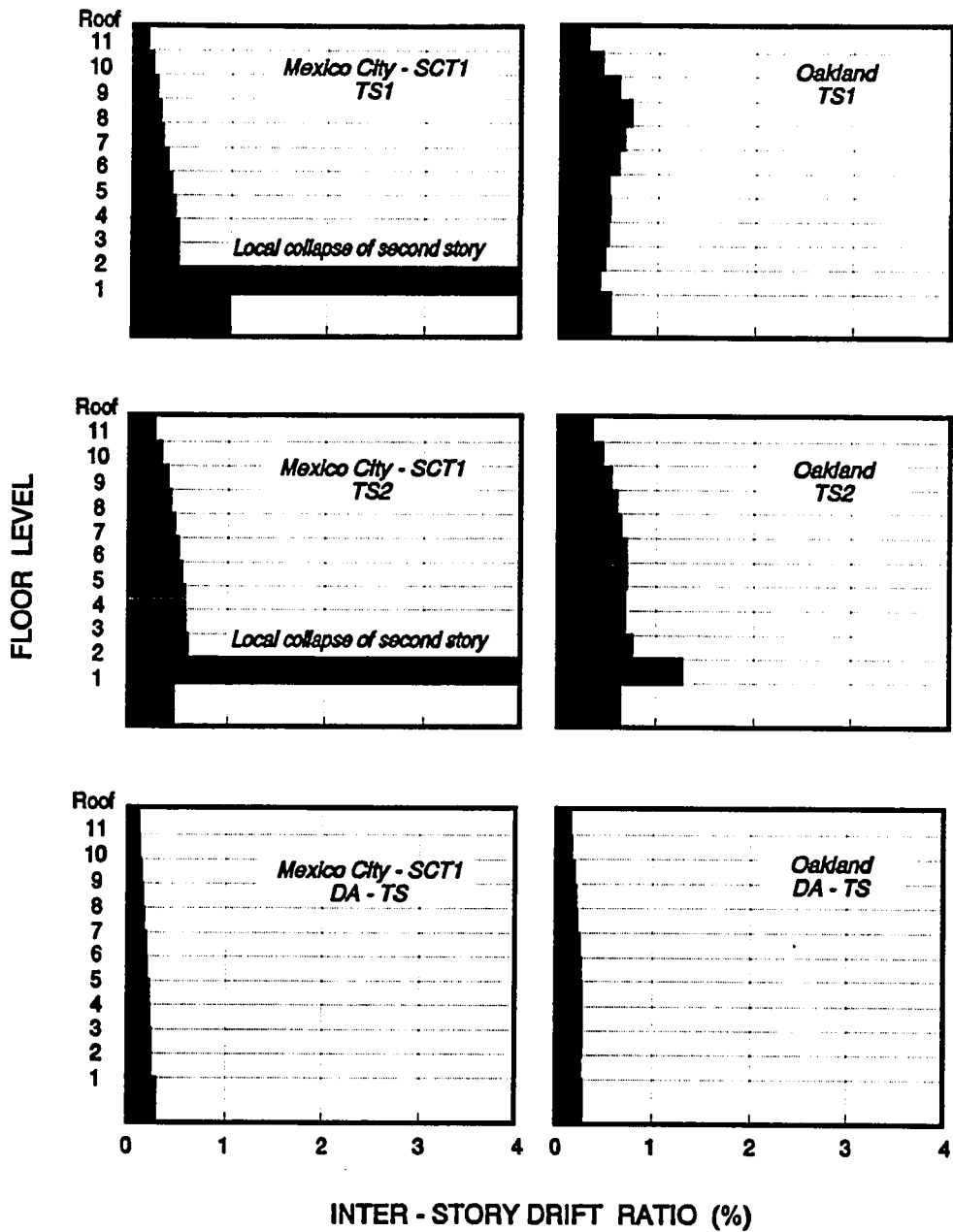
Figure 6.42 Maximum inter-story drift ratios for the braced building (configurations TS1, TS2 & DA-TS) subjected to the records on soft soil.

a) Performance of Reinforced Concrete Members

To evaluate the behavior of the building, the results obtained for configuration TS2 with the scaled El Centro record will be used. From the records on firm soils, the scaled El Centro record imposes the largest demands on the building with scheme TS2. In Fig. 6.43, plastic hinges developed in the perimeter frames for configuration TS2 is presented. Also shown in this figure are the members that fail in shear during the scaled El Centro record. (In Fig. 6.43, the length of the short exterior bays are shown larger than the actual scale)

BRACED TS2

O   *Hinge In only one direction of bending*

●   *Hinge In both directions of bending*

—   *Member shear failure*
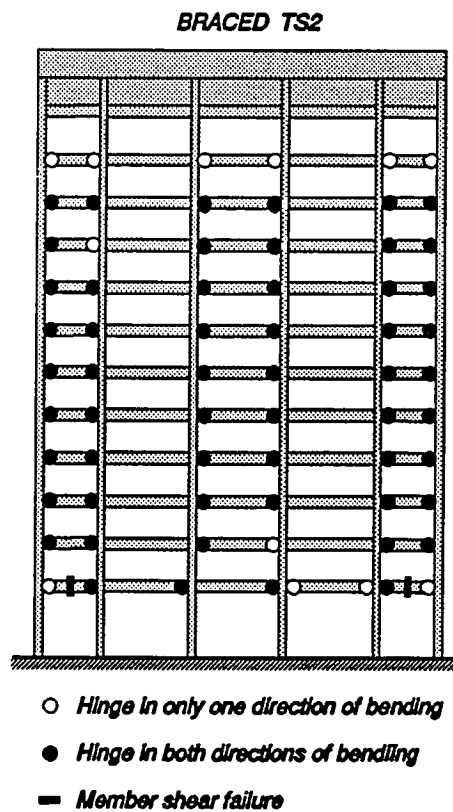
Figure 6.43   Hinge location for the perimeter frames of the braced building with configuration TS2 when subjected to the scaled El Centro record. (Exterior bays are not drawn to scale for clarity)

As can be seen, shear failure is prevented in all columns through the height of the building, and it is only anticipated for the short spandrel beams of the first floor. However, shear forces in some of the second story columns reached 92% of the shear capacity. The possibility for column shear failure in similar or larger events is evident. The latter result suggests that columns will require external jacketing to guarantee the adequate performance of scheme TS2.

Plastic hinges are developed only in beams. Pull-out of bottom beam reinforcement is predicted in many of the short spandrels but with minor reductions in strength which are not considered to affect the integrity of the structure.

The axial force distribution in columns with configuration TS2 subjected to the scaled El Centro record is presented in Fig. 6.44. The figure shows the maximum axial force developed in the members as a fraction of the corresponding capacity in pure compression or tension. It can be seen that the level of the tension forces developed in the columns of the bottom and top stories is high and exceeds the tension capacity in many cases. Compression capacity is never exceeded, but maximum compression forces reached up to 55% of the estimated capacity in some columns. Similar to the results obtained for the three-story buildings, the level of tension forces developed in columns with post-tensioned rods (see Fig. 6.37) is smaller than that obtained for scheme TS2. In addition, fewer columns showed tension forces for configuration C4B. This result is primarily attributed to the configuration adopted with scheme C4 and to the initial pre-compression induced in columns by initial prestressing of the rods.

Compressive axial forces in beams are, in general, lower than those obtained with configuration C4B with post-tensioned rods and remained below the compression capacity of these members. Tension forces are developed in beams of both braced and unbraced bays. Using the minimum amount of longitudinal reinforcement in the spandrels (typically at mid span) and neglecting any contribution of slab reinforcement, the maximum estimated tensile forces reach 25% of the capacity in pure tension.

While the flexural behavior of columns is adequate, the high level of tension forces induced in these members by the bracing system becomes a burden for the use of an X-bracing scheme. To prevent failure in tension and/or significant reductions in the flexural and shear capacity of columns, jacketing and collectors will have to be provided throughout
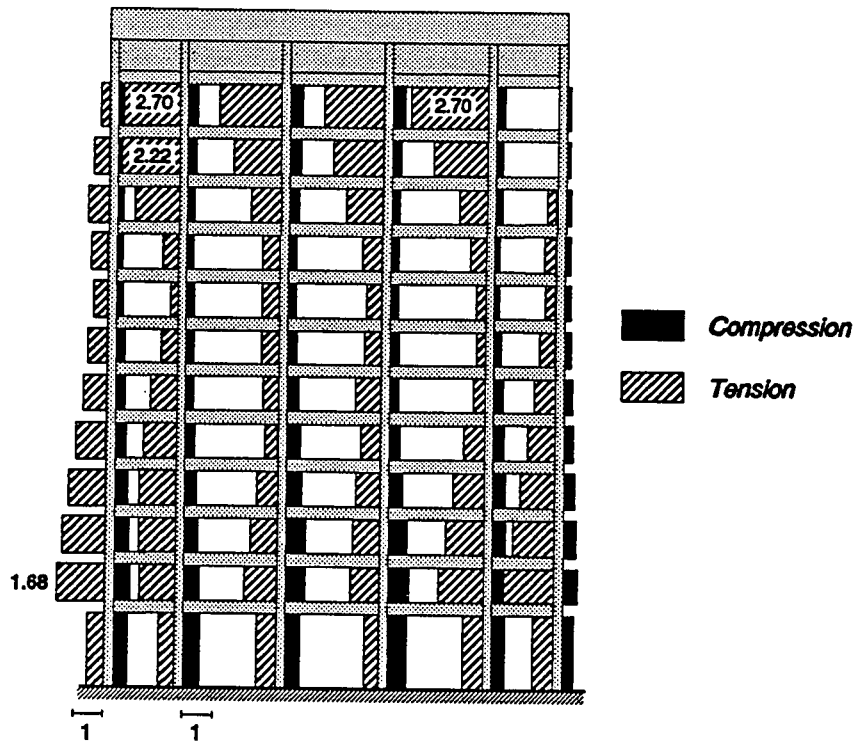
Figure 6.44 Axial force distribution in the perimeter frames of the braced building with configuration TS2 for the scaled El Centro record. (Axial force is shown as fraction of the capacity of the member in pure compression or tension)

the height of the building. Alternatively, to reduce the level of axial tension forces and to alleviate the design of collector members, braces could be distributed within the three middle bays using a configuration pattern similar to that of configuration DA-TS. Nonetheless, the latter configuration pattern will require a larger number of brace connectors. In addition, because of the high level of tension forces obtained it can be anticipated that collector members will most likely be required in most columns and beam members anyway.

b) Performance of Braces

Brace yielding and buckling of braces with configurations TS2 for the scaled El Centro record are presented in Fig. 6.45. Brace buckling is observed in most braces up to the ninth story; in the upper stories braces remain within the elastic range. In the second and upper stories braces never reach yielding and maximum elongations after buckling approach, at the most, 1.5 times the elongation at buckling load. In the first story, however, the braces yield and buckle with extensive inelastic excursions in both tension and compression, as illustrated by the hysteretic behavior of a typical first story brace in Fig. 6.45. Note that the brace buckles several times during the response of the structure and reaches the residual buckling load (P_r). Because the flat width to thickness ratio of the
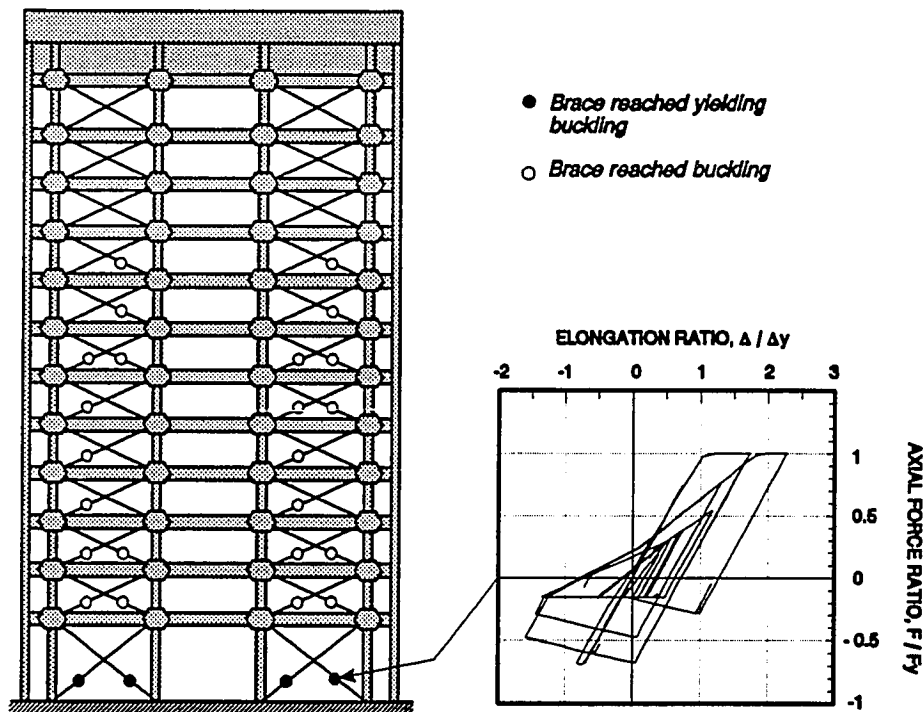
Figure 6.45   Yielding and buckling of braces, and typical hysteretic behavior of first story braces with configurations TS2 when subjected to the scaled El Centro record.

tube sections was selected to meet the LRFD recommendations for seismic behavior, fracture of the tube section due to repeated load reversals is not anticipated. However, it is clear that first story braces will experience a high level of damage after the earthquake.

The behavior of braces with configuration DA-TS for either the Mexico City - SCT1 or the Oakland record is in the elastic range in all but in the first story. First story braces only reach buckling (never reach yielding) with minimal reductions in strength and practically no hysteretic behavior.

6.3.3.3 Summary

The use of X-bracing as a retrofit scheme was studied by examining several possible configuration patterns, with different size and distribution of braces. From the retrofit schemes studied, three bracing configurations were considered to be viable alternatives for the retrofit of the building. These configurations are in increasing order of stiffness and strength: TS1, TS2 and DA-TS. Configuration TS1 was designed to provide the same initial stiffness as that of configuration C4B with post-tensioned rods, mainly for comparison.

For the records on firm soils, configurations TS2 and DA-TS both protect the building against collapse, with configuration TS2 being the most effective. However, retrofit scheme TS2 will require jacketing of columns throughout the height of the building to augment their shear strength. Beams will require collector elements to increase their axial load capacity.

For the records on soft soils, only configuration DA-TS prevents collapse of the structure under the Mexico City -SCT1 record, while for the Oakland record configurations TS1 and DA-TS protect the building from collapse. However, the response of the building on soft soils with configuration TS2 is the least effective and fails to prevent collapse of the structure. With bracing configuration DA-TS, the behavior of reinforced concrete members and steel braces is essentially in the elastic range, with little or no hysteretic behavior.

For the Mexico City - SCT1 record, the response of the braced building with lower stiffness and strength (schemes TS1 and TS2) led to collapse of the structure, despite the dissipation of energy through extensive yielding and buckling of braces. The key to the success of configuration DA-TS scheme was, for the Mexico City - SCT1 record, the large

stiffness of the bracing system and the reduction demands of the building due to shortening of the period of the building. Because of the large size of the braces, the use of configuration DA-TS as a retrofit scheme will most likely require large anchorage devices and the extensive use of collector members to transfer the large brace forces to the existing building. As noted earlier, the use of scheme DA-TS would probably be uneconomical and impractical.

The response of the X-bracing system for the records on *firm* soils is comparable to that of the post-tensioned bracing system. Both, configuration TS2 and C4B (or C4A) protect the building from collapse and result in a similar level of performance for the reinforced concrete members. The post-tensioned bracing system has the advantage that it would probably require fewer and smaller collector members than configuration TS2. On the other hand, configuration TS2 has fewer braces which would require fewer anchorage devices (brace forces are of the same magnitude for both configurations). Both schemes C4B (C4A) or TS2 offer comparable retrofit designs, and the final design is more a matter of economics and practicality rather than performance level.

6.3.4 Retrofit Scheme III - Structural Wall

The third retrofit scheme consisted of the addition of a structural wall *(shear wall)* to the perimeter frames. Two wall schemes with very distinct levels of stiffness and strength were selected for study. Typical dimensions and reinforcing details of the wall schemes are presented in Figs. 6.46 and 6.47, respectively. The first wall scheme, W1, consists of eccentric reinforced concrete walls, 15 in. thick, located in the outer bays (double column configuration bays), as shown in Fig. 6.46.

Walls are connected directly to existing columns by # 6 bar dowels to allow existing columns to act as boundary elements for the wall. Longitudinal reinforcement in these columns in the first floor is typically spliced in the mid-length region with a 40 bar diameter lap (see Fig. 4.12) which is barely sufficient to develop yielding of the reinforcement. In addition, spacing of transverse reinforcement (#3 bars) do not meet current ACI [4] requirements for confinement of concrete and lateral support of longitudinal reinforcement in boundary elements of structural walls. To avoid a premature bond failure of the longitudinal reinforcement and to provide additional confinement to the concrete and

WALL REINFORCING SCHEDULE			
Floor	Vertical	Horizontal	Dowels
1st - 9th	#11 @ 6	#6 @ 12	#6 @ 10
9th - Roof	# 9 @ 6	#6 @ 12	#6 @ 12

Existing Column   Existing Beam   Existing Column

28"   15"

26"   Dowels

120"

SECTION A - A
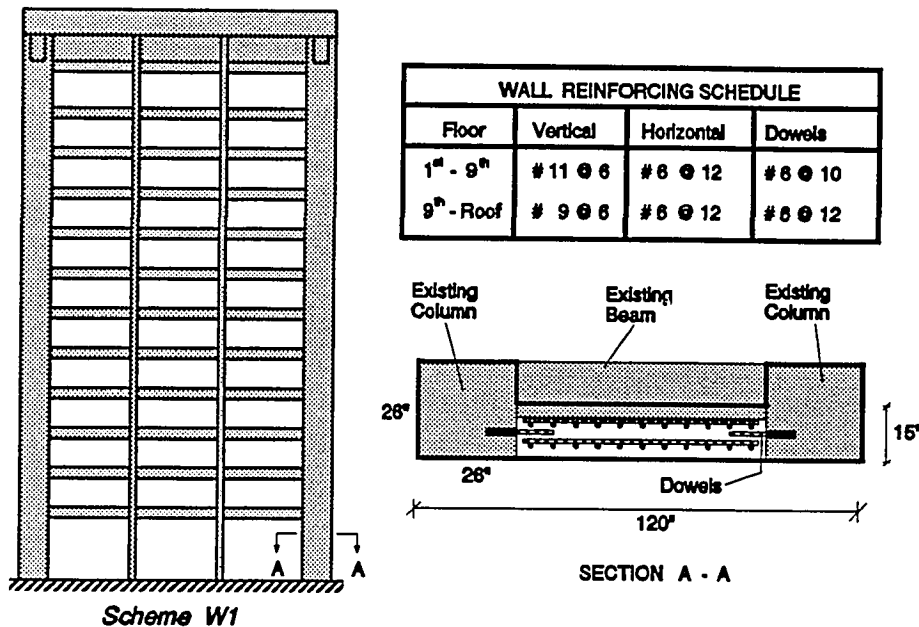
Scheme W1

Figure 6.46   Cross section dimensions and reinforcing details of structural wall scheme W1 for the twelve-story building.

compression reinforcement, existing columns will probably have to be confined with external steel straps, or reinforced concrete or steel jacketing [28, 50]. Note that because plastic hinges are expected to develop only at the base of the wall, the jackets would strictly be required in only the lower stories of the building, probably only in the first and second stories. The reinforcement layout shown in Fig. 6.46 was designed to satisfy the demands at the base of the wall, and it is likely that the longitudinal and transverse reinforcement could be gradually reduced with the height of the building to achieve a more economical design.

Shear reinforcement in wall scheme W1 consisted of two curtains of # 6 bars spaced at 12 in, as shown in Fig. 6.46. Design of the horizontal reinforcement followed capacity design principles to prevent shear failure prior to developing the flexural capacity at the base of the wall.

The second wall scheme, W2, consisted of one long structural wall that covered the central bay of perimeter frames of the building, as shown in Fig. 6.47. Similar to scheme W1, the wall is located eccentrically, flush with the exterior face of columns. The wall is 15 in. thick and is connected directly to the existing columns by dowels throughout the height of the building, as shown in Fig. 6.47. As above, existing columns are expected to act as boundary elements of the wall, and will have to be externally confined as described for scheme W1. Similarly, external confinement will probably be restricted to only the lower stories of the structure. Shear reinforcement consisted of two curtains of #8 (or #7 bars, see Fig. 6.47) and followed capacity design principles.

WALL REINFORCING SCHEDULE			
Floor	Vertical	Horizontal	Dowels
1st - 6th	#11 @ 12	#8 @ 12	#10 @ 10
6th - Roof	# 9 @ 12	#7 @ 12	# 8 @ 12

Scheme W2
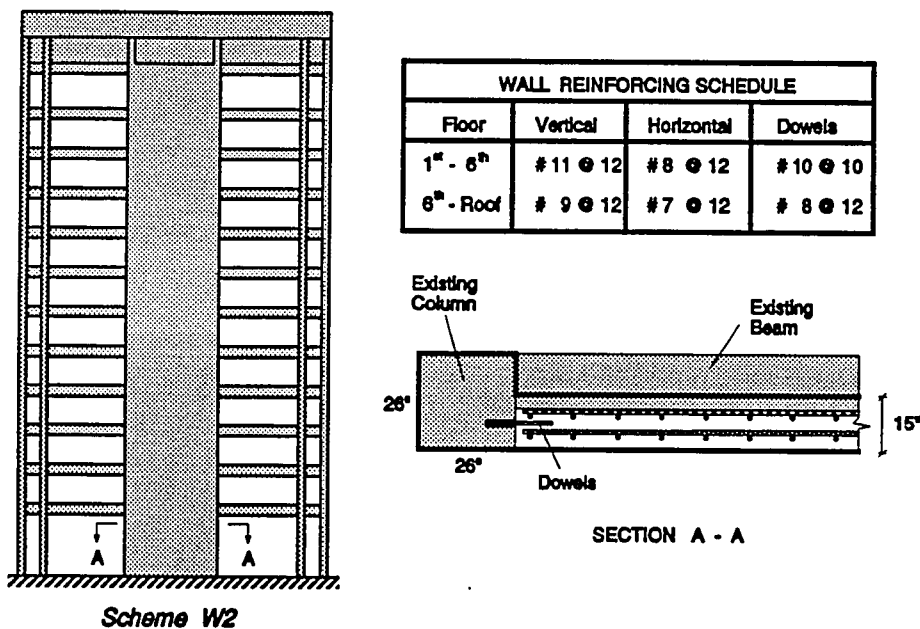
SECTION A - A

Figure 6.47 Cross section and reinforcing details of structural wall scheme W2 for the twelve-story building.

6.3.4.1 Lateral Stiffness and Strength

In Fig. 6.48, the relationships for the base shear coefficient and drift at the centroid of inertia forces for the original and braced building with wall schemes W1 and W2 are compared. In this figure, the relationships have been obtained using a uniform lateral distribution over the height of the building. For comparison, the relationships obtained for
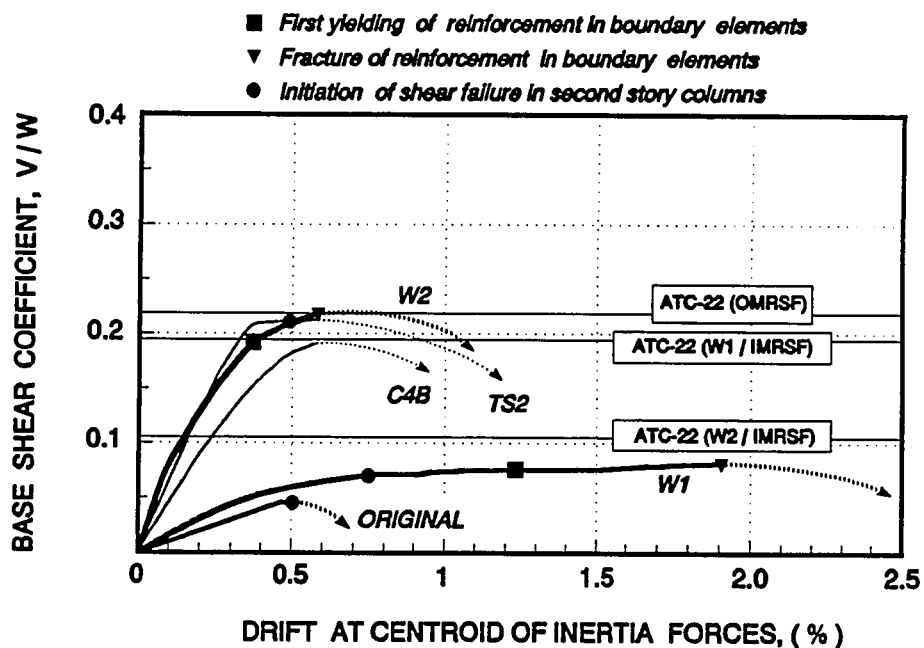
Figure 6.48 Base shear coefficient and drift at centroid of inertia forces relationship for the original and braced structure with wall schemes W1 & W2, with post-tensioned rods C4B and with tube sections TS2.

the post-tensioned bracing system with configuration C4B and for the X-bracing system with configuration TS2 are also shown in Fig. 6.48.

The building with structural scheme W1 shows only a moderate increase in initial stiffness. The sequence of events in the lateral response of the building indicates that shear failure in second story columns initiates prior to yielding of the flexural reinforcement in the wall. The shear failure of second story columns triggers the shear failure of columns in upper stories. The redistribution of forces after shear failure of these columns results in an increase in lateral drift and causes flexural yielding of the wall at the base. Failure of the wall - frame system is caused by fracture of the longitudinal reinforcement at the base of one of the walls at a drift which is essentially 4 times as high as that of the original structure (see Fig. 6.48). The main advantage of scheme W1 is not in an increased stiffness or strength, but rather in the increase of the deformation capabilities of the wall-frame system. The

presence of the walls restrains lateral drifts and prevents the sudden collapse of the structure observed for the original building upon shear failure of columns. Instead, the walls carry the additional shear forces from the failing columns and reach a more ductile flexural failure.

Wall scheme W2, on the other hand, provides a significant increase in stiffness and strength to the building. The increase in strength is as much as four times that of the original structure. Column shear failure occurs after yielding the longitudinal reinforcement in boundary elements, but prior to reaching ultimate strength of the wall. Failure of the wall is caused by fracture of the longitudinal reinforcement in the boundary elements. Unlike scheme W1, ultimate strength of the wall - frame structure is reached at drifts that are comparable to those at failure of the original structure. Note that shear failure of columns does not result in a significant deterioration of the lateral stiffness or strength of the building, because most of the stiffness and strength of the wall-frame system is provided primarily by the structural wall.

Fig. 6.48 also shows that the stiffness and strength of wall scheme W2 are quite similar to those of the X-bracing configuration TS2. At the same time, configuration C4B with post-tensioned rods has a lateral stiffness and strength that are only slightly smaller than those of wall scheme W2. Both steel bracing configurations, C4B and TS2, provide a much larger stiffness and strength than those of wall scheme W1.

For comparison, the base shear coefficient for a dual system consisting of a IMRSF capable of resisting at least 25% of the lateral forces and a reinforced concrete structural (shear) wall, as required by the provisions of the ATC - 22 is shown in Fig. 6.48. With wall scheme W1, column shear failure precedes flexural yielding of the wall. Therefore, it seemed appropriate to adopt response modification factors for brittle elements to compute the coefficient for this scheme. In contrast, with scheme W2 flexural yielding precedes column shear failure and thus a more ductile mode of failure is expected. Thus, modification factors corresponding to semi-ductile elements were adopted in the calculations.

The building under study does not satisfy the requirement of a IMRSF (ATC-22 does not include provisions for a structural wall with an OMRSF); however, it is reasonable to assume that the requirements of strength for a structural wall and an IMRSF are a lower bound for the strength required for a wall with an OMRSF. As can be seen, scheme W1

does not meet the lower bound for strength required by ATC-22. In fact, the required strength is several times larger than the estimated ultimate strength of scheme W1. On the other hand, ultimate strength of wall scheme W2 exceeds that required by ATC-22. A discussion of these results is presented later in Chapter VII.

6.3.4.2 Dynamic Response Analysis

Dynamic Properties

The fundamental period of vibration for the original and the braced structures with walls on firm and soft soil sites are presented in Table 6.10. Values for the period of the wall - frame system correspond to cracked properties of the walls in all cases. The reductions in the fundamental period of vibration of the structure are apparent. As expected, due to larger initial stiffness, the reductions in the fundamental period for wall scheme W2 are much larger than those for wall scheme W1. Similar to the results obtained for the three-story building, the addition of mass due to the self-weight the wall has only a minor influence in the period of the building.

For wall scheme W1, the lengthening in fundamental period of vibration of the building on soft soils is only moderate. Consequently, effective damping ratios are only slightly higher than the 2% damping ratio assumed for a fixed-base system. Note that for wall scheme W1 located on the San Francisco bay mud, calculated effective damping ratio is higher than that for the same building on the clays of Mexico City, even though the lengthening in period for the building on the San Francisco bay mud is smaller. The reason for this result is the higher hysteretic damping ratio assumed for the San Francisco bay mud (see Table 3.1). With wall scheme W2, period lengthening ratios ($\tilde{T}$ / T) are larger than with wall scheme W1, and higher effective damping values are obtained as shown in Table 6.10.

Dynamic Response

Maximum inter-story drifts obtained for wall schemes W1 and W2 for the records on firm soil sites are presented in Fig. 6.49. For the Californian earthquakes, scaled El Centro and Corralitos records, maximum drifts are larger with scheme W1 than those obtained with scheme W2. However, lateral deformations remain below 1% drift with both wall schemes

Table 6.10 Dynamic properties of the original and braced buildings with a structural wall.

Building	Fundamental Period (sec) [Effective Damping]*		
	Soil Type		
	Firm	Soft	
		Silty Clay Deposits (Mexico City)	San Francisco Bay Mud (California) Case II
Original	3.52 [2.0 %]	3.63 [2.3 %]	3.60 [2.6 %]
Wall Scheme W1	2.64 † [2.0 %]	2.79 † [2.5 %]	2.74 † [2.8 %]
Wall Scheme W2	1.22 † [2.0 %]	1.52 † [4.0 %]	1.44 † [3.7 %]

* values are based on a h^*/r ratio of 1.57 in accordance with the dimensions assumed for the foundation

† shown values correspond to cracked wall at the base.

in all cases. Column shear failure is eliminated with both wall schemes in all three records. Also, in both schemes, walls reach cracking over most of the height of the building, but they never reach yielding during the response. Inelastic behavior in frame members is restricted to flexural hinging in some of the spandrels; column hinging is prevented with both wall schemes.

For the records on soft soil sites, the response of the building varies significantly with each wall scheme. In Fig. 6.50, maximum inter-story drifts for wall schemes W1 and W2 subjected to the records on soft soil sites are compared. For the Mexico City - SCT1 record and wall scheme W1, maximum drifts reach about 1.5% in the upper stories of the building; however, column shear failure is prevented in all stories. In spandrels, pull-out of bottom reinforcement is anticipated in most beams with significant hinge rotation. Walls develop cracking throughout the height of the building, but they never reach yielding. With wall scheme W2, on the other hand, the response of the building is amplified and significant damage is expected for the existing members. Shear failure of columns and spandrels, as
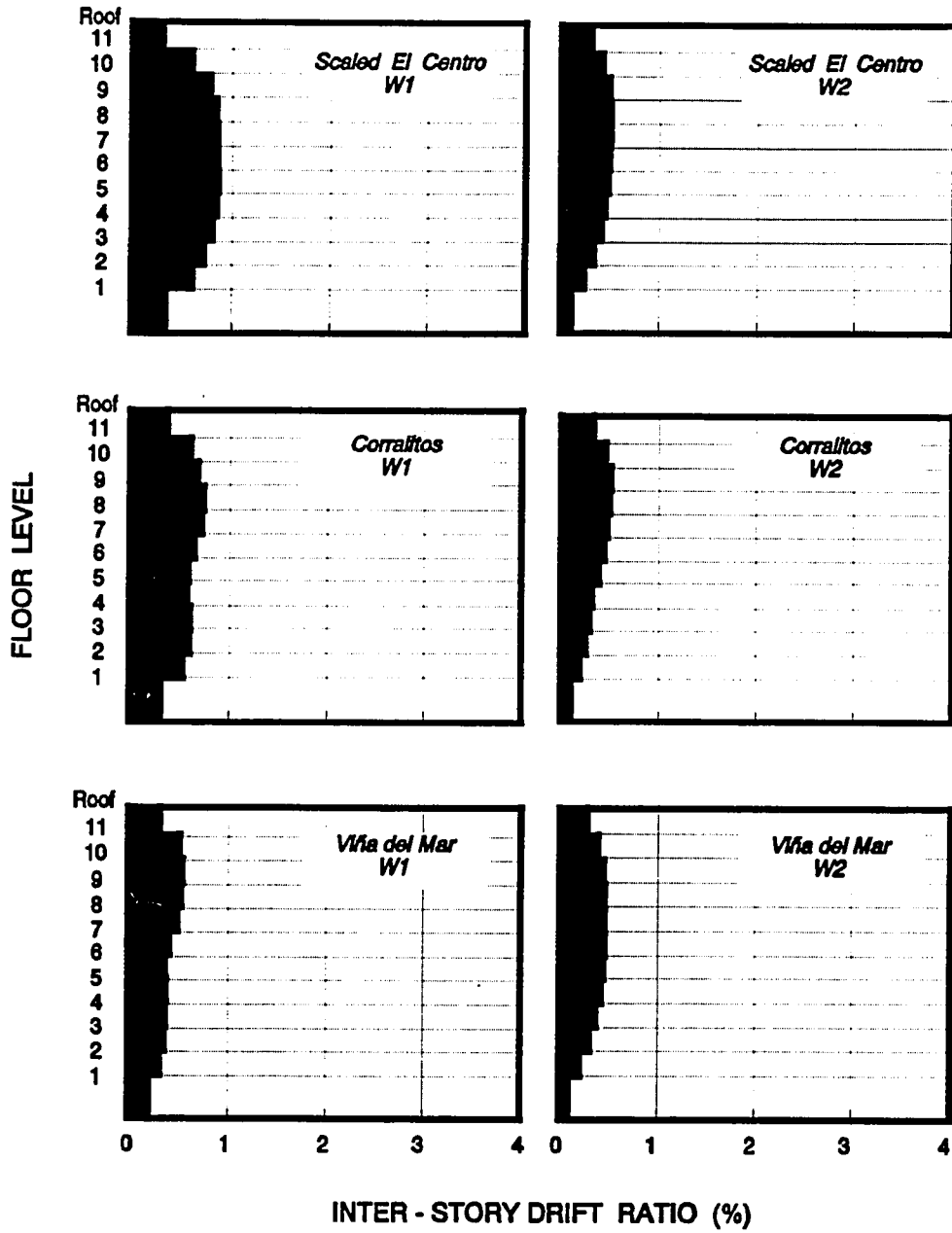
Figure 6.49 Maximum inter-story drifts for the braced building with wall schemes W1 & W2 subjected to the records on firm soil sites (scaled El Centro, Corralitos & Viña del Mar).

INTER - STORY DRIFT RATIO (%)
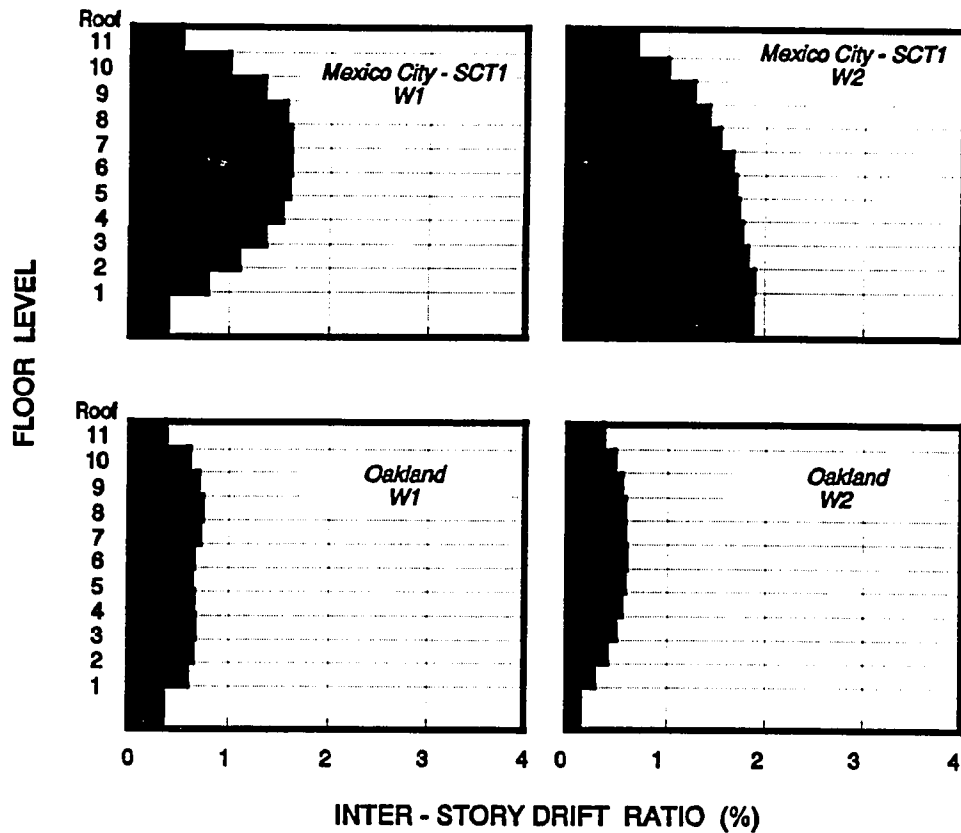
Figure 6.50 Maximum inter-story drift ratios for the wall - frame building subjected to the records on soft soil sites (Mexico City - SCT1 & Oakland (OHW)).

well as anchorage failure of bottom beam bars are observed in almost every floor level. In addition, and most important, the wall reaches its estimated flexural capacity by fracture of the longitudinal reinforcement in the boundary elements at the base. As a result, maximum inter-story drifts approach 2% in the first and second story, and due to the severe damage expected for the columns and the wall, partial collapse of the building is likely to occur.

For the Oakland record, maximum inter-story drifts remain below 1% and shear failure in columns and beams is prevented in all stories with both wall schemes. Walls develop cracking, but never reach yielding. Hinging is predicted only in beams with minor inelastic behavior.

Performance of Structural Wall System

Evaluation of the maximum inter-story drifts shows that wall scheme W1 is the most effective for controlling the response of the building on both firm and soft soil sites. From all the earthquake records considered in this study, the Mexico City - SCT1 record imposed the largest demands of strength and ductility on the wall - frame system. Thus, to examine the performance of the reinforced concrete members, the results obtained for wall scheme W1 subjected to the Mexico City - SCT1 record will be discussed in detail.

Performance of Reinforced Concrete Members

In Fig. 6.51, the profile of plastic hinges developed in columns and beams of perimeter frames during the response to the Mexico City - SCT1 record is presented. Also shown in the figure is the hinge rotation for "positive" moment in beams as a fraction of the rotation at failure in bond of bottom bars. Hinge rotations for negative moment were minimal (Θ_{max} / Θ_y < 1.1). As indicated earlier, flexural yielding of the wall is not anticipated, but rather extensive cracking of the wall throughout the height of the building. In Fig. 6.51, a possible crack pattern that could develop in the walls under the Mexico City - SCT1 record is indicated. The reader is cautioned to interpret the crack pattern *qualitatively*, even though the pattern was estimated from the magnitude of the moments and shear forces obtained at different levels of the wall.

Shear failure is prevented in columns and beams throughout the height of the building. Inelastic behavior is limited to hinging of the frame members and to cracking of the wall. As bending moments are maxima in the lower stories of the building, flexural cracking at the base of the wall is significant and is gradually reduced with height, as suggested in Fig. 6.51. In addition, maximum shear forces in the lower stories exceed the shear strength corresponding to flexure-shear cracking of the walls, and therefore diagonal cracking is anticipated. The magnitude of the shear forces at the base of the wall are moderate and approach only 57% of the estimated shear capacity of the wall. Web shear stresses at the wall base reach only 30% of the maximum recommended values for hinging regions [47]. Shear behavior of the wall is adequate.

In beams, plastic hinges develop throughout the height of the building, and are primarily due to the anchorage failure of bottom reinforcement. Pull-out of bottom

Scheme W1 - Mexico City - SCT1

1.4	1.4	1.0	1.0	1.2	1.6
2.2	2.6	2.2	2.4	2.4	2.4
2.7	3.5	2.2	2.4	3.1	3.2
4.0	4.3	2.6	3.1	3.5	4.8
4.0	4.4	2.6	3.2	3.6	4.8
3.9	4.5	2.7	3.2	3.6	4.8
3.7	4.2	2.7	3.4	3.3	4.8
3.3	3.9	2.4	3.2	2.9	4.4
2.7	3.2	1.9	2.6	2.4	3.7
2.5	3.2	1.7	2.4	2.4	3.3
1.0	1.8		1.2	1.3	1.1

O Hinge in only one direction of bending

● Hinge in both directions of bending
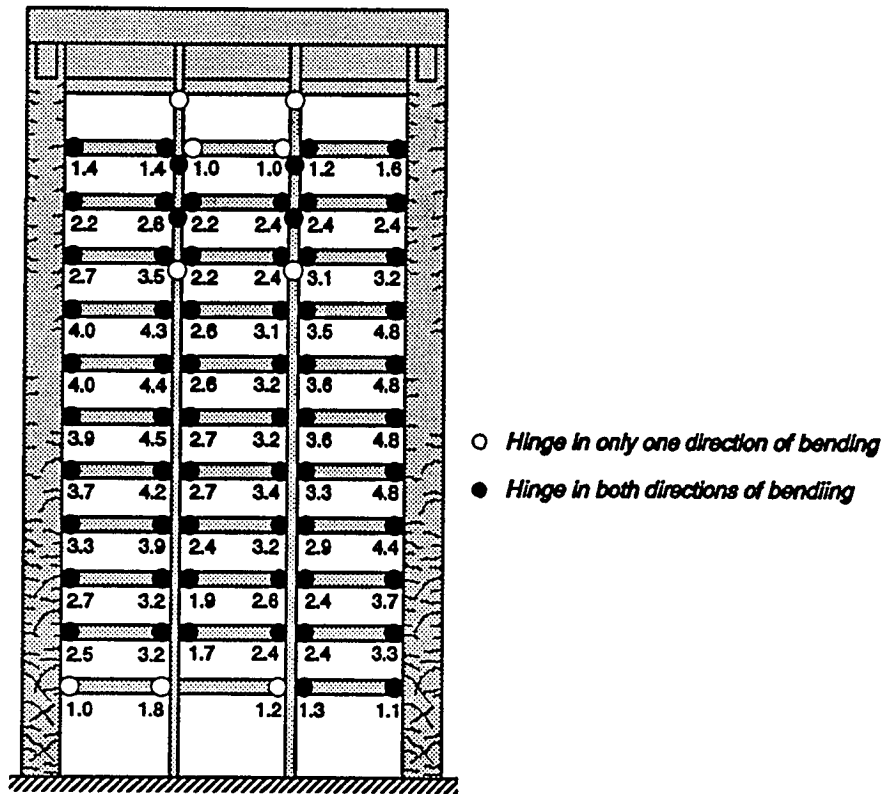
Figure 6.51   Hinge location for perimeter frames of the wall - frame system (Numbers indicate the hinge rotation for "positive" moment as a fraction of the rotation at failure in bond of bottom beam bars)

reinforcement is observed in all beams, with large hinge rotations and significant reductions in strength (see Fig. 6.51 and 4.16). In columns, plastic hinges only develop in the 9th to 12th story. However, hinge rotations are minimal and do not exceed 1.1 times the rotation at yielding of the sections.

The performance of the wall scheme W1 for the rest of the records considered in this study was better. Walls reached flexural cracking at the base, but they never reached flexural yielding. Plastic hinges developed only in spandrels (not in columns) with smaller hinge rotations than those anticipated for the Mexico City - SCT1 record.

6.3.4.3 Summary

The addition of structural walls to perimeter frames was examined as a possible retrofit strategy for the twelve-story building. Two wall schemes with distinct levels of stiffness and strength were investigated, namely W1 and W2.

For the records measured on firm soils, both wall schemes were able to protect the building from collapse and to prevent severe damage of the existing members in the structure. Furthermore, maximum inter-story drifts remained below 1% and column shear failure was prevented in all stories with both wall schemes. Walls reached cracking, but never developed flexural yielding.

For the records on soft soils, the response of the wall schemes varied depending on the earthquake record considered. For the Oakland record, both wall schemes improved the response of the building, and exhibited a level of performance that was very similar to that observed for the records on firm soil sites. However, for the Mexico City - SCT1 record, only one wall scheme was able to protect the building from collapse (scheme W1). Even though significant damage was anticipated in the hinging regions of spandrels with scheme W1, walls reached cracking only and never developed yielding. Shear failure of columns or beams was not anticipated. On the other hand, the response of the building with wall scheme W2 was inadequate. Column shear failure and flexural failure of the wall was anticipated during the response. Maximum inter-story drifts approached 2% in the lower stories of the building, and because of the high level of damage expected for columns and walls, partial collapse of the building is likely to occur.

6.4 PROTOTYPE STRUCTURE III - SEVEN-STORY BUILDING

Analyses of the original and retrofit buildings were conducted only in the longitudinal direction of the building, as lateral strength in the transverse direction was assumed to be adequate.

6.4.1 Original Building

6.4.1.1 Dynamic Response Analysis

Reinforcing details and, lateral stiffness and strength characteristics of the original building were presented in section 4.4. Table 6.11 shows the fundamental periods of vibration and the effective damping ratios of the building for the different types of soil conditions selected for study. For firm soil conditions, effective damping was selected as 2% of critical in all cases as indicated in Chapter III. For soft soil conditions, effective damping of the soil-structure system was determined using the procedure outlined in section 3.3.

Table 6.11 Dynamic properties of Seven-Story building (short direction).

Building	Fundamental Period (sec) [Effective Damping]*		
	Soil Type		
	Firm	Soft	
		Silty Clay Deposits (Mexico City)	San Francisco Bay Mud (California)
			Case II
Original	0.62 [2.0 %]	0.71 [5.3 %]	0.69 [6.0 %]

* values were based on a h*/r ratio of 0.60 in accordance with the dimensions of the foundation.

As can be seen from Table 6.11, the fixed-base period of the building is relatively short for a building of a seven story height (values shown in Table 6.11 are based on cracked properties for the reinforced concrete elements). The latter result is primarily due

to the deep spandrel beams of perimeter frames (see Figs. 4.20 and 4.21), which increase the lateral stiffness of the building significantly.

The lengthening in the fundamental period of the building located on soft soil sites is moderate ($\tilde{T}/T_{max} \approx 1.15$ for the building on clay deposits of Mexico City), but because of the relatively low effective height to radius of foundation ratio ($h^*/r \approx 0.60$, squat structure) the foundation damping ratio is high (see Fig. 3.15). As a result, the calculated effective damping ratios for the buildings located on soft soils are much higher than those assumed for the fixed-base building.

For the structure supported on the San Francisco bay mud, only one case (Case II) is presented for study. However, the overall results presented herein correspond, in general, to the most unfavorable situation, and differ little from the results obtained for the structure supported on soil Case I (see Table 3.1) or on a fixed-base.

Dynamic Response

a) Building Response on Firm Soil Sites

In Fig. 6.52, the maximum inter-story drifts obtained for the original building subjected to the records on firm soils are presented. As can be seen, inter-story drifts in excess of 4% are obtained in some stories during the response and collapse of the building is anticipated for the three records considered. For the Californian records, scaled El Centro and Corralitos, shear failure begins in the columns of the first story and propagates to the second and third stories. For the Viña del Mar record, however, shear failure begins and concentrates in the third and fourth story. The columns of the first and second story show no signs of failure in the latter case. In all the three cases, collapse of the building is produced by the generalized shear failure of columns in a given story (stories).

As indicated in Chapter IV, the primary load resisting system is a moment frame with deep spandrel beams and short columns (Figs. 4.20 and 4.21). Because of the low shear strength of columns, failure of these members occur at a relatively small lateral loads (drifts). Neither beams nor columns reach yielding at the ends prior to shear failure of columns and therefore the behavior of the building is brittle with no energy dissipation.
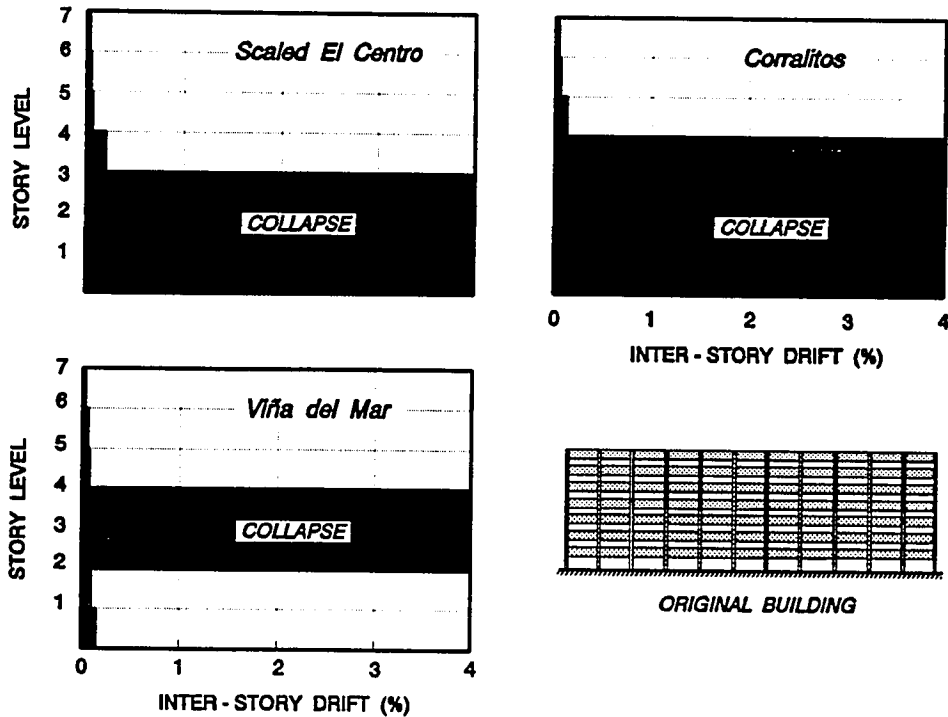
Figure 6.52   Maximum inter-story drift ratios for the original building subjected to the records on firm soil sites. (Scaled El Centro, Corralitos and Viña del Mar)

b) Building Response on Soft Soil Sites

Maximum inter-story drift ratios obtained for the original structure subjected to the two records on soft soil conditions are presented in Fig. 6.53. The drift values shown take due account of the lateral displacement and rocking motion of the foundation and correspond to the actual inter-story drift experienced by the building (Δ in Fig. 3.13). Because the structure is relatively squat, rocking motion of the foundation was negligible.

Similar to the results obtained for the structure subjected to the records on firm soil sites, inter-story drifts exceed 4% in some stories. Clearly, the original building would not have survived any of the records on soft soils. As above, collapse of the building is due to the generalized shear failure of the columns in a given story (or stories). The characteristics of both records on soft soils, Mexico City - SCT1 and Oakland, are such that shear failure of columns initiates in the second story, and not in the first story as anticipated for the
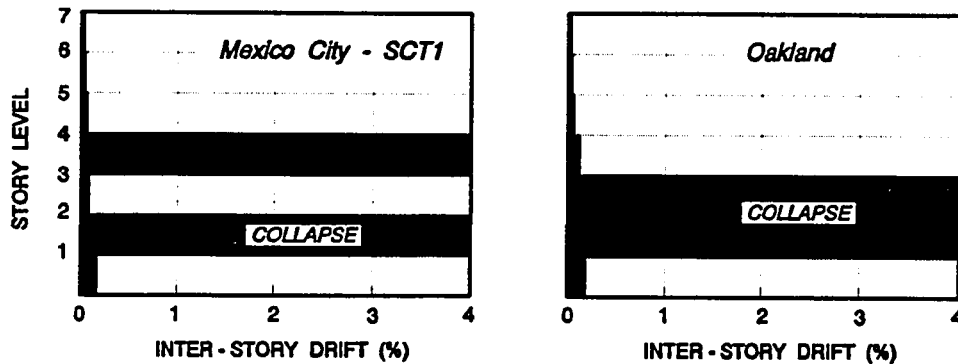
Figure 6.53   Maximum inter-story drift ratios for the original building subjected to the ground motion on soft soil sites. (Mexico City - SCT1 and Oakland)

scaled El Centro and Corralitos records above. First story columns do not exhibit shear failure and therefore inter-story drifts in the first story are minimal. As above, the behavior of the building is brittle without dissipation of energy.

6.4.1.2 Summary

The behavior of the original building for all of the earthquake records on firm and soft soils is inadequate. Collapse of the structure is anticipated for all the records. Failure is attributed to the generalized and premature shear failure of the columns in a given floor. The building exhibits brittle behavior and has no ability to dissipate energy. The need for seismic retrofit of the building is apparent.

6.4.2 Retrofit Scheme I - Post-Tensioned Bracing Systems

Evaluation of the post-tensioned bracing system considered several different configuration patterns and size of braces. Fig. 6.54 shows three of the configuration patterns considered for study. Brace size and brace distribution with height is presented in Table 6.12. In all cases, brace size was selected so that story stiffness and strength was either uniform or gradually reduced with the height of the building. Configuration patterns, brace size and brace distribution presented herein correspond to the minimum amount of bracing required to improve the response of the building. Lighter bracing schemes; i.e.
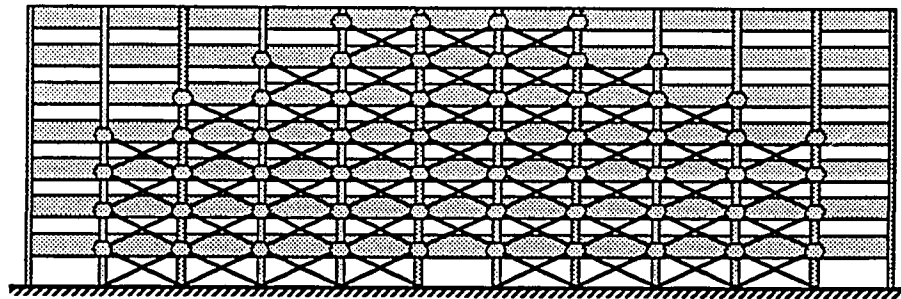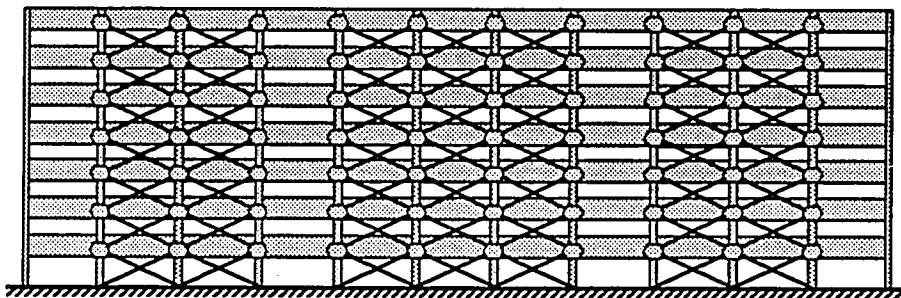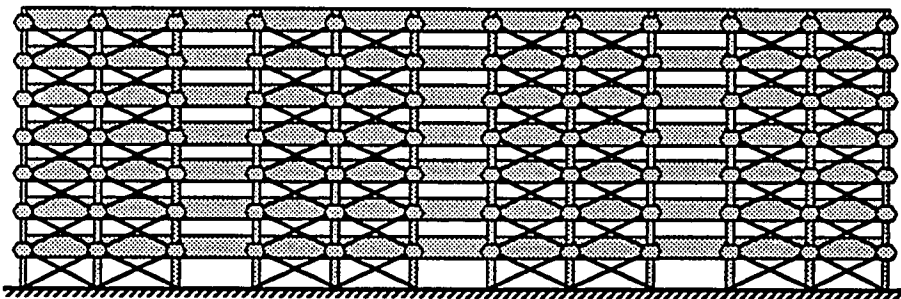
Figure 6.54 Bracing configurations for the seven-story building with post-tensioned bracing system. (perimeter frames only)

Table 6.12   Size and distribution of braces for configurations C1, C2 and C3.
(Seven-story building)

Story Level	Brace Size [Area (in^2)]		
	C1	C2	C3
2nd to Roof	2 - 1 3/8" ϕ rods [3.16]	3 - 1 1/4" ϕ rods [3.75]	3 - 1 1/4" ϕ rods [3.75]
1st	3 - 1 1/4" ϕ rods [3.75]	3 - 1 3/8" ϕ rods [4.74]	3 - 1 3/8" rods [4.74]

fewer braced bays and/or smaller brace size did not result in significant improvement of the behavior of the building.

Because of the large number of braced bays with all three configurations (7 to 8 braced bays), exterior columns are expected to be subjected to high bending moments and shear forces upon initial brace prestressing. Thus, the selection of an appropriate configuration becomes crucial for minimizing the forces induced in the existing elements.

In Fig. 6.55, the distribution of bending moments in columns with scheme C1 with an initial brace prestressing of 50% of the yield strength is presented. As expected, maximum bending moments (and shear forces) increase from interior to outer columns. Because outer bays are not braced with scheme C1, internal forces induced in exterior columns (column lines 11 and 22), show a reduction in the induced forces. Maximum bending moments occur in the first story columns of column lines 12 and 21. In these members, bending moments reach 65% of the moment capacity of the splice at the base, and shear forces approach 70% of the shear strength of the columns. If an initial brace prestressing of 75% of the brace yield strength were provided with scheme C1, the aforementioned columns would fail in shear due to brace prestressing alone (similar results would be obtained with bracing scheme C2). The use of a post-tensioned bracing system with configuration C1 jeopardizes the integrity of the existing structure upon prestressing of braces, and it is dangerous and inefficient. Even though a lower level of initial brace prestressing could be used (which is undesirable from an energy dissipation standpoint), column shear failure would occur prior to yielding of braces. Such a behavior is undesirable because it would not allow the bracing system to dissipate energy prior to column shear

$$\frac{M}{M_p} = 0.65 \quad (\frac{V}{V_u} = 0.70)$$

$$\frac{M}{M_p} = 0.65 \quad (\frac{V}{V_u} = 0.70)$$

BRACED C1 (Initial Pretress = 50% Fy)
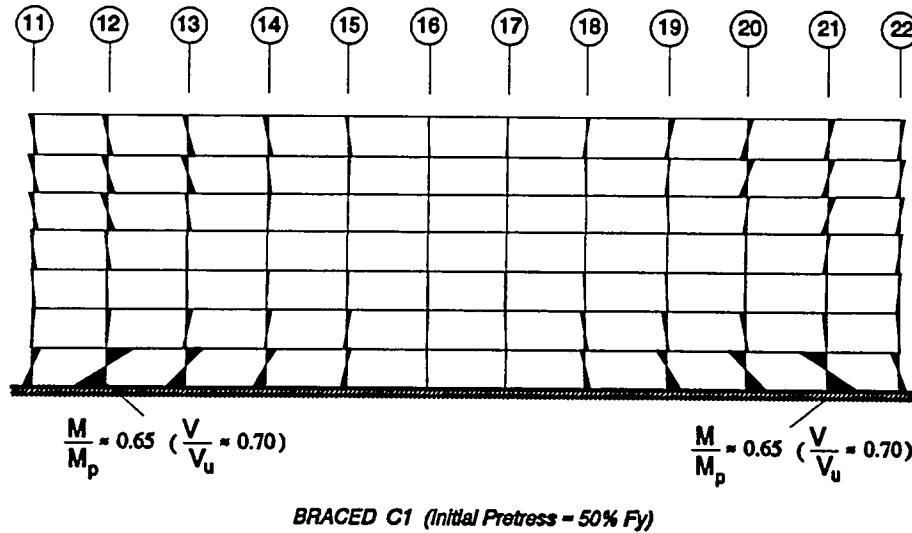
Figure 6.55 Effects of initial brace prestressing on the bending moment distribution in perimeter frame columns. Braced structure, scheme C1 with initial brace prestressing of 50% of brace yield strength.

failure during the response to the earthquake. Therefore, unless the bracing system provides significant lateral restraint to limit inter-story drifts without yielding of braces, column shear failure would not be prevented and collapse of the structure would most likely occur. Indeed, such was the behavior of configurations C1 and C2. Both bracing configurations failed to prevent column shear failure for all the records considered in the present study. Furthermore, following the generalized shear failure of the columns, schemes C1 and C2 were unable to limit lateral drifts, with maximum inter-story drifts that exceeded 4%, and failed to protect the structure from collapse.

Unlike schemes C1 and C2, first story columns do not fail in shear with scheme C3 when braces are initially prestressed to 75% of the brace yield strength. Notice that the distribution and size of braces with scheme C2 is the same as those of scheme C3 (see Table 6.11). However, the latter configuration provides a more uniform distribution of forces within the existing members, which eliminates the shear failure of columns upon prestressing of braces. Induced forces are still quite high with configuration C3; in first story columns (column lines 12 and 21) bending moments approach 70% of splice capacity at the base

and shear forces reach 75% of the shear strength. As above, the level of induced forces will likely cause extensive cracking in first story columns and jeopardize the integrity of the structure. It is clear that because of the level of induced forces, the size of braces is cannot be increased further.

Alternatively, the latter elements could be strengthened with a steel or reinforced concrete jacketing to reduce the relative force/strength ratio induced in the members prior to initial prestressing. However, such alternative seems unfeasible unless the post-tensioned bracing system shows significant improvements in the response of the building to warrant the strengthening of the elements. Thus, to examine the adequacy of the post-tensioned bracing system for the present structure, the behavior of only scheme C3 is presented in detail in the following sections.

6.4.2.1 Lateral Stiffness and Strength

In Fig. 6.56, the relationships for the base shear coefficient and the drift at the centroid of inertia forces for the existing and the braced building with scheme C3 are compared. In this figure, the relationships have been obtained using a uniform lateral load distribution over the height of the building. As can be seen, the increase in the initial stiffness provided by scheme C3 is moderate. Because of the high initial shear forces induced in first story columns upon initial brace prestressing, column shear failure begins at a smaller lateral load and drift than those observed for the original structure. At a drift of about 0.075%, there is an abrupt increase in lateral drift with almost no increase in lateral load. The reason for this behavior is that several columns fail in shear almost simultaneously at that drift level. Thus, according to the model used for member shear failure (see Chapter III), the forces carried by the failing elements are suddenly transferred to the remaining, more flexible, structure, almost as a shock loading.

Yielding of braces begins at a drift of about 0.18%. At this load level, almost 60% of the columns have already failed in shear. The remaining lateral stiffness and strength is thus dominated by the post-tensioned bracing system. Further increase in lateral load causes the shear failure of the remaining columns of the structure and the yielding of many braces. In Fig. 6.56, the lateral load and drift relationship for scheme C3 is terminated at a drift at the centroid of inertia forces of about 0.72%, which corresponds to a lateral drift of
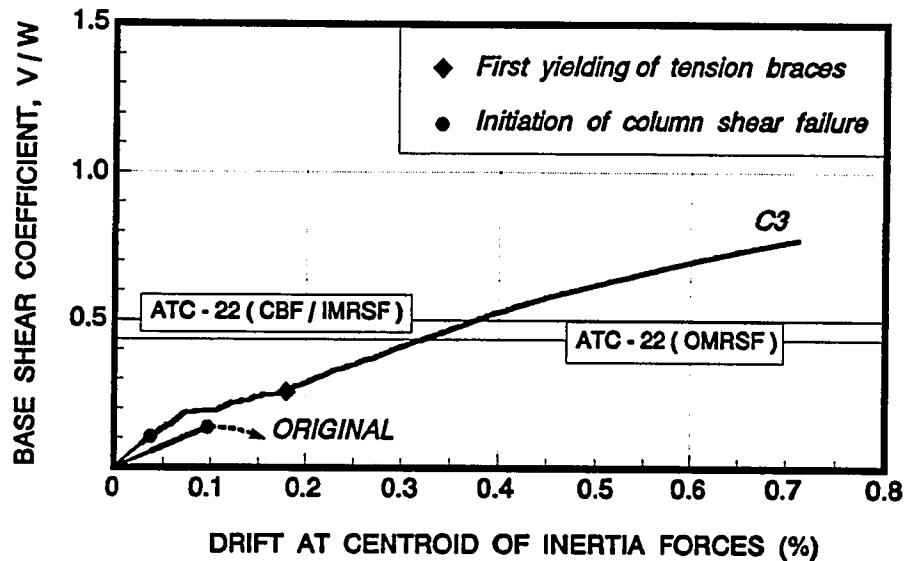
Figure 6.56 Base shear coefficient and drift at centroid of inertia forces relationship for the seven-story building. Original and braced structure with post-tensioned steel rods (scheme C3).

1% in the first story. At that drift level, more than 95% of the columns have failed in shear and braces have yielded in the first four stories of the building. In addition, braces which shorten have begun to sag in the first story. Even though the frame could carry further lateral loading through the resistance of the braces that remain elastic, the damage induced in the existing building is extensive and such behavior is considered terminal.

The results presented above suggest that the post-tensioned bracing may be detrimental rather than beneficial for the behavior of the building. With the addition of the post-tensioned bracing system, column shear failure is expedited rather than delayed. However, lateral strength at first yielding of braces is almost twice as that of the original structure. Since lateral drifts at first yielding of braces are small (less than 0.2%), it is reasonable to assume that columns would be able to maintain their axial load carrying capacity at such drift. Clearly, lateral resistance of the building would rely almost exclusively on the post-tensioned bracing system at that stage.

As indicated earlier, some columns could be strengthened prior to initial prestressing of braces to avoid an early column shear failure, provided that the bracing system were able to restrain lateral drifts. Based on the results obtained from the lateral load analyses discussed above, the drift at first yielding of braces is a reasonable drift limit criterion for the braced structure (at this load stage inter-story drifts are of the same magnitude as that of the drift at centroid of inertia forces). Thus, the post-tensioned bracing system would be considered a viable retrofit scheme only if lateral drifts obtained for the selected ground motions are limited to that corresponding to first yielding of braces. Notice that under this criterion, column shear in not prevented and is expected to occur in many columns. Also, the behavior of braces within the 0.2% drift is expected to be in the elastic range.

Also shown in Fig. 6.56 are the base shear coefficients required by ATC-22 for an OMRSF and for a dual system consisting of a CBF with an IMRSF capable of resisting 25% of the lateral loads. Brittle elements were assumed in estimating the coefficients shown in the figure. As discussed in previous sections, response modification factors embodied in the recommendations of ATC-22 for braced frames are intended for concentric bracing systems with structural steel sections, which are not considered appropriate for the evaluation of post-tensioned bracing systems. Also, the building under study does not correspond to an IMRSF, but rather to an OMRSF (ATC-22 does not include provisions for a CBF and an OMRSF). However, it is reasonable to assume that the required lateral resistance for a CBF with an IMRSF is a lower bound for the strength required for an OMRSF with a post-tensioned bracing system. Based on these premises, ultimate strength of the braced structure as defined above (resistance at first yielding of braces) is well below the lower bound implied by ATC-22, which would suggest that the resistance provided by the bracing system will be inadequate to resist the earthquake forces. Implications of the latter result will be discussed in Chapter VII.

6.4.2.2 Dynamic Response Analysis

Dynamic Properties

Table 6.13 shows the fundamental periods of vibration and the effective damping ratios for the original and braced structure corresponding to the different types of soil sites selected for study. For the braced building (scheme C3) on firm soils, the reductions in the

fundamental period of the building are significant. Note that the lengthening in the period of the braced building on soft soils is only minimal ($\tilde{T}/T_{max}$ = 1.03 for the clays of Mexico City), and consequently effective damping ratios of the system are similar to those of the building on firm soils.

For the buildings located on soft soil sites, the reductions in the fundamental period will probably result in lower strength and displacement demands, as suggested by the response spectra shown in Figs. 4.27 and 4.29. For the buildings located on firm soil sites, however, strength demands could increase; decrease or remain the same depending on the earthquake record considered (see Fig. 4.26). On the other hand, displacement demands are expected to be reduced in all cases (Fig. 4.28).

Table 6.13 Dynamic properties of the original and braced building with post-tensioned steel rods. (Seven-Story Building)

Building	Fundamental Period (sec) [Effective Damping]*		
		Soil Type	
	Firm	Soft	
		Silty Clay Deposits (Mexico City)	San Francisco Bay Mud (California)
			Case II
Original	0.62 [2.0 %]	0.71 [5.3 %]	0.69 [6.0 %]
Config. C3	0.44 [2.0 %]	0.46 [2.1 %]	0.45 [2.1 %]

* values are based on a h^*/r ratio of 0.60 in accordance with the dimensions of the foundation.

Dynamic Response

Maximum inter-story drift ratios for the braced building with scheme C3 obtained for the ground motions on firm and soft soil sites are presented in Figs. 6.57 and 6.58, respectively. The results presented for the building located on soft soils take due account
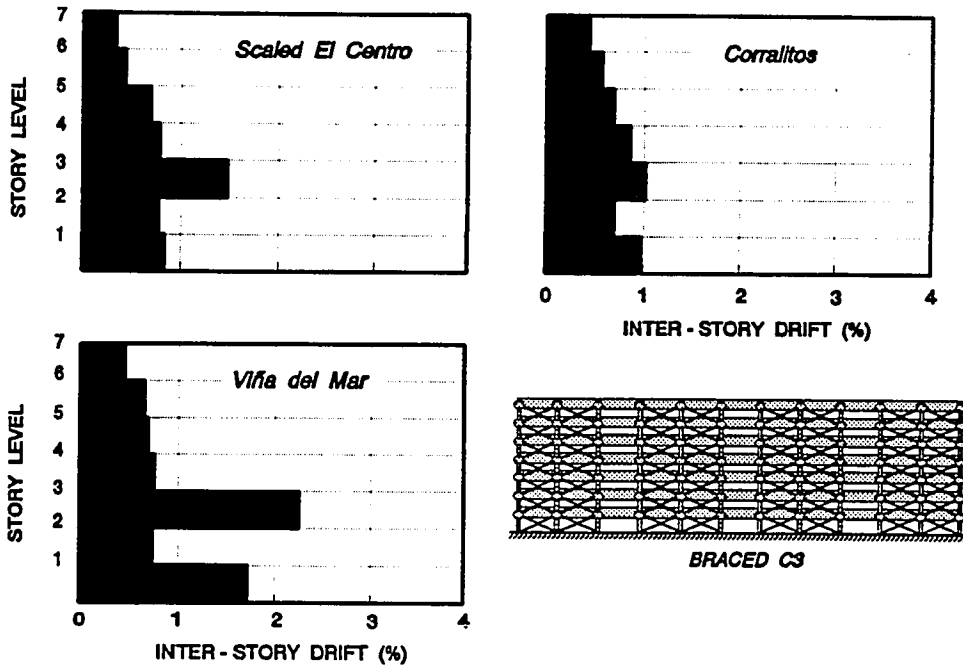
Figure 6.57 Maximum inter-story drift ratios for the braced building (scheme C3) subjected to the records measured on firm soil sites.
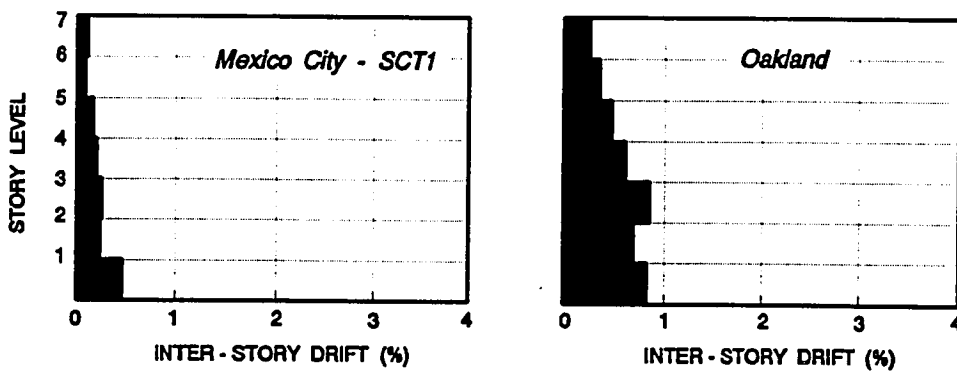
Figure 6.58 Maximum inter-story drift ratios for the braced building (scheme C3) subjected to the records measured on soft soil sites.

of the rocking motion of the foundation and correspond to the actual inter-story drifts for the building. In any case, rocking of the foundation was negligible in all cases studied.

Overall, inter-story drifts were significantly reduced with respect to those obtained for the original non-braced building. For the records on firm soils (Fig. 6.57), maximum inter-story drifts exceed the drift limit criterion established earlier for scheme C3 (Δ < 0.2%). The largest demands are imposed by the Viña del Mar record, with drifts in the first and third story in the order of 2%, which would likely cause the building to collapse.

For the records on soft soils, the response of the building is better than that observed for the records on firm soils, probably because of the reduced strength demands of the former records. Maximum inter-story drifts remain below 1% in all stories for both records. For the Oakland record however, drifts exceed the drift limit of 0.2% in most stories, and therefore a high level of damage is expected. On the other hand, for the Mexico City - SCT1 record, inter-story drifts remain in the order of 0.2%, except in the first story where lateral drift reach about 0.45%.

Performance of Post-tensioned Bracing System

The results presented above indicate that while the bracing system was able to reduce the response of the building, lateral drifts of the braced structure exceeded the drift limit criterion established for the building. The performance obtained for the Mexico City - SCT1 record is, perhaps, the only case in which the use of the post-tensioned bracing system is justified for the structure under study. Following is a general evaluation of the performance of the reinforced concrete elements and braces for the cases studied.

a) Performance of Reinforced Concrete Members

Column shear failure is observed in many columns for all the records considered in this study. For the three records on firm soil sites and for the Oakland record, column shear failure occurred in all columns. For the Mexico City - SCT1 record, column shear failure is observed in 77% of the columns, and is primarily concentrated in the lower stories of the building.

Because column shear failure develops in many columns and at rather small inter-story drifts (low level of lateral forces), beam hinging or column hinging is almost non-existent in the structure. Beams hinging is not observed in any of the cases studied, and column hinging occurs only at the base of exterior columns.

Axial forces in columns are quite high in general and exceed the axial compression and tension capacity of many columns in the structure for most of the records considered. An extreme case corresponds to the Viña del Mar record, where the axial compressive forces in the exterior columns of the first story exceed the compression capacity by a factor of about 2. Tensile forces are even more critical, maximum forces are about 5 times larger than the anticipated tension capacity. On the other hand, axial forces obtained for the Mexico City - SCT1 record remain within the axial capacity of columns. Maximum compressive forces in exterior columns remain high and reach about 76% of the compression capacity in the first floor, and in interior columns compressive forces reach 48% of the capacity in compression. Axial tension in columns is not developed during the response to the Mexico City - SCT1 record.

In beams, axial forces are smaller in magnitude than those developed in columns, and because of the relatively large cross section of the spandrels, maximum axial compressive forces represent only 48% of the capacity in pure compression, even for the largest demands (Viña del Mar record). Tensile forces develop in only a few spandrels and in some cases exceed the capacity in pure tension, even for the smallest demands (Mexico City - SCT1 record). The latter result suggests that steel collector elements will be required to augment the tensile capacity of columns and spandrels.

b) Performance of Steel Rod Braces

The behavior of braces is largely inadequate for the records on firm soil sites and for the Oakland record. For the Viña del Mar record (largest demands), braces yield extensively in all but in the top story of the building. Plastic deformations in the braces of the first and third story exceed the maximum allowable. Therefore, braces lose the prestress force completely. Also, a large number of braces become slack during the response to the event. Overall, braces are expected to suffer extensive damage and most likely would not safeguard the building against collapse when subjected to the records indicated above.

Braced C3 - Mexico City - SCT1

o : braces reached yielding, but never became slack
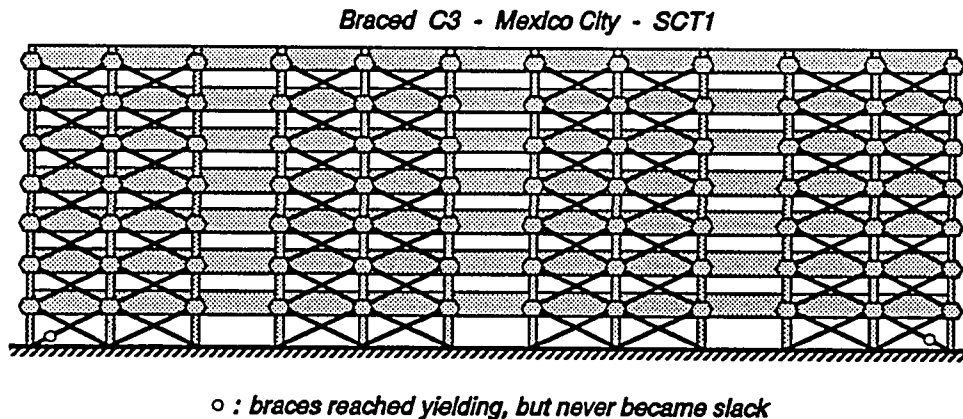
Figure 6.59 Distribution of inelastic response of braces with scheme C3 for the Mexico City - SCT1 record.

For the Mexico City - SCT1 record, the performance of braces is satisfactory. In Fig 6.59, the distribution of inelastic behavior in the braces with scheme C3 during the Mexico City - SCT1 record is presented. As can be seen, except for two braces in the first story, braces remain within the elastic range during the response to the earthquake record. In addition, braces that reach yielding during the response show minimal plastic elongations, with residual prestress forces that are 72% of the brace yield strength or higher. Based on the adequate performance of braces and the small lateral drifts, bracing scheme C3 represents a feasible retrofit alternative for the building for Mexico City. The latter case is the only case where the use of the post-tensioned bracing system is warranted.

6.4.2.3 Summary

Several post-tensioned bracing configurations with different size of braces were studied as possible retrofit schemes for the seven-story building. Because of the large number of braced bays required to stiffen and to strengthen the building, bending moments and shear forces induced in columns of the first story upon initial brace prestressing were quite high. Depending on the bracing configuration and on the level of initial prestress (typically 50% of the brace yield strength or higher), induced forces reached 70% or a higher percentage of the capacity of the member. In some cases, induced forces were so high that

column shear failure would be reached upon initial prestressing of braces. By selecting an appropriate configuration for the bracing system, it was possible to reduce the level of induced forces in existing elements. However, the level of forces was still quite high and significant cracking of columns could be generated. The latter result may be detrimental from a serviceability standpoint.

From the configurations studied, only one configuration, C3, was considered to be a feasible retrofit scheme. The level of induced forces was still quite high with this scheme, but it allowed the use of an initial prestress level of 75% of the brace yield strength. Because of the high level of forces induced in existing elements, static lateral load analyses indicated that column shear failure in the braced frame would begin at smaller load and drift levels than those expected for the original non-braced structure. Despite the early failure of columns, first yielding of braces began at load and drift levels larger than those corresponding to the ultimate strength for the bare frame. Thus, the use of scheme C3 was considered as a feasible alternative provided that lateral drift obtained for the selected ground motions did not exceed the drift at first yielding of braces.

The results from dynamic analyses indicated that the post-tensioned bracing scheme was unable to meet the drift limit criterion established for all the records on firm soil sites and for the Oakland record on soft soils. Column shear failure was observed in most of the columns in the structure and many braces yielded and lost prestress completely. Significant damage was expected for the existing members and the braces. The performance of the bracing system was inadequate and in most cases failed to protect the building from collapse.

On the other hand, the performance of bracing scheme C3 for the Mexico City - SCT1 record was satisfactory. Even though a large number of columns were expected to fail in shear, maximum inter-story drifts met, in general, the drift limit criterion established for the system. Furthermore, apart from two braces in the first story, braces remained elastic during the entire response to the earthquake. However, as discussed earlier, because of the large forces induced upon brace prestressing, the bracing system would not prevent the shear failure of most columns. To improve the performance level of the retrofit structure, columns can be encased with steel jackets that will enhance the shear capacity and the deformation capabilities of the members. Also, steel collector members are required to

enhance the compression capacity of exterior columns and the tensile capacity of a few spandrel beams. Tensile forces were not anticipated in columns.

6.4.3 Retrofit Scheme II - X-Bracing (Structural Steel Braces)

Two bracing schemes were selected for evaluating the response of structural steel braces, namely TS1 and TS2 as shown in Fig. 6.60. The configuration of both schemes (TS1 and TS2) consisted of two story high X-bracing over eight bays of the perimeter frames, except at the top story where diagonal bracing was provided. The two story X-bracing configuration was adopted after a similar retrofit design that was tested[51] and used as a retrofit scheme for an existing building[52]. Such bracing configuration avoids the problems associated with *chevron* bracing (or inverted V-bracing) and limits the unbraced lengths of the braces. It should be noticed that in the X-bracing scheme tested previously[51] and used for the retrofit of an existing building, braces were connected at the beam-column joint and at mid-span of spandrels with fixed-end connections. While the latter connection type would allow the use of a lower K factor and thus larger buckling load for the first cycle, it has been observed that buckling of the brace may cause local connection failure. The latter failure can be caused by excessive rotation at the brace ends and/or by substandard welds[51], which under load reversals will prevent the brace to reach the anticipated load capacity in compression and most important in tension. In the present study, braces were assumed to be connected with pinned-end connections, which avoid the problems associated with fixed-end connections mentioned above and provide a lower bound to the performance of the bracing system.

Braces consisted of tubular sections, and were, in general, selected to meet the slenderness requirements for seismic zones ($KL/r < 720/\sqrt{f_y}$) of the Load and Resistance Factor Design manual (LRFD)[45]. Also, tube sections followed the specifications for the flat width to thickness ratio of the LRFD manual (b/t$_w$ ≤ 110 / $\sqrt{f_y}$). Brace size and distribution of braces for both bracing schemes are presented in Table 6.14. Bracing scheme TS1 corresponds to the smallest brace size that would meet the requirements for slenderness and for flat width to thickness ratios of the LRFD. At the top story, however, braces would not meet the slenderness requirements mentioned above, but this is unimportant because braces are not expected to yield or to buckle in that story.

TS1 & TS2
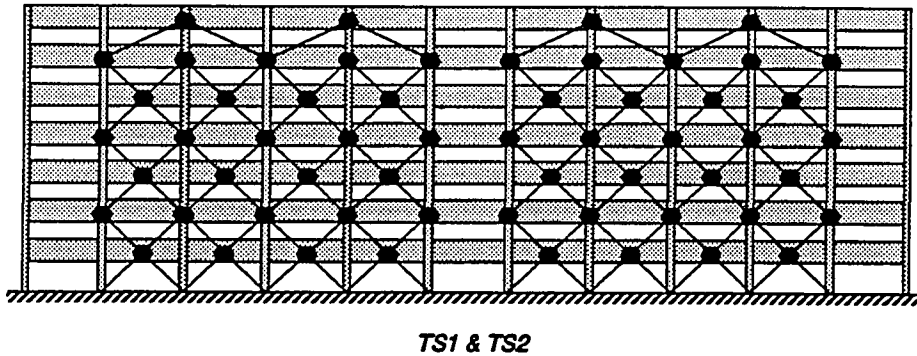
Figure 6.60 Bracing configuration pattern for the seven-story building with structural steel braces. (perimeter frames only)

Table 6.14 Size and distribution of braces for schemes TS1 and TS2. (Seven-story building)

Story Level	Brace Size [Area (in^2)]	
	TS1	TS2
All Stories	TS 5 x 5 x 1/4 [4.59]	TS 10 x 10 x 1/2 [18.40]

Bracing scheme TS2 was designed to meet the demands imposed by the ground motion selected for study, and has a much higher level of stiffness and strength. In both bracing configurations, brace size was selected to provide a uniform distribution of lateral stiffness and strength throughout the height of the building. The resulting slenderness ratios of braces varied from 91 for scheme TS1 to 45 for scheme TS2. Effective length of braces was considered equal to the unbraced length (K=1), a value that is consistent with the pinned-end connections assumed for the braces. Yield strength of tubular sections was 46 ksi in all cases.

6.4.3.1 Lateral Stiffness and Strength

In Fig. 6.61, the relationships for the base shear coefficient and drift at the centroid of inertia forces for the original building and the braced structures are compared. Also shown in this figure is the relationship for the post-tensioned bracing system obtained with scheme C3 with braces initially prestressed to 75% of the yield strength. The relationships shown were obtained using a uniform lateral load distribution over the height of the building.

Configuration TS1, which has the smallest brace allowed by the specifications of LRFD, has approximately the same initial stiffness as that of configuration C3. The similar initial stiffness of these two bracing schemes provide a basis of comparison for the two bracing systems without including the changes in the dynamic response due to different periods of vibration of the buildings. Because of the lower yield strength of the tubular

+ *First buckling of braces in schemes TS1 & TS2*

◆ *First yielding of tension braces*

● *Initiation of column shear failure*
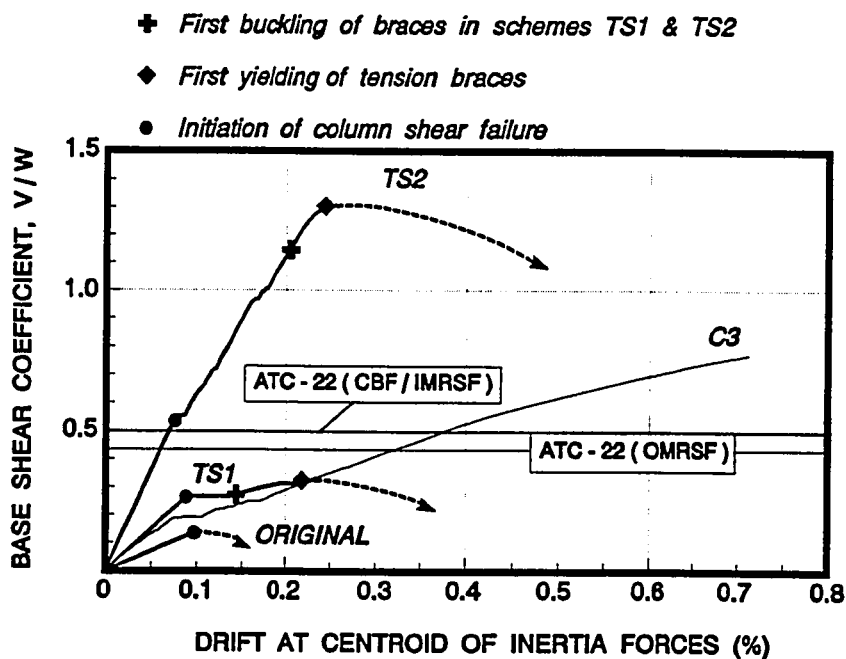
Figure 6.61   Base shear coefficient and drift at centroid of inertia force relationship for the seven-story building. Original and braced structure with configurations TS1, TS2, and C3.

sections, ultimate strength of bracing configuration TS1 is smaller than that of configuration C3. Bracing configuration TS2 has both higher initial stiffness and ultimate strength than configuration C3.

With bracing scheme TS1, shear failure of columns begins a load level that is almost twice of that carried by the original bare frame. Lateral drift at the initiation of column shear failure is similar for the braced (TS1) and original frame. Following the failure of columns in shear, there is an abrupt increase in lateral drift in the braced building. The reason for such behavior is that several columns fail in shear almost simultaneously at about the same drift level. Consequently, according to the model used for shear behavior (Chapter III), the forces carried by the failing elements are suddenly transferred to the rest of the structure and cause a large increase in the lateral displacement with no appreciably increase in lateral load. Due to this sudden redistribution of forces, braces in compression begin to buckle immediately after the onset of shear failure of columns in shear, as shown in Fig. 6.61. Further increase in lateral load results in the failure in shear of the remaining columns and in the buckling of the rest of the braces in compression which produce a continuous and gradual reduction in the lateral stiffness of the braced structure. Yielding of braces begins at a drift level of about 0.2% and occurs almost simultaneously in many braces. Soon after this event the building reaches its peak strength. Notice the similitude in the lateral load relationship of bracing schemes TS1 and C3 up to the 0.2% drift level.

With bracing configuration TS2, the increase in lateral stiffness with respect to that of the original building is substantial. Column shear failure begins at much higher load than that carried by the bare frame (about 5 times greater) but a similar lateral drift, in accordance with the higher initial stiffness of the building. Unlike the behavior observed for schemes TS1 or C3, the shear failure of columns has only a minimal impact on the lateral drift of the building, as shown in Fig. 6.61. The reason is that the bracing system carries most of the lateral load applied to the structure and the shear forces carried by the existing columns represent only a small fraction of the total lateral load. Thus, failure of the columns in shear requires relatively small force redistributions which result in minor increases in lateral displacements. Buckling of braces begins at a drift level of about 0.2%. Similar to the results obtained for scheme TS1, the sequential buckling of braces results in a gradual

reduction of the lateral stiffness of the building. Finally, at a drift of about 0.24% tension braces begin to yield and soon thereafter the building reaches its peak lateral load capacity.

Because of the low shear capacity and relatively high stiffness of the columns (short column), yielding of braces begins only after the shear failure of most of the columns in the building with both bracing schemes (TS1 and TS2). Such behavior is undesired because braces cannot dissipate energy prior to failure of the columns in shear. As result, significant damage of columns can be expected unless the bracing system is able to limit lateral deformations below the lateral drift associated to column shear failure.

Also shown in Fig. 6.61 are the base shear coefficients required by the ATC-22 for an OMRSF and for a dual system consisting of a CBF with and IMRSF capable of resisting 25% of the lateral loads. The coefficients shown were obtained assuming brittle elements (columns susceptible to shear failure) in the structure. As indicated earlier, the building under study does not meet the classification of an IMRSF, but rather that of an OMRSF (ATC-22 does include provisions for a CBF with an OMRSF). However, the required lateral strength for a concentrically braced frame with an IMRSF represents a lower bound for a building with CBF and an OMRSF.

Assuming that the lateral resistance of the braced building is given by the buckling capacity of the braces (as assumed in the design process of CBF systems), it is can be seen that strength provided by bracing scheme TS1 is well below than that required by ATC-22. On the other hand, the lateral resistance of scheme TS2 exceeds that required by the ATC-22. However, that the load level corresponding to the onset of shear failure in columns is about the same as that required by ATC-22. A discussion of these results is presented in Chapter VII.

6.4.3.2 Dynamic Response Analysis

Dynamic Properties

The fundamental periods of vibration and effective damping ratios for the original and the building with X-bracing are shown in Table 6.15. The reductions in the period of vibration of the braced structure are substantial, particularly for configuration TS2 which has the heaviest braces. In general, period lengthening ratios for the braced buildings are

Table 6.15 Dynamic properties of the original and buildings with X-bracing.

Building	Fundamental Period (sec) [Effective Damping]*		
	Soil Type		
	Firm	Soft	
		Silty Clay Deposits (Mexico City)	San Francisco Bay Mud (California) Case II
Original	0.62 [2.0 %]	0.71 [5.3 %]	0.69 [6.0 %]
Scheme TS1	0.43 [2.0 %]	0.44 [2.8 %]	0.44 [2.9 %]
Scheme TS2	0.28 [2.0 %]	0.30 [3.6 %]	0.29 [3.7 %]

* values are based on a h^*/r ratio of 0.60 in accordance with the dimensions of the foundation

relatively small and therefore effective damping ratios are not significantly higher than those adopted for the structures on a fixed-base. For bracing scheme TS2, effective damping ratios are somewhat larger mainly because of a relatively higher period lengthening ratio ($\tilde{T}/T \approx 1.07$ for the clay deposits of Mexico City).

For the buildings located on firm soils, the reductions in the period of vibration do not permit to anticipate substantial changes in the demands of strength for the braced building. Strength demands could increase, decrease or remain the same depending on the earthquake record considered (see Fig. 4.26). For the buildings located on soft soils, however, the reductions in the periods of vibration of the braced buildings clearly indicate reductions in strength demands, which would be substantial for the Oakland record (see Fig. 4.27).

Dynamic Response

Maximum inter-story drifts for the braced building with the two bracing schemes TS1 and TS2 obtained for the records measured on firm soil sites are presented in Fig. 6.62. As can be seen, bracing scheme TS1 is unable to limit lateral drift and collapse of the building is anticipated for the three records studied. In all cases, collapse of the structure is predicted by large lateral displacements at the second story level which led to instability of the building. Notice that even though the lateral load relationships for bracing schemes TS1 and C3 were similar up to yielding of braces (see previous section), the post-tensioned bracing system was more effective to limit inter-story drifts than scheme TS1 (see Figs. 6.57 and 6.61). The better performance of scheme C3 is probably due to the fact braces which shorten begin to sag after yielding of braces which provides scheme C3 with a higher
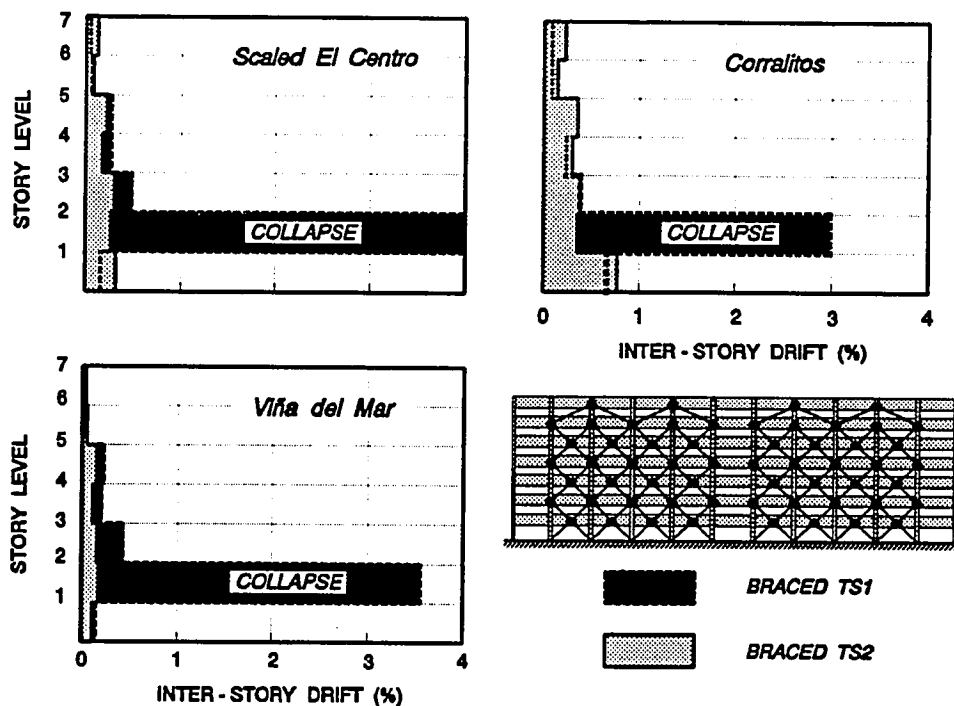
Figure 6.62   Maximum inter-story drift ratios for the braced building (schemes TS1 and TS2) subjected to the records measured on firm soil sites.

stiffness beyond yielding of braces (see Fig. 6.57). Lateral stiffness after yielding of braces with scheme TS1 is negligible as suggested in Fig. 6.61.

Bracing scheme TS2, on the other hand, limits inter-story drifts to less than 1% in all three cases. For the scaled El Centro and Viña del Mar records, inter-story drifts are less than 0.4% in all stories. Although, lateral drifts are controlled with scheme TS2, columns shear failure is not prevented.

In Fig. 6.63, maximum inter-story drifts for the bracing schemes subjected to records on soft soils are presented. For the Oakland record, bracing scheme TS1 is unable to limit inter-story drifts and collapse of the structure is anticipated. The mode of failure of the structure is similar to that described above for the records on firm soils. As above the performance of bracing scheme C3 during the Oakland record (Fig. 6.58) is better than that of scheme TS1. For the Mexico City - SCT1 record, inter-story drifts with scheme TS1 are minimal. The response of the structure with configuration TS2 is minimal for both records on soft soils. Column shear failure is observed in only a few columns and only for the Oakland record. Braces remain elastic during both earthquake records.
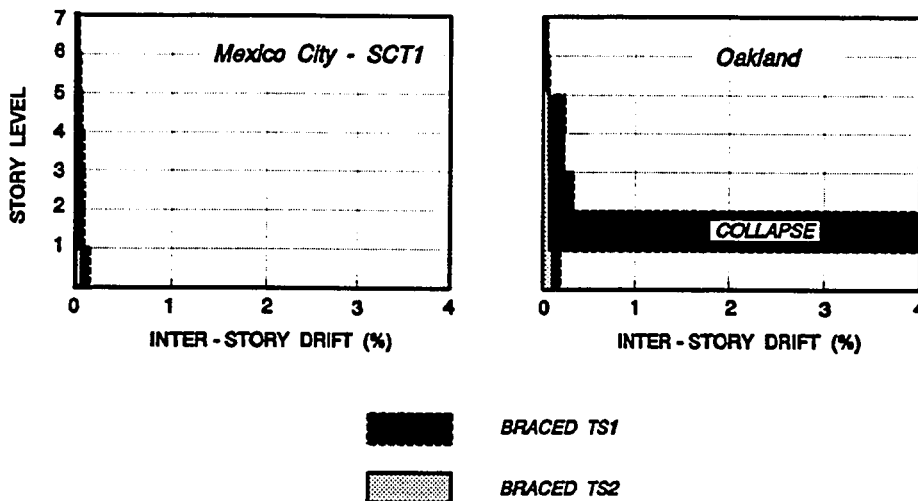
Figure 6.63   Maximum inter-story drift ratios for the braced building (schemes TS1 and TS2) subjected to the records measured on soft soil sites.

Performance of X-Bracing System

The preceding results show that X-bracing can be designed to reduce the response and control lateral drift of the building under study for the records on both firm and soil sites. Similar to the results obtained for the three-story building, the X-bracing system is more effective for structures on soft soil conditions than for those supported on firm soils. Overall, bracing scheme TS2 which has stiffer and stronger braces, exhibited better behavior than scheme TS1.

Following is an evaluation of the performance of the X-bracing system as a retrofit strategy for the building under study. Examination of maximum inter-story drifts reveals that bracing scheme TS2 is the most effective to limit lateral drift of the building on both firm and soft soil conditions. At the same time, from all the records considered for study, the Corralitos record imposes the largest demands of strength and ductility on the bracing scheme TS2. For this reason the results obtained for the latter record will be used as a basis for evaluating the performance of the reinforced concrete members and the braces.

a) Performance of Reinforced Concrete Members

Fig. 6.64, shows the degree of damage that can be expected for the building with scheme TS2 under the Corralitos records. In this figure, columns that are expected to fail in shear during the record are presented. Also shown are the plastic hinges developed in beams and columns. As can be seen, columns shear failure is not prevented and is spread over most of the columns in the building. Plastic hinges are developed only at the base of exterior columns in the first floor. Beams behave essentially in the elastic range; no hinges developed in these members. Because of the generalized failure of columns, the lateral stiffness and resistance of the frame is provided almost exclusively by the braces. While significant damage is expected in columns, lateral drifts under the Corralitos record are controlled by the bracing system. For the rest of the records on firm soil, scaled El Centro and Viña del Mar records, and for the Oakland record on soft soil, column shear failure is not prevented, but the number of columns failing in shear is reduced. For the Mexico City - SCT1 record, column shear failure is prevented with scheme TS2.

The axial force distribution in columns with configuration TS2 subjected to the Corralitos record is presented in Fig. 6.65. In this figure, the maximum axial force developed

— *Member shear failure*

○ *Hinge in only one direction of bending*
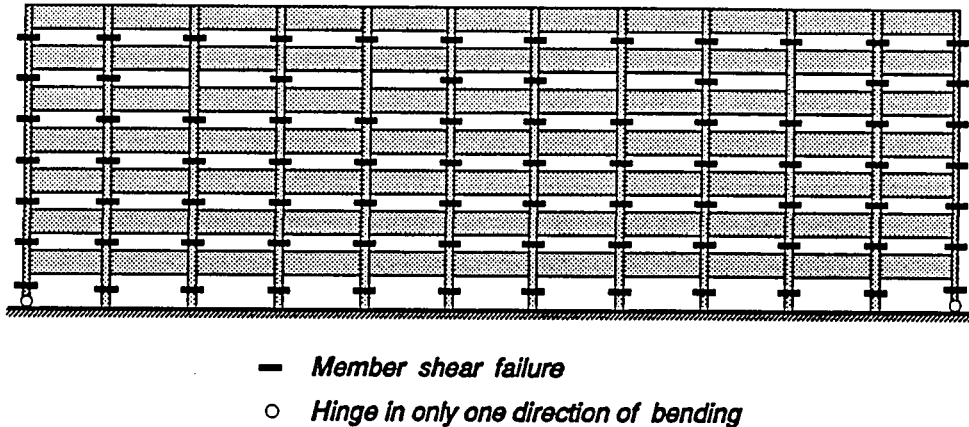
Figure 6.64 Hinge location and member shear failure for the perimeter frames of the braced building with configuration TS2 when subjected to the Corralitos record.

In the members is shown as a fraction of the corresponding capacity in pure compression or tension. As expected, maximum axial forces developed in columns that share a braced and an unbraced bay (column lines 12, 16, 17 and 21). The magnitude of the tension forces developed in columns of lower stories is substantial and exceed the capacity in pure tension in many instances. At the fourth story level there is an abrupt increase in the magnitude of the axial force ratio in columns, mainly because the amount of longitudinal reinforcement is reduced at that level. Such reduction in the amount of reinforcement followed the design of columns of the original bare frame, in which axial tension forces were not anticipated. Compressive axial forces are also quite high along the column lines indicated above, and exceed the maximum capacity in pure compression of several members.

The magnitude of axial forces in beams are, in general, much smaller than those induced in columns. Because of the relatively large cross section of spandrels, compression forces remained well below the compression capacity of these members. However, tension forces developed in spandrels of both braced and unbraced bays. Using the minimum amount of longitudinal reinforcement in the spandrels (typically at mid span) and neglecting any contribution of slab reinforcement, it was estimated that tensile forces would reach the capacity in pure tension for some spandrels in the lower stories.
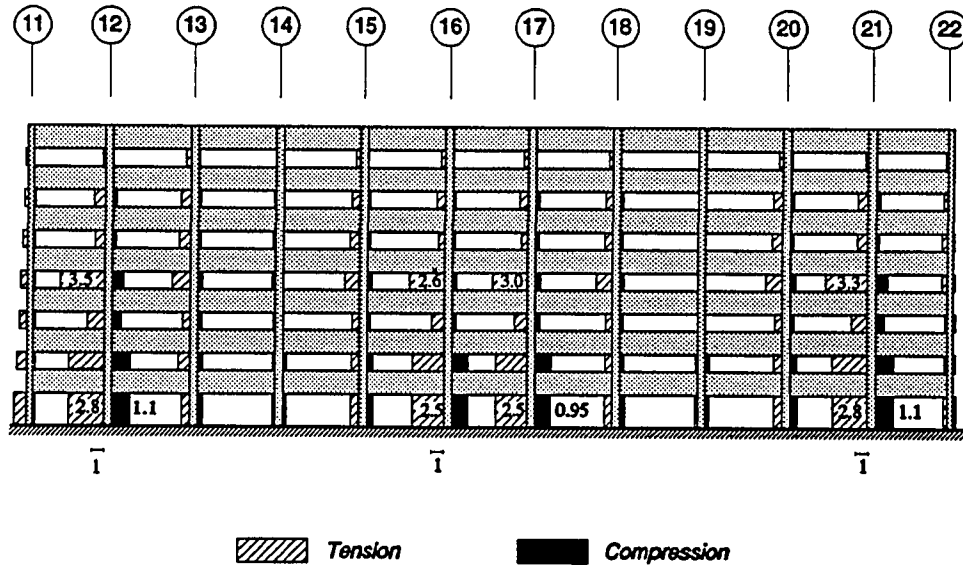
Figure 6.65   Axial force distribution in columns of perimeter frames of braced building with scheme TS2 for the Corralitos record. (Axial force is shown as a fraction of the capacity of the member in pure compression or tension)

Based on the results presented above, the need for collector elements to augment the tensile and compression capacity of columns is apparent and essential for the success of the X-bracing system. Also, to reduce the level of damage and to improve the shear and deformation capacity, columns could be encased with jacketing along the height of the building.

b) Performance of Braces

Inelastic behavior of braces with configurations TS2 for the Corralitos record are presented in Fig. 6.66. Brace yielding and/or buckling is confined to the braces of the lower three stories; braces in the upper stories remained within the elastic range. In the third story, braces only reach buckling and they never reach yielding. In the first story, braces yield and buckle with extensive inelastic excursions in both tension and compression. The latter behavior is shown in Fig. 6.66, for one of the most stressed braces in the first story. The brace buckles several times during the response of the structure and reaches the
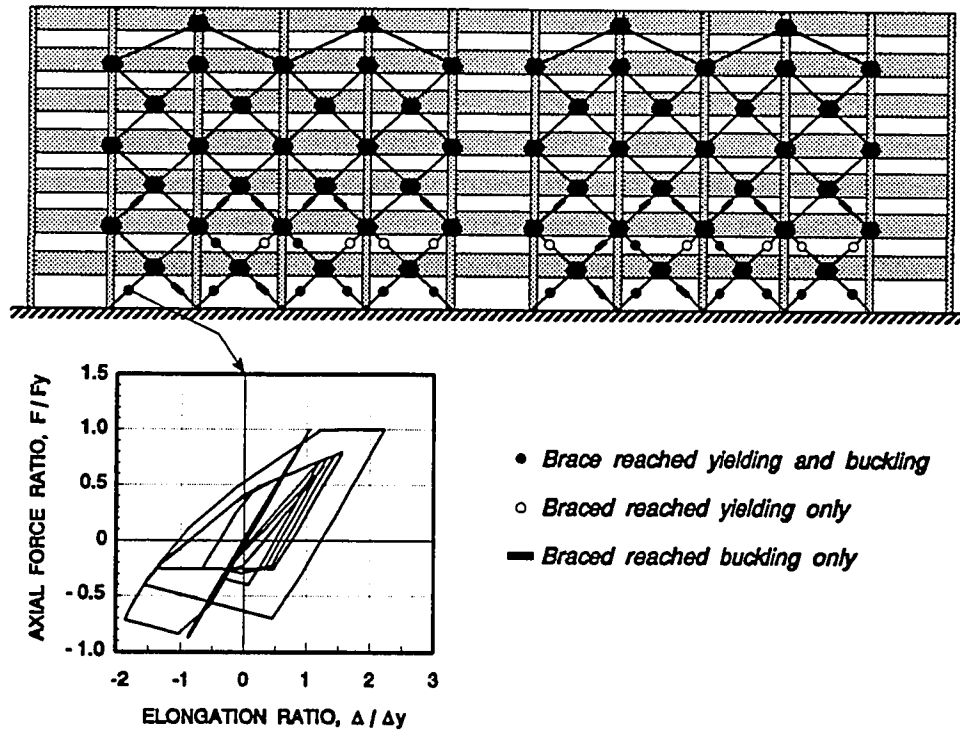
Figure 6.66 Yielding and buckling of braces, and typical hysteretic behavior of first story braces with scheme TS2 when subjected to the Corralitos record.

residual buckling load (P_r). Because the flat width to thickness ratio of braces was selected to meet the LRFD recommendations for seismic behavior, fracture of the tube section due to repeated load reversals is not anticipated. Note that because of the low slenderness ratio of the brace ($KL/r \approx 45$), the brace has a buckling load capacity (first cycle) of about 80% of the yield load in tension and displays good energy absorption capacity. Nonetheless, first story braces will experience a high level of damage after the earthquake.

Since the behavior of braces in the fourth and upper stories remained within the elastic range, it would appear that smaller sections could be used in these stories in order to obtain a more economical and efficient design. However, the use of smaller sections will also reduce the lateral stiffness of the story and will most likely increase lateral drifts and produce damage of braces. Thus, while the use of a smaller section could lead to a more

economical design, a larger lateral deformation and a higher degree of damage could be expected.

6.4.3.3 Summary

The use of X-bracing as a retrofit strategy was studied by examining two possible schemes which had the same bracing configuration but different size of braces, namely TS1, and TS2. Bracing scheme TS1 was designed for the smallest size of braces that would meet the requirements for concentric bracing of the LRFD seismic provisions, and had a similar initial stiffness to that of configuration C3 with post-tensioned rods.

For the records on both firm and soft soils, scheme TS1 was unable to prevent collapse of the building, except for the Mexico City - SCT1 record where the response of the building was minimal with small inter-story drifts (less than 0.2%). A comparison of retrofit schemes TS1 with C3, revealed that the post-tensioned braces were more effective in controlling lateral drifts than scheme TS1.

Bracing scheme TS2 provided an adequate safety level against collapse for the records on firm and soft soils. However, the bracing system was unable to prevent column shear failure, mainly because of the low shear capacity of the short stiff columns of the existing frame. Expected damage in columns is substantial despite the fact that the bracing system was able to control lateral drift to less than 1%. Also, retrofit scheme TS2 will require collector members in columns and beams throughout the height of the building to help carry the high axial forces induced by the bracing system. To improve performance level of the retrofit scheme, it is suggested that steel or reinforced concrete jacketing or steel collector elements be provided to improve the shear strength and deformation capabilities of columns.

CHAPTER VII

DISCUSSION OF RESULTS AND DESIGN IMPLICATIONS

7.1 GENERAL

In this chapter, the results obtained from inelastic analyses of the buildings are examined by comparing the strength and ductility capacities with the demands imposed by the earthquake records studied. The capacity of the buildings is estimated from the lateral load and drift relationships derived in previous sections (Chapter IV and VI). Earthquake demands are estimated from equivalent single-degree-of-freedom (SDOF) systems used to represent the behavior of the buildings. In addition, elastic and smoothed inelastic response spectra are used to compare maximum response of the buildings.

Based on these comparisons, simpler procedures for estimating the response of the buildings are suggested. Also, design strategies for the retrofit of reinforced concrete frames are re-evaluated and design recommendations are proposed.

The adequacy of ATC-22 for evaluating the performance of existing buildings and the suitability of the provisions for evaluating retrofit schemes considered in this study are examined.

7.2 DISPLACEMENT DUCTILITY REQUIREMENTS

7.2.1 Equivalent SDOF System

Several researchers [49, 53, 54] have attempted to model the resistance and displacement of multi-story buildings (multi-degree-of-freedom system, MDOF) using an equivalent SDOF system. The development of equivalent SDOF systems often involves several assumptions which are sometimes mathematically inconsistent. Despite these approximations, they can provide a reasonable estimate of the maximum response of multi-story structures and comprise an important tool for understanding the dynamic response of structures. In this study, the equivalent SDOF system follows assumptions that are similar to those used in previous studies [49, 53, 54], but includes some modifications that are explained in the following.

276

The equivalent SDOF system used in the present study consists of a bi-linear, stiffness degrading, fixed-base model, similar to the one used to produce the inelastic displacement ductility spectra presented in section 4.5.3 (Figs. 4.30 and 4.31). To model the inelastic behavior of the multi-story buildings with equivalent SDOF systems, the base shear coefficient and drift relationships obtained for each of the buildings studied were fit to a bi-linear relationship. Initial stiffness of the SDOF system is defined as the tangent at the origin of the base shear coefficient and drift relationship, as shown in Fig. 7.1. Thus, the period of vibration of the equivalent SDOF system is the same as that corresponding to the fundamental period of the building structure.

DRIFT AT CENTROID OF INERTIA FORCES
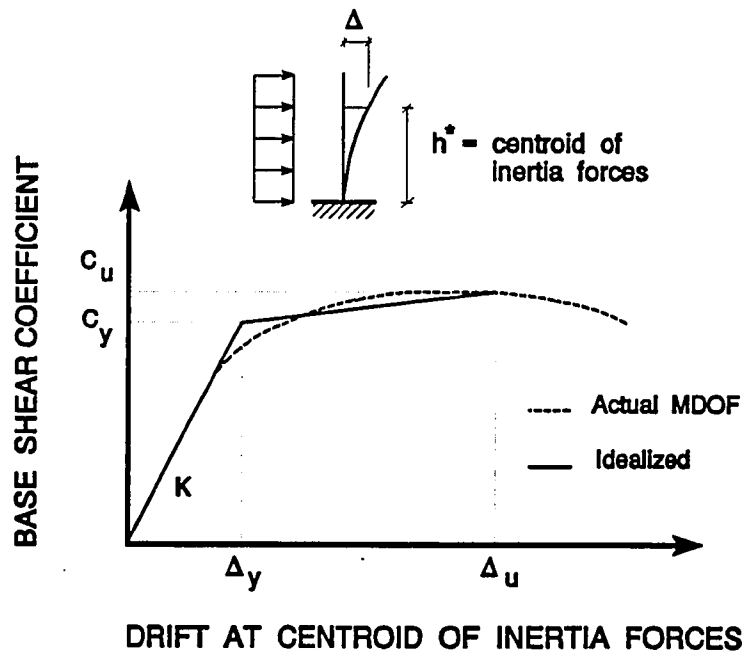
Figure 7.1   Typical idealization of the base shear and drift curve with a bi-linear relationship.

To determine the yield strength in the bi-linear relationship, strain hardening and drift corresponding to the ultimate state need to be defined first. Because the behavior and modes of failure of the buildings considered in this study are substantially different, the

definition of ultimate state is not unique. Such a definition will, in general, depend on the performance criteria established for the structure specified by the designer. Since lateral drift and structural damage are interrelated, the degree of damage can be established in terms of the drift level experienced by the structure. In this study, ultimate state of the buildings is defined by the maximum allowable drift that would not jeopardize the integrity and stability of the building. Both non-structural and structural damage can be allowed under the latter definition, provided that lateral drifts are controlled. Such a criterion is aimed at providing an adequate safety level against collapse, and it is not intended to safeguard existing elements against severe damage.

Once the drift at ultimate state is determined, strain hardening of the bi-linear system is defined by the line that passes through the point of ultimate state with a slope such that the areas under the bi-linear and the calculated base shear coefficient and drift curve are equal. In this manner, the energy absorption capacity at ultimate is maintained. The yield strength of the bi-linear system corresponds then to the point defined by the intersection of the initial stiffness and the strain hardening lines, as shown in Fig. 7.1.

In previous studies, bi-linear relationships were determined using base shear and *roof* drift values. In this study, bi-linear relationships are based on drift at the *centroid of inertia forces* (effective height of the building for motion in its fundamental period of vibration). The *centroid of inertia forces* is believed to represent better the inelastic deformations of the buildings because in most cases inelastic behavior tends to concentrate in the lower stories of the buildings. As a result of "yielding" in the structure, increments in lateral displacement in the lower stories can be significantly larger than those in the upper stories. Therefore, a relationship based on roof drifts is likely to underestimate the deformation capabilities of the structure. On the other hand, a relationship based on the lateral drift of the first story, for instance, would probably overestimate the deformation capacity of the building in the inelastic range.

Once the bi-linear relation is completely defined, the *global ductility capacity*, μ_c, of the buildings is estimated as the ratio between the drift at ultimate and the drift at yield. The ductility capacity, μ_c, will be compared to the requirements for ductility as obtained from the response of the equivalent SDOF systems to the earthquake records studied. To compare the response of the SDOF system with that of the multi-story buildings, the yield

strength of the bi-linear curve calculated as above is divided by the "effective weight" (participating mass) in the first mode of vibration of the buildings. Such an approximation is intended to account for multi-mode effects on the response of the buildings and can be justified by the fact that the response of the buildings studied is dominated by the first mode of vibration. Note that rigorous application of dynamic principles would require that the base shear coefficient and drift relationships be obtained using a load distribution that would produce a deflected shape corresponding to the first mode. However, the uniform lateral load distribution used to calculate the base shear and drift curves produced deflected shapes that are similar to those obtained in the first mode.

In a previous study, Jordan [49] proposed a simplified relationship that permits estimation of the ductility capacity of retrofitted buildings. The relationship is based on the lateral strengths and periods of vibration of the original and retrofitted structures, and on the ductility capacity of the original building. The use of such a relationship for estimating the ductility capacity is attractive because it does not require derivation of the lateral load and drift relations for the retrofitted buildings but only for the original building, thus reducing the computation effort. The proposed relation is as follows:

$$\mu_c = \mu_o \frac{C_{yo} \, T_o^2 \, \Sigma_i \, (\phi_o)_i \, \Sigma_i \, (\phi_r)_i^2}{C_{yr} \, T_r^2 \, \Sigma_i (\phi_o)_i^2 \, \Sigma_i(\phi_r)_i} \qquad (7.1)$$

where:

μ_o, μ_c	= ductility capacities of the original and retrofitted buildings respectively.
C_{yo}, C_{yr}	= yield strength of the original and retrofitted buildings respectively.
T_o, T_r	= periods of vibration of the original and retrofitted building respectively
$(\phi_o)_i, (\phi_r)_i$	= deflection in a first mode shape at level i of the original and retrofitted structure respectively, normalized with respect to the roof displacement.

The terms involving the summations of the deflected shapes of the buildings may be omitted if the mode shapes for the original and retrofitted buildings are similar. Such is

the case for the buildings considered in this study and therefore the summation terms are neglected in the following.

The main assumptions involved in the derivation of Eq. 7.1 are that the drift level at ultimate state and modes of failure of the original and the retrofitted buildings are the same. Also, the relationship was based on moment frames of reinforced concrete retrofitted with either reinforced concrete jacketing or structural walls. The values obtained from Eq. 7.1 will be used to determine the validity of the expression for buildings retrofitted with bracing systems.

Soil-structure interaction effects are neglected in the SDOF model. Because interaction effects showed only a minor influence in the overall evaluation of the buildings, a fixed-based SDOF system should suffice to estimate the response of the buildings on soft soil sites.

7.2.1.1 Prototype Building I - Three-Story Building

Idealization of Bi-Linear relationships

The base shear coefficient and drift relationships for the original and retrofitted buildings investigated for the three-story building are reproduced in Fig. 7.2. Also shown in this figure are the bi-linear relationships used to idealize the behavior of the three-story buildings as described above. The definition of ultimate state for the original and retrofitted buildings follow the criterion indicated earlier with specific failure modes as follows:

a) *Original Building:*

The ultimate state is defined by the drift corresponding to failure of all splices in the first story columns (see Fig. 7.2 a) because the lateral stiffness and resistance of the building is expected to degrade significantly soon after failure of all column splices.

b) *Post-Tensioned Bracing Schemes:*

As noted in Chapter VI, lateral stiffness and strength of the braced buildings is governed by the behavior of the braces. Maximum strength of the braced structure is reached when braces that shorten in the first story become slack. Failure of column splices occurs before the braces begin to sag and it does not

● *Splice failure of all first story columns*

✛ *First buckling of braces*

✕ *Braces sag (no tension)*

◆ *First yielding of braces in tension*

▲ *First yielding of reinforcement in boundary elements*

▼ *Fracture of reinforcement in boundary elements*

a) ORIGINAL

b) POST - TENSIONED SCHEMES

c) X - BRACING SCHEMES

d) STRUCTURAL WALL SCHEME

BASE SHEAR COEFFICIENT, V/W

DRIFT AT THE CENTROID OF INERTIA FORCES, (%)

Figure 7.2 Idealization of base shear and drift relationships for the original and retrofit three-story buildings.

cause an appreciable degradation of stiffness or strength of the retrofitted buildings. Accordingly, ultimate state is defined by the drift at which braces that shorten begin to sag.

c) *X-Bracing Schemes:*

Ultimate state is defined as the drift corresponding to failure of splices in all columns in the first floor. The reason for adopting this criterion is that both buckling and yielding of braces precede failure of splices in all first story columns, as shown in Fig. 7.1 c. Thus, lateral stiffness and strength of the building is expected to degrade rapidly after failure of splices.

d) *Structural Wall Scheme:*

Because the structural wall is a very rigid system compared to the existing frame, the strength of the wall is reached before failure of splices occurs in any of the columns. The ultimate state is defined as the drift at fracture of the reinforcement in the boundary elements of the wall, as shown in Fig. 7.1 d.

Displacement Ductility Requirements

In Table 7.1, the main properties of the equivalent SDOF model are represented by the "effective" base shear coefficient at yield, C_{eff} , (base shear coefficient corresponding to yield of bi-linear curve divided by the weight participating in the first mode), the drift at ultimate state, Δ_u , and the global displacement ductility capacity of the buildings, μ_c , as obtained from the bi-linear relations (Fig. 7.2) and Eq. 7.1.

Maximum allowable drifts (drifts at ultimate state, Δ_u) are all below or equal to 1%. Global displacement ductility capacities, μ_c , as obtained from the bi-linear relation for the original and the retrofitted structures with post-tensioned bracing and X-bracing are relatively low. For the wall scheme, however, the displacement ductility capacity is estimated at 7.2 even though the maximum allowable drift is relatively small (0.57%). The reason is that yielding, and thus energy dissipation in the wall, begins at very low drifts.

Global ductility capacities computed according to Eq. 7.1 are generally lower than those estimated from the bi-linear relations and therefore they are conservative. However, for scheme DA2, Eq. 7.1 overestimates the ductility capacity of the structure. The reason

Table 7.1 Computed properties and predicted response of equivalent SDOF system for the three-story buildings

Bldg. [T (sec)]	SDOF Model			r_c / r_r **				
	C_{eff}	Δ_u / h^* [%]	r_c	Records on Firm Soil			Records on Soft Soil	
				Scaled El Centro	Corralitos	Viña del Mar	Mexico City SCT1	Oakland
Original [1.11]	0.15	0.78	1.35	0.45	0.64	0.41	0.19	0.33
C1 [0.52]	0.51	1.00	2.86 (1.80)▼	0.93	1.02	1.17	+	2.11
C2 [0.46]	0.50	0.82	2.52 (2.36)▼	0.99	0.72	1.87	+	2.23
C3 [0.44]	0.67	0.93	2.64 (1.92)▼	1.33	1.00	2.15	+	+
C4 [0.40]	0.84	1.00	2.86 (1.86)▼	2.36	1.04	+	+	+
DA1 [0.40]	0.68	0.71	2.33 (2.29)▼	1.38	0.82	2.06	+	2.16
DA2 [0.30]	0.89	0.45	1.91 (3.11)▼	1.39	1.11	+	+	+
Wall [0.25]	0.61	0.57	7.2 (6.5)▼	3.50	2.06	5.69	+	+

T : fixed-base period of vibration
h* : height to the centroid of inertia forces
+ : response is elastic
▼ : global ductility capacity computed according to Eq. 7.1
** : values less than one indicate inadequate behavior

is that, as noted earlier, Eq. 7.1 assumes that the maximum allowable displacements and the mode of failure in the original and retrofitted structures are the same. However, the drift at ultimate for scheme DA2 is significantly lower than that of the original structure. Note that for the wall scheme the mode of failure of the retrofitted building is different than that of the original building. However, the ductility capacity obtained for the wall scheme is a conservative value.

In Table 7.1, the ratios between the global displacement ductility capacity, μ_c (as obtained from the bi-linear relations in Fig. 7.2), and the displacement ductility requirements, μ_r, are presented for the five earthquake records studied. In this table, the performance of a structure is considered adequate if the displacement ductility ratio, μ_c / μ_r, is greater or equal to one (i.e. capacities exceed demands). Otherwise, behavior is predicted to be inadequate for the buildings. For the original building, the displacement ductility demand obtained with SDOF model during the scaled El Centro record was 2.97 which compared with the ductility capacity of 1.35 resulted in a ductility ratio (capacity divided by demand) of 0.45 as shown in Table 7.1.

For the original building, inadequate behavior is predicted for all five earthquake records. Considering the records on firm soil, the SDOF model predicts larger displacement ductility requirements for the scaled El Centro and for the Viña del Mar records than for the Corralitos record. For the records on soft soils, the displacement ductility requirements are even larger than those for the records on firm soil, particularly for the Mexico City - SCT1 record. These results match very closely the results obtained from the dynamic analyses of the three-story building, as can be seen by comparing the maximum inter-story drifts presented in Fig. 6.2 and 6.3 for the records on firm and on soft soils, respectively.

A similar comparison for the post-tensioned bracing systems, schemes C1, C2, C3 and C4, shows the same correlation between the results of the SDOF model and those of the three-story structures. In Table 7.1, adequate behavior is predicted for the Viña del Mar record and for both records on soft soils, with all four post-tensioned bracing schemes. Maximum inter-story drifts presented in Fig. 6.10 for the Viña del Mar record and in Figs. 6.11 and 6.12 for the records on soft soils reveal the same conclusion. Further, it is predicted that for the Mexico City - SCT1 record, the response with all post-tensioned bracing schemes is in the elastic range. It can also be concluded from table 7.1 that

scheme C4, which displays the highest displacement ductility ratios, is the best alternative among the post-tensioned bracing schemes. Clearly, the Corralitos record imposes the largest ductility demands on configuration C4. The same conclusions were obtained from analyses of the three-story buildings.

For the X-bracing and the wall schemes, the correlations between the SDOF model and the MDOF structure are similar to those described above, and can be readily verified by comparing the results of Table 7.1 with those described in Chapter VI.

In summary, the predictions for the performance level of the original and retrofitted buildings using the equivalent SDOF model show remarkable agreement with the results from inelastic analyses of the three-story frames.

7.2.1.2 Prototype Structure II - Twelve Story Building

Idealization of Bi-Linear relationships

Following the procedure described earlier, the base shear coefficient and drift relations for the original and retrofitted buildings were used to define a bi-linear response. It can be recalled that the mode of failure of the buildings was, in general, governed by column shear failure in the lower stories of the buildings. The criterion used to determine ultimate state (Δ_u) was unique for all cases and was defined as the drift at the centroid of inertia forces at the onset of column shear failure. For the original building, column shear failure is clearly an appropriate definition for the ultimate state as lateral stiffness and strength will degrade rapidly soon after such failure (see Fig. 4.23). For the retrofit schemes, the criterion is appropriate because column shear failure begins after significant "yielding" in the structure (yielding and buckling of braces, or yielding of reinforcement in walls). Thus, it is reasonable to assume that only limited strength and deformation capacity will remain after failure of columns (see Figs. 6.33, 6.40 and 6.48). In wall scheme W1 (Fig. 6.46), however, column shear failure occurs prior to yielding of the wall at its base (see Fig. 6.48). Therefore, the criterion for determining the ultimate state may be somewhat conservative for scheme W1 since the loss of column shear capacity does not lead to an immediate loss of lateral capacity in the frame-wall system.

Displacement Ductility Requirements

The main properties of the equivalent SDOF system are presented in Table 7.2 for the original and most of the schemes considered for the twelve-story building. Bracing scheme DA-TS was not included here because it was not considered a viable alternative (expensive and impractical) as noted in Chapter VI.

Maximum allowable drifts (drifts at ultimate state, Δ_u) for the twelve-story structure are all under 0.8%, and are lower than the calculated drifts for the three-story buildings (Table 7.1). The main reason for such low limits on the ultimate drifts is the failure of columns in shear at small drifts. Similarly, global displacement ductility capacities are in general lower than those obtained for the three-story retrofit schemes. Notice that the displacement ductility capacity for the original building is calculated as 1 (no ductility), since column shear failure begins prior to significant yielding in the structure.

Similar to the results obtained for the three-story structure, global ductility capacities estimated from Eq. 7.1 are lower than those computed from the bi-linear relations. Except for wall scheme W2, Eq. 7.1 yields conservative values for the retrofitted twelve story buildings.

A comparison of the displacement ductility ratio, μ_c / μ_r, reveals that overall the performance of the original and the retrofit schemes predicted by the SDOF model are in good agreement with results obtained from the building analyses. For the original building, inadequate behavior is predicted for the scaled El Centro, Corralitos and the Mexico City - SCT1 records (in Table 7.2 a value for the ratio μ_c / μ_r greater or equal to 1 indicates adequate performance). These results match closely the behavior obtained from building analyses (see Fig. 6.29 and 6.30). Note that for the original structure inadequate behavior indicates shear failure of columns and, probably, collapse of the building.

For the post-tensioned schemes (C4A and C4B), adequate behavior is anticipated for all the records measured on firm soils, with the largest ductility requirements obtained for the scaled El Centro record. Similar conclusions were obtained from building analyses (see Fig. 6.34). For the records on soft soils, inadequate performance is predicted for the Mexico City - SCT1 record with both bracing schemes, and for the Oakland record with scheme C4B. The behavior predicted for the Mexico City - SCT1 record shows excellent

Table 7.2 Computed properties and predicted response of equivalent SDOF system for the twelve-story buildings

Bldg. [T (sec)]	SDOF Model			μ_c / μ_r **				
	C_{eff}	Δ_u / h^* [%]	μ_c	Records on Firm Soil			Records on Soft Soil	
				Scaled El Centro	Corralitos	Viña del Mar	Mexico City SCT1	Oakland
Original [3.52]	0.056	0.47	1.00	0.56	0.93	+	0.38	+
C4A [1.87]	0.172	0.76	2.05 (1.15)▼	1.41	1.78	+	0.45	1.55
C4B [1.71]	0.190	0.58	1.71 (1.25)▼	1.18	1.45	1.50	0.36	0.99
TS1 [1.74]	0.136	0.48	1.80 (1.69)▼	0.98	1.18	1.13	0.34	1.02
TS2 [1.42]	0.254	0.58	1.86 (1.35)▼	1.54	1.60	1.25	0.44	1.05
W1 [2.64]	0.058	0.74	2.35 (1.72)▼	0.64■	1.22	2.11	0.45■	1.26
W2 [1.22]	0.159	0.49	3.18 (2.93)▼	1.36	1.73	1.18	0.59	0.99

T : fixed-base period of vibration
+ : response is elastic
h* : height to the centroid of inertia forces
▼ : global ductility capacity computed according to Eq. 7.1
** : values less than one indicate inadequate behavior
■ : SDOF predictions do not match results from building analyses

agreement with the results from building analyses where collapse of the building was predicted with both bracing schemes (see Fig. 6.35). The behavior predicted for the Oakland record with scheme C4B does not match the results obtained from building analyses (see Fig. 6.35). However, because the displacement ductility ratio is very close to one, this case can be considered as borderline in which a definite conclusion cannot be made without conducting more elaborate analyses. In any case, the results using the SDOF model are conservative.

. For the X-bracing schemes (TS1 and TS2), adequate behavior is anticipated for all the records on firm soils, except for the scaled El Centro record with scheme TS2. For the records on soft soils, inadequate behavior is predicted only for the Mexico City - SCT1 record. These results show excellent agreement with those obtained from building analyses, as evidenced by the maximum inter-story drift ratios presented in Figs. 6.41 and 6.42. The low ductility ratios obtained for the Oakland record are somewhat conservative when compared to the behavior obtained from building analyses.

The results for the two wall schemes, W1 and W2, are dissimilar. With wall scheme W2, the SDOF model predicts adequate behavior for all the records on firm soil. Also, inadequate behavior is predicted for the Mexico City - SCT1 and the Oakland records. The predicted behavior for the Oakland record, however, can be considered a borderline case as explained above for scheme C4B. All these results for wall scheme W2 are in good agreement with those obtained from building analyses (see Figs. 6.49 and 6.50).

For wall scheme W1 (see Fig. 6.46) adequate behavior is predicted for the Corralitos, Viña del Mar, and Oakland records, and correlates well with that obtained from building analyses (Figs. 6.49 and 6.50). However, for the scaled El Centro and the Mexico City - SCT1 records the behavior predicted by the SDOF model is inadequate. While maximum inter-story drifts obtained for the latter two records are the largest compared to the drifts obtained for the rest of the records, the low displacement ductility ratios obtained in Table 7.2 do not explain the behavior obtained from building analyses, particularly for the scaled El Centro record. As noted in Chapter VI, the response of the building with wall scheme W1 for the scaled El Centro record indicated that lateral drifts were controlled (maximum inter-story drifts were all under 1%, as shown in Fig. 6.49) and there was minor damage to the members. Column shear failure was prevented over the entire height of the

building, and walls reached cracking but never reached yielding. For the Mexico City - SCT1 record, maximum inter-story drifts on the order of 1.5 % were obtained, but column shear failure was prevented over the entire height of the building. Walls suffered extensive cracking, but never developed flexural yielding (see Fig. 6.51).

A possible explanation for such a discrepancy is that the double wall configuration at the exterior of perimeter frames with a relatively flexible interior frame changed the dynamic characteristics of the building during earthquake response (participation of higher modes and elongation of the period after cracking of the walls and yielding at the beam ends). Such a behavior could have allowed the building to reach lateral drifts larger than those producing column shear failure under a uniform distribution of lateral loads in a static analysis.

Except for the cases just noted, the SDOF model helps explain the behavior of the buildings in terms of the ductility requirements imposed by the earthquake records selected in this study. Despite all the simplifications introduced, the predictions of the SDOF model show good agreement with the results from building analysis in most cases.

7.2.1.3 Prototype Structure III - Seven Story Building

Idealization of Bi-Linear Relationships

In the evaluation of the SDOF model, only the original and the X-bracing retrofit schemes were included. As noted in Chapter VI, the post-tensioned bracing system was found to be a viable alternative only for the Mexico City - SCT1 record, and therefore it was not considered in the present evaluation. The criterion used to determine the ultimate state of the original and retrofit schemes varied and was defined as follows.

The mode of failure of the original building was governed by column shear failure in the lower stories of the building. Following column shear failure, degradation of stiffness and strength is expected to be rapid (see Fig 4.23) and therefore the ultimate state was defined by the drift corresponding to the onset of column shear failure.

For retrofit schemes TS1 and TS2 (Figs. 6.61), the criterion was defined as the drift corresponding to first yielding of the braces. With both schemes, column shear failure and buckling of braces precede yielding of braces and therefore substantial damage to columns

can be expected using this criterion. However, for scheme TS2, column shear failure did not appear to have a substantial influence on the stiffness nor on the strength of the scheme because of the relatively large stiffness and strength provided by the braces. With scheme TS1, the columns failing in shear caused a significant reduction in stiffness and strength of the structure (Fig. 6.61). However, the presence of the bracing system provided the building with some deformation capacity following column shear failure, even though buckling and yielding of braces is expected to occur soon after the failure of columns. Scheme TS1 was rendered adequate if lateral drifts remained below that corresponding to yielding of braces, and therefore the criteria defined above is appropriate.

Displacement Ductility Requirements

The calculated properties of the equivalent SDOF system for the seven-story buildings are presented in Table 7.3. Notice that because of the premature shear failure of columns, maximum allowable drifts, Δ_u, are significantly smaller than those defined for the previous two buildings. Even after retrofitting with the X-bracing system, the permissible drifts are still very low (< 0.25 %). Global displacement ductility capacities are also shown in Table 7.3. Clearly, the original building has no deformation capability after column shear failure ($\mu_c = 1$).

Global ductility capacities estimated from Eq. 7.1 are too conservative in this case. The ductility capacity estimated for the retrofitted buildings is essentially the same as that of the original structure, whereas the addition of the braces result in added deformation capacity beyond the shear failure of columns (see Fig. 6.61). As noted earlier, the assumptions involved in Eq. 7.1 consider the original and retrofitted structures have the same maximum deformation capacity.

The displacement ductility ratios shown in Table 7.3 indicate that the original building would be inadequate, and because of the low ductility ratios obtained, collapse could be expected for all five earthquake records. Such a result is in good agreement with the conclusions obtained from building analyses (Figs. 6.52 and 6.53).

For bracing scheme TS1, inadequate behavior is predicted for all records, except for the Mexico City - SCT1 record, where elastic behavior would be anticipated. As above, good agreement is obtained between the predictions of the SDOF model and the results

Table 7.3 Computed properties and predicted response of equivalent SDOF system for the seven-story buildings

Bldg. [T (sec)]	SDOF Model			$*_c / *_r$ **				
	C_{eff}	Δ_u / h^* [%]	$*_c$	Records on Firm Soil			Records on Soft Soil	
				Scaled El Centro	Corralitos	Viña del Mar	Mexico City SCT1	Oakland
Original [0.62]	0.162	0.1	1.00	0.15	0.16	0.14	0.41	0.14
TS1 [0.43]	0.325	0.22	2.75 (1.04)▼	0.46	0.49	0.63	+	0.94
TS2 [0.28]	0.719	0.24	3.20 (1.10)▼	2.00	1.00	3.14	+	+

T : fixed-based period of vibration
h* : height to the centroid of inertia forces
+ : response is elastic
▼ : global ductility capacity computed according to Eq. 7.1
** : values less than one indicate inadequate behavior

obtained from building analyses (Figs. 6.62 and 6.63). Also, retrofit scheme TS2 is adequate for all five earthquake records, with the largest demands imposed by the Corralitos record. Furthermore, for the records on soft soils, elastic behavior is predicted. The predictions of the SDOF model correlate very well with results from building analyses (see Figs. 6.62 and 6.63). In addition, the ductility ratio of one obtained for the Corralitos record with scheme TS2, correlates well with the degree of damage anticipated for the building shown in Fig. 6.64.

Similar to the results obtained for the three and twelve story buildings, the correlations between the equivalent SDOF model and the results obtained from building analyses for the seven-story frame are remarkable.

7.2.2 Discussion

The results presented above suggest that the behavior of the buildings considered in this study can be reasonably well predicted by an equivalent bi-linear SDOF model idealized from relations between base shear coefficient and drift at the centroid of inertia forces. These results will serve to provide a basis for a simplified design procedure for retrofit schemes as discussed in the following section.

Also, the equivalent SDOF model could be used to estimate global displacement ductility demands of buildings similar in height and layout to those examined in this study. The main advantage in the use of the equivalent SDOF system is the significant reduction in the computer effort to carry out inelastic dynamic analyses. A broader range of earthquake records could be employed which would give a better representation of the possible different responses for a given structure. The procedure can be used for preliminary analyses of different scheme(s) prior to performing more elaborate analyses.

Ductility capacities calculated from the equation proposed by Jordan [49] yielded, overall, very conservative results. However, the use of such an equation has the advantage that, except for the ductility capacity of the original structure, the parameters involved in the equation (lateral strengths and periods of the original and retrofitted structures) can be estimated using current available elastic analysis procedures.

7.3 LATERAL DRIFT REQUIREMENTS

The behavior of the buildings can also be examined by comparing the maximum allowable drift (drift at ultimate state) with the lateral drift requirements of the earthquake records studied. Drift requirements (demands) can be estimated by dividing spectral displacements by the corresponding height to the centroid of inertia forces of each building.

In the following the *inelastic* drift at ultimate state is compared with the *elastic* response spectra of the earthquake records. Such a comparison is strictly valid for medium-to-long period structures where inelastic and elastic displacements are approximately the same [55]. For short period structures, inelastic displacements will, in general, be larger than the corresponding elastic displacement [55] and therefore such a comparison would not be valid. However, because the retrofitted buildings possess, in general, relatively low ductility

capacities (an exception to this result is the wall scheme used to retrofit the three-story building, Table 3.1), inelastic displacements for a building that is adequate should not differ significantly from the elastic displacement.

In Figs. 7.3 through 7.8, the elastic displacement response spectra for the records on firm and soft soils are compared to the maximum allowable drifts (Δ_u in Tables 7.1, 7.2 and 7.3) for the original and retrofitted buildings. In these figures, a structure is adequate if the maximum allowable drift (capacity) is greater than or equal to the spectral drift (demands) corresponding to the fundamental period of the building.

A detailed examination of results presented in Fig. 7.3 through 7.8 reveals that, overall, the adequacy of the original and retrofitted buildings can be approximately determined by comparing the maximum allowable drifts with elastic displacement (drift) response spectra. Consider for example in Fig. 7.3 the original three-story building and retrofit schemes C1 and C4. The original building (O) is inadequate as the maximum allowable drift is well below the drift requirements for the three records on firm soil (a similar conclusion is obtained for the records on soft soils, Fig. 7.4). Similarly, scheme C1 would probably be just adequate for the Viña del Mar record, but inadequate to satisfy the demands of the other two records on firm soils. Scheme C4 would be just adequate to satisfy the demands of the Corralitos record and adequate for the scaled El Centro and Viña del Mar. For the records on soft soils, a similar comparison would show that all retrofit schemes would perform satisfactorily. These results are in good agreement with the results obtained from building analyses and with those obtained from the SDOF system. An exception is scheme DA2, which according to the spectral displacements in Fig. 7.3 would perform inadequately during the Corralitos record; building analyses indicated that the performance of scheme DA2 was satisfactory. In any case, the results obtained from the comparison of lateral drifts are conservative.

For the twelve story buildings, the comparisons show similar correlations for the records on firm soils (Fig. 7.5). The behavior of the original building (O) is expected to be adequate only for the Viña del Mar record, a result that matches the performance obtained from building analyses. Schemes C4A, TS2 and W2 display maximum allowable drifts that are equal to or greater than the drift requirements imposed by the earthquake records, and

Figure 7.3   Maximum allowable drifts for original and retrofitted three-story buildings, and drift requirements of records on firm soil sites.

Figure 7.4   Maximum allowable drifts for original and retrofitted three-story buildings, and drift requirements of records on soft soil sites.

Figure 7.5   Maximum allowable drifts for original and retrofitted twelve-story buildings, and drift requirements of records on firm soil sites.
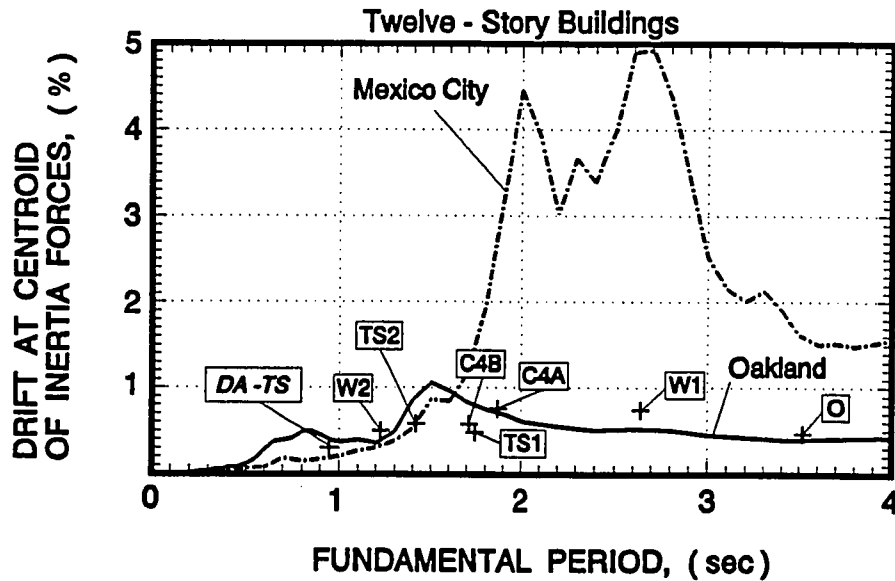
Figure 7.6   Maximum allowable drifts for original and retrofitted twelve-story buildings, and drift requirements of records on soft soil sites.
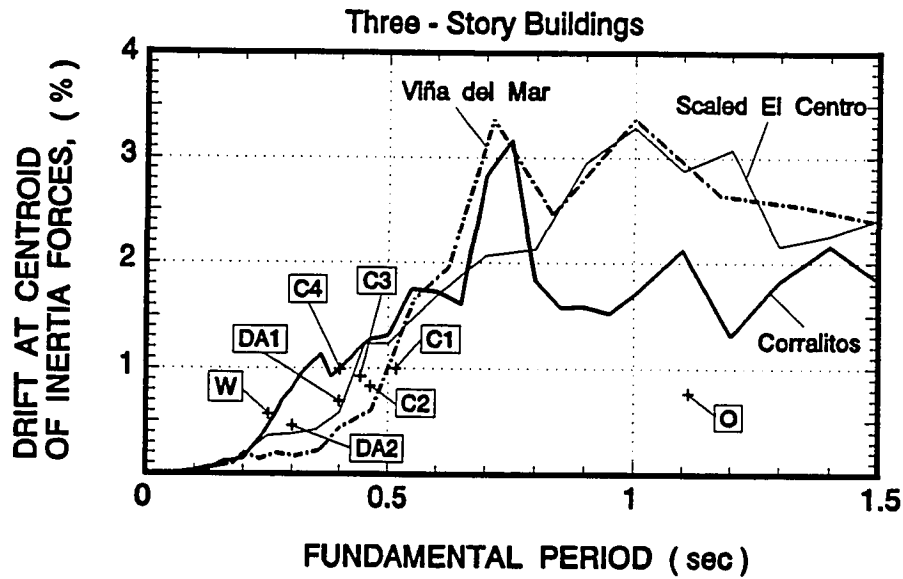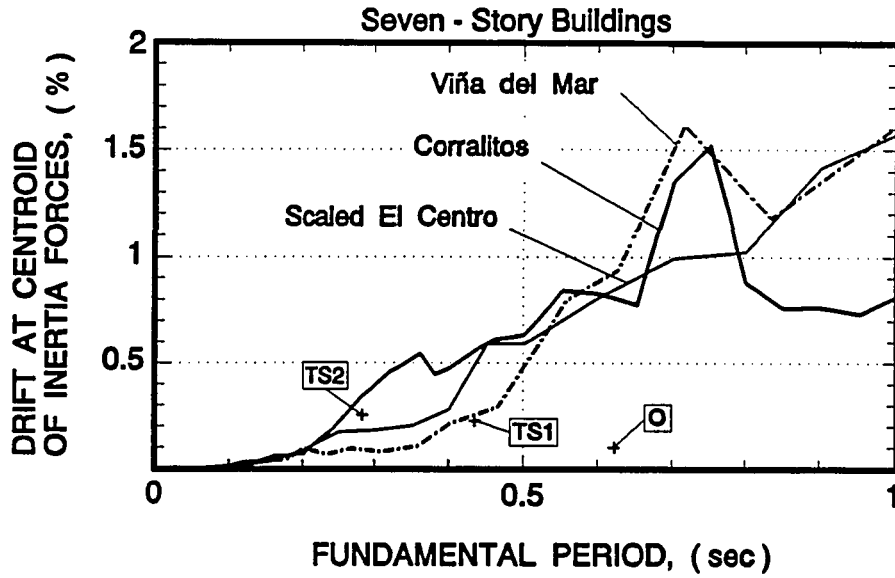
Figure 7.7   Maximum allowable drifts for original and retrofitted seven-story buildings, and drift requirements of records on firm soil sites.
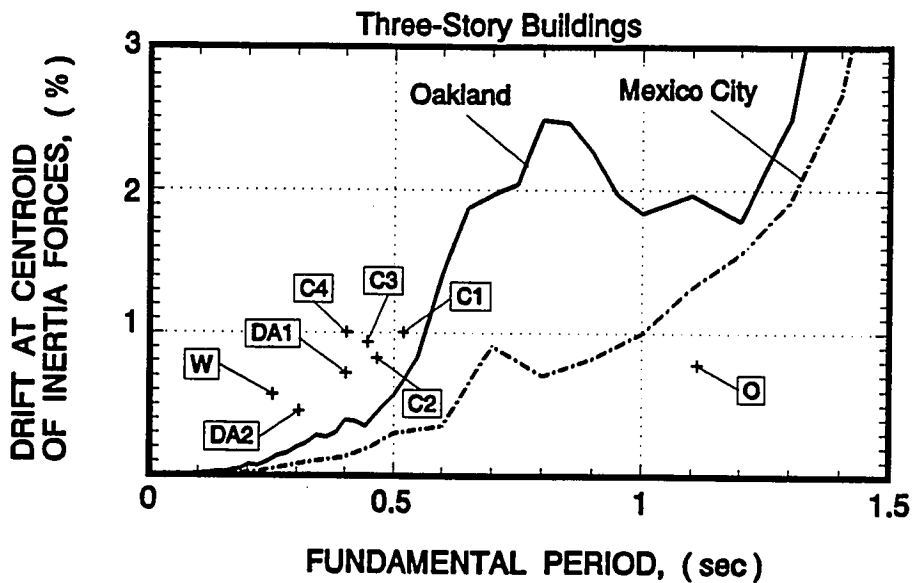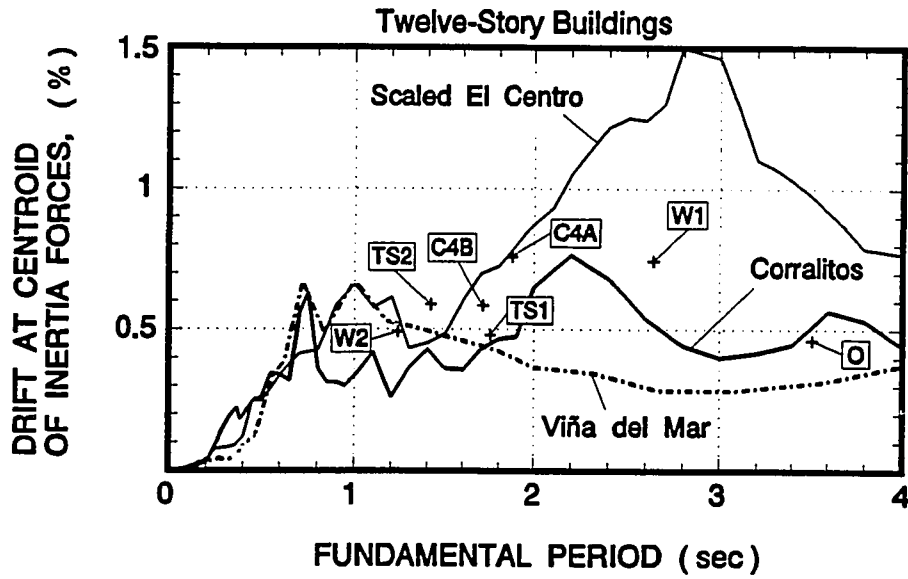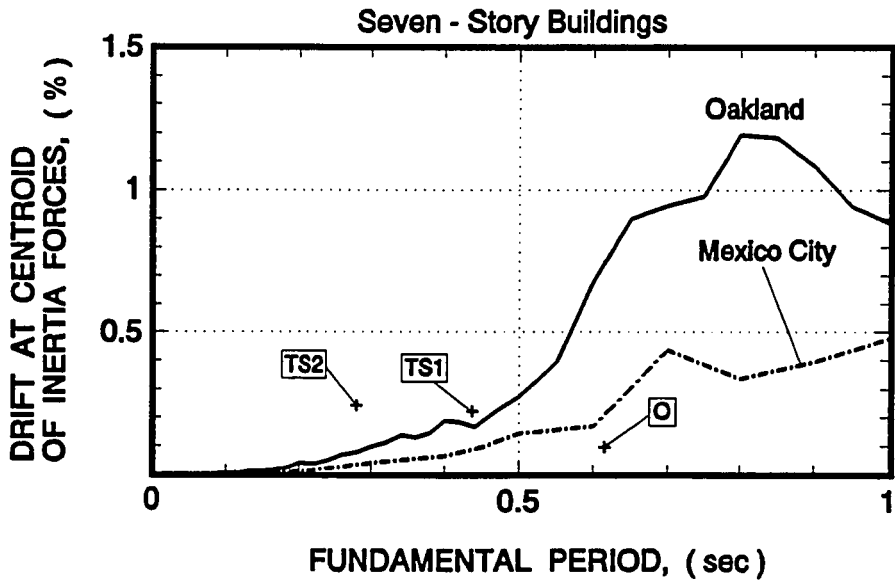

Figure 7.8   Maximum allowable drifts for original and retrofitted seven-story buildings, and drift requirements of records on soft soil sites.

therefore adequate behavior is anticipated. As noted in the previous Chapter, building analyses showed that these three schemes displayed adequate behavior for the records on firm soil sites. Similarly, schemes C4B and TS1 should display adequate performance for the Corralitos and Viña del Mar records, but inadequate behavior for the scaled El Centro record. Also, scheme C4B should perform better than scheme TS1 because of the larger allowable drift of scheme C4B. Such behavior shows, overall, good correlation with the results obtained from building analyses, except that the performance of scheme C4B was *better* than that implied in Fig. 7.5. However, because the difference between the estimated allowable drift for scheme C4B and the drift requirements of the scaled El Centro record are relatively small, this case can be considered as a borderline situation which would call for more elaborate analyses to draw a final conclusion.

As noted earlier, the behavior of scheme W1 for the scaled El Centro and the Mexico City - SCT1 records are the only cases in which the correlations between the maximum allowable drift and drift demands are not in good agreement with the results from building analyses. A possible explanation for this result was discussed earlier in this Chapter.

For the Oakland record (Fig. 7.16), good correlations are obtained for the original building (O) and retrofit schemes C4A, TS2, W1 and W2. With schemes C4B and TS1, inadequate behavior would be predicted whereas building analyses indicated a satisfactory performance for these schemes. These results are conservative and could be explained by the reductions in the demands of drift that would occur with elongations of the fundamental periods due to inelastic behavior in the structure. In Fig. 7.6, an elongation in the periods of the buildings from 1.7 secs. to 2 secs. would render schemes C4B and TS1 adequate.

For the Mexico City - SCT1 record, the comparisons show good correlation for all buildings except for schemes TS2, W1 and W2. The results for scheme W1 have been discussed previously. Notice the high drift demands for buildings with fundamental periods between 2 and 3 secs (more than 4%). For schemes TS2 and W2, adequate behavior would be predicted whereas building analyses and the equivalent SDOF system indicated unsatisfactory performance with probable collapse of the building. These results could be explained by the tremendous increases in drift demands with relatively small elongations in

the fundamental periods of the buildings. Furthermore, the drift demands would continue to increase up to a period of 2 secs.

For comparison, scheme DA-TS is included in Fig. 7.6. This scheme performed satisfactorily during the Mexico City - SCT1 record, but it was considered too expensive and impractical, thus a non viable alternative. In Fig. 7.6, it can be seen that adequate behavior would be predicted for scheme DA-TS; a result that matches that obtained from building analyses even though drift demands also increase with elongations in period. However, the increment in drift demands over similar elongations in period are significantly smaller for scheme DA-TS than for either scheme TS2 or W2. Because of the extremely high drift demands of the Mexico City - SCT1 record between periods of 2 and 3 secs., it is unlikely that a retrofit scheme would be able to supply such high drift demands. These results suggest that the only feasible strategy for the retrofit of medium rise frame buildings in Mexico City is to stiffen the building (shorten the period) to such a degree that significant increases in drift demands with elongating periods are avoided. From the results of this study and those of Jordan [49], it appears that a maximum period of 1 sec. is an adequate limit. It is clear, however, that the retrofitted structure still has to satisfy the minimum drift demands for the corresponding period of vibration.

For the seven story building, the results are, in general, in good agreement with those obtained from building analyses (see Figs. 7.7 and 7.8).

In summary, a comparison between maximum allowable drifts with elastic displacement (drift) spectra provided an adequate (or conservative) estimate of the behavior of the buildings subjected to the records on firm soils and to the Oakland record. For the buildings subjected to the Mexico City - SCT1 record the predictions may be unsafe for structures with periods of vibration larger than 1 sec.

7.4 IMPLICATIONS FOR DESIGN

Within the approximations involved in the previous analyses, the results obtained above show that the performance of an existing or retrofitted frame building can be approximately predicted by comparing the maximum drift capacity with the displacement demands obtained from elastic response spectra. Such a result has significant implications for the design strategies of retrofit schemes for existing buildings. The design strategies

suggested in the following are strictly applicable for buildings located on firm soil sites although based on the results obtained for the Oakland record, it appears that a similar strategy could be used on soft soils in the U.S. provided that appropriate response spectra are used. Design strategies for medium rise buildings located on the clay deposits of Mexico City were briefly discussed above, and are different from the procedures described below.

Also, the discussion assumes that the existing structure does not undergo any significant changes in mass upon retrofit. Therefore, the changes in period of vibration of the building are attributed to changes in stiffness only.

The lateral load analyses (base shear coefficient and drift relations) of the frame buildings considered in this study (and also those considered by Jordan [49]) showed that the drift at ultimate of the retrofitted structure may increase, decrease or remain the same as that of the original building (see Fig. 7.2 and Table 7.1). Nevertheless, the allowable drifts of the retrofitted structure are expected to be, in general, of the same magnitude as that of the original structure. Such a behavior is the result of the presence of "non-strengthened" elements in the structure which limit the maximum lateral deformations of the retrofitted structure (failure of splices and/or shear failure of columns).

Consider in Fig. 7.9 typical smoothed displacement response spectra for ground motions on firm soils that represent a design earthquake. Such spectra can be derived using the familiar Newmark-Hall rules for a given design earthquake. Notice that there are two distinct regions indicated as the "short" and medium-to-long period ranges. It might be recalled that in accordance with the rules of Newmark-Hall, maximum inelastic and elastic displacements are assumed to be the same in the medium-to-long period range. In the short period range, maximum inelastic displacements are always larger than maximum displacements of the same structure responding elastically to the earthquake [55].

An existing medium-to-long period building with maximum allowable drift, Δ_o, and fundamental period, T_o, is indicated in the figure. The existing structure would be inadequate because its maximum allowable drift is less than the demands of the design earthquake. Also shown in Fig. 7.9 is the idealized bi-linear relation for the existing building. According to the results presented in the previous section, a retrofit will be successful only if the retrofitted structure meets the drift demands of the design earthquake. In Fig. 7.9,

SMOOTHED INELASTIC DISPLACEMENT SPECTRA
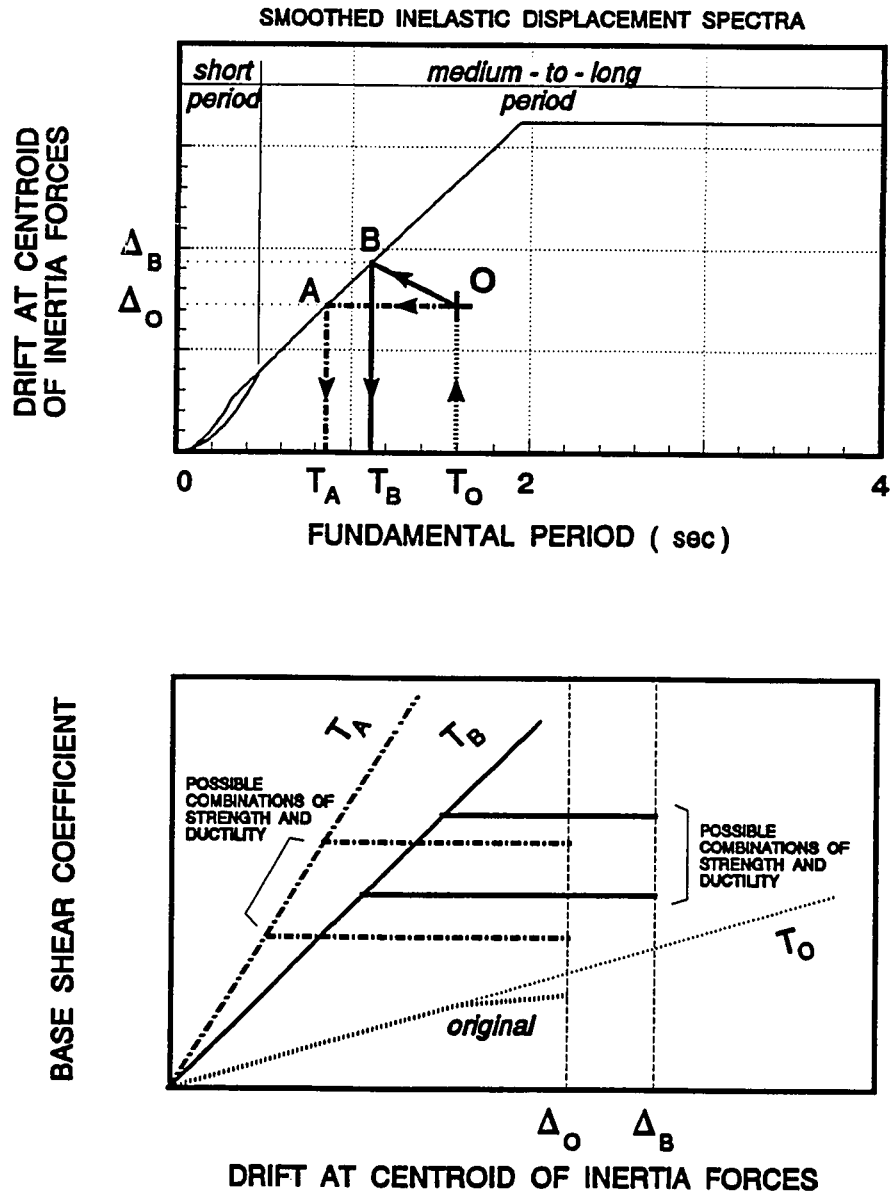
Figure 7.9 Design strategies for medium to long period structures on firm soils.

segments OA and OB illustrate two possible paths that would lead to a successful retrofit. Segment OA represents the path to follow if, after retrofitting, the drift at ultimate remains the same as that of the original building. Segment OB represents the path to follow if the drifts at ultimate are increased upon retrofit. Points A and B define the **maximum periods of vibration** or **minimum stiffnesses** that have to be provided by the retrofit schemes for adequate performance of the retrofitted building under the design earthquake. Once the minimum stiffness requirement is met there exist a variety of strength/ductility relationships that will lead to a successful retrofit, as suggested in Fig. 7.9. Such a result is a consequence of the approximation that inelastic and elastic displacements in the medium-to-long period range are the same, regardless of the level of strength or ductility in the structure.

These concepts of minimum stiffness requirements were also indicated by Jordan [49] in the analyses of reinforced concrete jacketing (and addition of structural walls) as retrofit for reinforced concrete frames. Based on the results of the present study and those obtained by Jordan, it is apparent that the retrofit strategies for non-ductile reinforced concrete frames with medium-to-long periods are controlled by the lateral stiffness of the retrofitted structure, and not by strength or ductility.

Notice that while strength or ductility play an indirect role in determining the adequacy of a retrofit scheme in the medium-to-long period range, they should not be regarded as unimportant. The retrofitted structure must have enough ductility to achieve the drift demands of the earthquake. Also, ductility in the structure will provide the building with a greater deformation capability which might be indispensable in the event of ground motions larger than those anticipated for the site.

For short period (low-rise) structures displacements will increase with inelastic behavior. In such cases, the retrofit scheme must satisfy minimum strength requirements in addition to the requirements of minimum stiffness requirements only. Consider in Fig. 7.10 an existing building with maximum allowable drift, Δ_o, and period T_o, which is inadequate to satisfy the demands of the design earthquake. Note that the original building is located in the medium-to-long period range. Assuming that the drift at ultimate of the retrofitted structure is the same as that of the original building, Fig. 7.10 shows that there are several alternatives for a successful retrofit. Point B represents the maximum period of

SMOOTHED INELASTIC DISPLACEMENT SPECTRA

DRIFT AT CENTROID OF INERTIA FORCES

short period | *medium - to - long period*

$1 < \mu_0 < \mu_1$

μ_1 μ_0

$\mu = 1$

Δ_o

Δ^A_{elas}

A

B

O

0   T_A T_B 0.5 T_O 1

FUNDAMENTAL PERIOD (sec)

BASE SHEAR COEFFICIENT

Δ^A_{elas}

C^A_{elas}

$C^B_{y\,min}$

$C^A_{y\,min}$

T_A

T_B

T_O

original

$\Delta_Y = \Delta_o / \mu_1$ Δ_o
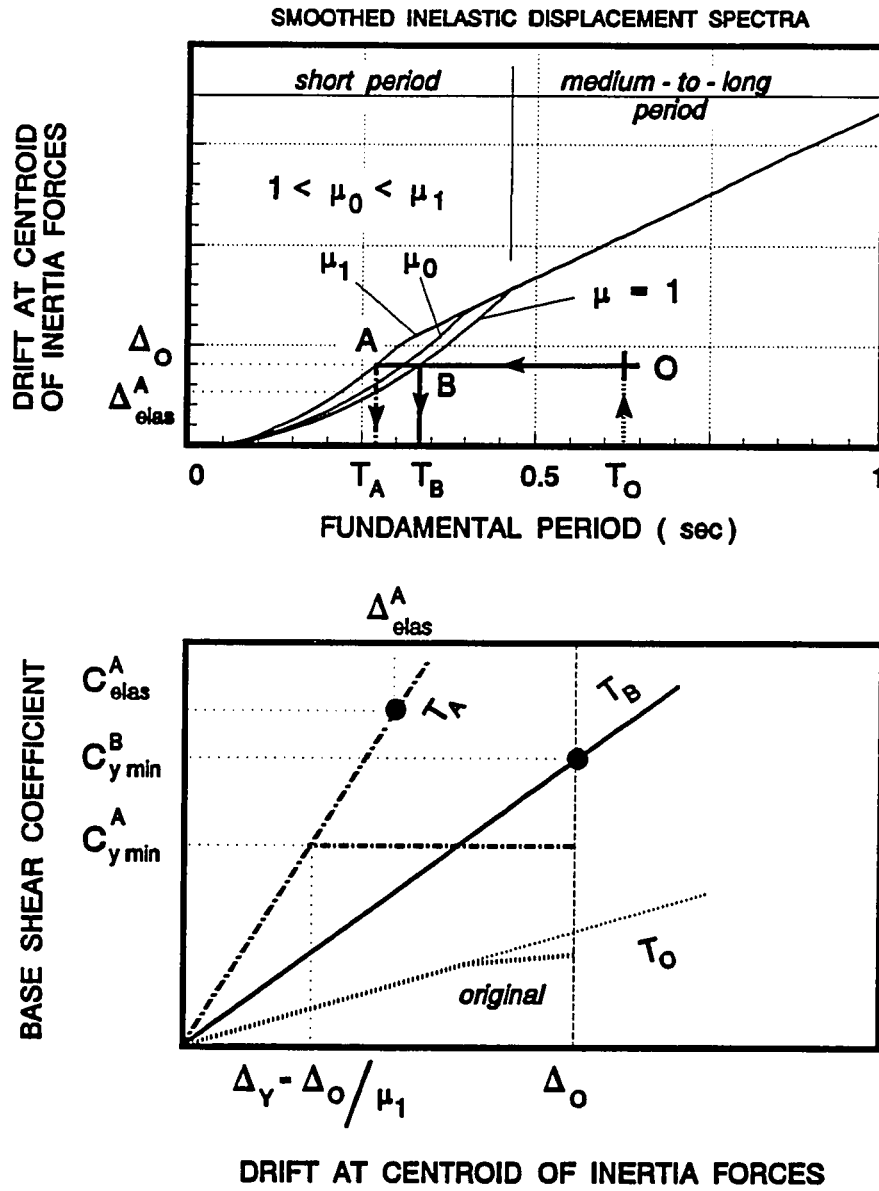
DRIFT AT CENTROID OF INERTIA FORCES

Figure 7.10 Design strategies for short period structures on firm soils.

vibration of a retrofitted structure that would satisfy the demands of the design earthquake. Note, however, that point B intercepts the *elastic* spectrum ($\mu = 1$), and therefore a retrofitted structure with period T_B would have to respond elastically to the earthquake to develop a maximum drift Δ_o. Since the period of the retrofitted structure T_B falls within the "short" period range, inelastic behavior at drifts smaller than Δ_o will result in drifts larger than the maximum allowable Δ_o and cannot be allowed. From the load and drift relationship shown in Fig. 7.10, the stiffness associated with the period T_B and the maximum drift Δ_o define the minimum strength required for the structure, C^B_{ymin}.

Alternatively, point A defines the maximum period T_A for a retrofitted building that may be allowed to experience inelastic behavior. The amount of inelastic behavior is defined by the global displacement ductility μ_1. By equating the *ductility demands* of the earthquake μ_1 with the global ductility capacity of the desired retrofit scheme, a minimum "yield" displacement and therefore a minimum "yield" strength, C^A_{ymin}, can be defined as shown in Fig. 7.10. Because the period of the retrofitted structure falls within the short period range, a retrofitted structure with period T_A but with a yield strength lower than the minimum strength C^A_{ymin} would result in drifts larger than the maximum allowable and therefore rendered inadequate. The retrofitted structure may have a strength higher than C^A_{ymin}, in which case the maximum drifts will be smaller than Δ_o. However, the strength of the retrofitted structure need not be larger than that defined by the maximum elastic displacement, Δ^A_{elas} shown in Fig. 7.10. Clearly, strengths larger than C^A_{elas} will not reduce the maximum drifts in the structure.

The concepts of minimum stiffness and "yield" strength can be illustrated by comparing the base shear and drift relationships of schemes C4 and TS1 used to retrofit the three-story building (see Fig. 7.2). These two schemes were designed to have the same initial stiffness (periods of vibration). However, for the records on firm soils the performance of scheme TS1 was inadequate, while scheme C4 performed satisfactorily. Using the design concepts presented above, the inadequate behavior of scheme TS1 can be attributed to the lower "yield" strength and to the lower deformation capacity at ultimate, as shown in Fig. 7.2.

The design strategies presented are intended primarily for the design of retrofit schemes for buildings on firm soils and it is believed that represents a valuable and relatively simple tool to determine minimum requirements of stiffness and strength for adequate

performance of the retrofit scheme. Such a procedure should be used as a preliminary design of the retrofit scheme(s) prior to conducting more elaborate design analyses procedures.

Also note that the design procedure is based on response spectra derived for SDOF systems with an elasto-plastic behavior (Newmark-Hall [55]) which may not be representative of structures with strain hardening and /or stiffness degradation. Alternatively, rules to construct inelastic response spectra for stiffness and strength degrading systems have been proposed elsewhere [74].

7.5 COMPARISON WITH ATC-22 PROVISIONS

As discussed earlier in Chapter II, ATC-22 provides minimum requirements for the *evaluation of existing buildings*, but contains no provisions for the *design* or *evaluation* of retrofit systems. Thus, the ATC-22 document should be used to evaluate the performance of only existing (original) buildings. Currently, there are no code provisions for the design of retrofit schemes in the U.S., and as a result, the performance level of retrofit schemes (design forces and drift limits), has to be determined with little or no guidance. Even though ATC-22 is not oriented towards the design of retrofit schemes, a comparison of the behavior of the retrofitted buildings of the present study with the provisions of ATC-22 can provide valuable insights for the evaluation and design of retrofitted structures. In the following, the behavior of the buildings studied is examined in light of the ATC-22 document by comparing the lateral strength of the buildings with that required by the provisions. Because of the significant difference in the response spectra of U.S. records with that of the Mexico City - STC1 spectra, the provisions of ATC-22 do not contemplate large responses for buildings in the long period range. Therefore, ATC-22 can only be compared with the behavior of buildings with available ground motions from U.S. events.

The prescribed design forces in current codes and those of ATC-22 correspond to the lateral load level where "significant yielding" occurs in the structure. The term "significant yielding" is defined as that level causing complete plastification of at least the most critical region of the structure (not the level where first yielding occurs in any member in the structure) [15]. For comparison, the load level corresponding to "significant yielding" was determined as the *yield strength* of the bi-linear relation used to idealize the base shear

coefficient and drift relationship of the buildings, as described earlier in this Chapter (see Fig. 7.1).

In Table 7.4, the *yield strength* of the buildings (as defined above) and the minimum base shear coefficient prescribed by ATC-22 are compared (a summary of the ATC-22 provisions pertaining to the structural systems considered in this study are presented in Appendix A). The base shear coefficients prescribed by ATC-22 shown in Table 7.4 are the same as those indicated in the base shear coefficient and drift presented in previous chapters. As noted earlier (Chapters IV and VI), many of the retrofit schemes included in the present study do not conform with the structural systems contemplated in ATC-22. Specifically, ATC-22 does not contemplate dual systems consisting of steel bracing systems or "shear" walls with ordinary moment resisting space frames (OMRSF) of reinforced concrete, which correspond to the cases investigated in this study. Thus, the buildings with steel bracing or wall systems are compared to dual systems with intermediate moment resisting space frames (IMRSF) to observe the structural systems specified within ATC-22. An IMRSF is presumed to have more ductility than an OMRSF and therefore the prescribed code forces for an IMRSF should be smaller than those for OMRSF. In view of this assumption the specified base shear coefficients for these systems can only be considered as a lower bound for the retrofit schemes included in this study which considered OMRSF.

In addition to specifying different load levels for different structural systems, ATC-22 provides different load factors depending on the expected behavior of the elements in the structure (brittle, semi-ductile or ductile. See Chapter II and Appendix A). The assumptions involved to select appropriate load factors for the buildings studied were discussed in previous Chapters; the assumed element behavior for each building is indicated in Table 7.4. For comparison, the strength ratio between the computed lateral strength, C_y, and the prescribed strength by ATC-22, C^{ATC-22} are indicated in the last column of Table 7.4. In this table, the performance of a building is considered adequate if the strength ratio C_y / C^{ATC-22} is greater than or equal to one.

a) *Three-Story Buildings:*

The results of Table 7.4 show that an evaluation of the original building using the ATC-22 document would consider the building inadequate, a result that is in good agreement with the results obtained from building analyses for the U.S. records.

Table 7.4 Comparison of ATC-22 provisions with calculated lateral strength of buildings.

Building		Computed Base Shear at "Yielding" c_y	ATC - 22		c_y / c^{ATC-22}
			Minimum Base Shear Coefficient c^{ATC-22}	Structural System [Element Behavior]	
3-Story	Original	0.150	0.408	OMRSF [Brittle]	0.37
	C1	0.420	0.278		1.51
	C2	0.450	"	CBF w/ IMRSF	1.62
	C3	0.570	"	[Semi-Ductile]	2.05
	C4	0.700	"		2.52
	DA1	0.580	0.278	CBF w/ IMRSF	2.08
	DA2	0.790	"	[Semi-Ductile]	2.84
	Wall	0.500	0.248	R/C WALL w/ IMRSF [Semi-Ductile]	2.02
12-Story	Original	0.045	0.213	OMRSF [Brittle]	0.21
	C4A	0.137	0.214	CBF w/ IMRSF	0.64
	C4B	0.152	"	[Brittle]	0.71
	TS1	0.109	0.214	CBF w/ IMRSF	0.51
	TS2	0.203	"	[Brittle]	0.95
	W1	0.046	0.194	R/C WALL w/ IMRSF [Brittle w/ W1, Semi-Ductile w/ W2]	0.24
	W2	0.127	0.107		1.19
7-Story	Original	0.130	0.422	OMRSF [Brittle]	0.31
	TS1	0.260	0.497	CBF w/ IMRSF	0.52
	TS2	0.515	0.497	[Brittle]	1.03

For the retrofitted buildings, all schemes meet the lower bound coefficient of ATC-22. However, because the base shear specified by ATC-22 for these systems contemplated IMRSF instead of OMRSF, a conclusion regarding the adequacy of ATC-22 force level cannot be drawn. Building analyses indicated that schemes C4, DA2 and the wall system performed satisfactorily for the U.S. records considered in this study. The strength ratios C_y / C^{ATC-22} obtained in table 7.4 suggest that the required design base shear coefficient for structural systems that include OMRSF instead of IMRSF is, for steel bracing systems, 2.5 times larger than that implied by ATC-22. For wall systems with OMRSF the required base shear is about twice that suggested by ATC-22.

b) _Twelve-Story Buildings_

Similar to the results obtained for the three-story building, the provisions of ATC-22 indicate that the building would perform inadequately under the design lateral forces. Building analyses revealed the same conclusion for the original building.

For the retrofitted buildings, the level of forces prescribed by ATC-22 suggest inadequate performance of the buildings for all schemes with the exception of wall scheme W2. However, inelastic dynamic analyses of the buildings on firm soils showed adequate performance for all retrofit schemes, but scheme TS1. These results are conservative, but, in general, they do not match the results obtained from building analyses. The main reason for such a discrepancy in the results is attributed to the significant difference between the calculated fundamental period and the minimum value for the period ($T \leq C_a T_a$, see Appendix A) specified by ATC-22. Because of the unusual long period of vibration calculated for the twelve-story building, a base shear coefficient based on the calculated period for the building rather the minimum value specified by the code would result in lower strength demands. Such a large discrepancy between the periods was not observed in the retrofitted three-story buildings. In addition, for the retrofitted three-story buildings, the base shear coefficient was governed by the maximum value allowable by ATC-22 (see Appendix A).

Note, that for retrofit schemes TS2 and W2, where the difference between the calculated and the prescribed period was not as significant as for the rest of the schemes, the computed "yield strength" and the prescribed level of forces are quite similar.

c) *Seven-Story Buildings*

As for the two previous buildings, the provisions of ATC-22 would have rendered the original building inadequate, a result that correlates well with the behavior obtained from building analyses. For the braced buildings, the provisions would indicate inadequate behavior for scheme TS1 and adequate behavior for scheme TS2. These results are in agreement with those obtained from building analyses, despite the fact that an IMRSF instead of a OMRSF was considered in calculations of the ATC-22 provisions. The predictions of ATC-22 are adequate in this case.

CHAPTER VIII

SUMMARY, CONCLUSIONS AND RECOMMENDATIONS

8.1 SUMMARY

The study focusses on the use of a retrofit technique that involves the addition of post-tensioned braces with high slenderness ratios (such as steel rods or strands) to improve the seismic resistance of existing reinforced concrete frames. The use of high strength steel rods or strands braces can significantly increase the lateral strength of a frame structure with relatively small amounts of material and is envisioned as an alternate system to structural steel braces. Steel rods or strands can be initially prestressed to increase the initial stiffness of the structure and to reduce the likelihood of shortening the braces to the point where they become slack. If braces remain in tension, stiffness reductions during an earthquake are minimized.

The main objective of this study was to evaluate the performance of post-tensioned bracing systems to improve the seismic response of low and medium rise reinforced concrete frames. The study was aimed at identifying benefits and inadequacies of the system and at identifying cases for which the post-tensioned technique was most suitable. The behavior of the post-tensioned bracing system was evaluated analytically by examining the inelastic dynamic response of three buildings. In addition, the behavior of the post-tensioned bracing system was compared with two alternate schemes that involved the addition of X-bracing and the addition of structural walls. All schemes included in this study confine retrofit operations to the exterior of the building by providing braces or walls only to perimeter frames.

The buildings selected for study were prototype designs and represented typical low and medium rise construction of the 1950's and 1960's in the United States. Low-rise construction was represented by a three-story reinforced concrete frame, while medium-rise construction was represented by seven and twelve story high frame buildings of reinforced concrete.

Frame members in the three-story building featured reinforcing details that are typical of structures not designed to resist seismic forces. The main deficiencies in the three-story building included lightly-confined, short splices at the base of columns (24 bar diameters) and short embedment lengths of bottom beam reinforcement into columns (6 in.).

The second structure considered for study was a twelve story frame building that featured a "soft" first story and a massive parapet at the top of perimeter frames. The weak links in the structure were the small size and wide spacing of the transverse reinforcement outside the hinging region in beams and columns. Such reinforcing details made columns and beams susceptible to potential shear failures. Anchorage of reinforcement was, in general, adequate to develop yielding of reinforcement, but insufficient to develop the ultimate flexural strength of the member.

The seven-story building featured deep spandrel beams (6 ft. deep) and short "captive" columns (4 ft.) in the longitudinal direction of the building. The main inadequacies in frame members were poor column shear strength and short lap splices at the base of columns (20 bar diameters).

To idealize inelastic behavior of the buildings, an existing non-linear analytical model was modified to include failure of reinforced concrete members that exhibit strength degradation and lack ductility. In particular, supplementary hysteretic laws were implemented to emulate strength degradation following anchorage failure in reinforced concrete members. Such a model was used to simulate failure in bond of embedded reinforcement in beams and failure of short splices in columns. A further modification was introduced in the model to idealize failure of members in shear using a relatively simple model. The model was aimed at representing sudden changes in stiffness and strength induced in the structure by member shear failure rather than reproducing behavior of members failing in shear.

Modeling of the behavior of steel braces followed existing non-linear models derived for braces with medium and high slenderness ratios.

Based on these models, inelastic static lateral load analyses were conducted to estimate the lateral stiffness, strength and global displacement ductility of the existing and retrofitted buildings. The static analyses revealed that lateral strength of the existing three-

story building was governed by failure of column splices. For the twelve and seven story buildings, lateral strength was governed by shear failure of columns.

Inelastic dynamic response of existing and retrofitted buildings was evaluated for five earthquake records. Selected ground motions were representative of major earthquakes in the U.S and elsewhere on firm and soft soil conditions. The effects of soil-structure interaction for buildings located on soft soil sites were included in the analyses using a simplified procedure.

The dynamic response was evaluated in terms of maximum displacements, inter-story drifts and ductility demands imposed by the earthquake records. The criterion for determining adequacy of existing and retrofitted buildings was based on providing life-safety to the occupants; i.e. buildings must withstand ground motions with non-structural and structural damage but without collapse. Based on this criterion, dynamic analyses showed that all three existing buildings were inadequate to withstand one or more of the earthquakes records studied, and therefore, seismic retrofit was warranted.

8.2 CONCLUSIONS AND DESIGN RECOMMENDATIONS

On the basis of the results obtained from analyses on the existing and retrofitted buildings the following conclusions can be drawn:

8.2.1 Post-Tensioned Bracing Systems

a) In general, the post-tensioned bracing system is a viable alternative to control lateral drift and to prevent collapse of low and medium-rise reinforced concrete frames on firm and soft soil sites. While the technique is most suitable for low-rise buildings on soft soil sites, it can also be used for low and medium rise buildings located on firm soils. The adequacy of the post-tensioned bracing systems for medium-rise frame buildings on soft soils will depend on the characteristics of the ground motion.

b) Dynamic analyses indicated that the use of high levels of initial prestress of braces reduced the overall response of the buildings. Initial prestress levels of 50% or higher should be used in design to maximize energy dissipation of the system through yielding of braces.

c) Yielding of braces in tension reduces the amount of initial prestress in the braces, but it does not necessarily lead to total loss of prestress. Braces can be allowed to yield in tension without completely losing the initial prestress force, provided that the maximum elongation of the brace beyond that at prestressing does not exceed elongation at yield.

d) The higher strength of steel strands as opposed to steel rods showed no significant influence on the overall dynamic response of the structure. Axial compressive and tension forces in columns or beams were higher when steel strands were used. Because of the lower strength of steel rods, it can be anticipated that the design of anchor systems and potential modifications to foundations may be more economical if rods are used in lieu of strands.

e) Initial brace prestressing can significantly modify the distribution of internal forces of existing reinforced concrete members. The magnitude of induced forces depends on the bracing configuration, brace size, number of braced bays and initial prestress level. A particular problem arises if induced forces are high enough to cause or to augment cracking of existing members. In such cases, the use of post-tensioned bracing may be limited by serviceability and/or durability requirements. The results of this study suggest that long, squat concrete frames are unlikely candidates for the use of a post-tensioned bracing system. In such structures, brace prestressing is realized over a long length which may cause large deformations at the ends of the building and may induce large forces in exterior columns/beams.

8.2.2 Comparison of Post-Tensioned Bracing with X-Bracing and Structural Walls

a) For the low and medium rise buildings studied, the post-tensioned bracing system offers a performance level comparable to that of an X-bracing system or the addition of a structural wall. Such a result is valid for firm soils and soft soils, but it does not include the results obtained for medium rise buildings located on clay deposits of Mexico City.

b) Maximum axial tensile forces developed in columns using post-tensioned bracing were, in general, lower than those induced by an X-bracing system of a comparable level of performance. The lower level of tensile forces obtained with a post-tensioned bracing system is attributed to the initial pre-compression of columns due to initial brace prestressing. Maximum axial compressive forces in columns were similar in magnitude for

both bracing systems. The height of the building did not appear to limit the use of the post-tensioned bracing system.

c) The use of infill walls in low-rise buildings on soft soils appears to be an excessive and expensive solution, because minimum dimensions and requirements for reinforcement of the wall may lead to a lateral capacity larger than what is needed. In addition, extensive modifications to existing foundations are likely with such a scheme and may substantially increase rehabilitation costs. Although not included in this study, the addition of wing walls may be a less expensive solution than infill walls, if a bracing system is considered undesirable.

8.2.3 Soil Structure Interaction Effects

In general, the effects of soil-structure interaction resulted in an increased response of the buildings, although interaction effects occasionally decreased or did not appreciable influence the response of the buildings. However, consideration of soil-structure interaction effects did not affect the conclusions regarding the adequacy of the buildings to withstand the earthquake records analyzed.

8.2.3 Proposed Design Strategies

The results obtained in this and in previous studies indicate that drifts at ultimate of the retrofitted structure are similar to those of the existing structure, or of the same magnitude, irrespective of the retrofit scheme. Such a behavior is the result of the presence of "non-strengthened" elements which possess limited deformation capacity. On the basis of this result, a design strategy is proposed for preliminary design of retrofit schemes. The procedure allows the designer to determine the minimum stiffness and strength requirements for the retrofit scheme to perform adequately under a design earthquake. Such a design procedure was derived for buildings located on firm soils only, but a similar strategy could be used for buildings located on soft soils in the U.S. if appropriate response spectra are used.

Due to the peculiar characteristics of the response of medium-rise buildings located on the clay deposits of Mexico City, the design strategy for these types of buildings is different. Drift demands of the Mexico City - SCT1 record for medium rise buildings

(T = 1.5 to 3 secs) may reach extremely high values (on the order of 4%) and it is unlikely that a retrofitted structure will be able to withstand such high drift demands without severe damage or collapse. In addition, for buildings with fundamental periods less than 2 secs., strength and drift demands increase with an elongation of the period due to inelastic behavior. The retrofit strategy for the kind of motion measured in Mexico City must involve shortening of the fundamental period of the building to a point where significant increases in drift demands with elongations in period are avoided.

8.2.5 Design Recommendations

a) If the lateral strength of the frame structure is governed by shear failure of columns, it is unlikely that a bracing system alone (either post-tensioned or X-bracing) will be able to prevent such a failure. Even if shear failure is prevented, shear forces developed in columns are likely to be very high. Thus, unless shear forces are very low, columns will most likely have to be strengthened to either reduce the shear demand/strength ratio induced in columns or to modify the brittle shear failure to a more ductile flexural failure.

b) High levels of axial forces were induced on the buildings studied by the bracing system (post-tensioned or X-bracing). As a result, members of braced frames (usually members of perimeter frames) would have to be reinforced by either collector elements or jackets to augment the axial capacity of the existing members. However, the retrofit scheme may also consider the addition of jackets to members of unbraced frames (usually members of interior frames) to avoid brittle failure and to increase their deformation capabilities. The addition of collectors or jackets will permit larger drifts in the structure and therefore a lighter (more flexible) bracing system may be required. In addition to providing the structure with more ductile behavior, the resulting scheme may be less expensive even though it might increase disturbance to the occupants during retrofit operations. Such a strategy may be particularly suitable for buildings that exhibit potential column shear failures at relatively low lateral drifts.

c) The use of steel bracing (post-tensioned or structural steel bracing) proved to be a feasible retrofit scheme for relatively flexible reinforced concrete frame buildings. In such buildings, the bracing system can provide substantial increases in strength and dissipate energy at drifts small enough that severe damage to existing members and lateral drift are

controlled. In contrast, for relatively stiff buildings, such as low-rise structures with short stiff columns or with infills, the steel bracing system is not likely to perform well because significant damage or failure of existing elements occurs at relatively small drifts. In such cases, the stiffness requirements of the bracing system for preventing severe damage to elements will be so high that the use of such a system will generally be economically and practically unfeasible. Retrofit schemes such as jacketing of elements or the addition of wing walls may be more viable alternatives.

8.3 SUGGESTIONS FOR FUTURE RESEARCH

a) Additional studies are required to evaluate the behavior (strength and ductility) of existing building components and building structures of reinforced concrete. In particular, studies regarding the capacity of short columns with short lap splices under load reversals are needed.

b) The effects of initial prestressing on the behavior of reinforced concrete members were not included in the present study and need to be evaluated. Initial pre-compression can either delay (improve the performance) or precipitate failure of splices in columns of a post-tensioned bracing system.

C) The use of steel bracing systems as a retrofit scheme for reinforced concrete frames points out the need for studying the behavior and design of connections for both, post-tensioned and structural steel bracing systems. Because of the special problems associated with steel-to-concrete connections the design of efficient and reliable connection devices requires particular attention and needs further investigation.

APPENDIX A

SUMMARY OF RELEVANT PROVISIONS OF ATC-22

The ATC-22 provisions described herein pertain only to the structural systems and components for the buildings considered in the present study. These provisions correspond to the equivalent lateral force procedure, which forms the basis of the ATC-22 document. A dynamic analysis is required for "tall" buildings with vertical irregularities caused by significant changes in mass or geometry. However, the base shear forces obtained from dynamic analyses, such as a response spectrum analysis, need not be greater than that required by the equivalent force procedure.

A.1 BASE SHEAR

The seismic base shear , V, in a given direction is determined by the familiar relationship:

$$V = C_s W \qquad (A.1)$$

where W is the total dead load of the building (for storages and warehouses 25% of the floor live load shall be applicable. Also other restrictions apply but that are not relevant to this study). C_s is the seismic design coefficient determined below. To specify lateral forces for existing buildings, ATC-22 uses a mean response spectra instead of the mean plus one standard deviation usually specified for new construction. The base shear coefficient, C_s , in ATC-22 is thus reduced from that prescribed for new construction and corresponds to 67% of the value specified in the NEHRP provisions [15] for new buildings as follows:

$$C_s = 0.67 \frac{1.2 A_v S}{R T^{2/3}} = \frac{0.8 A_v S}{R T^{2/3}} \qquad (A.2)$$

where:

A_v = velocity-related acceleration coefficient which varies depending on the seismic zone considered and is equal to 0.4 for zones of high seismic risk.

S = soil profile coefficient given in Table A.1 (In locations where soil properties are unknown or where the profile does not meet any of the four types indicated in Table A.1, the value of S shall be taken as 1.5).

R = response modification coefficient as shown in Table A.2.

T = fundamental period of the building, as defined below.

The value of C_s need not be greater than 85% of the limiting value of the NEHRP provisions [15]:

$$C_s = 0.85 \frac{2.5 A_a}{R} = 2.12 \frac{A_a}{R} \qquad (A.3)$$

where:

A_a = acceleration coefficient which varies depending on the seismic zone and is equal to 0.4 for zones of high seismic risk.

A.2 FUNDAMENTAL PERIOD

The value of the fundamental period T is calculated from one of the following two methods:

A.2.1 Method A

a) For buildings in which the lateral resistance consists of moment resisting frames capable of resisting 100% of the required lateral force and such frames are not enclosed or adjoined by more rigid components tending to prevent the frames from deflecting when subjected to seismic forces, the fundamental period of the building T_a can be approximated by:

$$T_a = C_T h_n^{3/4} \qquad (A.4)$$

where:

C_T = 0.030 for concrete frames.

h_n = the height in feet above the base to the highest level of the building.

Table A.1 Soil profile coefficients

Soil Profile Type	Soil Profile Coefficient, S
Rock (characterized by a shear wave velocity greater than 2500 feet per second), or Stiff soil conditions where the soil depth is less than 200 feet and the soil types are stable deposits of sands, gravels, or stiff clays.	1.0
Deep cohesionless or stiff clay conditions, including sites where the soil depth exceeds 200 feet and the overlying soils are stable deposits of sands, gravels or stiff clays.	1.2
Soft- to medium-stiff clays and sands, characterized by 30 feet or more of soft- to medium-stiff clays with or without intervening layers of sand or other cohesionless soils	1.5
Soft clays with more than 70 feet deep or silts characterized by a shear wave velocity less than 400 feet per second.	2.0

Table A.2 Response modification factors and element behavior modification coefficients

Structural System	Response Modification Factor, R	Element Behavior Modification Factor, C_d
Ordinary Moment Frames of Reinforced Concrete	2	2
Concentrically Braced Frames with Intermediate Moment Frame of Reinforced Concrete*	5	4.5
Reinforced Concrete Shear Walls with Intermediate Moment Frame of Reinforced Concrete*	6	5

* moment frame must be capable of resisting 25% of the prescribed seismic forces

b) For all other buildings (braced frames, structural (*shear*) walls):

$$T_a = 0.05 \frac{h_n}{\sqrt{L}} \qquad (A.5)$$

where:

L = overall length (in feet) of the building at the base in the direction under consideration.

A.2.2 Method B

The fundamental period may be estimated using the structural properties and deformation characteristics of the resisting elements in a properly substantiated analysis (such a procedure is used in the present study). The fundamental period so determined **shall not exceed** $C_a T_a$, where C_a takes a value of 1.2 in zones of high seismic risk.

A.3 STRENGTH DEMANDS

The load combinations specified in ATC-22 are the same as those required by the NEHRP provisions [15], as follows:

$$Q = (1.1 + 0.5 A_v) \, Q_D + 1.0 \, Q_L + 1.0 \, Q_S \pm (1.0 Q_E)^* \qquad (A.6)$$

and

$$Q = (0.9 - 0.5 A_v) \, Q_D \pm (1.0 Q_E)^* \qquad (A.7)$$

where:

Q = effect of combined loads.

Q_D = effect of dead load.

Q_L = effect of live load.

Q_S = effect of snow load.

Q_E = effect of seismic forces.

The seismic portion of the demand Q_E, is obtained from analysis of the building using the base shear, V, from Eq. A.1.

*   ATC-22 modifies the term (1.0 Q_E) in accordance with the expected behavior for the member being considered for analysis.

a) *For elements that behave in a ductile manner* the demands obtained from analyses are estimate from Eqs. A.6 and A.7 without modification.

b) *For brittle elements* which are expected to exhibit a sudden mode of failure, the basic earthquake effect should be multiplied by the factor 0.75 C_d, where C_d is the system factor obtained from Table A.2.

c) *For semi-ductile elements*, defined by the provisions as elements whose behavior is intermediate between that of types a) and b), the term 1.0 Q_E should be replaced by 0.375 $C_d Q_E$. (C_d is obtained from Table A.2)

Load factors are applied to building components rather than to building structures. However, to compare the provisions of the ATC-22 with the behavior obtained for the buildings of this study, it is assumed that the overall response is governed by the response of critical elements in the structure, brittle or semi-ductile elements, as described in Chapters IV and VI. Thus, the lateral strength of the building is estimated using the load factors associated with the behavior of the elements that govern the response of the building.

To compute the base shear coefficient, load factors for dead load and gravity loads were weighed against the loads for seismic forces. For the purpose of comparison, load factors for seismic forces were weighed higher than gravity loads. The distribution of between dead loads, live loads and earthquake forces was as follows: 30% for dead load, 10% for live load and 60% for earthquake forces.

In addition to load factors, the seismic coefficient was modified by strength reduction factors, ϕ. A value of 0.85 was adopted when brittle element behavior was expected, and 0.9 was adopted for semi-ductile and ductile modes of failure. Thus, the final value for the base shear coefficient was calculated as:

$$C_s^* = \frac{C_s Q}{\phi} \qquad\qquad (A.8)$$

REFERENCES

1.- Report on Workshop, "Repair and Retrofit of Existing Structures," *PMFSEL Report No. 87-6*, December 1987, 69 pp.

2.- ACI Committee 318, "Building Code Requirements for Reinforced Concrete (ACI 318 - 63)," American Concrete Institute, Detroit, Michigan, 1963, 144 pp.

3.- International Conference of Building Officials, "Uniform Building Code," Whittier, California, 1991.

4.- ACI Committee 318, "Building Code Requirements for Reinforced Concrete (ACI 318 - 89)," American Concrete Institute, Detroit, Michigan, 1989, 353 pp.

5.- International Conference of Building Officials, "Uniform Building Code," Whittier, California, Volume I, 1967, 595 pp.

6.- International Conference of Building Officials, "Uniform Building Code," Whittier, California, 1964.

7.- Wyllie, Jr., L. A., "Seismic Strengthening Procedures for Existing Structures," *IABSE Symposium*, Venice, Italy, 1983, pp. 363 - 370.

8.- International Conference of Building Officials, "Uniform Building Code," Whittier, California, 1955.

9.- ACI Committee 318, "Building Code Requirements for Reinforced Concrete (ACI 318 - 56)," American Concrete Institute, Detroit, Michigan, 1956.

10.- Orangun, C. O., Jirsa J. O., and Breen J. E., "A Reevaluation of Test Data on Development Length and Splices," *Journal of the American Concrete Institute*, Vol. 74, March 1977, pp. 114-122.

11.- Pessiki, S. P., Conley, C. H., Gergely P. and White R.N., "Seismic Behavior of Lightly-Reinforced Concrete Column and Beam-Column Joint Details," *Technical Report NCEER-90-0014*, National Center For Earthquake Engineering Research, Red Jacket Quadrangle, Buffalo, NY 14261.

12.- Applied Technology Council, " A Handbook for Seismic Evaluation of Existing Buildings (Preliminary)," ATC-22, Redwood City, California, 1989.

13.- Farahany, M. M., "Computer Analysis of Reinforced Concrete Cross Sections," M.Sc. Thesis, The University of Texas at Austin, May 1977.

14.- Kent, D.C. and Park, R., " Flexural Members with Confined Concrete," *Journal of the Structural Division*, ASCE, Vol. 97, No. ST7, July 1977.

15.- Building Seismic Safety Council, "NEHRP Recommended Provisions for the Development of Seismic Regulations for New Buildings", Code (Part I) and Commentary (Part II), Washington D.C., 1988.

16.- National Institute of Standards and Technology, "Performance of Structures During the Loma Prieta Earthquake of October 17, 1989," *NIST Publication 778*, January 1990.

17.- Boubenider, R., "Foundation Effects on the Inelastic Response of Frames to Seismic Excitation," M.Sc. Thesis, The University of Texas at Austin, August 1988, 116 pp.

18.- Kannan, A. E. and Powell, G. H., "DRAIN - 2D: A General Purpose Program for Dynamic Analysis of Inelastic Plane Structures," *Reports No. EERC 73-6 and EERC 73*

- 22, University of California at Berkeley, April 1973 (Revised Sept. 1973 and August 1975).

19.- **Newmark, N. M.,** " A Method of Computation for Structural Dynamics," *Transactions ASCE,* Vol. 127, Part I, 1962, pp. 1406 - 1435.

20.- **Wakabayashi, M.,** *Design of Earthquake-Resistant Buildings,* McGraw-Hill Book Company, 1986, 310 pp.

21.- **Bertero, V., Aktan A. E., Charney, F. and Sause R.,** "Earthquake Simulator Tests and Associated Experimental, Analytical, and Correlation Studies of One-Fifth Scale Model," *Earthquake Effects on Reinforced Concrete Structures (U.S. - Japan Research),* SP-84, American Concrete Institute, Detroit, Michigan, 1985, pp. 375-424.

22.- **Aktan, A. E., Bertero V., Chowdhury, A. and Nagashima,T.,** "Experimental and Analytical Predictions of the Mechanical Characteristics of a 7-Story 1/5 Scale Model R/C Frame-Wall Building Structure," *Report No. EERC-83/13,* University of California at Berkeley, 1984.

23.- **Giberson, M. F.,** "Two Nonlinear Beams with Definition of Ductility," *Journal of the Structural Division,* ASCE, Vol. 95, February 1969, pp. 137 - 157.

24.- **Takeda, T, Sozen, M. A. and Nielsen, N.,** "Reinforced Concrete Response to Simulated Earthquakes," *Journal of the Structural Division,* ASCE, Vol. 96, December 1970, pp. 2557 - 2573.

25.- **Badoux, M.E.,** "Seismic Retrofitting of Reinforced Concrete Structures with Steel Bracing Systems," Ph.D. Dissertation, The University of Texas at Austin, May 1987, 275 pp.

26.- Hoedijanto, D., "A Model to Simulate Lateral-Force Response of Reinforced Concrete Structures with Cylindrical and Box Sections," Ph.D. Dissertation, University of Illinois, Urbana, 1983.

27.- ACI-ASCE Committee 352, "Recommendations for Design of Beam-Column Joints in Monolithic Reinforced Concrete Structures," *Journal of the American Concrete Institute*, Vol. 82, May-June 1982, pp. 266 - 283.

28.- Valluvan, R., Kreger, M. E. and Jirsa, J. O., "Strengthening of Column Splices in Infilled Shear Walls," *paper for oral presentation at the 10 th World Conference in Earthquake Engineering*, Madrid, Spain, 1992.

29.- Jain, A. K. and Goel S. C., "Hysteresis Models for Steel Members Subjected to Cyclic Buckling or Cyclic End Moments and Buckling (User's Guide for DRAIN-2D: EL9 and EL10)," *Report No. UMME 78R6*, Department of Civil Engineering, The University of Michigan, Ann Arbor, Michigan, December 1978.

30.- "Load & Resistance Factor Design Manual of Steel Construction", American Institute of Steel Construction, First Edition, March 1990.

31.- Lee, S. and Goel S., "Seismic Behavior of Hollow and Concrete-Filled Square Tubular Bracing Members," *Research Report UMCE 87-11*, The University of Michigan, December 1987, 249 pp.

32.- Goel, S. C. and Hanson, R. D., "Behavior of Concentrically Braced Frames and Design of Bracing Members for Ductility," *Proceedings of the 56 th Annual Convention of the SEAOC*, San Diego, October 1987, pp. 167 - 192.

33.- Anderson, J. C. and Naeim, F., "Design Criteria and Ground Motion Effects on the Seismic Response of Multistory Buildings," ATC 10-1, Critical Aspects of Earthquake Ground Motion and Building Damage Potential, Applied Technology Council, Palo Alto, Ca., 1984.

34.- **Veletsos, A. S.,** "Dynamics of Structure-Foundation Systems," *Structural and Geotechnical Mechanics, A Volume Honoring N. M. Newmark,* edited by W. J. Hall, Prentice-Hall, 1977, pp. 333 - 361.

35.- **Kausel, E.,** "Forced Vibrations on Circular Foundations on Layered Media," *Research Report R74-11,* Civil Engineering Department, Massachusetts Institute of Technology, January 1974.

36.- **Kausel, E., Roesset, J. M. and Waas, G.,** "Dynamic Analyses of Circular Footings on Layered Media," *Journal of the Engineering Mechanics Division,* ASCE, Vol. 101, October 1975.

37.- **Kausel, E., Whitman, R. V., Murray, J. P. and Elsabee, F.,** "The Spring Method for Embedded Foundations," *Nuclear Engineering and Design,* Vol. 48, 1978, pp. 377 - 392.

38.- **Isenhower, W. I.,** "Torsional Simple Shear/Resonant Column Properties of San Francisco Bay Mud," Geotechnical Engineering Thesis GT80-1, The University of Texas at Austin, December 1979, 307 pp.

39.- **Veletsos, A. S. and Meek J. W.,** "Dynamic Behavior of Building Systems," *Int. Journal of Earthquake Engineering and Structural Dynamics,* Vol. 3, No. 2, 1974, pp. 121 - 138.

40.- **Veletsos, A. S. and Nair V. V.,** " Seismic Interaction of Structures on Hysteretic Foundations," *Journal of the Structural Division,* ASCE, Vol. 101, No. ST1, 1975, pp. 109 -129.

41.- **Veletsos, A. S. and Verbic B.,** "Dynamics of Elastic and Yielding Structure-Foundation Systems," *Proceedings of the Fifth World Conference on Earthquake Engineering,* Rome, 1974, pp. 2610 - 2613.

42.- **Romo, M. P. and Seed H. B.,** "Analytical Modeling of Dynamic Soil Response in the Mexico Earthquake of Sept. 19, 1985," *Proceedings*, The Mexico Earthquakes-1985, Factors Involved and Lessons Learned, American Society of Civil Engineers, 1987, pp. 148 - 162.

43.- **Lodde, P. F.,** "Dynamic Response of San Francisco Bay Mud," Geotechnical Engineering Thesis GT82-2, The University of Texas at Austin, June 1982, 295 pp.

44.- **Tarquis, F. and Roesset, J. M.,** "Structural Response and Design Criteria for the 1985 Mexico City Earthquake," Geotechnical Engineering Dissertation GD89-1, The University of Texas at Austin, December 1988, 208 pp.

45.- **"Seismic Provisions for Structural Steel Buildings - Load and Resistance Factor Design,"** American Institute of Steel Construction, Chicago, Illinois, Nov. 1990.

46.- **Jimenez, L,** "Strengthening of Reinforced Concrete Frame using an Eccentric Wall," M. Sc. Thesis, The University of Texas at Austin, May 1989.

47.- **Paulay, T.,** "The Design of Ductile Reinforced Concrete Structural Walls for Earthquake Resistance," *Earthquake Spectra*, Vol. 2, No. 4, 1986.

48.- **Filippou, F. and Issa, A.,** "Nonlinear Analysis of Reinforced Concrete Frames under Cyclic Load Reversals," *Report No. UCB/EERC-88/12*, Earthquake Engineering Research Center, University of California, Berkeley, California, September 1988, 114 pp.

49.- **Jordan, R. M.,** "Evaluation of Strengthening Schemes for Reinforced Concrete Moment-Resisting Frame Structures subjected to Seismic Loads," Ph.D. Dissertation, The University of Texas at Austin, May 1991, 207 pp.

50.- **Aboutaha, R. and Engelhardt, M**, (private communication) Research in progress on the behavior of short lap splices in columns, The University of Texas at Austin, February 1992.

51.- **Bush, T. D.**, "Seismic Strengthening of a Reinforced Concrete Frame," Ph.D. Dissertation, The University of Texas at Austin, May 1987, 326 pp.

52.- **Wyllie, L. and Dal Pino, J. A.**, "Seismic Upgrade Preserves Architecture," *Modern Steel Construction*, Jan 1991, pp. 20 - 23.

53.- **Saiidi, M. and Sozen, M. A.**, "Simplex and Complex Models for Non-Linear Seismic Response of Reinforced Concrete Structures," *Structural Research Series No. 465*, University of Illinois at Urbana-Champaign, Urbana, Illinois, August 1979, 188 pp.

54.- **Moehle, J. P. and Sozen, M. A.**, "Experiments to Study Earthquake Response of R/C Structures with Stiffness Interruptions," *Structural Research Series No. 482*, University of Illinois at Urbana-Champaign, Urbana, Illinois, August 1980, 421 pp.

55.- **Newmark, N. M.and Hall W. J.**, *Earthquake Spectra and Design*, Engineering Monographs on Earthquake Criteria, Structural Design and Strong Motion Records, Earthquake Engineering Research Institute, 1982, 103 pp.

56.- **Jones, E. A. and Jirsa, J. O.**, "Seismic Strengthening of a Reinforced Concrete Frame using Structural Steel Bracing," *PMFSEL Report No. 86-5*, The University of Texas at Austin, May 1986, 147 pp.

57.- **ACI Committee 318**, "Building Code Requirements for Reinforced Concrete (ACI 318 - 71)," American Concrete Institute, Detroit, Michigan, 1971, 78 pp.

58.- **Fintel, M. and Khan F. R.**, "Shock-Absorbing Soft Story Concept for Multistory Earthquake Structures," *Journal of the American Concrete Institute*, Vol. 66, No. 5, May 1969, pp. 381 - 390.

328

59.- **Japan Disaster Prevention Association,** "Standard for Evaluation of Existing Reinforced Concrete Buildings," revised in 1990.

60.- **Japan Disaster Prevented Association,** "Guidelines for Seismic Retrofitting of Existing Reinforced Concrete Buildings," revised in 1990.

61.- **Applied Technology Council,** "Evaluating the Seismic Resistance of Existing Buildings," ATC-14, Redwood City, California, 1987, 370 pp.

62.- **Federal Emergency Management Agency,** "Techniques for Seismically Rehabilitating Existing Building (Preliminary)," Earthquake Hazards Reduction Series, FEMA 172, May 1989.

63.- **Alcocer, S. M. and Jirsa, J. O.,** "Reinforced Concrete Frame Connections Rehabilitated by Jacketing," *PMFSEL Report 91-1*, The University of Texas at Austin, July 1991, 221 pp.

64.- **Gaynor, P. J.,** "The Effect of Openings on the Cyclic Behavior of Reinforced Concrete Infilled Shear Walls," M. Sc. Thesis, The University of Texas at Austin, August 1988, 245 pp.

65.- **Miranda, E. and Bertero, V. V.,** "Post-Tensioning Technique for Seismic Upgrading of Existing Low-Rise Buildings," *Proceedings of the Fourth U.S. National Conference on Earthquake Engineering*, Palm Springs, California, Vol. 3, May 1990, pp. 393 - 402.

66.- **Miranda, E.,** "Upgrading of a School Building in Mexico City," *Proceedings of the Fourth U.S. National Conference on Earthquake Engineering*, Palm Springs, California, Vol. 1, May 1990, pp. 109 - 118.

67.- **Sugano, S. and Fujimura, M.,** "Aseismic Strengthening of Existing Reinforced Concrete Buildings," *Proceedings of the Seventh World Conference in Earthquake Engineering*, Istanbul, 1980.

68.- **Jirsa, J. O. and Badoux, M.,** "Strategies for Seismic Redesign of Buildings," *Proceedings of the Fourth U.S. National Conference on Earthquake Engineering*, Palm Springs, California, Vol. 3, May 1990, pp. 343 - 351.

69.- **Chai, Y. H., Priestly, M. J. N. and Seible, F.,** "Seismic Retrofit of Circular Bridge Columns for Enhanced Flexural Performance," *ACI Structural Journal*, Vol. 88, No.5, September - October 1991, pp. 572 - 584.

70.- **Bett, B. J.,** "Behavior of Strengthened and/or Repaired Reinforced Concrete Columns Under Reversed Cyclic Deformations," M. Sc. Thesis, The University of Texas at Austin, August 1985.

71.- **Migliacci, A., et al.,** "Repair Techniques of Reinforced Concrete Beam-Column Joints," *IABSE Symposium*, Venice, 1983, pp. 355-362.

72.- **Riddell, R. and Newmark N. M.,** "Statistical Analysis of the Response of Non-Linear Systems Subjected to Earthquakes," *Structural Research Series No. 468*, University of Illinois at Urbana-Champaign, Urbana, Illinois, August 1979, 291 pp.

73.- **Umehara, H. and Jirsa, J. O.,** "Shear Strength and Deterioration of Short Reinforced Concrete Columns under Cyclic Deformations," *PMFSEL Report 82-3*, The University of Texas at Austin, July 1982, 256 pp.

74.- **Al-Sulaimani, G. J. and Roesset J. M.,** "Design Spectra for Degrading Systems," *Journal of Structural Engineering*, ASCE, Vol. 111, December 1985, pp. 2611 - 2623.

VITA

José Antonio Pincheira was born in Santiago, Chile, on September 13, 1960, the son of Guillermo Pincheira Squella and Paulina Peña González.

In 1978, he entered the University of Chile where he received the degree of Bachelor of Science in Civil Engineering and the diploma of Ingeniero Civil, graduating with unanimous distinction. In August 1986, he attended the graduate school at the University of Manitoba, Canada, where he was awarded the degree of Master of Science in Civil Engineering. In August 1988, he entered the graduate school of the University of Texas at Austin.

José A. Pincheira married Paulette G. Berthelon in Santiago, Chile, on August 23, 1986. They have one son, José Pablo, who was born in Austin, Texas, on October 12, 1989.

Permanent Address:

        Consejo de Indias 1360-B
        Providencia
        Santiago, CHILE

This dissertation was typed by the author.